



## **ROLE OF THE KIDNEY ANDROGEN-REGULATED PROTEIN IN THE DEVELOPMENT OF THE METABOLIC SYNDROME**

Tesis presentada por:

**Beatriz Bardají de Quixano**

Para optar al grado de doctor en Bioquímica, Biología molecular y  
Biomedicina

Tesis inscrita en el departamento de Bioquímica de la Universidad Autònoma de Barcelona y realizada en el grupo de Fisiopatología Renal del CIBBIM-Nanomedicina/Institut de Recerca Hospital Universitari Vall d'Hebron y dirigida por la doctora Anna Meseguer Navarro.

Dra. Anna Meseguer Navarro

Beatriz Bardají de Quixano

Barcelona, septiembre 2013

## ACKNOWLEDGEMENTS

Cuando me senté el primer día (de muchos) a escribir esta tesis estaba muy preocupada por recopilar una introducción que explicara bien lo que iba a venir después, por no pasarme con los detalles en los materiales y métodos, por ordenar los resultados de la manera más inteligible posible, por construir una discusión realista, razonable y razonada que no ocupara dos tomos... Todo parecía difícilísimo. Pensé en dejar los agradecimientos para el final porque, rubia de mí, llegué a la conclusión de que sería la parte más fácil, vamos, que los podría hacer un mono amaestrado. Y ahora que me siento a escribirlos, me doy cuenta de han sido muchos años de trabajo duro, de emociones fuertes (ilusiones y desilusiones), que hay muchas personas que han estado ahí en todos estos momentos y que lo difícil va a ser no dejarme a nadie que haya sido importante para mí durante estos años.

En primer lugar, quería dar las gracias a mi madre, por todo en general, pero en este caso en concreto, por apoyarme siempre en todos mis proyectos, planes y decisiones bajo cualquier circunstancia y por muy locos que fueran. Gracias por enseñarme que las cosas no se dejan a medias, que si algo vale pena hay dejarse la piel para conseguirlo y que no hay que conformarse con dar el 100% cuando se puede dar el 110%.

A los bros también hay que reservarles un lugar especial.

Gracias a Juancho (hey yo) por venir a sacarme del laboratorio en mil ocasiones en las que yo no era capaz de dejar lo que estaba haciendo y por quedarte conmigo el rato que hiciera falta hasta que yo acababa para llevarme a casa.

Gracias a Alberto (cohete) por creer siempre que era buena en lo que hacía hasta el punto de querer llevarme a trabajar contigo en varias ocasiones y por escuchar las cosas que les hacía a los ratones a pesar de que a ti sí que te gustan los animales.

A la dra. Anna Meseguer, jefa, directora y tutora, gracias por haberme dado la oportunidad de realizar este trabajo, incluso sin expediente. Por haber confiado en mí para llevar a cabo un proyecto de esta envergadura, para tutorizar y enseñar a otros y por haberme dado libertad para decidir y organizar.

A la dra. Luz Barreiro, en ocasiones post-doc, en otras canguro, en algunas, mala influencia (recordemos las carreras de carros ya sabes dónde), pero siempre mi amiga. Gracias por no perder nunca la paciencia conmigo y por todo lo que me has enseñado dentro y fuera del laboratorio, excepto lo del arroz, eso no molaba nada. Fuiste un gran apoyo durante el tiempo que compartimos.

Al dr. Pep Villena gràcies per la teva col·laboració a l'estabulari i per haver estat sempre accessible i proper a tots els dubtes que t'he volgut preguntar.

A la dra. Olga Tornavaca, gràcies per ensenyar-me els secrets del disseny experimental, del controls, de les repliques i a saber organitzar-me el temps per no haver d'anar els caps de semana al laboratori.

Vecinos de fisiopatología renal: Natàlia Enguix, Jaime Lasheras y Rosi Pardo gracias por dejar a mano vuestro material para cuando nosotros andábamos escasos... Que noooo... Gracias por participar con nosotros en celebraciones y disgustos como si fuéramos del mismo grupo. Y gracias a Marta García (no me he olvidado de ti) por la buena acogida que me diste nada más llegar.

Tengo que dar muchas gracias a las chicas que han pasado por el laboratorio para hacer prácticas de la carrera o de máster, que fueron a parar a mi poyata para que les enseñara los misterios de la investigación y acabaron convirtiéndose en una ayuda inestimable. No dejo de preguntarme cómo he tenido tanta suerte de que todas hayáis coincidido conmigo porque ya es casualidad que todas las que aparecéis a continuación hayáis resultado tan trabajadoras, bien predisuestas y encima buena gente. Gracias por haberme dejado que os enseñara, por haber aprendido tan rápido, por haber sido de tan gran ayuda en este trabajo y por haberme hecho sentir orgullosa en todas y cada una de vuestras defensas de másters.

Marie Defays, thank you so much for your jokes and good temper all times no matter what.

Sonia Díez, gracias por haber estado siempre tan bien dispuesta a ayudar a otros.

Cristina Suárez, gracias por tu trabajo tan meticuloso y cuidado.

Andrea Caballero, gracias por el intercambio de conocimientos y por el tiempo que sé que sacaste de debajo de las piedras para sacar el trabajo adelante.

Haizea Lekuona, gracias por tomarte siempre las cosas con filosofía.

Ayleen de la Rivera, por desgracia coincidimos poco tiempo y aun así pude contar con que me echara una mano con los últimos toques experimentales.

A la gente del servicio de nefrología de Vall d'Hebron que conocí de rebote. Especialment gràcies a la Carme Canatarell pel teu recolzament incondicional.

Y también un agradecimiento especial a María Sarrias por tu paciencia y buen juicio para controlar la situación el día que me convertí en la niña del exorcista, gracias por ayudarme a solucionar ese tema.

A las amigas del Oak House, especialmente Jana Tarrida y Carol de Britos, y afines como Natalia Mantecón y Mónica la otra rubia, gracias por vuestro apoyo y comprensión aunque ya sé que veces ha sido difícil entenderme.

Binonenas, algunas habéis hecho tesis (Gèraldine Joanny), otras no (Immaq Soria) y otras ni siquiera sois bio (Marta) y aun así te acogimos y te queremos igual. Algunas de las decisiones más importantes las hemos tomado juntas y gracias a los consejos de las demás, gracias porque os he podido encontrar siempre que os he necesitado.

A las ingenieras, aunque algunas no ejerzan según dicen, gracias por vuestro apoyo incondicional en todo momento y por el interés que habéis mostrado siempre en las freakadas que yo hacía. Y sobre todo, Gracias a Noemí Ayesa, por los conciertos, los restaurantes japoneses (en concreto el de “por favor deja de coger comida de una vez”), los viajes, los planes alternativos y la “fiesta definitiva”.

Amigos playeros, gracias por haberme recogido todos los 12 de octubre y 15 de agosto (y alguno que otro día más) incondicionalmente y dispuestos a playear conmigo para olvidar los disgustos que da a veces la investigación.

També voldria dedicar unes línies als meus ja no tan nous companys de feina:

Gràcies al dr. Lluís Guirado per donar-me l'oportunitat d'entrar al món dels assajos clínics, per creure't les coses bones que havies sentit de mi i per la bona acollida que em vas donar al meu nou lloc d'experiments.

Muchas gracias a Irene Silva por enseñarme con paciencia infinita los secretos de las bases de datos, los eCRDs, las visitas de inicio y de monitorización, la recuperación de muestras despistadas, la ubicación de todo en general y de algunos lugares en concreto cuando llamaba en crisis porque me había perdido por los pasillos de Puigvert.

A les adjunts del despatx, a la Cristina Canal per haver estat sempre tan propera, a la Núria Garra per haver-te preocupat pel meu benestar quan m'has trobat a les mil de la tarda al despatx escrivint tesi, a la Carme Facundo per explicar-me les coses dels nefros de manera que jo les pugui entendre i a la Núria Serra per animar-me sempre a mantenir la calma.

A las chicas experimentales: a la dra. Elisabet Ars, a la dra. Paola Krall, a Gemma Bullich, a Olga Sancho, a Lluïsa Carnero, a Patricia y a Ania por haberme dejado trastear puntualmente en vuestro lab y por haber aguantado con paciencia las quejas interminables sobre la escritura de la tesis. Y concretamente a la dra. Elena Guillén, gracias por tu apoyo y tus palabras de ánimo en todo momento.

Mil mishones de gracias al dr. Fede Grünbaum y a Deborah LoGiaccio por Volver a traer la música a mi vida y porque ya no somos Como Tres Extraños. Ah bueno, y por haber ayudado a crear el grupo del brote psicótico...

Fede, lo prometido es deuda y por eso apareces dos veces en estos agradecimientos. También tengo que darte las gracias por tu ayuda, tu apoyo, tu paciencia infinita, tu psicoterapia y por las burbujas, y porque siempre he podido contar contigo en los momentos alegres y en los difíciles.

Y como no, grazie mille a Chiara Chianese por tu buen humor y tu optimismo siempre, por tu cariño y tu risa súper contagiosa.

Als antics de Fisopatologia Renal:

Dra. Marta Riera, aquestes paraules no són per fer-te la pilota, jeje, ja estaven escrites d'abans. Moltes gràcies per la bona acollida que em vas donar quan vaig arribar al laboratori, gràcies per haver estat sempre propera i per ser un exemple a seguir en el treball de poiatà.

Dra. Maya Vilà, gràcies per posar el punt políticament incorrecte a totes les situacions i per estar sempre disposada a compartir els teus coneixements amb persistència i paciència.

Dr. Guillermo Suñé, el otro maño del lab, sobre todo y más importante tengo que agradecerte que me advirtieras del peligro de no equilibrar bien las centrífugas.

A todo el personal del estabulario, muchas gracias por vuestra buena predisposición a ayudarnos a los investigadores en todo lo que necesitamos. Y especialmente, gracias a Álex Rojo porque has aguantado el ataque de una de las predocs más pesada y puntillosa (por no decir otra cosa) que ha pasado por el VHIR. Gracias por estar siempre para resolver dudas y echar una mano en todo lo que he necesitado.

Many thanks to Luka Ozretic for the tour around Barcelona and for your help with the histology slides.

Muchas gracias a José Luís Mosquera por el rescate del último momento y por quedarte a darme lecciones de estadística más allá de tu hora de salir.

A Elena Estremera, la auténtica, no la otra, muchas gracias por cuidarnos a todas siempre, por adoptarnos en tu casa, por darnos shisha y por darnos apoyo en todo momento.

A todos los hijos adoptivos de fisiopatología renal gracias por vuestras visitas diarias para hacernos pasar un rato divertido.

Sunny Malhotra, gracias tu buen humor siempre.

Dra. Lide Alaña, gracias por tus locuras y tus burradas.

Dr. Marc Cuadros, gracias por tu paciencia y tu calma.

Jordi Vilardell, gràcies per les teves visites acompanyades de xerrades interminables, pel teu ajut incombustible i gràcies per fer de guia pels racons de la UAB.

Jordi Romero, gràcies per organitzar i apuntar-te a qualsevol festa, dinar, celebració, reunió, guateque, copeo, sopar, café, cervesa, aperitiu, comiat, pasar l'estona, o qualsevol altre tipus d'event. Gràcies per portar sempre bon rollo i gràcies pels bons moments a l'estabulari inhalant isofluorà i CO<sub>2</sub> i perseguint rates i ratolins pel terra. Ha estat tota un experiència compartir aquests anys amb tu.

Esto ya casi se acaba, y por eso les ha llegado el turno a los compañeros de alegrías y penas más cercanos: mis AMIGOS de Fisiopatología Renal.

A María Fernández, gracias por tenernos siempre todo a punto para que pudiéramos ponernos a investigar nada más llegar al laboratorio. También gracias por el cariño e interés que has mostrado siempre en las cosas rarísimas que hemos hecho a lo largo de estos años.

Natàlia Puig, tot i que vam coincidir poc al laboratori, me'n alegro molt d'haver continuat mantenint el contacte i haver-te pogut conèixer millor. Gràcies per l'organització (aquesta frase s'ha repetit molt recentment) i gràcies per afegir-te sempre a les coses que hem organitzat els altres amb tanta il·lusió i carinyo.

Gracias a Toni Cuevas por la KAP procariota recombinante sin modificaciones post-traduccionales. Y ahora en serio, gracias por haber ayudado a que no acabara electrocutada, quemada con fuego, ácido, nitrógeno líquido, nieve carbónica, atacada por un rotor de centrífuga... enseñándome que las máquinas del laboratorio tienen instrucciones y no funcionan mejor por darles golpes en el lado.

Al dr. Edu Sarró, moltes gràcies pels teus bons consells sobre el western blot, pels dolents no. Pero sobre tot moltes gràcies per no deixar-me mai sola fent el hooligan I per haver estat sempre disposat a donar-me un cop de mà en els moments que t'he necessitat.

Bruja mayor, bruja mayor, gràcies per haver ajudat a fundar l'aquellarre sense el qual ni jo ni la bruixa petita haguèssim sobreviscut amb dignitat a totes les circumstàncies viscudes. Gràcies a la dra. Thais Cuadros per haver-me aportat tranquil·litat i cordura sempre que ha estat possible, gràcies per la teva paciència, per saber escoltar quan cal escoltar i per parlar quan s'ha de parlar, gràcies pels teus consells tant científics com de la vida en general.

Dr. Joan López Hellín, I'm lost for words. Como no puedo resumir todas las cosas por las que tendría que darte las gracias, para abreviar, GRACIAS por todo. De todos los laboratorios en todas las ciudades del mundo, tuve que entrar en el tuyo.

A la meva Maite, la Conxi Jacobs, la deixo pel final, per a que quan llegeixi aquestes pàgines (ja no sé quantes en porto), es pugui trovar fàcilment.

Amb un començament no gaire amistós (no ens posarem a recordar l'incident del PBS, ni el del màster), de seguida, l'ou i la castanya van congeniar (encara ningú s'explica com). Hem viscut milers d'aventures: hem anat de festa, al teatre, a fer birres, vins i altres, ens hem apuntat a balls rars i a balls raríssims, hem intentat fer veure que anàvem a conferències, hem posat a prova la màquina de triturar paper fins a límits indescriptibles, hem convertit el lab en una rave, fins i tot hem anat a pescar foques... Primer de tot t'haig d'agrair que m'hagis seguit sempre en les meves bogeries i segon de tot, que m'hagis aturat quan ja eren massa boges. Tercer, quart, cinqué... n-é, no sé per on continuar, perquè són tantes les coses que podria agrair-te que això s'allargaria fins a l'infinit i ningú es llegiria la tesi. Ho resumiré (potser ja he après) en que has estat la millor amiga que mai hagués desitjat trobar en una situació com la nostra i el millor recolzament que mai hagués esperat tenir i només espero haver estat la meitat de bona amiga per a tu del que tu has estat per a mi.

Y finalmente, quería agradecerte, Marcos, que hayas intentado enseñarme a pedir ayuda cuando lo necesitaba (y recalco "intentado") y que hayas persistido mañamente aunque yo, por cabezonería, no hiciera ni caso. Lo que sí que me has enseñado, viniendo de propio a Barcelona, es que no hay distancia suficientemente larga (al menos entre Zaragoza y Barcelona), ni mar suficientemente profundo (al menos en "La Playa"), y que ain't no Vueling high enough. Gracias por haber acudido a levantarme todas las veces que me caído (muchas), por haberte caído conmigo e incluso haberte chipiado en aquella ocasión. Gracias por aguantar los capazos de lo que iba sucediendo con la KAP. Y gracias por haber hecho que estos "dos días" (que a mí me han parecido años), hayan sido legen-wait for it-darios.

¿Ya os creíais que se había acabado?

Pues a parte de los agradecimientos, me gustaría tener un recuerdo especial para dos personas con las que me hubiera gustado compartir este momento pero que se perdieron por el camino, una de ellas al principio y la otra al final.

La primera es Silvia Costamagna, nefróloga y nutricionista, que me animó a entrar en el mundillo del riñón con tan buena vista que resulta que me gustó y me quedé.

La segunda es Laia Soler, amiga amiguísima de la infancia, ¿hace falta decir algo más?

*“Hay que estar en los sitios para que pasen cosas”*

Cuatro amigos

David Trueba

# INDEX

---

# INDEX

<b>ABBREVIATIONS</b>	<b>1</b>
<b>SUMMARY</b>	<b>10</b>
<b>INTRODUCTION</b>	<b>13</b>
<b>I. THE METABOLIC SYNDROME</b>	
1. Definition	14
1.1. Diagnostic	15
1.2. Epidemiology	17
2. Disorders leading to metabolic syndrome: Organs and signaling pathways involved	18
2.1. Arterial hypertension	18
2.2. Impaired glucose metabolism	25
2.3. Obesity	29
2.4. Dislipidemia	34
3. Consequences	39
3.1. Cardiovascular disease	39
3.2. Diabetes mellitus	39
3.3. Kidney failure	40
<b>II. THE KIDNEY ANDROGEN-REGULATED PROTEIN</b>	
1. KAP and the androgens	43
2. The KAP gene	44
3. The KAP protein	46
4. Interaction of KAP with other proteins	47
<b>III. THE KAP TRANSGENIC MICE</b>	
1. Designing of the transgenic mouse	50
2. Regulation of the transgene	50
3. Effect of the over-expression of KAP on kidney	51
4. Transcriptomic assays of the transgenic mice's kidney	53
5. Effect of the transgene of the animals' blood pressure	55



<b>AIMS</b>	<b>59</b>
<b>MATERIALS AND METHODS</b>	<b>61</b>
EXPERIMENTAL DESIGN	62
MATERIALS:	
1. The mice	63
1.1. KAP transgenic mice	63
1.2. Leptin deficient (ob/ob) mice	63
1.3. Ppar $\gamma$ 2 knock-out mice	63
1.4. Poko mice	63
1.5. The diets	64
2. The cell lines	64
2.1. PKSV-PCT3	64
2.2. HepG2 (human hepatocellular liver carcinoma)	65
2.3. The clones	65
2.4. The culture media	65
3. The bacteria	67
3.1. D32 $\alpha$ TM	67
3.2. One-shot <sup>®</sup> TOP 10	67
3.3. The culture media	67
4. The plasmids	68
4.1. pCR <sup>®</sup> 2.1-TOPO <sup>®</sup>	68
4.2. pCMV-HA	68
4.3. pBIG2i	69
5. The buffers	70
METHODS:	
1. Genomic techniques	72
1.1. DNA extraction	72
1.1.1. From animal tissue	72
1.1.2. From bacterial cultures	73
1.1.3. Quantitative and qualitative analysis of DNA	73
1.2. Polymerase Chain Reactions	73
1.2.1. Genotyping PCR	
1.2.2. pCMV-HA insert amplification for further cloning in pCR <sup>®</sup> 2.1-TOPO <sup>®</sup>	

1.2.3. Detection presence of the insert cloned in pBIG2i	
1.2.4. DNA Sequencing	
1.2.5. PCR product checking on agarose gel	
1.2.6. Purification and ligation of DNA bands from agarose gels	
2. Expression analysis techniques	77
2.1. RNA preparation	77
2.1.1. RNA isolation	
2.1.2. Quantitative analysis of RNA	
2.1.3. Qualitative analysis of RNA	
2.2. RT-PCR	78
2.2.1. RNA from animal solid organs for endogenous genes checking for microfluidic cards	78
2.2.2. RNA from animal solid tissue for microfluidic cards	78
2.2.3. RNA from cell pellets for NFκB RT-PCR profiler	78
2.3. Real Time qPCR	78
2.3.1. Search of best endogenous (housekeeping) genes for the microfluidic cards	
2.3.2. Real Time qPCR	
2.4. Microfluidic cards	81
2.5. RT-PCR Profiler	82
3. Protein analysis and proteomic techniques	83
3.1. Protein isolation	83
3.1.1. Protein isolation from cell pellets	
3.1.2. Protein isolation from animal solid tissue	
3.1.3. Protein quantitative analysis	
3.2. Sample concentration	85
3.3. Immunoblotting or Western blot analysis	85
3.4. Two-dimensional (2D) analysis	87
4. Histochemistry and other tissue methods	89
4.1. Tissue extraction and conservation	89
4.2. Paraffin blocks	90
4.3. Paraffin-embedded tissue sections	90
4.4. Tissue staining	90
4.5. Assembly	91
4.6. Microscopy observation and image acquiring	91
5. In bacteria methods	91
5.1. Bacteria cultures	91

5.2. Bacteria transformation	91
5.2.1. Transformation of competent bacteria from D32 $\alpha$ TM strain	
5.2.2. Transformation of competent bacteria from One-Shot® TOP10 strain	
6. In cell methods	93
6.1. Cell cultures	93
6.2. Cell thawing	93
6.3. Trypsinization	94
6.4. Cell counting	95
6.5. Cell freezing	95
6.6. Stable transfection of cells	96
6.7. Cell clones picking	98
6.8. Toxicity assays	98
6.9. Viability assays	99
6.10. Hoechst staining	99
6.11. Oil red o staining	99
6.12. Experiments in isolated culture cell models	100
6.12.1. Development of mouse proximal tubule cell systems with controlled expression of KAP	
6.12.2. Stably transfected KAP	
6.13.2.1. NF $\kappa$ B in PCT3 cells	
6.13.2.2. Secretion of eukaryotic recombinant KAP	
6.12.3. Prokaryotic recombinant KAP	
6.13.3.1. Oxidative stress assays in PCT3 and HK cells	
6.13.3.2. Oleic acid + recombinant prokaryotic KAP in HepG2 cells	
7. In vivo methods	109
7.1. Animal weighing	109
7.2. Food and H <sub>2</sub> O intake register	109
7.3. Glucose tolerance test	110
7.4. Insulin tolerance test	110
7.5. Collection of blood samples	111
7.6. Blood pressure measurement	113
7.7. Animal sacrifice and tissue collection	114
7.8. High fat diet experiments	115
8. Data treatment, statistical analyses and calculation of the N for experiments on live animals	117
<b>RESULTS</b>	<b>119</b>

1. Phenotype of the animal experimental models:	120
1.1. Blood pressure measurements	120
1.2. Evaluation of glucose metabolism	121
1.3. Body weight	124
1.4. Lipid profile	127
1.5. Effect of KAP and hfd on inflammation	128
1.6. Serum proteomic assay	129
1.7. Effect of stably transfected KAP on NFκB inflammation pathway in PCT3 clones	130
2. Studies in isolated organs:	135
2.1. Organs' weight	135
2.2. Adipose tissues histology	136
2.3. Liver histology	137
2.4. Effect of prokaryotic recombinant KAP on lipid storage in HepG2 cells	138
2.5. Kidney histology	146
2.6. Study of the secretion of KAP	148
3. Differential gene expression assays in adipose tissue, liver and kidney:	151
3.1. Differentially expressed genes in inguinal white adipose tissue	151
3.2. Differentially expressed genes in liver	159
3.3. Differentially expressed genes in kidney	162
4. Other metabolic syndrome models	163
4.1. Characterization of the phenotype	163
4.2. Characterization of the kidney	163
<b>DISCUSSION</b>	<b>167</b>
1. Animals' body weight is controlled in a multigenic and multitissular manner independently of the over-expression of KAP	171
2. Interaction of the transgene with the high fat diet diminishes the deleterious effects produced by these separately on lipid metabolism	177
3. The high fat diet but not the over-expression of KAP demonstrates an evident role in the development of impaired glucose metabolism	180
4. The over-expression of KAP, high fat diet and interaction of both are differentially involved in the development of inflammation in the different animals' tissues	183
5. Blood pressure is more affected by a high fat diet than by the over-expression of KAP	185
6. Kidneys are more affected by high fat diet than by over-expression of KAP	188
<b>CONCLUSIONS</b>	<b>193</b>

**REFERENCES** **195****PUBLISHED ARTICLES** **204**

Tornavaca O, Sarro E, Pascual G, **Bardaji B**, Montero MA, Salcedo T, López-Hellin J, Itarte E, Meseguer A.(2011) **KAP Degradation by Calpain is Associated with CK2 Phosphorylation and Provides a Novel Mechanism for Cyclosporine A-induced Proximal Tubule Injury.** PLoS ONE 6(9):e25746. Doi10.1371/journal.pone.0025746.

Grande MT, Pascual G, Riobos AS, Clemente-Lorenzo M, **Bardaji B**, Barreiro L, Tornavaca O, Meseguer A, López-Novoa JM. **Increased oxidative stress, renin-angiotensin system and sympathetic overactivation induce hypertension in kidney androgen-regulated protein (KAP) transgenic mice.** Free Radical Biology & Medicine. 2011 Aug 25.

Tornavaca O., Pascual G., Barreiro M. L., Grande M. T., Carretero A., Riera M., Garcia-Arumi E., **Bardaji B.**, González-Núñez M., Montero M.A., López-Novoa J.M. i Meseguer A. **Kidney Androgen-Regulated Protein Transgenic Mice Show Hypertension and Renal Alterations Mediated by Oxidative Stress.** Circulation (2009) 119; 1908-1917.

# **ABBREVIATIONS**

---

**ABBREVIATIONS**

20-HETE	20-hydroxyeicosatetraenoic acid
2D	two dimensions / bidimensional
2YH	yeast two-hybrid assays
8-OHdG	8-hydroxydeoxyguanosine
Acaa	acetyl-Coenzyme A acyltransferase
Acaa1b	acetyl-Coenzyme A acyltransferase 1b
Acca2	acetyl-Coenzyme A acyltransferase 2
ACE	angiotensinogen converting enzyme
Acsn3	Acyl-CoA synthetase medium-chain family member 3
ADH	antidiuretic hormone
Agt1a	angiotensin II receptor, type 1a
AKI	acute kidney injury
Akt	serine-threonine protein kinase
AMP	adenosine monophosphate
Ang II	angiotensin II
AplnR	apelin receptor
APS	ammonium persulphate
ARB	angiotensin receptor blocker
ARE	androgen-response element
ATP	adenosine triphosphate
ATR1	angiotensin II receptor 1
BAT	brown adipose tissue
BCA	bicinchoninic acid
BCL3	B-cell lymphoma 3-encoded protein
BMI	body mass index
bp	base pair
BP	blood pressure

## ABBREVIATIONS

BSA	bovine serum albumin
BUN	blood urea nitrogen
C/EBPA	CCAAT/enhancer-binding protein alpha
C3	complement component 3
cAMP	cyclic adenisine monophosphate
Card10	caspase recruitment domain-containing protein 10
Casp1	caspase 1/interleukin-1 converting enzyme
CCL2	chemokine C-C motif ligand 2
CD27	tumor necrosis factor receptor
CDK2	cyclin-dependent kinase 2
cDNA	complementary DNA
CEEA	Comitè Ètic d'Experimentació Animal
Cf	final cocentration
CISH	cytokine-inducible SH2-containing protein
CK2	casein kinase 2
CKD	chronic kidney disease
cm	centimeters
cM	centiMorgans
Co	original concentration
CO <sub>2</sub>	carbon dioxide
co-IP	co-immunoprecipitation
CREBBP	CREB-binding protein
CsA	cyclosporin A
Ct	total concentration
CVD	cardiovascular disease
Cyp4a12A	cytochrome P450, family 4, subfamily a, polypeptide 12a
Cyp4a14	cytochrome P450, family 4, subfamily a, polypeptide 14
CypB	cyclophilin B
DCFH-DA	2',7'-dichlorofluorescein diacetate
DHT	dihydrotestosterone



## ABBREVIATIONS

DIA	diastolic blood pressure
dl	deciliters
DM	diabetes mellitus
DMSO	dimethyl sulfoxide
DNA	deoxyribonucleic acid
dNTP	deoxyribonucleotides triphosphate
DPX	distyrene plasticizer and xylene
DTT	dithiothreitol
EDTA	ethylenediaminetetraacetic acid
EGF	epidermal growth factor
eGFR	estimated glomerular filtration rate
E-H	Eosin-Haematoxylin
Eif2ak2	eukaryotic translation initiation factor 2-alpha kinase 2
ERK	extracellular signal-regulated kinases
EtBr	ethidium bromide
EtOH	ethanol
FA	fatty acid
FBS	foetal bovine serum
FELASA	Federation of European Laboratory Animal Science Associations
FFA	free fatty acids
fig	figure
Fw	forward
g	grams
GAPDH	glyceraldehyde 3-phosphate dehydrogenase
GFR	glomerular filtration rate
GLUT4	Solute carrier family 2 facilitated glucose transporter, member 4
GTT	glucose tolerance test
h	hours
H <sub>2</sub> O	water
HA	hemagglutinin

## ABBREVIATIONS

hAGT	human angiotensinogen
HCl	hydrogen chloride
HDL	high density lipoproteins
HED	hydroxiethyl disulfide
hfd	high fat diet
Hmgsc2	3-hydroxy-3-methylglutaryl-CoA synthase 2
HPA-axis	hypothalamic-pituitary-adrenal axis
HQ	histochemistry
HSD11B1	hydroxysteroid-11- $\beta$ -dehydrogenase type 1 enzyme
HSPA5	heat shock 70 kDa protein 5
HT	hypertension
i/p	intra peritoneal
IEF	isoelectric focusing
IGF-1	insulin-like growth factor 1
IGT	impaired glucose tolerance
IHC	immunochemistry
IKBKB	inhibitor of nuclear factor kappa-B kinase subunit beta
IL-6	interleukin 6
IP	immunoprecipitation
IRAK2	interleukin-1 receptor-associated kinase-like 2
IRS1	insulin receptor substrate 1
IRS2	insulin receptor substrate 2
ITT	insulin tolerance test
IU	international units
KAP	kidney androgen-regulated protein
KCl	potassium chloride
kDa	kiloDaltons
kg	kilograms
KO	knock out
l	liters

## ABBREVIATIONS

LB	Luria-Broth
LBC	lower buffer chamber
LDH	lactate dehydrogenase
Lep	leptin
LipA	lipase A
Lipe	hormone-sensitive lipase
LPL	lipoprotein lipase
M	molar
m <sup>2</sup>	squared meters
mA	milliamperes
MAP	mean arterial pressure
MAPK3	mitogen-activated protein kinase 3
MCP-1	monocyte chemotactic protein-1
MDRD	Modification of Diet in Renal Disease
MED	mean arterial pressure
MetOH	methanol
mg	milligrams
MgCl <sub>2</sub>	magnesium chloride
MHC	major histocompatibility complex
μg	micrograms
μl	microliters
μmol	micromols
min	minutes
ml	milliliters
mM	millimolar
mmHg	mercury millimeters
mmol	millimols
MP	Mean blood pressure
mQ	milliQ
mRNA	messenger RNA

## ABBREVIATIONS

MS	Metabolic syndrome
MT	Masson's trichrome
mV	millivolts
MW	molecular weight
NaCl	sodium chloride
NADPH	nicotinamide adenine dinucleotide phosphate
NaOH	sodium hydroxide
NES	nuclear export signal
NF $\kappa$ B	nuclear factor NF-kappa-B
ng	nanograms
nl	nanoliters
nm	nanometers
nM	nanomolar
nmol	nanomols
NO	nitric oxide
Nox4	NADPH oxidase 4
nt	nucleotides
o/n	over night
°C	degrees centigrades
PAI-1	plasminogen activator inhibitor-1
p-Akt	phospho serine-threonine protein kinase
PAS	periodic acid-Schiff
PBS	phosphate buffered saline
PCR	polymerase chain reaction
PEST	peptide sequence which is rich in proline (P), glutamic acid (E), serine (S), and threonine (T)
PFA	paraformaldehyde
p-IRS1	phospho insulin receptor substrate 1
PKR	protein kinase R
PNPLA2	patatin-like phospholipase domain containing 2
POKO	ppary-ob knock out

## ABBREVIATIONS

PPAR- $\gamma$	peroxisome proliferator-activated receptor gamma
PPIA	peptidyl-prolyl cis-trans isomerase (CypA)
PT	proximal tubule
PVDF	polyvinylidene difluoride
qRT-PCR	quantitative retrotranscription polymerase chain reaction
RAAS	renin-angiotensin-aldosterone system
Rbp4	retinol binding protein 4
RNA	ribonucleic acid
ROS	reactive oxygen species
rpm	revolutions per minute
RT	room temperature
RT-PCR	retrotranscription polymerase chain reaction
Rv	reverse
SA	Acyl-CoA synthetase medium-chain family member 3
SDS	sodium dodecyl sulfate
SDS-PAGE	sodium dodecyl sulfate polyacrylamide gel electrophoresis
sec	seconds
siRNA	small interfering RNA
Slc20a1	sodium-dependent phosphate transporter 1
SLC2A4	gene encoding for GLUT4
Slc2A4	Solute carrier family 2 facilitated glucose transporter, member 4
STAT	signal transducer and activator of transcription
SYS	systolic blood pressure
TAE	Tris-Acetate-EDTA
TEMED	tetramethylethylenediamine
tg	transgenic
TG	triglycerides
Tgf- $\beta$ 1	transforming growth factor-beta 1
TH/T <sub>3</sub>	thyroid hormone
TMR	TMR

## ABBREVIATIONS

TNF $\alpha$	tumor necrosis factor-alpha
tPA	tissue plasminogen activator
TRAF3	TNF receptor-associated factor 3
TZD	thiazolidinediones
UBC	upper buffer chamber
uPA	urokinase plasminogen activator
UV light	ultraviolet light
V	volts
V <sub>c</sub>	circulating volume
VEGF	vascular endothelial growth factor
V <sub>f</sub>	final volume
V <sub>o</sub>	original volume
V <sub>s</sub>	serum volume
V <sub>t</sub>	total volume
WAT	white adipose tissue
WB	western-blot
wce	whole cell extract
WHO	World Health Organization
WIP	working IP buffer
wt	wild type
XTT	tetrazolium salt

## **SUMMARY**

---

## SUMMARY

The metabolic syndrome (MS) includes signs such as obesity, insulin resistance, compensatory hyperinsulinemia, dyslipidemia (DLP) and hypertension (HT) together leading to diabetes mellitus (DM) and cardiovascular disease (CVD). HT, DM and DLP are the main risk factors for endothelial dysfunction (decreased GFR and increased vascular permeability), inflammatory response, oxidative stress, activation of the rennin-angiotensin-aldosterone system (RAAS) and arteriosclerosis. These are all common signs to CVD, MS and chronic kidney disease (CKD).

CKD (decreased renal function expressed as glomerular filtration rate (GFR) or creatinine clearance less than 60 mL/min/1.73 m<sup>2</sup>) is mainly caused by HT, CVD and DM. CKD is associated with a significant increased risk of cardiovascular morbidity and mortality and is the major cause of death (mediated by HT) in diabetic individuals. This suggests that the kidney may be playing a key role in the MS based on the existence of a relationship between CKD and MS.

The general aim of this work is to study the molecular mechanisms underlying the MS, based on the study of the role of the kidney androgen-regulated protein (KAP), a protein of unknown function that is expressed exclusively in proximal tubule of mouse kidney and is regulated mainly by androgens, in the development of hypertension and MS.

The transgenic mouse (Tg) over-expressing KAP, a HT model with an apparent genetic predisposition to DLP and insulin resistance, shows cardiovascular and renal alterations that match some of those defining the MS (HT, endothelial dysfunction, oxidative stress and activation of RAAS), it is intended to clarify the environmental and molecular circumstances which trigger the MS assuming that KAP could be involved or related to the development of MS.

These three lines of study were followed in the present work:

1. Physiology of MS in whole body in controls (C) and Tg male mice fed on a control diet (chow) or high fat diet (HFD) containing 45% of calories in the shape of lipids (commonly used to induce obesity, hypertension and insulin resistance).
2. Histological and molecular (both proteomic and differential gene expression) analyses of study target organs and tissues.



3. Comparison of "in vivo" results with isolated cell systems:

- a) Effects of induced KAP expression on murine proximal tubule isolated cell cultures.
- b) Effects of prokaryotic recombinant KAP and oleate on human liver isolated cell cultures.

All results were statistically analyzed through standard t-tests.

These results demonstrated an involvement of the protein KAP in the development of MS opposite to what was initially hypothesized, since the consequences of HFD analyzed in the ways described above appear attenuated in over-expression of KAP. On the other hand, alterations associated with MS are manifested most strongly in the presence of HFD than in over-expression of KAP and appear to be diminished in the presence of both factors together.

# INTRODUCTION

---

# INTRODUCTION

## I. THE METABOLIC SYNDROME

### 1. Definition

There is certain controversy in the definition of the metabolic syndrome (also called cardiometabolic syndrome, insulin resistance syndrome or syndrome X) since it manifests with wide phenotypic variances in people with endogenous predisposition genetically determined and conditioned by environmental factors [1]. These are the reasons why there is no precise definition since many health organizations and associations have different visions of this syndrome [2]. However, all of the definitions agree in that metabolic syndrome is not a unique disease but a cluster of disorders comprising a group of conditions that converging in one same individual put them at risk of cardiovascular disease (CVD) and diabetes mellitus (DM), these conditions include somehow impaired glucose metabolism, high blood pressure, alterations in lipid metabolism and abdominal obesity [3].

Abdominal obesity is directly proportional to increase of waist circumference, being the metabolically more active adipose tissue depot, since the adipocytes of abdominal fat increase plasma levels of tumour necrosis factor  $\alpha$  (TNF $\alpha$ ) and release a number of other products such as non-esterified fatty acids (NEFA) or cytokines such as adiponectin, resistin, plasminogen activator inhibitor 1 (PAI-1) leading to a pro-inflammatory state. TNF $\alpha$  has shown not only to cause the production of inflammatory cytokines but also to activate cell signalling by interaction with a TNF $\alpha$  receptor that may lead to insulin resistance. High blood NEFA levels overload muscle and liver with lipids and this ends up in insulin resistance. Besides, increased levels of PAI-1 enhance a pro-thrombotic state that might be connected to the pro-inflammatory state. Obesity is usually accompanied of low adiponectin levels. High resistin levels have been associated with inflammation, endothelial dysfunction, thrombosis and other CVD risk factors. Chronic inflammation contributes to an increased risk of hypertension, atherosclerosis and diabetes [4].

Impaired glucose metabolism or insulin resistance is present in the majority of people suffering from metabolic syndrome either in the shape of impaired glucose tolerance (IGT), impaired fasting glucose (IFG) or even type 2 diabetes. Long-lasting insulin resistance often leads to glucose intolerance that might develop in diabetic hyperglycaemia, constituting one of the major risks of CVD. However, presence of metabolic syndrome in insulin resistant people is more strongly correlated with CVD risk than type 2 diabetic patients [5].

Alterations in lipid metabolism in the shape of dyslipidemia (DLP) usually manifested by high blood levels of triglycerides and low blood levels of high density lipoprotein (HDL) cholesterol, which have shown to be atherogenic lipid alterations [6].

Increased blood pressure, although being multi-factorial in origin, is intimately associated with obesity, for instance, the atherogenic state that enhances the stiffness of arteries contributes to a raise in blood pressure.

Although relationship among DM, HTA and DLP is known since the 20s, it was Gerald Reaven who suggested in 1988 that these factors tended to occur in one same individual either simultaneously or sequentially in the shape of a syndrome to which he named X syndrome or Reaven's syndrome.

Nowadays, there are many health associations interested in studying the metabolic syndrome such as (US) National Cholesterol Education Program (NCEP) - Adult Treatment Panel III (ATP III), American Heart Association (AHA), World Health Organization (WHO), International Diabetes Federation (IDF) or (US) National Institute of Health (NIH). Among these, it is the Adult Treatment Panel III the one giving the criteria differing most from all the others, identifying the following six conditions leading to the metabolic syndrome: abdominal obesity, atherogenic dyslipidemia, increased blood pressure, insulin resistance (may be accompanied with glucose intolerance), pro-inflammatory state, pro-thrombotic state [3].

The definition of the metabolic syndrome is closely related to the diagnostic criteria proposed by each one of these organizations.

### 1.1. Diagnostic

Diagnostic clinical criteria are similar according to the organizations described above; however they show important differences specially when detecting the main cause of the syndrome. The three most recent are described below, criteria are listed in order of importance or priority in the development of the metabolic syndrome [3].

#### *Diagnostic according to NCEP-ATP III*

Metabolic syndrome is diagnosed when 3 of the following 5 are present [7]:

<b>Risk factor</b>	<b>Defining level</b>
Abdominal obesity, given as elevated waist circumference:	
Men	$\geq 102$ cm
Women	$\geq 88$ cm
Hypertriglyceridemia	$\geq 1.7$ mmol/l
Low HDL cholesterol:	
Men	$< 1.03$ mmol/l

Women	< 1.3 mmol/l
Blood pressure	systolic blood pressure $\geq$ 130 mmHg and/or diastolic blood pressure $\geq$ 85 mmHg and/or pharmacological treatment
Elevated fasting glucose	$\geq$ 5.6 mmol/l and/or pharmacological treatment

*Diagnostic according to IDF:*

Metabolic syndrome is diagnosed when waist circumference appears elevated and 3 of the others are present [8]:

<b>Risk factor</b>	<b>Defining level</b>
Abdominal obesity, given as elevated waist circumference:	
non-Hispanic white men	$\geq$ 94 cm
Mexican-American men	$\geq$ 90 cm
Women	$\geq$ 80 cm
Hypertriglyceridemia	$\geq$ 1.7 mmol/l
Low HDL cholesterol:	
Men	< 1.03 mmol/l
Women	< 1.3 mmol/l
Blood pressure	systolic blood pressure $\geq$ 130 mmHg and/or diastolic blood pressure $\geq$ 85 mmHg and/or pharmacological treatment
Elevated fasting glucose	$\geq$ 5.6 mmol/l and/or pharmacological treatment

*Diagnostic according to WHO:*

Metabolic syndrome is diagnosed when impaired glucose metabolism appears in the shape of one of the factors listed in block A. and 2 of the factors listed in block B. are present [9]:

**A. Insulin resistance identified****by 1 of the following:**

- type 2 DM
- impaired fasting glucose  $\geq 75^{\text{th}}$  percentile
- impaired glucose tolerance  $\geq 6.1$  mmol/l

**B. Plus any 2 of the following:**

- High blood pressure                      systolic blood pressure  $\geq 140$  mmHg and/or diastolic blood pressure  $\geq 90$  mmHg and/or pharmacological treatment
  - Hypertriglyceridemia                    $\geq 1.7$  mmol/l
  - Low HDL cholesterol
    - Men    $< 0.9$  mmol/l
    - Women                                       $< 1.0$  mmol/l
  - BMI    $> 30$  kg/m<sup>2</sup>
- and/or
- waist/hip ratio
- Men    $> 0.9$
  - Women                                       $> 0.85$
- Urinary albumin excretion rate    $\geq 20$   $\mu$ g/min
- or
- albumin/creatinine ratio                $\geq 30$  mg/g

**1.2. Epidemiology**

The metabolic syndrome is a rising pathology in the developed world, reaching around 24% of the over 20 years old population in the United States in 2007, which is a leading country in the prevalence of metabolic syndrome [10]. However, both European and Latin-American countries are currently experiencing an increase in the prevalence of metabolic syndrome slowly reaching US levels.

According to a study published in 2012 [11], prevalence of metabolic syndrome in Spain in population aged 35-74 was of 31% (29% in women and 32% in men). Among the men, most frequent conditions were glycaemia and hypertriglyceridemia, and among the women, abdominal obesity and low levels of HDL. Among the people diagnosed of metabolic syndrome, CDV risk was moderate and higher in men (8%) than women (5%) and higher than in general population.

Prevalence of metabolic syndrome increases with age and increasing body weight. In the developed world, population is ageing and the prevalence of obesity is increasing, justifying the increase in the prevalence of metabolic syndrome in these countries.

In countries such as Europe or US, there is not much gender difference in the prevalence, however in African-American or Mexican-American population prevalence is lower in men than women.

Genetic factors predisposing to metabolic syndrome are: hypertriglyceridemia, CKD and DM family background.

## **2. Disorders leading to metabolic syndrome: Organs and signalling pathways involved**

### **2.1. Arterial hypertension**

Hypertension (HT) or arterial hypertension (high blood pressure) means high blood pressure. Blood pressure is the force of blood pushing against the walls of arteries as it flows through them [12]. Blood pressure involves two measurements, systolic and diastolic, which depend on whether the heart muscle is contracting (systole) or relaxed (diastole) between beats. Normal blood pressure is within the range of 100-140 mmHg systolic (top reading) and 60-90 mmHg diastolic (bottom reading). Although there are several criteria, high blood pressure is most frequently said to be present if it is persistently at/or above 140 mmHg for systolic and 90 mmHg for diastolic.

Hypertension is classified as either primary (essential) hypertension or secondary hypertension; about 90–95% of the cases are primary hypertension which means high blood pressure with no obvious underlying medical cause. The remaining 5-10% (secondary hypertension) is caused by other conditions that affect the kidneys, arteries, heart or endocrine system [13].

Hypertension is a major risk factor for stroke, myocardial infarction, heart failure, aneurysms of the arteries), peripheral arterial disease and is a cause of chronic kidney disease.

### **Signalling pathways controlling blood pressure:**

Blood pressure is controlled by the renin-angiotensin-aldosterone system (RAAS), being a hormone system which involves several organs such as kidney (majorly), liver, lungs and brain [14]. The RAAS consists on a cascade of proteins and hormones that activate whenever blood pressure needs to be regulated; it is in charge of balancing body water by compensating hypovolemia, hyponatremia and hypotension (fig. 1).

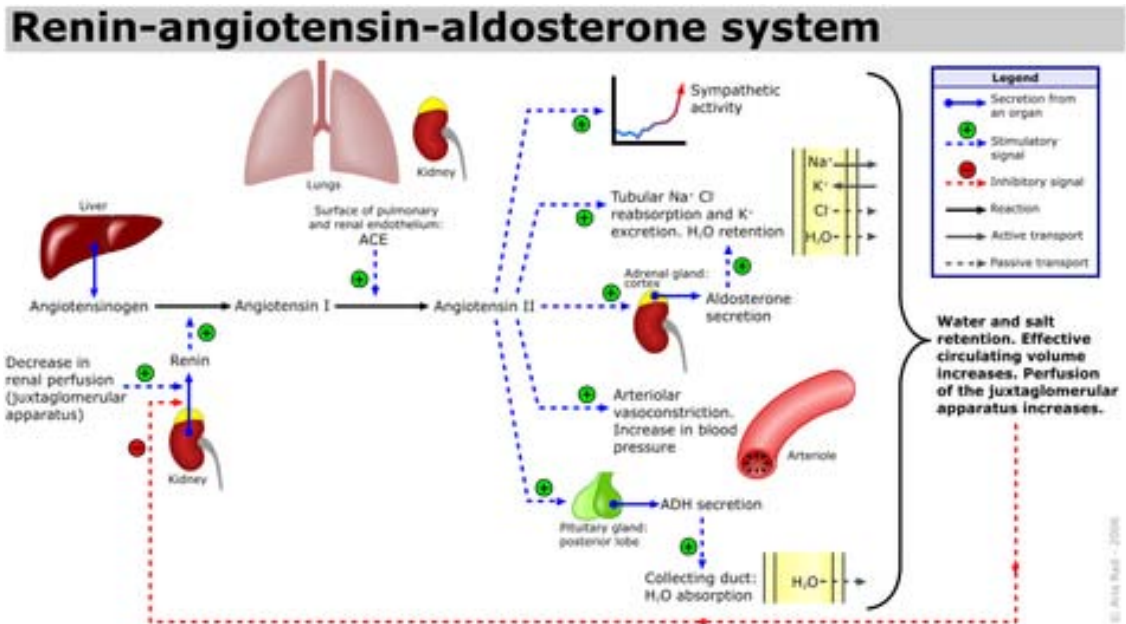


**Figure 1.** Renin-angiotensin-aldosterone system. Scheme extracted from [www.wikipedia.org](http://www.wikipedia.org)

Renin is an enzyme secreted into blood by specialized cells that surround the arterioles at the entrance to the glomeruli of the kidneys called juxtaglomerular cells (the renal capillary networks that are the filtration units of the kidney, see block below). The renin-secreting cells, which compose the juxtaglomerular apparatus, are sensitive to changes in blood flow and blood pressure. The primary stimulus for increased renin secretion is decreased blood flow to the kidneys or decreased renal perfusion in the juxtaglomerular apparatus, which may be caused by loss of sodium and water. When renin secretion is activated, it cleaves angiotensinogen to its active form angiotensin I.

Angiotensinogen is produced and released to circulation in liver. It is an  $\alpha$ -2-globulin that belongs to the serpin family. It is expressed in a constitutive manner, however it will remain inactive until it is cleaved by renin. Stimuli such as corticosteroids, androgens, estrogens thyroid hormones and angiotensin II may increase angiotensinogen blood levels [15].

Angiotensin I is the product of the cleavage of angiotensinogen by the action of renin, it is a well inactive being the precursor of angiotensin II. Angiotensin I is converted to angiotensin II by the action of the angiotensin-converting enzyme (ACE), a kinase that removes 2 C-terminal residues from angiotensin I. ACE is secreted majorly by kidney but there is also lung secretion of it, and it constitutes an important target in the pharmacological control of blood pressure since the use of ACE inhibitor drugs decrease the production of angiotensin II.

Angiotensin II is the major bioactive product of the RAAS acting as an endocrine, autocrine/paracrine and intracrine hormone. It has its action enhancing sympathetic activity. It acts directly on renal tubules (see block below) activating reabsorption of  $\text{Na}^+$ ,  $\text{Cl}^-$ , excretion of  $\text{K}^+$  and retention of  $\text{H}_2\text{O}$ . It also acts on the kidney adrenal cortex activating the secretion of



aldosterone that enhances action already described on renal tubules. Angiotensin II has also a direct vasoconstrictor function on arterioles. Finally, it stimulates posterior hypophysis to secrete antidiuretic hormone (ADH) that enhances the reabsorption of H<sub>2</sub>O by the collecting duct. All these actions end up on the aim of increasing the circulating volume through the retention of water and salt and increasing the perfusion of the juxtaglomerular apparatus in order to raise blood pressure. When blood pressure is balanced again, the raise in water and salt retention in circulating volume and in yuxtaglomerular apparatus perfusion acts as negative feed-back signal that inhibits the secretion of renin.

It has been demonstrated that angiotensin II has also a role in oxidative stress generation since it activates endothelial and endocardial NADPH oxidase which the major producer of reactive oxygen species (ROS) by catalyzing the production of superoxide (O<sub>2</sub> •-), which is reduced to hydrogen peroxide (H<sub>2</sub>O<sub>2</sub>) by superoxide dismutases. Although it is not a free radical, hydrogen peroxide is an oxidant capable of initiating lipid peroxidation chain [16].

Angiotensin II has also shown to up-regulate NF-κB and inflammatory genes related to this pathway [16].

#### **Organs involved in blood pressure control:**

Although many organs, such as liver, lungs, hypophysis or nervous system, have shown to have a role in blood pressure control, it is the kidney that is more intimately related to this function.

#### The kidney

Besides blood pressure control already described, the major function of the kidneys is to remove waste products and excess fluid from the body, process taking place through the urine. The production of urine involves highly complex steps of excretion and re-absorption. This process is necessary to maintain a stable balance of body chemicals. Kidneys also perform the critical regulation of plasma osmolarity and acid content. The kidneys also produce hormones that affect the function of other organs such as production of blood cells (such as erythropoietin), blood pressure regulation (such as renin) and control calcium metabolism (through vitamin D) [17].

Kidney disease damages kidneys, preventing them from properly cleaning blood. This damage can cause wastes to accumulate in the body and lead to other health problems, including heart disease, anaemia, and bone disease. Chronic kidney disease can eventually cause kidney failure if it is not treated. Disorders such as high blood pressure, type 2 diabetes or dyslipidemia are likely to damage the kidneys. The final stage of chronic kidney disease is kidney failure, or end-stage renal disease. People with kidney failure need dialysis, in which blood is cleaned through a machine or a new, healthy kidney through transplantation in order to be able o keep up with kidney physiological functions [18].

*Anatomy of the kidney:*

The human kidney is fairly typical of that of mammals. Differential features of the mammalian kidney, compared to other vertebrates, include the presence of the renal pelvis and renal pyramids, and of a clearly distinguishable cortex and medulla. The latter feature is due to the presence of elongated loops of Henle. It is only in mammals that the kidney takes on its classical bean-like shape.

The kidneys are two organs located evenly on the back of the abdomen, under the rib cage, one on each side of the spine. They are wrapped by a fibrous envelope constituting a strong film that covers the entire organ. In most mammals each kidney is irrigated by one single renal artery connecting directly from the abdominal aorta so that it receives the arterial blood at the maximum pressure. Once filtered at the glomerulus, blood leaves the kidney through the renal vein. From a structural point of view, two areas may be differed in kidney: one granular looking located in the sub-capsular region, named cortex, and another internal known as medulla (fig. 2). The medulla consists of several pyramids, whose vertices (renal papillae) end into the renal calyces. In the medulla an outer zone (adjacent to the cortex) and an inner zone may be distinguished. The calyces converge in the renal pelvis, which proceeds to the ureter.

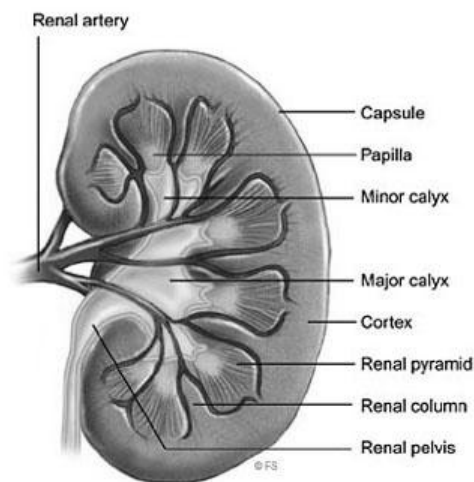


**Figure 2.**  
Scheme of the anatomy of the kidney.  
Obtained from [www.scioly.org](http://www.scioly.org).

**-The nephron:**

Structurally the kidney is composed of about one million nephrons (functional units of the kidney) enveloped in conjunctive tissue. Each nephron consists sequentially of the renal corpuscle or filter unit, the juxtaglomerular apparatus, the proximal tubule, the loop of Henle and distal tubule (fig. 3). Based on the location of the renal corpuscle, there are three types of nephrons: surface cortical, middle cortical and juxtamedullar, with several structural differences.

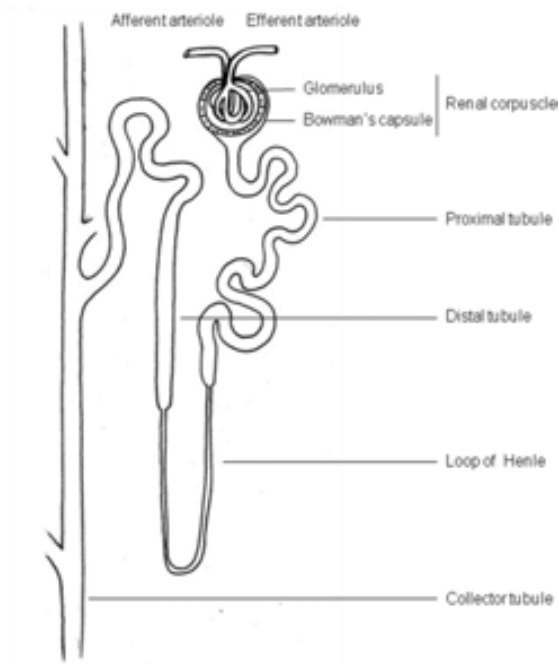


**Figure 3.**  
Scheme of the structure of the nephron.  
Modified from [www.aic.cuhk.edu.hk](http://www.aic.cuhk.edu.hk)

**-The renal corpuscle:**

The renal corpuscle comprises a tangle of capillaries, located between the afferent and efferent arterioles and called glomerulus, as well as a hollow cavity called Bowman's capsule, bulging in the glomerulus and the light falls into the tubules. Glomerular filtration surface is formed by three elements: the vascular endothelium, the glomerular basal membrane and the Bowman's capsule epithelium (fig. 4). Renal vascular endothelium is fenestrated, and the limit of pore size is 70 nm. Glomerular basal membrane is formed by fusion of the endothelial and epithelial cells, and is basically composed of collagen IV. Epithelial cells remain "floating" in the Bowman's capsule and attached to the glomerular basal membrane by cytoplasmic extensions called podocytes. The glomerular core is called mesangium and consists, besides the extracellular matrix, of two different cells types: mesangial cells, with contractile capacity, and macrophages with phagocytic capacity.

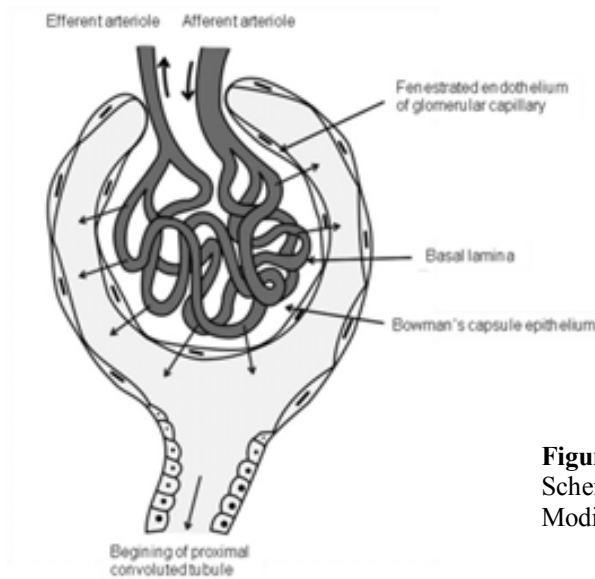


**Figure 4.**  
Scheme of the structure of the renal corpuscle.  
Modified from [www.wikipedia.org](http://www.wikipedia.org)

#### -Renal tubules:

The renal tubules are divided into several segments, which according to their functional classification are: the proximal tubule, the loop of Henle or intermediate tubule, distal tubule and collecting ducts.

In general, cells of each segment have similar morphological and functional characteristics with two exceptions: the proximal tubule (which has three cell types: S1, S2 and S3 with some functional differences) and collecting ducts (composed of principal and intercalary cells, serving very different).

#### -The juxtaglomerular apparatus:

Located in the vascular region of the glomerulus, is primarily responsible for regulating blood pressure by controlling the renin-angiotensin-aldosterone system (RAAS), through the secretion of renin.

#### *Kidney Functions:*

The kidneys are essential in the urinary system and also serve homeostatic functions such as the regulation of electrolytes, maintenance of acid–base balance, and regulation of blood pressure (via maintaining salt and water balance). They serve the body as a natural filter of the blood, and remove wastes which are diverted to the urinary bladder. In producing urine, the kidneys excrete wastes such as urea and ammonium, and they are also responsible for the reabsorption of water, glucose, and amino acids. They also produce hormones including calcitriol (active shape of vitamin D), erythropoietin, and the renin enzyme.

The kidney has three main groups of functions; in order to develop these functions properly a rigorous control of the renal circulation is necessary.

- Endocrine function: synthesis and secretion of hormones such as erythropoietin, renin, and vitamin D.
- Excretory function: excretion of waste products derived from metabolism, which are basically water and nitrogen wastes such as creatinine, urea and uric acid.
- Homeostatic function: regulating the hydroelectric and acid-base balance.

Among the hormones secreted by the kidneys, there is erythropoietin, calcitriol and the enzyme renin. Erythropoietin is released in response to hypoxia (low levels of oxygen at tissue level) in the renal circulation. It stimulates erythropoiesis (production of red blood cells) in the bone marrow. Calcitriol, the activated form of vitamin D, promotes intestinal absorption of calcium and the renal reabsorption of phosphate. Renin is part of the renin-angiotensin-aldosterone system; this enzyme is involved in the regulation of aldosterone levels.

Regulatory and excretory functions are performed by the formation and elimination of urine, formed by a suitable composition depending on the needs of the organism.

The renal system is primarily responsible for removing from circulation all catabolic final products and waste substances, which majorly come from the cellular metabolism. The excretory system of mammals is formed mainly by the kidney and its associated ducts. The urinary tract consists of the kidneys, producing and secreting urine, the ureters which are the tubes that carry urine to the bladder and urethra which will transport urine to the outside of the body (fig. 5).

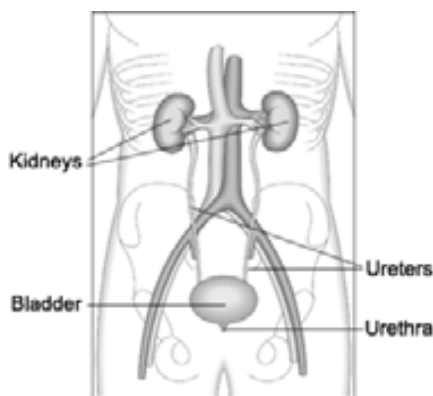


**Figure 5.**

Location of the kidneys and urinary system in the human body. Obtained from [www. faculty.college-prep.org](http://www.faculty.college-prep.org)

The kidney participates in whole-body homeostasis, regulating acid-base balance, electrolyte concentrations, extracellular fluid volume, and regulation of blood pressure. The kidney accomplishes these homeostatic functions both independently and in concert with other organs, particularly those of the endocrine system. Various endocrine hormones coordinate these endocrine functions; these include renin, angiotensin II, aldosterone, antidiuretic hormone (ADH), and atrial natriuretic peptide, among others.

Many of the kidney's functions are accomplished by relatively simple mechanisms of filtration, reabsorption, and secretion, which take place in the nephron.

## 2.2. Impaired glucose metabolism

Glucose is a rapid source of energy for the body. Regular glucose blood level is of 5 mM. Its metabolism comprises two different activities: anabolism, or synthesis of glucose, and catabolism, or degradation of glucose. Between meals or in short fasting periods, blood glucose decreases and glucagon hormone secreted by pancreas alpha-cells activates glucose synthesis or gluconeogenesis in liver in order to raise glucose blood levels. In postprandial state, pancreas beta-cells secrete insulin in order to lower down circulating glucose levels by activating glucose storage and catabolism. There are two different pathways in glucose catabolism: aerobic and anaerobic. Anaerobic pathway takes place in the cytoplasm and is moderately efficient in terms of energy; aerobic pathway takes place in mitochondria through the use of oxygen and ends up in a great release of energy [19].

Glucose enters the cells via facilitated diffusion with the help of specialized membrane transporters called GLUTs. These GLUTs are expressed by insulin sensitive cells and they remain in the cytoplasm until insulin reaches its own cell receptor and activates the insulin signalling pathway, which, among other functions, activates the translocation of the GLUTs to the cell membrane in order to enhance the entrance of glucose. There are different types of GLUTs depending on the tissue and they are classified with numbers. GLUTs and insulin receptors are only present in cells from tissues that use glucose as the main source of energy.

Once glucose has entered the cell, first step of its catabolism takes place in the cytoplasm in an anaerobic manner and second step takes place inside the mitochondria needing oxygen. Energy obtained from glucose is converted to heat or stored in the shape of adenosine triphosphate (ATP), the breaking up of these molecule also supplies energy. Glucose entering hepatocytes is stored in the shape of glycogen.

Any cell type containing mitochondria is suitable for using glucose as a source of energy such as adipose tissue or brain and liver which are obligate glucose consumers, in the absence of glucose the brain is able to use ketone bodies as a source of energy. However the main glucose user tissue is muscle, which is able to use glucose as a source of energy both in the presence and the absence of oxygen, when myocytes may convert glucose to energy through fermentation, a process that gives lactic acid as a waste product [19].

Impaired glucose metabolism usually involves insulin resistance (IR) that is a condition in which normal amounts of insulin are inadequate to produce normal insulin response from fat, muscle or liver cells. As a result, higher levels of insulin are needed in order to achieve normal insulin effects; the raise of insulin is called compensatory hyperinsulinemia. Resistance to insulin occurs both with the body's endogenous insulin and with exogenously administered insulin (insulin injections). There are many risk factors associated to insulin resistance; among

the most important causes are genetic factors, obesity, over dosing of carbohydrates and inactivity.

Insulin resistance in adipocytes results in elevated hydrolysis of stored triglycerides and increased mobilization of these lipids which will elevate circulating free fatty acids. Insulin resistance in muscle reduces glucose uptake, permitting the glucose to remain circulating. Insulin resistance in hepatocytes results in impaired glycogen synthesis and failure to suppress glucose production [20]. All of these results contribute to elevate circulating glucose concentration.

People manifesting long-lasting insulin resistance, often develop glucose intolerance or impaired glucose tolerance (IGT), where circulating glucose is raised beyond normal range but not as high to suffer from diabetes [6].

High glucose and insulin levels have been tightly associated to metabolic syndrome and are the origin of type 2 diabetes.

#### **Signalling pathways controlling glucose metabolism:**

Insulin signalling pathway is the main way in which glucose metabolism is controlled. Alterations along this pathway may lead to insulin resistance.

In a postprandial situation, insulin is secreted and reaches glucose-user cells and binds to the extracellular portion of the alpha subunits of the dimeric insulin receptor placed in the membrane of these cells. This causes a conformational change in the insulin receptor that activates the kinase domain residing on the intracellular portion of the beta subunits. The activated kinase domain autophosphorylates tyrosine residues at the C-end of the receptor and phosphorylates tyrosine residues in the IRS-1 protein attached to beta subunit, activating it.

p-IRS1 binds to phosphoinositol 3 kinase (PI3K) in order to activate it. Activated PI3K converts the membrane lipid PIP<sub>2</sub> into PIP<sub>3</sub> by catalyzing the reaction  $PIP_2 + ATP \rightarrow PIP_3$ . PIP<sub>3</sub> generates a binding site both in protein kinase B (PKB or Akt) and pyruvate dehydrogenase kinase, isozyme 1 (PDK1) so that they can be phosphorylated and activated. Active Akt phosphorylates glycogen synthase kinase (GSK) and in order to inactivate it, so that GK can no longer phosphorylate glycogen syntase (GS). When GS is not phosphorylated, it enhances the production of glycogen.

Akt together with PDK 1 facilitate the vesicle fusion and translocation from cytoplasm to membrane of GLUTs facilitated diffusion glucose transporters. Akt reaches the cell nucleus and also stimulates the expression of GLUTs at transcriptional level through NFκB pathway (fig. 6).

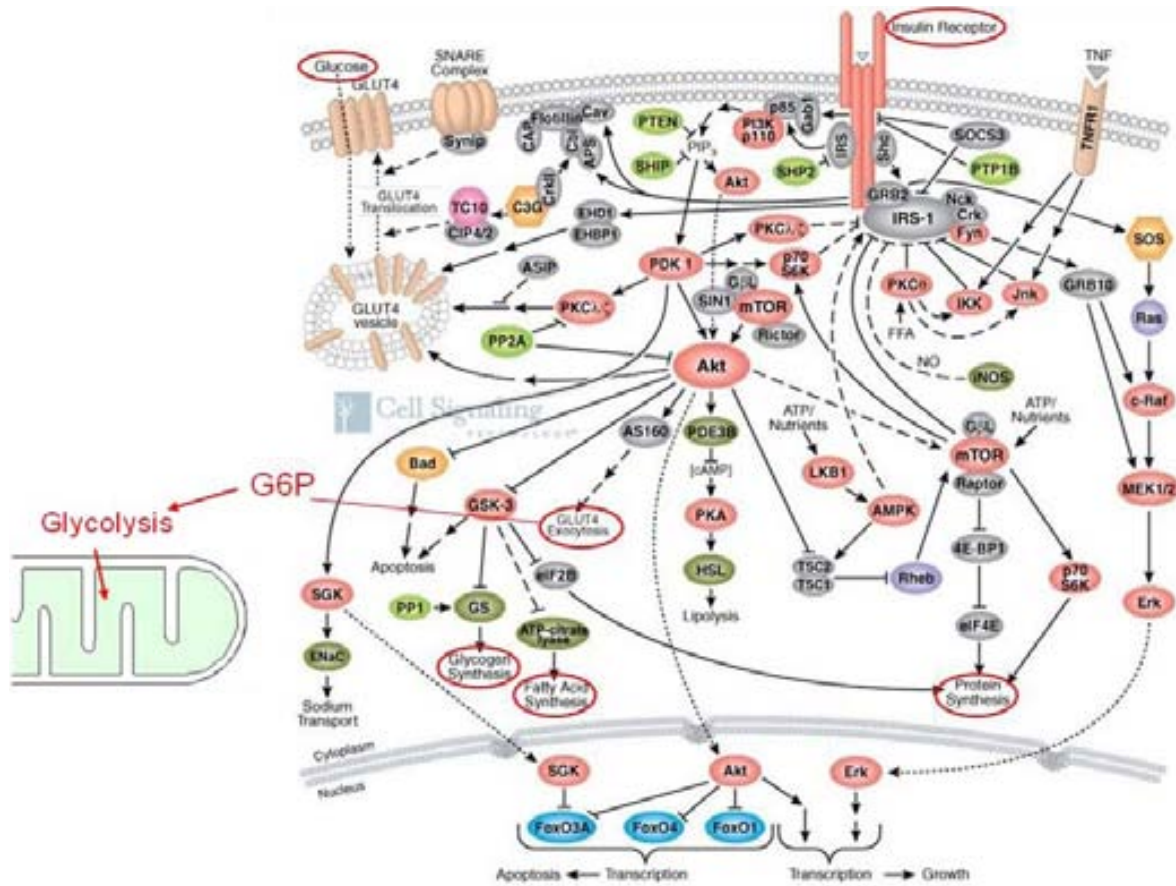


**Figure 6.** Schematic view of the insulin signalling pathway. Scheme modified from [www.cellsignal.com](http://www.cellsignal.com).

GLUTs are insulin regulated glucose transporters present in insulin sensitive tissues such as muscle, adipose tissue or liver. There are different GLUTs found in different tissues:

GLUT1: brain and erythrocytes.

GLUT2: liver, kidney, intestine and beta-cells.

GLUT3: is similar to GLUT1

GLUT4: muscle and adipose tissue. This isoform is insulin-dependent.

In the absence of insulin, GLUT4 is retained in the inside of the myocytes or adipocytes in the vesicles' bilayers. The presence of insulin induces translocation of GLUT4 from the intracellular storage to the cell membrane.

Once glucose enters the cell, it is immediately phosphorylated by glucokinase in liver and hexokinase in other tissues and converted to glucose-6-phosphate (G6P), so that it is no longer able to go back through GLUT and outside of the cell. G6P is ready for glycolysis (fig.6).

The final main aim of insulin is to lower down glucose circulating levels, and it exerts its action by enhancing glycogen synthesis, fatty acid synthesis and protein synthesis through the use of glucose as a substrate.

Alterations in the insulin signalling pathway classified as insulin resistance usually take place in the first steps already described of the process.



**Organs involved in glucose metabolism:**

As already mentioned, muscle is the major glucose consumer in the body and therefore, where peripheral insulin resistance is first shown.

The muscle

Since muscles are so crucial to animals, they are very sophisticated. They are efficient at turning fuel into motion; they are long-lasting, self-healing and able to grow stronger with practice [21]. Muscles are primarily responsible for maintenance of posture and changes in it, locomotion of the body itself, as well as movement of internal organs, such as the heart contraction and movement of food through the digestive system through peristalsis. Myocytes contain protein filaments that glide past one another, producing a contraction that changes the shape and size of the cell. Muscles work to produce force and cause motion.

Muscular tissues are classified as skeletal, cardiac, or smooth muscles. Cardiac and smooth muscle contraction occurs automatically and involuntarily and is necessary for survival. Voluntary contraction of the skeletal muscles serves to move the body and can be finely controlled. These three types of muscle have significant differences. However, all three create contraction through the use the movement of actin against myosin. In skeletal muscle, contraction is stimulated by electrical impulses transmitted by the nerves (motoneurons). Cardiac and smooth muscle contractions are stimulated by internal pacemaker cells which contract regularly, and propagate contractions to other muscle cells they are in contact with. All skeletal muscle and many smooth muscle contractions are facilitated by the neurotransmitter acetylcholine.

Muscular activity is responsible for much of the body's energy consumption. All muscle cells produce ATP, molecules which are used to power the movement of the myosin heads. Muscles conserve energy in the shape of creatine phosphate which is generated from ATP and can regenerate ATP when needed through creatine kinase. Muscles also keep storage of glucose in the form of glycogen. Glycogen can be rapidly converted to glucose when energy is required for sustained, powerful contractions. Within the voluntary skeletal muscles, the glucose molecule can be metabolized anaerobically in a process called glycolysis which produces two ATP and two lactic acid molecules in the process (in aerobic conditions, lactate is not formed, instead pyruvate is formed and transmitted through the citric acid cycle). Since glucose is muscle's main source of energy, in the case of peripheral resistance to insulin, this tissue is one of the firsts were to detect this alteration. Muscle cells also contain lipid vacuoles, which are used to obtain energy during aerobic exercise. The aerobic energy systems take longer to produce the ATP and reach peak efficiency, and require many more biochemical steps, but produce significantly more ATP than anaerobic glycolysis.

### 2.3. Obesity

Obesity is a condition in which a high proportion of body adipose tissue is present that puts the individual at greater risk of developing hypertension, insulin resistance, dyslipidemia and other health problems associated to CVD risk.

Most frequently, the origin of this excess of adipose tissue and therefore, weight, is a result of the imbalance between calories intake and calories consumed. Excess of calories is stored as lipid energy depots. In less frequent cases, obesity comes from a genetic and/or hormonal origin.

Central adiposity (or abdominal adipose tissue) is a key feature of the metabolic syndrome, reflecting the fact that the syndrome's prevalence is driven by the strong relationship between waist circumference and increasing adiposity. However, despite the importance of obesity, patients that are regular weight may also be insulin-resistant and have the syndrome.

#### **Signalling pathways involved in obesity development**

Obesity has demonstrated to be a multifactor dependent disorder and has demonstrated to be a risk factor for hypertension, atherosclerosis and diabetes. However, it is not body mass increase itself that is predictive of these disorders, but the altered lipid metabolism as well as adipose tissue secreted hormones and inflammatory mediators secreted in this pathological state that have shown to have an important role in the development of metabolic syndrome [22].

Adipose tissue has not only demonstrated to be actively pro-inflammatory in obese individuals, but also in non obese individuals with impaired lipid metabolism in adipose tissue [23]. Thus adipose tissue has demonstrated not only to be an energy reservoir but also to be an active endocrine organ secretor of humoral factors called adipokines (cell-to-cell signalling proteins) and pro-inflammatory cytokines such as leptin, adiponectin, resistin, TNF $\alpha$ , IL-6 or PAI-1 [24]. Leptin is a hormone that has demonstrated to have an important role in energy balance through the regulation of appetite and metabolism, being one of the most important adipose derived hormones. The effects of this hormone were able to be studied thanks to spontaneously leptin mutated mice ob/ob that show a mutation in the leptin gene Ob (Lep) and db/db that show a mutation in the leptin receptor gene. These animals showed massive obesity that reverted with leptin injections only in the case of ob/ob. This hormone is mainly secreted by white adipose tissue, being an indicator of adiposity or amount of lipid in the body. It is released to the circulation as a satiety signal when stomach is full. It has been demonstrated that many obese subjects are leptin resistant [25].

Adiponectin is a high concentration circulating adipokine, the levels of which are inversely correlated to obesity, insulin resistance and type 2 diabetes. Visceral adipose tissue has demonstrated to be a negative indicator of adiponectin. Moreover, most of the conditions defining the metabolic syndrome have demonstrated negative associations with adiponectin.

This adipokine has shown to increase fatty acid oxidation and inhibit glucose production by the liver and this is thought to be the main mechanism in which low expression levels of adiponectin are related to insulin resistance, possibly being an insulin enhancer. Pro-inflammatory cytokines also seem to reduce adiponectin levels [26].

Resistin levels have been suggested to link obesity, insulin resistance and diabetes. It increases the production of LDL in human liver cells and also degrades LDL liver receptors. Thus, the liver is less able to clear LDL cholesterol from the body accelerating the accumulation of LDL in arteries, increasing the risk of atherosclerosis and CVD [27]. It also participates in the inflammatory response and increases transcriptional events, leading to an increased expression of pro-inflammatory cytokines interleukin-1 (IL-1), interleukin-6 (IL-6), interleukin-12 (IL-12), and tumour necrosis factor- $\alpha$  (TNF- $\alpha$ ) in an NF- $\kappa$ B-mediated fashion. There seems to be a strong correlation between resistin and obesity, serum resistin levels will increase with increased adiposity, specifically, abdominal obesity.

TNF $\alpha$  (tumor necrosis factor-alpha) is a central regulator of inflammation, and TNF- $\alpha$  antagonists may be effective in treating inflammatory disorders in which TNF- $\alpha$  plays an important pathogenetic role. TNF $\alpha$  is mainly secreted by macrophages and is involved in a wide variety of biological processes including cell proliferation, differentiation, apoptosis, lipid metabolism, and coagulation.

IL-6 (interleukin 6) acts as both a pro-inflammatory and anti-inflammatory cytokine. It is secreted by T cells and macrophages to stimulate immune response. IL-6's role as an anti-inflammatory cytokine is mediated through its inhibitory effects on TNF- $\alpha$  and IL-1, and activation of IL-1ra and IL-10. IL-6 produced by adipocytes is thought to be a reason why obese subjects have higher endogenous levels of C-reactive protein. IL-6 supports the growth of B cells and is antagonistic to regulatory T cells [28].

PAI-1 or plasminogen inhibitor 1 is the major physiologic inhibitor of plasminogen activator in plasma. A variety of clinical situations that are associated with increased risk of ischemic cardiovascular events show high levels of PAI-1. Increased PAI-1 levels have been associated to high blood pressure, demonstrated to be a pro-atherosclerotic and pro-thrombotic factor, and may also enhance the progression of CVD [29].

### **Organs involved in obesity development**

Disorders in the physiology of adipose tissue are a major event in the development of pathologies associated to metabolic syndrome. The knowledge of this tissue from a multidisciplinary perspective would help to learn about features underlying the development of obesity.

The adipose tissue

Adipose tissue plays a fundamental role in maintaining energy balance and as hibernating gland for some mammals [30]. However, it is not only a passive tissue that stores energy. Recent studies have published that it is an endocrine tissue that secretes important molecules linked to processes such as immune response, lipid metabolism and vascular function among others.

The importance of adipose tissue in the disorders leading to metabolic syndrome are due to the large number of receptors (adrenergic and insulin) expressed in this tissue in front of different stimuli explaining the adjustment of sensitivity to various metabolic circumstances. It is known that lipids intake through the diet are stored as fat and that an excess in adipose tissue leads to the increase of serum free fatty acids, stimulating the production of triglyceride-rich lipoproteins and insulin resistance. Furthermore, through the study of mice fed on a high fat diet, it was found that adipose tissues together with the liver were affected in weight by intake and accumulation of lipids.

Adipose tissue or lipid depot is loose connective tissue built from cells called adipocytes, composed of roughly 80% lipid. Uncomplexed lipids are found in liver and muscles. Its main role is to store energy in the form of lipids, although it also cushions and insulates the body. Body fat is a hormonally active tissue, recognized as a major endocrine organ, as it produces hormones such as leptine, resistin, and the TNF $\alpha$  cytokine. Moreover, adipose tissue can affect other organ systems of the body and may lead to disease. Obesity or being overweight in humans and most animals does not depend on body weight but on the amount of body adipose tissue. There are two types of adipose tissue: white adipose tissue (WAT) and brown adipose tissue (BAT).

*Types of adipose tissue:*

Adipose tissue is composed of adipocytes, which contain lipid droplets, and several other cell types, including fibroblasts, macrophages, and endothelial cells. Adipose tissue contains many small blood vessels.

In humans, adipose tissue is found in specific locations, which are referred to as adipose depots: subcutaneous fat (under the skin), visceral fat (around internal organs), in bone marrow (yellow bone marrow) and in breast tissue. The subcutaneous layer of adipose tissue provides insulation from heat and cold. Around organs, it provides protective filling. However, the main function of this tissue is to act as lipid storage that can be burned to face the energy needs of the body. Adipose depots in different parts of the body have different biochemical profiles.

Visceral or abdominal fat is located inside the abdominal cavity, packed in between organs (stomach, liver, intestines, kidneys, etc.). Visceral fat is different than subcutaneous fat underneath the skin, and intramuscular fat interspersed in skeletal muscles. Fat in the lower body, as in thighs and buttocks, is subcutaneous, whereas fat in the abdomen is mostly visceral.

Visceral fat is composed of several adipose depots including mesenteric, epididymal white adipose tissue, and perirenal depots. This latter is thought to be the most metabolically active adipose tissue. An excess of visceral fat is known as central obesity, in which the abdomen protrudes excessively. There is a strong correlation between central obesity and cardiovascular disease. Excess of visceral fat is also linked to type 2 diabetes, insulin resistance inflammatory diseases, and other obesity-related diseases.

Sexual dimorphism in the adiposity distribution in humans induces differences in the predisposition to lipid-related metabolic alterations. Female sex hormones cause lipids to be stored in the buttocks, thighs, and hips in women, while to male sex hormones cause lipids to be stored in the abdomen in men. Abdominal adipose tissue is metabolically more active than all others; lipolysis is found enhanced over lipogenesis mobilizing large quantities of fatty acids towards the liver to be processed. This overloading of lipids in liver leads to hyperinsulinism (alterations in insulin induced catabolism), hyperglycemia (due to a raise in the gluconeogenic activity) and hypertriglyceridemia [31]. Femoro-gluteus adipose tissue is subcutaneous fat defining the typical female pattern of body fat distribution, metabolically less active, more prompt to lipid storage and therefore poses less of a health risk compared to visceral fat. Most of the remaining non-visceral fat is found just below the skin in a region called the hypodermis. Subcutaneous fat is not related to many of the classic obesity-related pathologies, such as heart disease, cancer, and stroke, and there are even some evidences that suggest that it might be protective. Like all other fat organs, subcutaneous fat is an active part of the endocrine system, secreting the hormones leptin and resistin.

In mice, there are eight major adipose depots, four of which are located in the abdominal cavity: The paired gonadal depots are attached to the uterus and ovaries in females and the epididymies and testes in males; the paired retroperitoneal depots are found along the dorsal wall of the abdomen, surrounding the kidney, and, when massive, extend into the pelvis. The mesenteric depot forms a net that supports the intestines, and the omental depot, which has its origin near the stomach and spleen, and, when massive, extends into the ventral abdomen. Both the mesenteric and omental depots incorporate much lymphoid tissue as lymph nodes and milky spots, respectively. The two superficial depots are the paired inguinal depots, which are found anterior to the upper segment of the hind limbs (underneath the skin) and the subscapular depots, paired medial mixtures of brown adipose tissue adjacent to regions of white adipose tissue, which are found under the skin between the dorsal crests of the scapulae. The layer of brown adipose tissue in this depot is often surrounded by a cover of white adipose tissue; sometimes these two types of fat (brown and white) are hard to distinguish. The inguinal depots enclose the inguinal group of lymph nodes. Minor depots include the pericardial, which surrounds the heart, and the paired popliteal depots, between the major muscles behind the knees, each containing one large lymph node. Of all the depots in the mouse, the gonadal depots

are the largest and the most easily dissected, comprising about 30% of dissectible fat and being the more metabolically active adipose tissue.

*Adipose tissue Functions:*

Adipose tissue may be divided into two different types. White adipose tissue is that the functions of which are related to energy storage, storing and releasing fatty acids as triglycerides by simultaneous processes of lipolysis and lipogenesis. In the case of mice, it can be subdivided in gonadal and inguinal adipose tissue, depending on their location. Adipocyte nucleus is located in the periphery as well as organelles displaced by large lipid vacuoles filling the cytoplasm. The brown adipose tissue in contrast, stands at the back of the chest, between the scapulas and plays a fundamental role in regulating body temperature, producing heat. Unlike white adipose tissue, adipocyte size is smaller, the cells are multilocular and have a brownish colour, due to their high number of mitochondria and cytochromes involved in the generation of heat (fig. 7) [32].

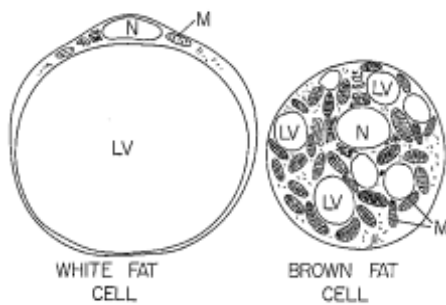


**Figure 7.**  
Scheme of white and brown adipocytes.  
Obtained from [www.sportsci.org](http://www.sportsci.org)

**Brown adipose tissue:**

A specialised form of adipose tissue in humans, most rodents and small mammals, and mainly hibernating animals, is brown adipose tissue. It is located mainly around the neck and large blood vessels of the thorax. This specialized tissue can generate heat by uncoupling the respiratory chain of oxidative phosphorylation within mitochondria. The process of uncoupling means that the energy from this process is released as heat rather than being used to generate ATP when protons transit down the electrochemical gradient across the inner mitochondrial membrane. This thermogenic process may be vital in neonates exposed to the cold, which then require this thermogenesis to keep warm, as they are unable to shiver, or take other actions to keep themselves warm.

**White adipose tissue:**

Free fatty acids are released from lipoproteins by Lipoprotein lipase (LPL) and enter the adipocyte, where it is reassembled into triglycerides by esterifying them onto glycerol.

In humans, lipolysis is controlled through the balanced control of lipolytic B-adrenergic receptors and  $\alpha_2A$ -adrenergic receptor-mediated anti-lipolysis.

Fat is not laid down when there are surplus calories available and stored passively until it is needed; rather, it is constantly being stored in and released from the adipose tissue.

Storage in the adipose tissue is catalyzed by insulin, the activity of which is stimulated by high blood glucose.

Adipocytes have an important physiological role in maintaining triglyceride and free fatty acid levels, as well as determining insulin resistance. Abdominal fat has a different metabolic profile, being more likely to induce insulin resistance. This explains partially why central obesity is related to impaired glucose tolerance and is an independent risk factor for cardiovascular disease (even in the absence of diabetes mellitus and hypertension).

Adipose tissue is the greatest peripheral source of aromatase in both males and females, contributing to the production of estradiol (E<sub>2</sub>). Other adipose tissue derived hormones include adiponectin, resistin, PAI-1 and leptin. Adipose tissues also secrete a type of cytokines (cell-to-cell signalling proteins) called adipokines (adipocytokines) and including TNF $\alpha$ , IL-6, which play a role in obesity-associated complications.

Genetically obese mice lack leptin protein. Leptin is produced in the white adipose tissue and signals to the hypothalamus. When leptin levels decrease, the body understands this as loss of energy, and hunger increases. Mice lacking this protein lack satiety signal and may eat until they are four times their normal size [33].

Leptin, however, plays a different role in diet-induced obesity in rodents and humans. Since adipocytes produce leptin, the levels of this are elevated in the obese individuals. However, hunger remains, and, when leptin levels drop due to weight loss, hunger increases. The drop of leptin is better viewed as a starvation signal than the rise of leptin as a satiety signal. Elevated leptin in obesity is known as leptin resistance. The changes that occur in the hypothalamus as a result of leptin resistance in obesity are currently the focus of obesity research.

#### **2.4. Dyslipidemia**

Dyslipidemia is a term that involves abnormal amount of circulating lipids due to a disorder of lipoprotein metabolism, including lipoprotein overproduction or deficiency. This may manifest as a circulating increase in total cholesterol, low density lipoproteins (LDL) and triglycerides, and a decrease in high density lipoproteins (HDL). This disorder is one of the major risk factors for CVD and DM.

Diabetic dyslipidemia is attributed to an increase in the fatty acid flux to liver due to insulin resistance, and is characterized by high circulating triglyceride levels, low HDL and high LDL. This pathologic state is directly linked to hepatic steatosis or fatty liver [34].

As previously described, subjects on a standard weight may also be at risk of insulin resistance and subsequent metabolic syndrome, since it is not just lipid accumulation in adipose tissue what enhances this risk, but the distribution of the lipid excess around the body, especially in liver. An excess of body fat accumulated in the liver is a stronger endangering factor for metabolic syndrome than an excess of adipose tissue [35].

### **Signalling pathways involved in dyslipidemia**

Hepatic steatosis has been recognized as a condition of the metabolic syndrome as well as a key feature in the development of dyslipidemia, coming from an imbalance between the influx and synthesis of fatty acids and the use of fatty acids for beta-oxidation or secretion as very low density lipoprotein (VLDL) triglycerides. Thus, there is a relationship between increased liver lipids and overproduction of large VLDL particles. Moreover, in subjects with high lipid levels insulin is not able to regulate VLDL synthesis increasing concentrations of circulating VLDL. This leads to alterations in the metabolism of other lipoproteins that interact with VLDL, resulting in decreased HDL cholesterol and increased formation of LDL [36].

Dietary lipids are supplied in the form of triacylglycerols which must be hydrolyzed to fatty acids and monoacylglycerols before they can be absorbed. Lipid digestion is nearly completed in the small intestine, the free fatty acids and monoglycerides are absorbed by the enterocytes of the intestinal wall. Short chain fatty acids enter directly into the portal vein system and are transported to the liver, while long chain fatty acids are re-esterified in the enterocyte and enter the circulation via the lymphatic route as chylomicrons.

Fatty acids are transported in the blood as complexes with albumin or as esterified lipids in lipoproteins. Lipoproteins comprise a core of triacylglycerols and fatty acid esters of cholesterol, and an outer layer of a single layer of phospholipids interspersed with unesterified cholesterol.

Chylomicrons are lipoproteins from dietary lipids that are packaged by enterocytes. They enter the blood stream through the lymph vessels. Lipoprotein lipase located on the interior walls of the capillary blood vessels hydrolyses the triacylglycerols, releasing fatty acids. These enter the adipose tissue where they will be stored and the muscles where they serve as fuel.

Very-low density lipoproteins (VLDL) are large triacylglycerol-rich lipoproteins produced in the liver from endogenous lipid. VLDL are the major carriers of triacylglycerols which are also processed by lipoprotein lipase and supply fatty acids to adipose tissue and muscles. Low-density lipoproteins (LDL) are the end products of VLDL metabolism. LDL delivers cholesterol to the liver and HDL may transfer cholesterol to other lipoproteins. There is evidence that HDL actively protects vessel walls (fig. 8).



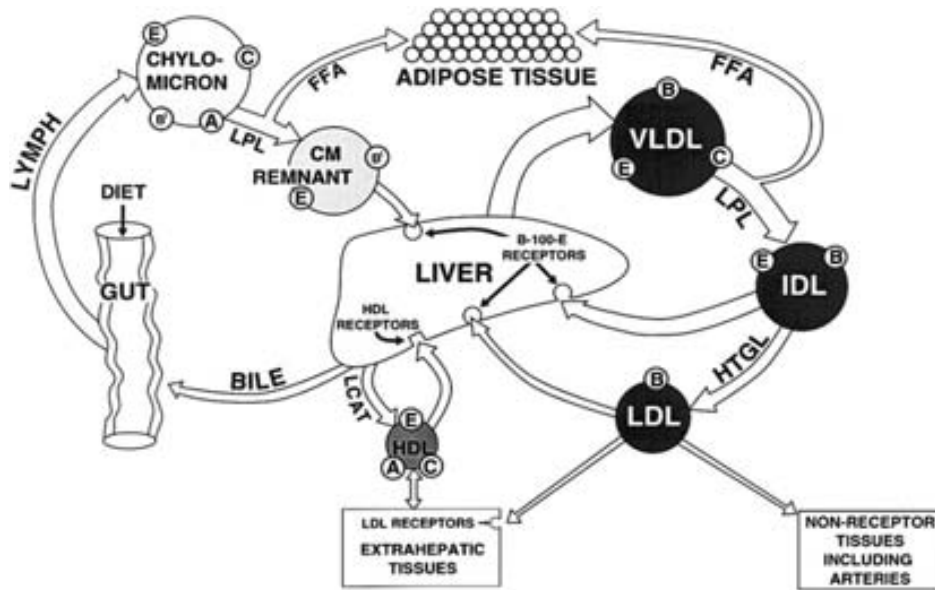


**Figure 8.** Metabolism of lipoproteins and lipids. Obtained from <http://jn.nutrition.org>.

### Organs involved in dyslipidemia

The liver plays a key role in lipid metabolism by being responsible for fatty acid synthesis and lipid circulating levels through the synthesis of lipoproteins. If lipid droplets pathologically accumulate inside hepatocytes, hepatic steatosis develops and this is the onset for further lipid metabolism dysfunctions [37].

#### The liver

The liver is thought to be responsible for up to 500 separate functions, usually in combination with other systems and organs. The main functions of the liver include to process nutrients from food, produce bile, and remove toxic products from the body and synthesise proteins. Inflammation of the liver, or hepatitis, and other liver damages may interfere with these important functions and can lead to poor health. Currently, there is no artificial organ or device capable of emulating all the functions of the liver. Some functions can be emulated by liver dialysis, an experimental treatment for liver failure.

The liver is a reddish brown organ with four lobes of unequal size and shape. It is both the largest internal organ and gland in the human body. It is found in all vertebrates, and is typically the largest visceral organ. Its shape varies considerably in different species, and is largely determined by the shape and arrangement of the surrounding organs. Nevertheless, in most species, including mammals, it is divided into right and left lobes. The internal structure of the liver is quite similar in all vertebrates.

It is located in the right upper quadrant of the abdominal cavity, resting just below the diaphragm. The liver lies to the right of the stomach and overlies the gallbladder. It is connected to two large blood vessels: the hepatic artery and the portal vein. The hepatic artery carries

blood from the aorta, whereas the portal vein carries blood containing digested nutrients from the entire gastrointestinal tract and also from the spleen and pancreas. These blood vessels subdivide into capillaries, which then lead to a lobule. Each lobule is made up of millions of hepatic cells which are the basic metabolic cells.

The liver gets a dual blood supply from the hepatic portal vein and hepatic arteries. The hepatic portal vein carries venous blood drained from the spleen, gastrointestinal tract, and its associated organs. The hepatic arteries supply arterial blood to the liver, accounting for the remainder of its blood flow. Oxygen is provided from both sources; approximately half of the liver's oxygen demand is met by the hepatic portal vein, and half is met by the hepatic arteries. Blood flows through the liver sinusoids and empties into the central vein of each lobule. The central veins converge into hepatic veins, which leave the liver.

### *Anatomy of the liver:*

#### Surface anatomy:

The liver is divided into four lobes based on surface features. The falciform ligament is visible on the front of the liver. This divides the liver into a left anatomical lobe, and a right anatomical lobe. When turning the liver over, to look at it from the back side (the visceral surface), there are two additional lobes between the right and left. These are the caudate lobe (superior) and the quadrate lobe (inferior). Each of the lobes is made up of lobules; a vein goes from the centre, which then joins to the hepatic vein to carry blood out from the liver.

On the surface of the lobules, there are ducts, veins and arteries that carry fluids to and from them.

#### Functional anatomy:

The central area where the common bile duct, hepatic portal vein, and hepatic artery proper enter is the hilum. The duct, vein, and artery divide into left and right branches, and the portions of the liver supplied by these branches constitute the functional left and right lobes.

The caudate lobe is a separate structure which receives blood flow from both the right- and left-sided vascular branches (fig. 9).

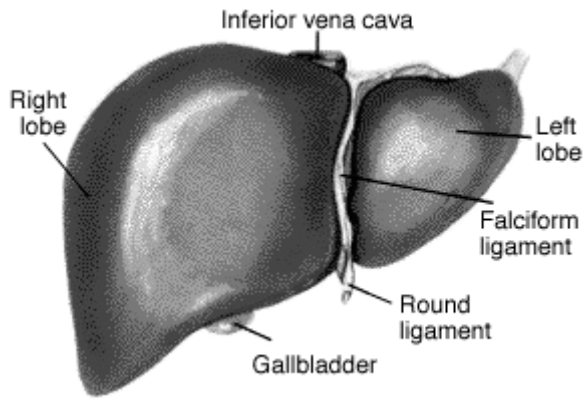


**Figure 9.** Scheme of the anatomy of the liver and biliary system. Obtained from [www.hanumanmedical.com](http://www.hanumanmedical.com).

#### *Liver Functions:*

The various functions of the liver are carried out by the hepatocytes. The liver is a metabolically active organ responsible for many vital functions. The primary functions of the liver are bile production and excretion, excretion of bilirubin, cholesterol, hormones, and drugs, metabolism of fats, proteins, and carbohydrates, enzyme activation, storage of glycogen, vitamins, and minerals, synthesis of plasma proteins, such as albumin, and clotting factors and blood detoxification and purification.

Anabolic functions include amino acid synthesis, gluconeogenesis (synthesis of glucose from amino acids, lactate or glycerol), glycogenolysis (catabolism of glycogen into glucose), glycogenesis (formation of glycogen from glucose, muscle tissues can also do this), protein synthesis, cholesterol synthesis, lipogenesis (production of triglycerides), synthesis of most of the lipoproteins, production of coagulation factors I (fibrinogen), II (prothrombin), V, VII, IX, X and XI, as well as protein C, protein S and antithrombin. Production and excretion of bile required for emulsifying fats. One fraction of the bile drains directly into the duodenum, and another is stored in the gallbladder. Production of insulin-like growth factor 1 (IGF-1), a polypeptide protein hormone that plays an important role in childhood growth and continues to have anabolic effects in adults. Thrombopoietin production, a glycoprotein hormone that regulates the production of platelets by the bone marrow.

Catabolic functions include breakdown of insulin and other hormones, glucuronidation of bilirubin, facilitating its excretion into bile, breaking down or modification of toxic substances (such as methylation), and conversion of ammonia to urea (urea cycle).

Other functions of the liver are storage of many substances, including glucose (in the shape of glycogen), vitamin A, vitamin D, vitamin B6, iron, and copper. Including immunological effects since it contains many immunologically active cells. Synthesis of angiotensinogen, a hormone that is responsible for raising the blood pressure when activated by renin, an enzyme that is released when the kidney senses low blood pressure.

### **3. Consequences**

#### **3.1. Cardiovascular disease**

Cardiovascular disease is a general term that describes pathology of the heart or blood vessels. Blood flow to the heart, brain, or rest of the body could be reduced due to thrombosis (blood clots) or atherosclerosis (stiffness and narrowing of the arteries due to accumulation of fatty acids).

There are four types of CVD: coronary heart disease, stroke, peripheral arterial disease and aortic disease, which are linked among them. Coronary heart disease and stroke may be caused by the same problem and that is atherosclerosis. This happens when arteries become narrowed by a build-up of atheroma within their walls. Arteries may become so narrow that they cannot deliver enough oxygen-rich blood to the heart. A piece of the atheroma that breaks may cause a blood clot to form. If the blood clot blocks the coronary artery and cuts off the supply of oxygen-rich blood to myocardium, this latter may become permanently damaged (heart attack). If a blood clot blocks an artery that carries blood to the brain, it can cut off the blood supply to part of the brain and this is when a stroke happens.

CVD is the leading cause of death and hospitalization Spanish population. Currently there are more than 125,000 deaths in Spain and more than 5 million hospital stays due to cardiovascular diseases (CVD) per year.

Many subjects showing no symptoms are at severe risk of suffering a cardiovascular event for presenting two or more risk factors. In over 60% of cases these risk factors are not controlled. Over one third of patients with acute myocardial infarction die before reaching the hospital without receiving effective treatment. Thus, the incidence and coronary mortality has not improved appreciably in the last decade in Spain [38].

#### **3.2. Diabetes mellitus**

Diabetes mellitus type 2 is a metabolic disorder that is characterized by high blood glucose in the context of insulin resistance and relative insulin deficiency. The classic symptoms are polyuria, polydipsia and polyphagia. Type 2 diabetes represents about 90% of cases of diabetes with the other 10% due primarily to diabetes mellitus type 1 and gestational diabetes. Obesity is thought to be the primary cause of type 2, rates of diabetes have increased markedly over the last 50 years in parallel with obesity. Long-term complications from high blood glucose can include heart attacks, strokes, diabetic retinopathy where eyesight is affected, kidney failure which may require dialysis, and poor circulation of limbs leading to amputations. The acute complication ketoacidosis is uncommon unlike in type 1 diabetes, non-ketonic hyperglycemia however may occur.

Type 2 diabetes is more common in old age, when existing a family background with diabetes and in people with obesity. Over 75 years of age the prevalence is 41.3% in women and 37.4% in males, while the overall average prevalence in Spain in people over 18 years is 13.8%.

More recent data allow us to state that the incidence has suffered a progressive increase in recent years in all regions of Spain, in some cases reaching figures of around 20 per 100,000 individuals [39].

### **3.3. Chronic Kidney disease**

Chronic kidney disease (CKD) has kidney failure as the most serious outcome. Kidney failure or renal failure describes a medical condition in which the kidneys' structure and functions are affected so that they fail to adequately filter waste products from the blood. There are two forms of kidney failure, acute (acute kidney injury, AKI) and chronic (chronic kidney disease, CKD); a number of other diseases or health problems may cause either form of renal failure to occur.

Renal failure is described as a decrease in glomerular filtration rate (GFR) and albuminuria. Biochemically, renal failure is typically detected by an elevated serum creatinine level. Problems frequently encountered in kidney unpaired function include abnormal fluid levels in the body, altered acid levels, abnormal levels of potassium, calcium, phosphate, and (in the longer term) anaemia as well as delayed healing in broken bones. Depending on the cause, haematuria (blood loss in the urine) and proteinuria (protein loss in the urine) may occur. Long-term kidney problems have significant repercussions on other diseases, such as cardiovascular disease. When the GFR has fallen very low or if the renal dysfunction leads to severe symptoms renal replacement therapy as dialysis or kidney transplantation, is indicated [40].

The type of renal failure is determined by the trend in the serum creatinine. Other factors which may help differentiate acute kidney injury from chronic kidney disease include anaemia and the kidney size on ultrasound. Chronic kidney disease generally leads to anaemia and small kidney size [41].

#### **a) Acute kidney injury:**

Acute kidney injury (AKI), is a rapidly progressive loss of renal function, generally characterized by oliguria (decreased urine production, quantified as less than 400 ml per day in adults); and fluid and electrolyte imbalance. AKI can result from a variety of causes, generally classified as prerenal, intrinsic, and postrenal. An underlying cause must be identified and treated to arrest the progress, and dialysis may be necessary as a substitutive therapy while finding the fundamental causes.

#### **b) Chronic kidney disease:**

CKD can develop slowly and, initially, show few symptoms. CKD can be the long term consequence of irreversible acute disease or part of a disease progression.

CKD is measured in five stages, which are calculated using a patient's GFR. A normal GFR varies according to many factors, including sex, age, body size and ethnicity [42]. Renal professionals consider the GFR to be the best overall index of kidney function, it is calculated using several equations based on serum creatinine level. Stage 1, renal function mildly diminished, with few symptoms. Stages 2 and 3 need increasing levels of supportive care from their medical providers to slow and treat the renal dysfunction. Stages 4 and 5 usually require preparation of the patient towards active treatment in order to survive. Stage 5, CKD is considered a severe illness and requires some form of renal replacement therapy (dialysis) or kidney transplant if possible [43].

Data from experimental and clinical studies suggest that proteinuria plays an important role in the pathogenesis of the progression of CKD since most proteins are usually too big to pass through the kidneys, but they do pass through when the glomeruli are damaged. This does not cause symptoms until extensive kidney damage has occurred [44]. According to these findings, the disease classification to indicate prognosis of every stage is based on albuminuria levels.

CKD has numerous causes; however, in developed countries the most common is diabetes mellitus (DM), accounting for 40% of new CKD patients [44]. The second most common causes are long-lasting, uncontrolled, hypertension (HT), obesity and CVD. In all these cases, it is thought that diabetic glomerulosclerosis and hypertensive nephrosclerosis might be the pathological entities. The former is defined by a worsening of hypertension, an increase in albuminuria and a progressive decrease in the GFR. The latter does not show characteristic markers but an increase in albuminuria [44].

Diabetic glomerulosclerosis is caused by angiopathy of capillaries in the kidney glomeruli. It is sometimes associated with by nephrotic syndrome and diffuse glomerulosclerosis. These features may appear in patients with chronic diabetes (usually less than 15 years after onset). The disease is progressive and may cause death 3-5 years after the initial lesions, and is more frequent in men [44]. Given that diabetic nephropathy is the most common cause of chronic kidney failure and end-stage kidney disease, it is known that the risk is increased if blood-glucose levels are poorly controlled. Furthermore, once nephropathy develops, the greatest rate of progression is seen in patients with poor control of their blood pressure. Also subjects with high cholesterol level in their blood have increased risk than others.

Diabetic nephropathy continues to get gradually worse. Complications of chronic kidney failure are more likely to occur earlier, and progress more rapidly, when it is caused by diabetes than other causes. Even after initiation of dialysis or after transplantation, diabetic patients tend to progress worse than non-diabetic.

Increasing prevalence of kidney failure and early stages of CKD, and the high costs and poor outcomes of treatment constitute a worldwide public health concern. Ageing of the population

and the increase in obesity prevalence mean that this disease will probably be an issue for both developed and developing countries in the future.

## II. THE KIDNEY ANDROGEN-REGULATED PROTEIN

### 1. KAP and the androgens

Androgens are cholesterol-derived steroid hormones that activate gene transcription after binding to specific intracellular receptors. Although androgens are primarily involved in the establishment of male reproductive function, they act as well on other non-reproductive tissues such as bone, nerve, fat, skeletal muscle, liver and kidney [45-48].

Murine kidney represents a singular model where to study androgen action at transcriptional level since, opposite to what happens in accessory sex organs of the reproductive system, androgens cause hypertrophy without DNA synthesis, [49]. The renal pathophysiology group, interested in studying the mechanisms controlling the regulation of androgen-mediated gene expression in kidney and its pathophysiological significance, identified new target genes for androgen action in this tissue. Using differential expression techniques [50, 51], besides kidney androgen-regulated protein (KAP) and Acyl-CoA synthetase medium-chain family member 3 (AcsM3 or SA), several genes co-ordinately expressed by androgens were identified in the kidney [52] encoding for proteins involved in oxidative metabolism [53], lipid metabolism and hypertension [54] in the transport of organic anions and cations [55] or inflammation [52] (fig. 10).

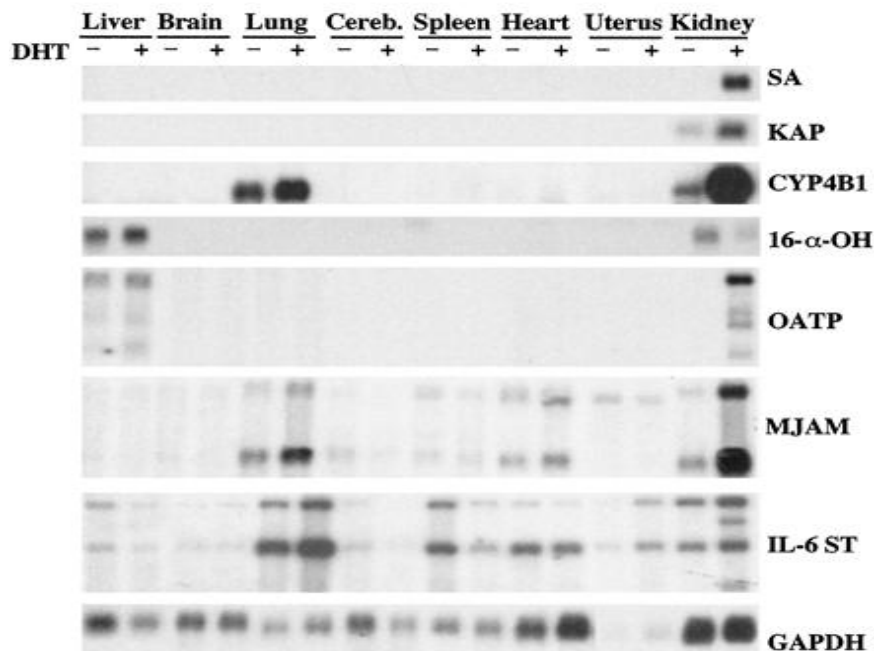


**Figure 10.** Identification of androgen-regulated genes in kidney by PAP-PCR and cDNA RDA.

Our group's results together with those of others indicated that genes coding for enzymes involved in metabolism, elimination and detoxification of xenobiotics and drugs from the body,



as well as organic anions and cations transporters are co-ordinately expressed and subjected to strong androgenic control in the kidney. It is known that the induction of these genes occurs after cellular stress induced by xenobiotics or other harmful intermediates, such as, reactive oxygen species (ROS), and that the adaptive response is related to the protection against environmental aggressions [56].

From a clinical point of view, has been described that there are gender differences in the impact of acute renal damage caused by nephrotoxic drugs or ischemia-reperfusion, as well as progression to chronic kidney damage caused by hypertension, nephron mass loss or age. Although classically attributed a protective role for estrogens, studies in humans and experimental animals have shown a certain role of male hormones in these differences [57]. Thus, it has been reported that androgens may increase blood pressure and compromise renal function [58, 59] by different mechanisms including increased sodium reabsorption in proximal tubule [59], and control over vasoconstrictor systems as endothelin [60], nitric oxide [61], angiotensin II [62], or by activation of the arachidonic acid metabolism by CYP450 [63]. Androgens have also been associated with stimulation of apoptotic pathways and renal cell loss [64] and, involved in this process, with progression to chronic renal disease characterized by glomerulosclerosis and renal interstitial fibrosis [65].

The study of androgen-regulated genes in the kidney, and especially those displaying a restricted expression to kidney, was thought to be relevant in understanding the pathophysiological mechanisms of renal disease and its consequences in the cardiovascular system. Among the identified genes we concentrated preferentially in the study of KAP gene expressed co-ordinately with the other genes of our panel, which encodes a protein of unknown function.

## **2. The KAP gene**

The KAP gene is a single copy gene located at position 63.7 cM of mouse chromosome 6, comprising 3,807 nucleotides distributed in 4 exons and 3 introns and generates a cDNA consisting of 607 nucleotides [66, 67] (fig. 11).

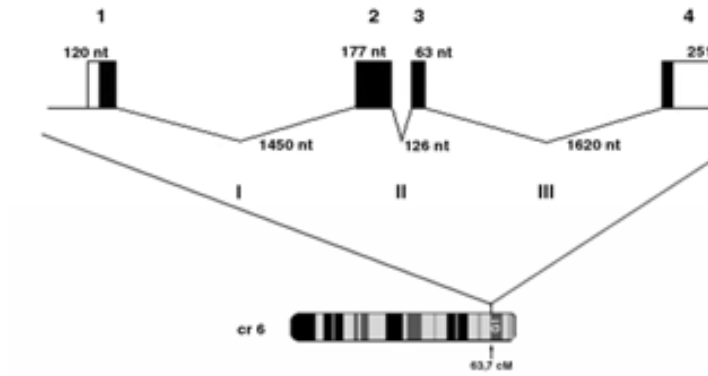


**Figure 11.** Gene structure and chromosomal location of the KAP gene.

KAP is one of the most abundant and specific gene expressed in renal proximal tubule epithelial cells [68-70]. It is regulated by the action of steroid and thyroid hormones along the different segments of the proximal tubule (fig. 12).

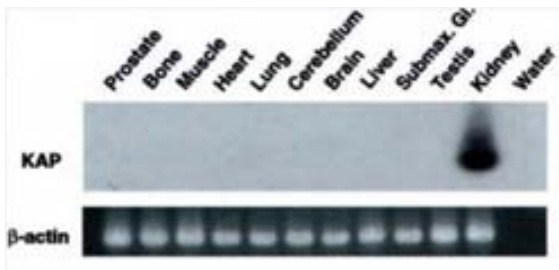
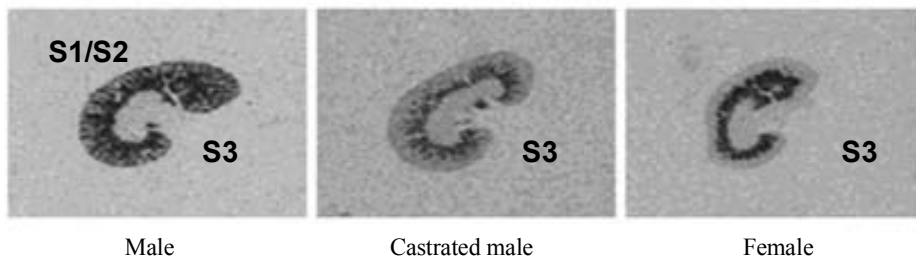


**Figure 12.** **Left:** Tissue distribution of KAP mRNA: RT-PCR of total RNA extracted from various tissues of male mice, using specific KAP mRNA murine primers. **Down:** In situ hybridization using probes of single stranded RNA KAP. In the presence of androgens (intact males), KAP is expressed in S1, S2 and S3 segments of the proximal tubule.



In vivo studies have shown that while S3 cells (pars recta) express the gene in the presence of thyroid hormone (TH/T<sub>3</sub>) and are responsive to sex hormones [71], segments S1/S2 (pars convoluta) express the gene in only presence of androgens and functional androgen-receptor [72]. Thus, it is observed that castrated males and females express the gene in S3, while intact males or androgen-induced females, and so do in S1/S2 [68]. The cortical expression due to androgens can be modulated by TH. In TH genetically-deficient adult males or in animals in which hypothyroidism was drug-induced, cortical expression of androgen-dependent KAP is diminished, or even inhibited, and can be completely reconstituted by the exogenous administration of TH [73]. Studies have shown that complete androgen-dependent expression of KAP in the renal cortex is conditioned upon the presence of thyroid hormone [74] (fig. 13).

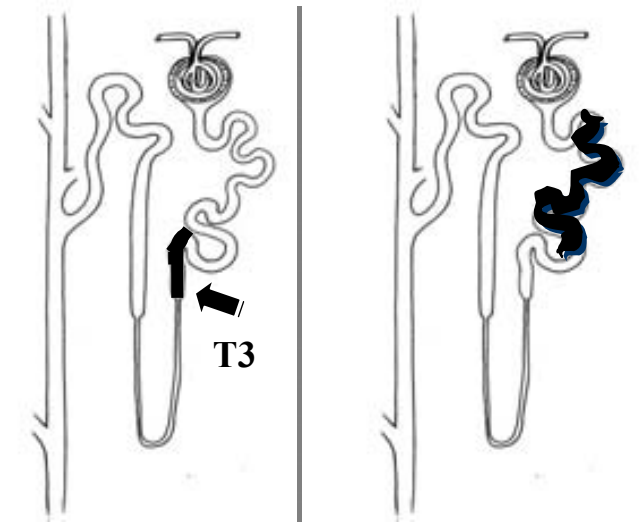


**Figure 13.**

In the absence of androgens, castrated males and females, KAP is expressed in S3 segment (**left**). In the presence of androgens, male, it is expressed as well in S1 and S2 segments (**right**).

KAP expression in S3 cells depends on T3 and is enhanced by the presence of androgens and estrogens.

Ovariectomy does not decrease expression of KAP in S3, but hypothyroidism does.

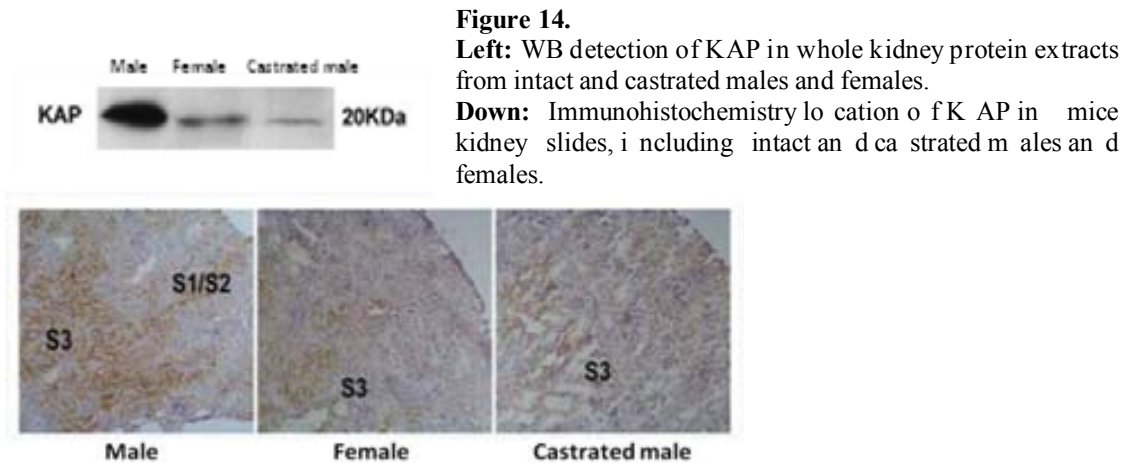
KAP expression in S1 and S2 requires the presence of androgens and their functional receptor. Lack of T3 decreases expression at any age.

### 3. The KAP protein

Although KAP's mRNA is very abundant in kidney, and its expression is strict and controlled in the proximal tubule, there is a lack of information on the function of the protein. In order to identify and characterise this protein, antibodies were generated against two synthetic peptides and it was determined that KAP (protein) is expressed in the same cell types and under the same hormonal stimuli than its mRNA.

Using raw kidney extracts a protein of 20 kDa apparent molecular weight was detected by SDS-PAGE gels [67]. Although the expected MW was of 13 kDa (121 amino acids long) computational analysis of the amino acid sequence defines a negatively charged hydrophilic region that could explain the observed delay in the SDS-PAGE [75].

This protein showed, like the corresponding mRNA, to be more abundant in intact males than females or castrated males, an identical distribution (in the S3 segment in kidneys of females and whole PT in males) and a cytoplasmic pattern compatible with the localization of KAP in the endoplasmic reticulum (ER), further it was found that the protein is not only located in the ER, but also in Golgi apparatus and nucleus, being secreted to the extracellular medium [75] (fig. 14).



#### 4. Interaction of KAP with other proteins

The lack of homology between the sequence (both nucleotidic and peptidic) as well as functional domains of KAP with other known proteins prevents to predict or suggest a possible function for this protein. Identification of proteins capable of interacting with KAP was carried out by using yeast two-hybrid assays (2YH). Cyclophilin B (CypB) was found among the identified proteins and KAP-CypB interaction was subsequently confirmed by GST-pull down assays, co-IP and confocal microscopy [75]. CypB belongs to the family of cyclophilins, chaperones with peptidyl-prolyl cis-trans isomerase, first discovered as intracellular receptors of cyclosporin A (CsA) [76]. This immunosuppressant acts by inactivating the phosphatase calcineurin and thereby inhibiting NFAT pathway in T lymphocytes, but showed how serious renal toxicity undesirable effect. A large number of studies in the literature attributed CsA-mediated renal toxicity to hemodynamic changes produced by alterations in the balance between vasodilator and vasoconstrictor elements in the kidney [77], as well as direct effects on proximal tubule cells [78, 79]. Based on the interaction between KAP and CypB, we determined the effects of CsA on KAP in the kidney, showing a decrease of the protein, concomitantly with an increase of its mRNA, suggesting the implementation of a negative feedback system to recover the KAP protein levels after loss per share of CsA (fig. 15).

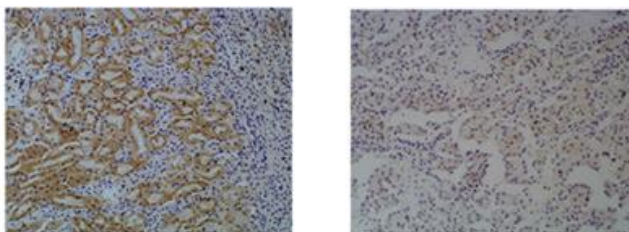


**Figure 15.**  
 Action of CsA on KAP detected by immunohistochemistry in kidney slides: CsA reduces KAP protein levels in mouse kidney as shown in this immunohistochemistry image with antiKAP specific antibodies.

The hypothesis that the KAP must be important for tubular function was reinforced when noting that the protein over-expression conferred increased resistance to CsA toxicity in a renal

proximal tubule isolated system [75]. Since cyclophilins have a broad tissue distribution, it is suggestive to think that the toxic effects that the immunosuppressive specifically exerts in renal tubule cells may be due to protein loss by this cell type, such as KAP (fig. 16).

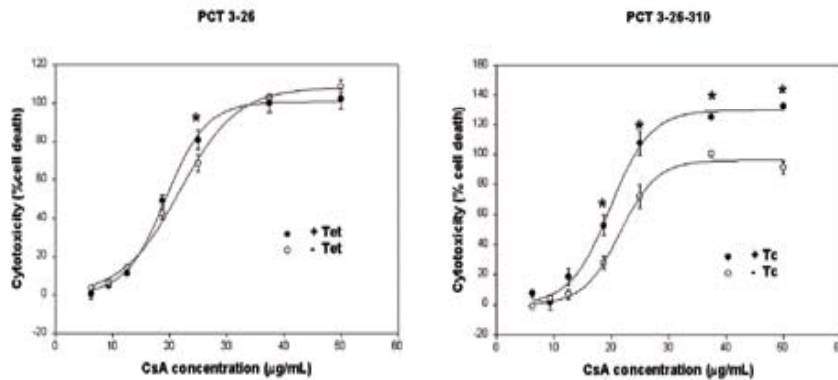


**Figure 16.** Action of KAP on CsA by LDH assays: KAP overexpression in a murine cellular model of proximal tubule cell decreases toxicity caused by CsA on a Tet-on system.

It has been discovered that the loss of KAP in the presence CsA is due to a slight increase in the secretion of the protein into the extracellular medium but mainly to the degradation that occurs in the presence of the immunosuppressant. Both effects occur preferentially when the protein is phosphorylated by CK2 in well identified residues and located in a PEST sequence present in KAP [80]. Specific inhibitors of calpain and caspases but not lysosomal proteases or proteasome prevented the degradation of protein by CsA, indicating the possible participation of calpain and caspase in the process. The effect of calpain on KAP has been demonstrated in vivo and in vitro and it has also been observed that this protease is activated by CsA in a proximal tubule cell system and also in animals with impaired renal function due to treatment with the immunosuppressant [81]. The loss of KAP by the action of CsA takes place by the activation of calpain and it is promoted by the CK2 mediated phosphorylation in well identified residuals of the protein:

- KAP is phosphorylated by casein kinase 2 in its phosphorylation residues corresponding to a PEST sequence.
- The phosphorylation of KAP promotes the degradation by CsA.
- CsA activates calpain protease both in kidney and in proximal tubule cultured cells.
- Calpain degrades KAP protein, preferably when the latter is phosphorylated by CK2.
- KAP co-localizes with CypB in the endoplasmic reticulum and the Golgi apparatus regardless of its phosphorylation status and is secreted to the extracellular medium. None of these facts, not the co-location or the interaction with CypB, are affected by mutations in the CK2 phosphorylation sites.

According to these observations, it has been suspected that KAP and CypB participate in the endoplasmic reticulum stress response and the metabolic system, as well as in the cell cycle

## INTRODUCTION

control and in proliferation/differentiation processes and kidney development, with probably very relevant functions for the proximal tubule cells and the kidney homeostasis control.

### III. THE KAP TRANSGENIC MICE

#### 1. Designing of the transgenic mouse

In order to determine the effects of KAP “in vivo”, Tg animals were generated in the laboratory by using the promoter of KAP itself: pKap2 construct, previously used for targeting genes to renal proximal tubule heterologously [82] (fig. 17).

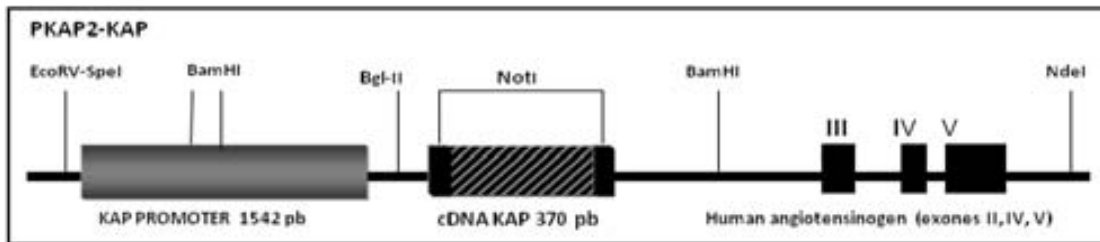


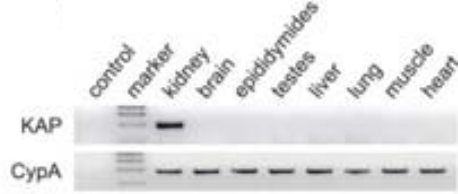
**Figure 17.** pKap2-KAP construct:

- KAP promoter to drive expression to renal proximal tubule epithelial cells.
- II-V exons and intronic regions of human angiotensinogen contain enhancer elements necessary for the expression of the transgene. It has been proven that human angiotensinogen gene is not expressed in Tg mice.
- Testosterone transgene regulation takes place in the same manner as the endogenous gene. It shows sensitivity to androgens as flutamide like the endogenous gene.
- The KAP cDNA is inserted into a NotI target generated in exon II of human angiotensinogen.

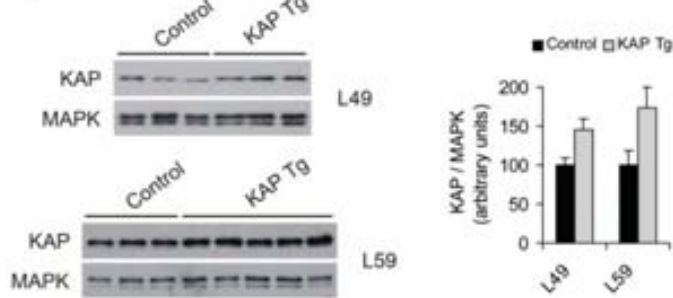
From nine original founder lines, two (L49 and L59) were finally selected for further studies. These were born at the expected Mendelian ratios, had normal growth curves and were fertile independently of their gender. Experimental procedures were performed in 4-6 months old males from both transgenic lines in order to characterize the transgenic mouse; the features detailed below are the same on both Tg lines [67].

#### 2. Regulation of the transgene

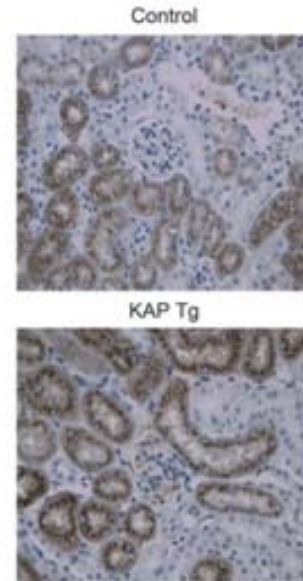
The transgene proved to be regulated in the same manner as the endogenous gene. The expression of KAP mRNA in Tg animals is limited to the kidney (quantitative RT-PCR), where it has been observed that the protein is increased about twice in Tg vs control littermates (WB), moreover the expression of the protein is limited to the proximal tubule of these animals (immunohistochemistry (IHC)) (fig. 18).

**Figure 18.** a. RT-PCR tissue distribution of KAP mRNA

b. WB detected expression of KAP



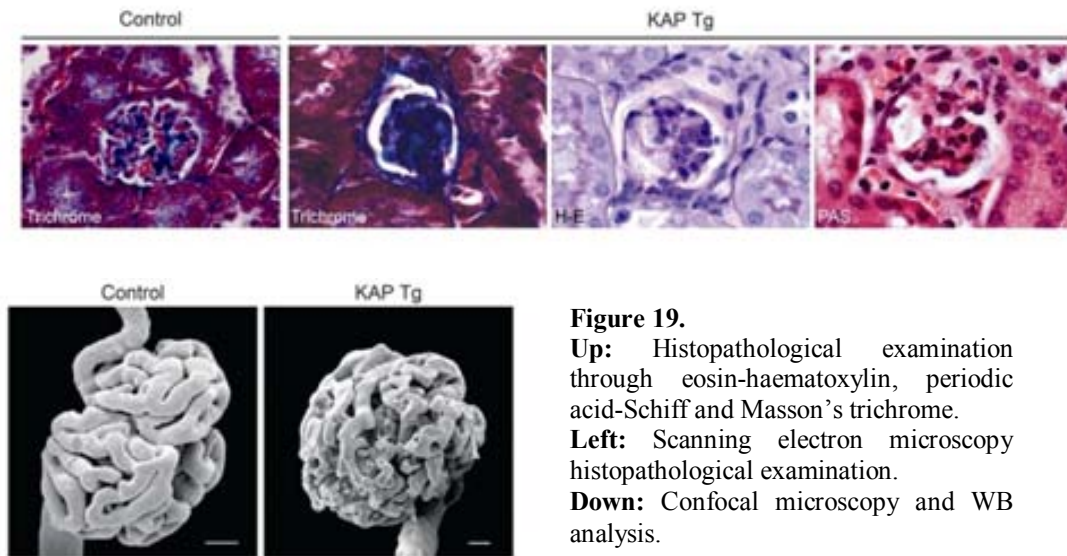
c. IHC immunolocation



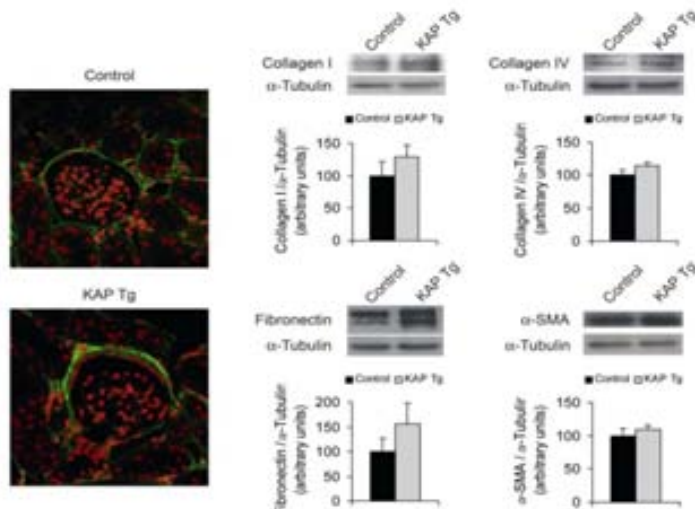
### 3. Effect of the over-expression of KAP on kidney

These animals showed no significant tubular injury but they do suffer from different glomerular alterations including afferent arteriole dilation and focal segmental glomerulosclerosis (histopathological examination of the kidneys using eosin-haematoxylin, periodic acid-Schiff and Masson's trichrome). The latter has been confirmed using confocal microscopy and by WB to demonstrate increased collagen-IV in the basal membrane and collagen-I and fibronectin in kidney extracts. Through scanning electron microscopy severe capillary collapse in affected glomeruli has been determined (fig. 19).



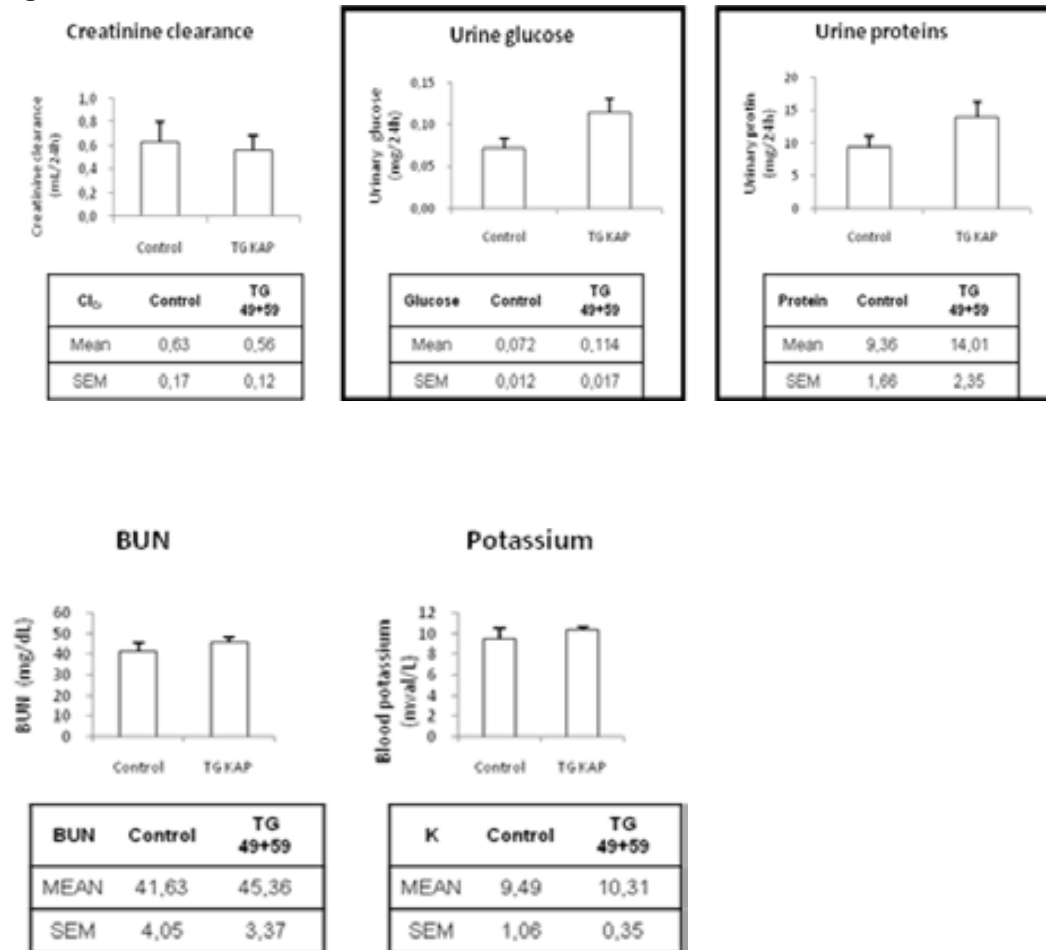


**Figure 19.**  
**Up:** Histopathological examination through eosin-haematoxylin, periodic acid-Schiff and Masson's trichrome.  
**Left:** Scanning electron microscopy histopathological examination.  
**Down:** Confocal microscopy and WB analysis.



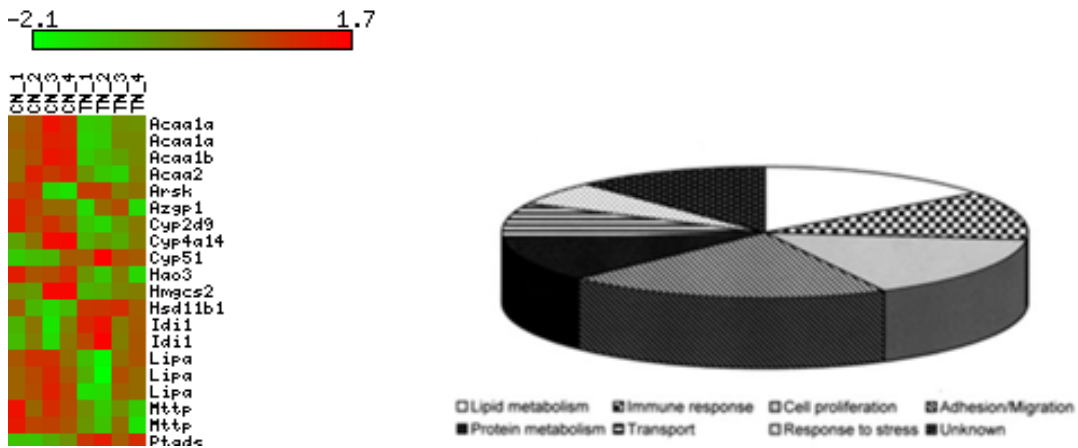
Regarding to renal function, the transgenic mouse displays proteinuria and glucosuria but not changes in creatinine clearance, plasma urea or potassium [67] (fig. 20). These renal alterations in over-expression of KAP reinforce the idea, previously discussed, of the need to maintain the levels of this protein in a strict physiological range, again demonstrating the importance of transcriptional and post-translational control to which the expression is subjected.

Figure 20.



#### 4. Transcriptomic assays of the transgenic mice's kidney

In order to explain the molecular mechanisms underlying the kidney alterations on KAP Tg mice, a transcriptomic analysis using MOE 430 2.0 Affymetrix microarrays was performed and revealed differences in lipid metabolism and Na<sup>+</sup> transport related genes, among others. Of all the genes that showed a FC equal or higher than 1.5, only those gene responses that occurred in both founder Tg lines and those that were statistically significant in one founder line or in both were further studied. Microarray results were further confirmed by quantitative real time RT-PCR assays [67] (fig. 21).



**Figure 21.**

**Left:** Example of the change in expression of genes related to lipid metabolism in kidneys of transgenic mice compared. The red color indicates that increased expression and green low.

**Right:** functional distribution of the genes found differentially expressed.

The relevance of the cytochrome family on kidney metabolism, and the androgenic-regulation of some of its members, indicate that Cyp4A14 and Cyp2D9 must be important genes in the KAP action mechanism. Moreover, these two genes are significantly down-regulated in both Tg lines. Other genes of interest found in the microarrays include the murine cytokine inducible SH2-containing (Cis) protein gene (Cish), a Stat5-responsive negative regulator of Jak/Stat signalling. In physiological conditions, androgens and all regulators that have an impact on KAP expression could control Stat-5 activation and consequently, the Jak/Stat signalling pathway in the kidney. Cyp2D9 constitutes an example of this KAP-controlled mechanism.

Down-regulation of Cyp4A14 in transgenic mice indicates that KAP, containing a functional and potent androgen-response element (ARE) on its proximal promoter, and representing an androgen-target gene, might be essential for downstream control of other androgen-regulated genes in mouse kidney. Besides the Stat-5 pathway, other mechanisms have also been studied. Cyp2D9, known as testosterone 16- $\alpha$ -hydroxylase, is involved in degradation of steroid hormones in liver cells; its low levels in transgenic mice might increase androgen levels in kidney, controlling expression of target genes, such as Cyp4A14. Cytochrome Cyp4A14, involved in the metabolism of arachidonic acid is strongly down-regulated in Tg kidneys as been shown to occur with increasing doses of circulating androgens in mice [83] (fig. 22).

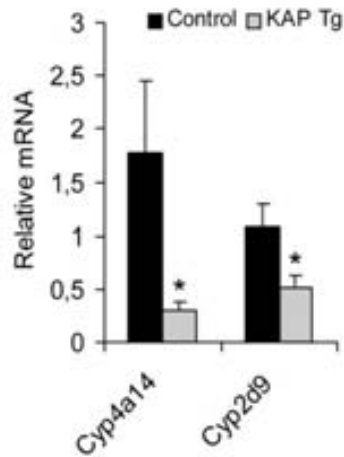


**Figure 22.** Real Time (quantitative) RT-PCR of Cyp4A14 and CypD9 in control and Tg mice kidneys.

### 5. Effect of the transgene of the animals' blood pressure

The existence of a Cyp4A14 KO model with a hypertensive phenotype [84], lead to the study of blood pressure of these Tg animals, in collaboration with Dr. José Miguel López-Novoa, University of Salamanca. Disruption of Cyp4A14 gene causes hypertension, which is more severe in males. Male Cyp4A14 (-/-) mice show increases in plasma androgens, up-regulation of kidney Cyp4a12 expression and increased formation of pro-hypertensive 20 hydroxyecosatetraenoic acid (20-HETE). Cyp4a12 is highly expressed in liver and kidney of control male mice but is expressed at very low levels in liver and kidney of female mice. Testosterone treatment increases slightly the level of its RNA in female mice liver, and even more in their kidney, thus representing a rather specific kidney target for testosterone. Both Cyp4a12a and Cyp4a12b isoforms efficiently hydroxylate arachidonic acid to 20-HETE, but only Cyp4a12a is expressed in the kidney. Thus Cyp4a12a is the predominant 20-HETE synthase in the mouse kidney. Castration normalizes blood pressure of Cyp4A14 (-/-) mice, minimized Cyp4A12 expression and 20-hydroxyarachidonate formation. Since KAP over-expression diminishes Cyp4A14 expression, arterial pressure was studied in KAP Tg mice in both founder lines by the tail cuff method, demonstrating that for KAP Tg animals are also hypertensive [67] (fig. 23).

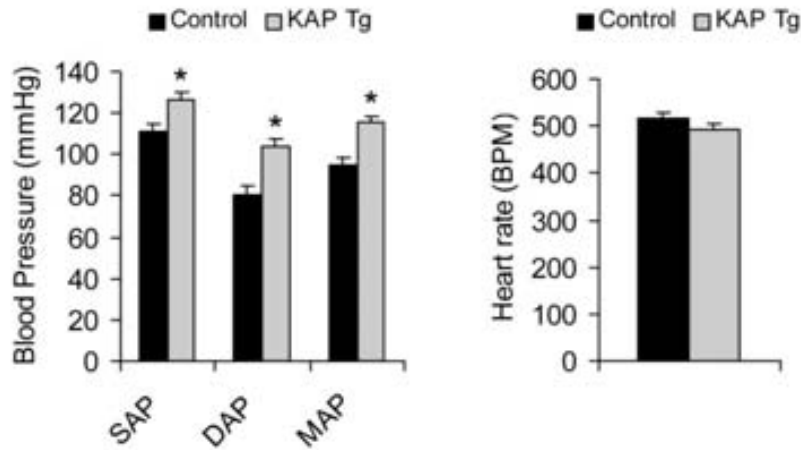


**Figure 23.**  
Blood pressure measurements by tail-cuff method, in mmHg.

To identify the causes of hypertension on KAP Tg mice were investigated through the role of several major pathways involved in hypertension including the renin-angiotensin-aldosterone system (RAAS), the endothelin system, activation of alpha and beta adrenergic receptors, and the production of reactive oxygen species. Blood pressure was measured in awoken mice using the tail cuff method and confirmed by telemetry. RAAS system was studied with oral administration of captopril, an inhibitor of the angiotensin I converting enzyme (ACE) or i.p. injection of the angiotensin II receptor (AT1) antagonist losartan, these were equally effective on decreasing the mean arterial pressure (MAP) of KAP Tg mice (about 15 mmHg). These drugs induced only minor changes in control mice, and were unable to restore MAP to normal control levels. The endothelin system was studied by administrating bosentan, a blocker of both ETA and ETB endothelin receptors, which caused milder effects than those observed with the drugs interfering in the RAAS system. The alpha adrenergic receptors blocker prazosin had almost no effect, while atenolol, a blocker of beta adrenergic receptors, reduced MAP to values similar to those of control mice. The most powerful effect was observed after the administration of 4-hydroxy-2,2,6,6-tetramethylpiperindine-N-oxyl (tempol), a membrane-permeable superoxide dismutase mimetic, with a decrease of MAP levels to normal or even lower values than those found in controls. Since tempol completely restored normal MAP values, it was assumed that increased blood pressure in KAP Tg mice is mediated by increased reactive oxygen species (ROS) production.

Continuous production of reactive oxygen species appears to be one of the most important outcomes of NADPH consumption by microsomal monooxygenases, meaning that these enzymes contribute significantly to the cellular production of oxygen-derived free radicals. These ROS play an important pathophysiological role in the development and maintenance of hypertension. Presence of ROS was studied both by analysing the increase of oxidative injury levels and the decrease in the antioxidative enzymes activity.

Mitochondrial DNA damage, protein and fatty acid oxidation to determine oxidative injury levels, as well as, Activity of ROS metabolising enzymes such as catalase, SOD and glutation peroxidase were measured in control and mice to determine the extent of ROS effect (fig. 24).

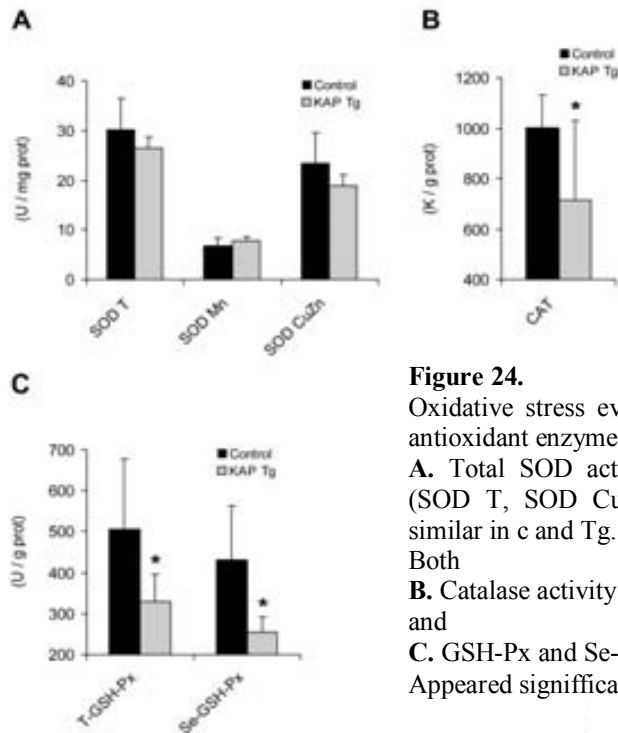


**Figure 24.**

Oxidative stress evaluation in control and Tg males by antioxidant enzymes activity analysis.

**A.** Total SOD activity, mitochondrial or cytoplasmatic (SOD T, SOD CuZn y SOD Mn, respectively), were similar in c and Tg.

Both

**B.** Catalase activity and

**C.** GSH-Px and Se-GSH-Px activities

Appeared significantly reduce in Tg animals.

Mitochondrial DNA damage, protein and fatty acid oxidation were evaluated to determine oxidative injury levels. Urinary excretion of 8-iso-PGF<sub>2α</sub> and 8-hydroxydeoxyguanosine (8-OHdG) was also measured through the use of ELISA and total daily excretion was calculated. 8-iso-PGF<sub>2α</sub> is an isoprostane that can be generated by a non-enzymatic oxidative reaction of arachidonic acid and has been used to quantify oxidative stress in vitro and in vivo. 8-Hydroxydeoxyguanosine (8-OHdG) is produced by oxidation of DNA, and its urinary excretion has been demonstrated to correlate with oxidative stress [85]. Urinary excretion of both iso-PGF<sub>2α</sub> and 8-OHdG were higher in Tg than in control mice, they were reduced to control levels by the superoxide dismutase mimetic tempol and only partially by atenolol (fig. 25).

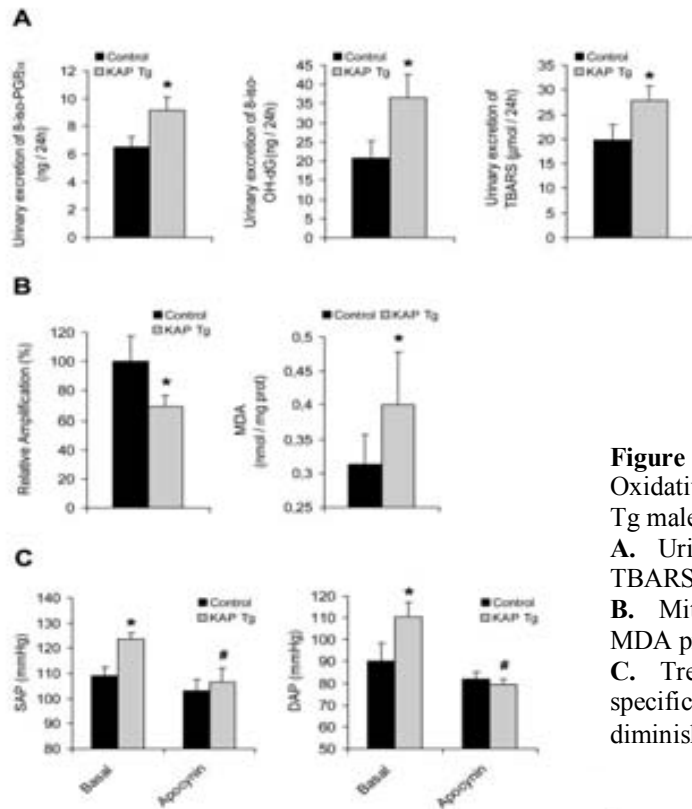


**Figure 25.** Oxidative stress evaluation in control and Tg males by oxidative damage analysis. **A.** Urinary excretion of 8-iso-PGF<sub>2α</sub>, TBARS and 8-OH-dG. **B.** Mitochondrial DNA damage and MDA production in renal tissue. **C.** Treatment with NADPH oxidase specific inhibitor apocynin significantly diminished both SAP and DAP in Tg.

KAP over-expression-induced hypertension is based in an increased oxidative stress, increased sympathetic activation and the subsequent increase in renin release and angiotensin II production.

Hypertension caused by angiotensin II increases superoxide production in the central nervous system. The pressor and sympatho-excitatory effects of Ang II administered directly to the central nervous system were completely cancelled by adenoviral vector-mediated expression of superoxide dismutase and central administration of tempol. Furthermore, the pressor effect of central Ang II was shown to be mediated by NAD(P)H-oxidase-dependent production of superoxide in the brain.

Some characteristics of KAP Tg model such as glomerulosclerosis, hypertension, proteinuria and glycosuria matched defining signs of cardiometabolic syndrome. The increasing incidence of this disease and its consequences make the KAP a protein of interest to investigate its involvement and, with it, the role of the kidney in this syndrome.

**AIMS**

---



## **AIMS**

The general aim of this work is to study the role of the kidney androgen-regulated protein (KAP) in the development of hypertension and metabolic syndrome. Focusing on the following more specific aims:

1. Study of the physiology of the metabolic syndrome in transgenic mice over-expressing KAP and the interaction of the transgene and a rich in fat diet by evaluating the main conditions altered in the metabolic syndrome: blood pressure, glucose metabolism, body weight and lipid profile.
2. Study of the effects of the over-expression of KAP and the interaction of the transgene with a rich in fat diet at a histological and molecular level in metabolic syndrome target organs and tissues.
3. Comparison of "in vivo" results with isolated cell systems:
  - a) Transfected murine renal proximal tubule (PCT3) with stable and controlled expression of wild type KAP: based on the cloning of KAP cDNA in pBIG2i eukaryotic expression vector and the empty vector as a negative control for all assays.
  - b) Human hepatoma (HepG2) treated with the KAP-His bacterial recombinant protein and sodium oleate with the aim of evaluating whether KAP affects lipid storage in human liver cells.

# **MATERIALS AND METHODS**

---

## MATERIALS AND METHODS

### EXPERIMENTAL DESIGN:

In order to achieve the aims of this work the following study lines were designed:

1. Physiology of MS in whole body: three studies were carried out in controls (c) and Tg male mice fed on a control diet (chow) or high fat (hfd) containing 45% of calories in the shape of lipids

1<sup>st</sup>) Designed to evaluate the evolution of the weight, water and food intake, blood pressure, glucose tolerance and insulin "in vivo" over seven months. These tests were performed every two months starting the first month after weaning.

Lipid profile and serum insulin levels were also studied every two months during this period.

At the end stage of this study, several tissues and organs were extracted (brain, kidney, liver, heart and different adipose tissues) to carry a comparison of subsequent molecular studies.

2<sup>nd</sup>) Designed exactly in the same way as the first to confirm results obtained.

3<sup>rd</sup>) Designed to evaluate food and water intake.

2. Histological and molecular analyses of the findings in animals: histopathological analyses in kidney, liver and adipose tissues; evaluation of the influence of the hfd in the KAP protein expression in kidney; studying alterations in proteins involved in the insulin signaling pathway in target tissues; differential gene expression analyses of genes involved in HT, RAAS axis, oxidative stress, glucose and lipid metabolism and inflammation in kidney, liver and inguinal white adipose; serum proteomic assays.

3. Comparison of "in vivo" results with isolated cell systems:

a) Transfection murine renal proximal tubule (PCT3) with stable and controlled expression of wild type KAP: based on the cloning of KAP cDNA in pBIG2i eukaryotic expression vector and the empty vector as a negative control for all assays. These clones are used to observe what molecular, functional and metabolic alterations found in the Tg animal kidney are reproduced in this isolated cell system. The protein secretion into the apical or basal cell culture medium and its effects are analyzed regarding viability, toxicity, and cell differentiation. Also studying differential gene expression of the NFκB pathway with and without wild type KAP to evaluate its role in inflammatory processes in the kidney.

d) Human hepatoma (HepG2) treated with the KAP-His bacterial recombinant protein and sodium oleate with the aim of evaluating whether KAP affects lipid storage in human liver cells. As well as, its effect on viability, toxicity, differentiation was analyzed in this system. All results were statistically analyzed through standard t-tests.

## **MATERIALS:**

### **1. The mice**

#### **1.1. KAP transgenic mice**

The transgenic mice were generated upon the pKAP2-KAP construct containing KAP's self promoter, 1542 base pairs (bp) from the 5-flanking region of the KAP gene, which proved to drive expression of a heterologous reporter gene in a tissue-specific, cell-specific, and androgen regulated manner [68] as well as several exons from the human angiotensinogen gene that are essential for the expression of the transgene but showed no expression of their own.

The transgene is regulated equally as the endogenous gene: both the mRNA and the protein are expressed exclusively in the kidney proximal tubule and this expression is regulated by androgens. Transgenic males show higher levels of KAP than controls.

These mice show hypertension from their fifth month of life. They suffer from renal damage (fibrosis, focal segmental glomerulosclerosis and tubular damage) and oxidative stress.

#### **1.2. Leptin deficient (ob/ob) mice**

Ob/ob mice show a spontaneous mutation in the leptin gene, causing them to gain weight rapidly reaching even 3 times the normal weight of wild type animals. Their obesity is characterized by an increase in the size and number of adipocytes [86]. These mutant mice show hyperphagia, hyperglycaemia similar to that shown in diabetes, glucose intolerance, elevated insulin plasma levels, infertility, defects in wound healing, and increased production of hormones by pituitary and adrenal glands. Leptin is a hormone that controls body weight by regulating appetite and metabolism. It is secreted by adipocytes, and also has other functions: endocrine, inflammatory, hematopoietic, angiogenesis among others. There are increasingly more data linking leptin with cardiovascular disease [87].

#### **1.3. Ppar $\gamma$ 2 knock-out mice**

Ppar $\gamma$ 2 knockout mice have a dominant autosomal punctual mutation silencing PPAR $\gamma$ 2 gene that mimics the dominant negative mutation of patients with metabolic syndrome. The PPAR $\gamma$  (Peroxisome Proliferators Activated Receptor  $\gamma$ ) receptor is a transcription factor that controls important metabolic pathways such as adipogenesis and insulin sensitivity. Although expressed primarily in adipose tissue, it is also present in other tissues such as liver in positive energy balance situations [88].

#### **1.4. Poko mice**

Poko mice are the result of mating Ppar $\gamma$ 2 mutated mice (PPAR $\gamma$ 2 -/-) and ob/ob mice, so that they are heterozygote's for the disruption of a region of the Ppar $\gamma$ 2 gene (PPAR $\gamma$ 2 +/-) and for the leptin deficiency (Lep ob / Lep +), and therefore show the ablation of the gene PPAR $\gamma$ 2 and the mutation of the leptin gene. However, these poko mice are not obese, but have a severe insulin resistance, failure of pancreatic  $\beta$  cells and dyslipidemia [89].



### 1.5. The diets

The control and KAP Tg animals were fed upon two different diets, in the first place, a regular chow diet as a control, and on the second place, a high fat diet (HFD) (Harlan TD.06415) in which 45% of the caloric content comes from a lipidic origin:

*CHOW DIET:* 2018 Harlan Global Diet

*HIGH FAT DIET:* TD.06415 Tekland custom research diet:

*Teklad Custom Research Diet Data Sheet*

TD.06415 Adjusted Calories Diet (45/Fat)		Key Features	
<b>Formula</b>	<b>g/Kg</b>	<ul style="list-style-type: none"> <li>Purified Diet</li> <li>Diet Induced Obesity</li> <li>High Fat</li> </ul>	
Casein	246.0	<b>Key Planning Information</b>	
L-Cystine	3.6	<ul style="list-style-type: none"> <li>Products are made fresh to order</li> <li>Store product at 4°C or lower</li> <li>Use within 6 months (applicable to most diets)</li> <li>Box labeled with product name, manufacturing date, and lot number</li> <li>Replace diet at minimum once per week</li> <li>More frequent replacement may be advised</li> </ul>	
Corn Starch	86.0	<ul style="list-style-type: none"> <li>Lead time:                             <ul style="list-style-type: none"> <li>2 weeks non-irradiated</li> <li>4 weeks irradiated</li> </ul> </li> </ul>	
Maltodextrin	116.0	<b>Product Specific Information</b>	
Glucose	200.0	<ul style="list-style-type: none"> <li>1/2" Pellet or Powder (free flowing)</li> <li>Minimum order 3 Kg</li> <li>Irradiation available upon request</li> </ul>	
Lard	186.0	<b>Options (Fees Will Apply)</b>	
Soybean Oil	30.0	<ul style="list-style-type: none"> <li>Rush order (pending availability)</li> <li>Irradiation (see Product Specific Information)</li> <li>Vacuum packaging (1 and 2 Kg)</li> </ul>	
Cellulose	68.0	<b>International Inquiry</b>	
Mineral Mix, AIN-93G-MX (B4046)	43.0	<ul style="list-style-type: none"> <li>Outside U.S.A. or Canada:                             <ul style="list-style-type: none"> <li>askanutritionist@harlan.com</li> </ul> </li> </ul>	
Calcium Phosphate, dbasic	3.4	<b>Place Your Order (U.S.A. &amp; Canada)</b>	
Vitamin Mix, AIN-93-VX (B4047)	19.0	<ul style="list-style-type: none"> <li>Place Order - Obtain Pricing -</li> <li>Check Order Status -</li> <li>(800) 483-5523</li> <li>(608) 277-2066 fax@harlan.com</li> <li>tekinfo@harlan.com</li> </ul>	
Choline Bitartrate	3.0	<b>Helping you do research better</b>	
Red Food Color	0.1		

**Footnote**  
Approx. 45% of total calories come from fat. Designed with similarities to Research Diets, Inc. formula D12451. For the series TD 06414-TD 06416. Approximate fatty acid profile (% of total fat): 35% saturated, 47% monounsaturated, 17% polyunsaturated.

Selected Nutrient Information <sup>1</sup>		
	% by weight	% kcal from
Protein	21.7	19.0
Carbohydrate	41.4	36.2
Fat	22.8	44.8
<b>Kcal/g</b>	<b>4.6</b>	

<sup>1</sup>Values are calculated from ingredient analysis or manufacturer data  
Teklad Diets are designed & manufactured for research purposes only.

**Speak With A Nutritionist**  
 • (800) 483-5523  
 • askanutritionist@harlan.com

Harlan Laboratories - PO Box 44220 - Madison, WI 53744-4220  
www.harlan.com

**harlan™**

Harlan, Harlan Laboratories, Helping you do research better, and the Harlan logo are trademarks and/or service marks of Harlan Laboratories, Inc.  
© 2018 Harlan Laboratories, Inc.

001088

## 2. The cell lines

### 2.1. PKSV-PCT3

This is an immortalized epithelial cell line that derives from the contorted segment of the kidney proximal tubule (pars convoluta, PCT). They were obtained from male mice transgenic for the simian virus 40 big-T and small-T antigen (SV40) under the control of the promoter of the pyruvate kinase [90]. This cell line shows an epithelial morphology, being adherent cells that

grow into monolayer and possess the capability of forming domes after several days post-confluence (when they have been fully differentiated) (fig. 1) [91].

The cell line was cloned on limit dilution in order to obtain the PCT3 cells (PKSV-PCT clone 3) that maintain the phenotype of the parental cells from which they come from [92]. The original cell line was ceded to our laboratory by Dr. Alain Vandewalle.

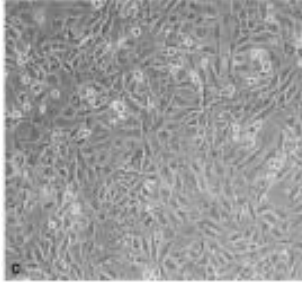


**Figure 1.** Cultured PCT3 cells. Obtained from Sarró et al., 2008.

## **2.2. HepG2 (human hepatocellular liver carcinoma)**

These are adherent, epithelial-like cells growing in monolayer and in small aggregates that have a model chromosome number of 55. HepG2 cell line was derived from the liver tissue of fifteen year old human male with differentiated hepatocellular carcinoma. This cell line is not tumorigenic in immunocompromised mice. HepG2 cells secrete plasma proteins, such as albumin, transferrin, fibrinogen,  $\alpha$ -2-macroglobulin, plasminogen. They also respond to stimulation with HGH [93].

## **2.3. The clones**

PKSV-PCT (PCT3 clones) were stably transfected with pBIG2i plasmidic vector into which the wt cDNA of KAP had been previously cloned:

- KAP wt: wild type protein
- pBIG2i empty vector as a negative control

A hemagglutinin (HA) tag had been added to the C-end and it had been initially cloned into the pHA-CMV vector. This expression vector adds an HA tag at the N-end of the insert cloned into it, but it happens that KAP contains a signal peptide at its N-end that directs the protein to the endoplasmic reticulum and is fatherly removed from the final protein by a post-translational modification, so the HA tag added to the clone in pHA-CMV would be lost. For this reason the tag was also added at the C-end by designing complementary primers encoding the C-end of KAP (eliminating the STOP codon) and the HA tag.

## **2.4. The culture media**

PCT3 and KAP clone cells were routinely cultured in DMEM:Ham's F12 (1:1, v/v) enriched with 20mM HEPES, 2mM L-glutamine, 12.5 mM D-Glucose, 60 nM sodium selenite, 5  $\mu$ g/ml transferrin, 50 nM dexametasone, 1% antibiotic-antifungal and supplemented with 2% foetal

## MATERIALS AND METHODS

bovine serum (FBS), 5 µg/ml insulin, 10ng/ml epidermal growth factor (EGF) and 1 nM triiodothyronine.

### *PCT3 CELLS RICH MEDIUM:*

	<b>Preparation and aliquots</b>	<b>Store at</b>	<b>Cf</b>	<b>Vf</b>
DMEM (Gibco ref.: 11880-036)		4 °C		250 ml
HAM F12 (Gibco ref.: 31765-068)		4 °C		250 ml
HEPES buffer (Gibco 1M-100 ml)		RT	20 mM	10 ml
Glutamine (Gibco 200 mM)	10 ml aliquots. Add when starting to use the medium.	-20 °C	2 mM	5 ml
Glucose anhydrous (Sigma G-7021)	Dissolve 1.12 g of glucose in 20 ml of DMEM/F12 at 37 °C and shake gently until it totally dissolves. Add to the medium.	RT	2.24 g/l	1.12 g
Apo Transferrin (Sigma T-8027)	Dissolve 100 mg in 20 ml de H <sub>2</sub> O. 0.5 ml aliquots.	-20 °C	5 µg/ml	500 µl
Insulin (Sigma I-6634 50 mg)	Resuspend in 5 ml of mQ H <sub>2</sub> O and 5 µl of concentrated (fuming) HCl. 1 ml aliquots.	-20 °C	5 µg/ml	250 µl
Dexametasone 10 <sup>-3</sup> M (Sigma D-8893)	Dissolve 1 mg in 2.5 ml 95% EtOH. 0.5 ml aliquots.	4 °C	5 · 10 <sup>-8</sup> M	25 µl
T3 10 <sup>-4</sup> M (Sigma T-5516)	Dissolve 1 mg in 15 ml KOH 10 mM. 1.5 ml aliquots.	4 °C	10 <sup>-9</sup> M	5 µl
EGF (Sigma E-4127)	Dissolve 100 µg in 1 ml mQ H <sub>2</sub> O. 50 µl aliquots.	-20 °C	10 ng/ml	50 µl
Selenium (Sigma S-9133)	Dissolve 1 mg in 20 ml mQ H <sub>2</sub> O UNDER A GASSES CABINETTE. 1 ml aliquots.	4 °C	60 nM	100 µl
Foetal bovine serum decomplemented (Biological Industries cat.: 04-007-1A)	Decomplement the serum by heating it at 56 °C 30 min. 40 ml aliquots.	-20 °C	2 %	10 ml
Antibiotic-antimycotic (Gibco cat.: 15240-062) 100 ml	10 ml aliquots.	-20 °C	1 %	5 ml

**Vf = 500 ml**

- Mix all the reagents in an appropriate container under a laminar flow hood.
- Stir.
- Filter using a 0.22 µm pore filter (Millipore Stericup® and Steritop™, PR01925).
- Divide the final volume into 500 ml bottles.
- Store at 4 °C.

HepG2 cells were routinely cultured in DMEM+GlutaMax™ enriched with 25 mM D-Glucose, 1% non-essential amino acids, 1% penicillin-streptomycin and supplemented with 10% foetal bovine serum (FBS).

*HepG2 CELLS RICH MEDIUM:*

	Preparation and aliquots	Store at	Cf	Vf
DMEM (Biological Industries cat.: 01-055-1A) 500 ml or DMEM + GlutaMAX™-1 (Gibco Invitrogen 31966)		4 °C		500 ml
Glutamine (Gibco 200 mM) Add if the medium does not contain Glutamax reagent.	10 ml aliquots. Add when starting to use the medium.	-20 °C	2 mM	5 ml
Glucose anhydrous (Sigma G-7021) Add if it is not supplemented in the medium.	Dissolve 2.25 g of glucose in 20 ml of DMEM at 37 °C and shake gently until it totally dissolves. Add to the medium.	RT	25 mM	2.25 g
Penicillin-Streptomycin solution (pen 10 i.u./ml, strep 10 mg/ml) (Biological Industries cat.: 03-031-3B)	10 ml aliquots.	-20 °C	1 %	5 ml
Non-essential amino acids MEM- EAGLE 100x (Biological Industries cat.: 01-340-1B) 100 ml	No aliquots.	4 °C	1 %	5 ml
Foetal bovine serum decomplexed (Biological Industries cat.: 04-007-1A) 500 ml	Decomplement the serum by heating it at 56 °C 30 min. 40 ml aliquots.	-20 °C	10 %	50 ml
Antibiotic-antimycotic (Gibco cat.: 15240-062) 100 ml Add instead of penicillin-streptomycin	10 ml aliquots.	-20 °C	1 %	5 ml

Vf = 500 ml

- Mix all the reagents in an appropriate container under a laminar flow hood.
- Stir.
- Filter using a 0.22 µm filter (Millipore Stericup® and Steritop™, PR01925).
- Divide the final volume into 500 ml bottles.
- Store at 4 °C.

**3. The bacteria****3.1. DH5α™**

Commercial bacterial cells strain, made chemically competent at our laboratory (Invitrogen, cat. no. K4520-01). Competent bacteria are those capable of incorporating exogenous DNA through transformation.

**3.2. One-shot® TOP 10**

Commercial chemically competent *E. coli* cell strain (Invitrogen, cat. no. C4040-10) which is easily transformed and used for cloning.

**3.3. Culture media**

Bacteria were routinely cultured in Luria Broth (-/+ agar) 50 µg/ml ampicillin medium.

*Liquid LB-ampicillin:*

Isolated bacteria colonies were cultured in liquid 25% Luria-Broth medium/50 µg/ml ampicillin (Invitrogen, cat. No.: 11593-019).

*Solid LB-agar-ampicillin:*



Bacteria were grown in 25% Luria-Broth medium/15 % agar/50 µg/ml ampicillin (Invitrogen, cat. No.: 11593-019) in order to select transformed colonies.

*S.O.C. Medium:*

Commercial rich medium for bacteria seeding included in the One Shot® TOP10 Competent Cells (Invitrogen cat. No.: 15544-034).

**4. The plasmids**

**4.1. pCR®2.1-TOPO®**

This plasmid vector is provided in the TOPO® TA-Cloning kit (Invitrogen, cat. No.: K4500-01) and is used for cloning PCR Taq polymerase amplified products. It is supplied linearised with single 3'-thymidine (T) overhangs for TA Cloning® and topoisomerase I covalently bound to the vector (referred to as “activated” vector) (fig. 2). Taq polymerase has a nontemplate-dependent terminal transferase activity that adds a single deoxyadenosine (A) to the 3' ends of PCR products. The linearised vector supplied in this kit has single overhanging 3' deoxythymidine (T) residues. This allows PCR inserts to ligate efficiently with the vector.

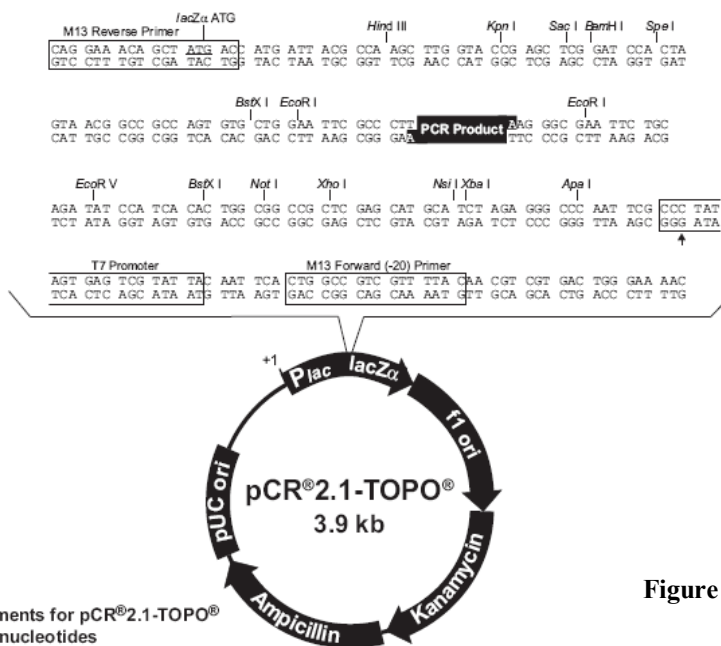


**Figure 2.** pCR® 2.1 plasmid map.

**4.2. pCMV-HA**

The cDNA inserts are often pre-cloned in pCMV-HA plasmid which attaches an HA tag to the cDNA insert (fig. 3), so that, when the construct is cut to be cloned in the definite vector, it will take the HA tag with it. Having an HA tag is interesting since it is much easier and clearer to detect than to detect, in our case, the exogenous KAP protein since the anti-HA antibody is

commercially available, whereas our anti-KAP is homemade. pCMV-HA was purchased to Clontech cat. no. 631604.

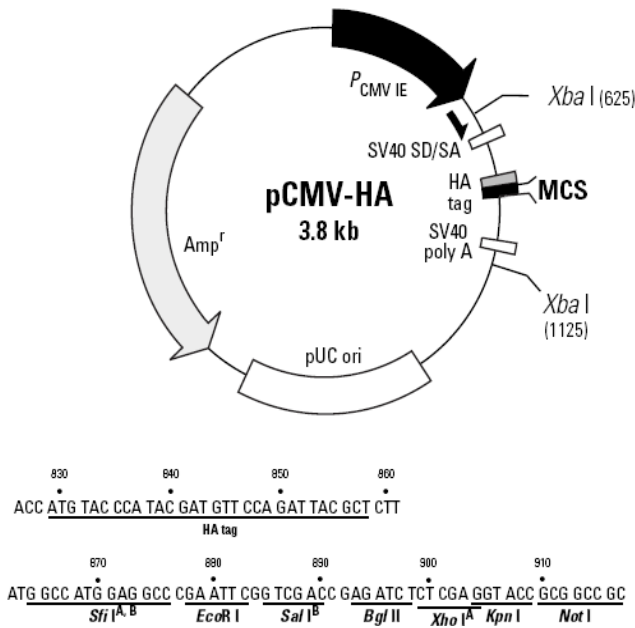


Figure 3. pCMV-HA plasmid map.

### 4.3. pBIG2i

This vector is based on a high copy of number plasmid backbone containing the *colE1* origin of replication and  $\beta$ -lactamase gene that confers resistance to ampicillin (fig.4). The bi-directional tetracycline-responsive promoter in the vector is comprised of a central tetON element, a stronger CMV element to drive cDNA expression, and a weaker TK element to drive expression of transactivator component. pBIG2i contains a selectable marker conferring resistance to Hygromycin B for the generation of stable cells lines [94].



Figure 4. pBiG2i plasmid map, drawn by Marie Defays.

**5. The buffers**

Reagents and preparation of the main buffers used in this work is detailed below:

*APS (ammonium persulphate)*

Reagents:

ammonium persulphate	1 g
mQ H <sub>2</sub> O	10 ml

Preparation:

- Mix reagents on ice.
- Filter with a 0.45 µm pore syringe filter.
- Aliquote.
- Store at -20 °C.

*EDTA 0.5 M pH 8*

Reagents:

EDTA (2 H <sub>2</sub> O)	93.05 g
mQ H <sub>2</sub> O	400 ml

Preparation:

- Adjust pH with NaOH (~20 g).
- Weigh EDTA.
- Add NaOH progressively until desired pH is reached.
- Add mQ H<sub>2</sub>O up to 500 ml.
- Autoclave.
- Store at RT.

*NaOH 5M*

Reagents:

NaOH	50 g
mQ H <sub>2</sub> O	250 ml

Preparation:

- Mix and shake.
- Autoclave.
- Store at RT.

*PBS 10x*

Reagents:

NaCl	160 g
KCl	4 g
Na <sub>2</sub> HPO <sub>4</sub> 2H <sub>2</sub> O	29 g
KH <sub>2</sub> PO <sub>4</sub>	4 g
Autoclaved mQ H <sub>2</sub> O	2 l

Preparation:

## MATERIALS AND METHODS

- Mix and shake.
- Autoclave.
- Store at RT.

### *PBS 1x TWEEN 0.1 %*

#### Reagents:

mQ H <sub>2</sub> O	6.3 l
PBS 10x	700 ml
Tween	7 ml

#### Preparation:

- Mix and shake.
- Store at RT.

### *SDS ELECTROPHORESIS BUFFER 5x*

#### Reagents:

MQ H <sub>2</sub> O	2 l
tris base	30.2 gr
glycine	144 gr
SDS 20 %	50 ml

#### Preparation:

- Mix and shake.
- Store at RT.

### *SEPARATING: 4x TRIS-CI/SDS, pH 8.8*

#### Reagents:

mQ H <sub>2</sub> O	250 ml
tris base	45.5 g
SDS 20%	5 ml

#### Preparation:

- Weigh Tris and add 200 ml H<sub>2</sub>O.
- Adjust pH 8.8 with HCl 1N.
- Adjust pH with NaOH 5M.
- Add SDS and then add H<sub>2</sub>O up to 250 ml.
- Filter with a syringe filter 0.45 µm pore.
- Store at RT (short term).
- Store at 4 °C (long term).

### *STACKING: 4x TRIS-CI/SDS, pH 6.8*

#### Reagents:

mQ H <sub>2</sub> O	200 ml
tris base	12.1 g
SDS 20%	4 ml

Preparation:

- Weigh Tris and add 150 ml H<sub>2</sub>O.
- Adjust pH 6.8 with HCl 1N.
- Adjust pH with NaOH 5M.
- Add SDS and then add H<sub>2</sub>O up to 200 ml.
- Filter with a syringe filter 0.45 µm pore.
- Store at RT (short term).
- Store at 4 °C (long term).

*TAE 50x*

Reagents:

mQ H <sub>2</sub> O	2 l
tris base	484 g
glacial acetic acid	114.2 ml
EDTA 0.5 M pH 8	200 ml

Preparation:

- Mix and shake.
- Autoclave.
- Store at RT.

*TRANSFER BUFFER 3x*

Reagents:

MQ H <sub>2</sub> O	2 l
glycine	217.5 g
tris base	45.81 g
SDS 20 %	37.5 ml

Preparation:

- Mix and shake
- Store at RT.

**METHODS:**

**1. Genomic techniques**

**1.1. DNA extraction**

**1.1.1. From animal tissue**

Extraction and purification of genomic DNA from mouse tail clippings was performed using the Promega Wizard<sup>®</sup> SV Genomic DNA purification kit (cat. #A2361) and took place using a maximum of 0.5 cm of tail fragments and following the manufacturer's instructions.

### **1.1.2. From bacterial cultures**

Plasmid DNA was isolated from transformed bacteria isolated colonies grown in liquid LB-ampicillin 50 µg/ml medium incubated o/n in a shaker at 37 °C 200 rpm with GE Healthcare Illustra™ PlasmidPrep MiniSpin Kit (ref.: 28-9042-70) for 5 ml cultures in order to obtain small amounts of DNA.

A 5 ml culture was seeded in 100 ml LB-ampicillin 50 µg/ml and incubated o/n in a shaker at 37 °C 200 rpm. The plasmid DNA was purified with Qiagen® Plasmid Maxi Kit (cat. no.: 12163) when large amounts of plasmid DNA were desired to obtain.

### **1.1.3. Quantitative and qualitative analysis of DNA**

Concentration, purity and quality of total DNA were determined by absorbance spectrophotometry using a Nucliber NanoDrop Technologies ND-1000 spectrophotometer using 1.5 µl of sample. The purity of DNA was assessed by absorbance ratios 260/280 nm (1.9-2.1) and 230/260 nm (1.8-2) obtained by spectrophotometry.

## **1.2. Polymerase Chain Reaction**

The polymerase chain reaction (PCR) is used to amplify a target region of DNA and generate a multycopy of this particular DNA sequence to be further detected.

All PCRs were performed under standard procedure. The master mixes were composed of nuclease-free H<sub>2</sub>O, Taq polymerase buffer, MgCl<sub>2</sub>, nucleotides, forward and reverse primers and Taq Polymerase enzyme (ratios varied according to the different Taq polymerases' manufacturers' instructions). Template DNA solutions were supplied by the users. All reactions took place in a Gene Technologies G-Storm thermal cycler (R/N GT-10834, Ref.: GS 00001).

### **1.2.1. Genotyping PCR**

When mice were to be genotyped, 2 genes were amplified from the DNA extracted from the tail clippings: a housekeeping gene (either p107 or p130 gene, both involved in cell cycle) and a fragment of the human angiotensinogen (hAGT) gene. The housekeeping genes were used as a positive control for the presence of DNA in our samples. hAGT gene was used to determine whether mice were transgenics or controls. This gene plays a role in the rennin-angiotensin human system. As mentioned before, several exons and introns of this gene were introduced in the construct used produce the transgenics as they had been previously proven to act as enhancer regions for the expression of the transgene; however hAGT is not expressed in the transgenic mice and is not involved in the phenotype of these animals.

*p107 and p130 PCRs:*

Primers:

Name	Sequence (5' → 3')	Annealing T (°C)	Amplified fragment (bp)
p130-F	TAC ATG GTT TCC TTC AGC GG	55	200
p130-R	ACG GAT GTC AGT GTC ACG	55	200
p107-F	TCG CTG GCA GTC TGA GTC AG	55	200
p107-R	TGT GCT GAG CAT GAA CAG AC	55	200

Enzyme:

Ecotaq Ecogen Ref.: ETAQ-500

Reaction:

Reagent	Co	Vo (µl)	Cf
Buffer	10x	2.5	1x
MgCl <sub>2</sub>	50 mM	1.75	3.5 mM
dNTPs	10 mM	2	0.8 mM
primer Fw	10 µM	2.5	1 µM
primer Rv	10 µM	2.5	1 µM
H <sub>2</sub> O		0	-
TaqPol		0.25	
Sample	H <sub>2</sub> O	13.5	40 ng DNA

Vf = 25 µl

94 °C	5 min
94 °C	30 sec
55 °C	30 sec
72 °C	30 sec
72 °C	5 min
CYCLES	30

*Transgene PCR:*

Primers:

Name	Sequence (5' → 3')	Annealing T (°C)	Amplified fragment (bp)
TG-F	CAT CTG TTG AGT GCC TCT GC	50	500
TG-R	CTG GTC TCT GTG CTT CCA	50	500

Enzyme:

Platinum® Taq DNA Polymerase High Fidelity Invitrogen Cat. No. 11304-011

Reaction:

Reagent	Co	Vo	Cf
Buffer	10X	2.5	1x
MgSO <sub>4</sub>	50 mM	1	2mM
dNTPs	10 mM	0.5	0.2 mM
primer Fw	10 µM	1	0.4 µM
primer Rv	10 µM	1	0.4 µM
H <sub>2</sub> O		5.4	-
TaqPol		0.1	
Sample	H <sub>2</sub> O	13.5	10 ng DNA

Vf = 25 µl

94 °C	5 min
94 °C	30 sec
50 °C	30 sec
68 °C	30 sec
68 °C	5 min
CYCLES	30

**1.2.2. pCMV-HA insert amplification for further cloning in pCR®2.1-TOPO®**

Primers:

Name	Sequence (5' → 3')	Annealing T (°C)	Amplified fragment (bp)
KAPstable-Fw	GCT AGC ATG TAC CCA TAC GAT GTT	50	500
KAPstable-Rv	ACT AGT TCA AGC GTA ATC TGG AAG	52	500

Enzyme:

Platinum® Taq DNA Polymerase High Fidelity Invitrogen Cat. No. 11304-011

Reaction:

Reagents	Co	Vo	Cf	
Buffer	10x	5	1x	94 °C 2 min
MgSO <sub>4</sub>	50 mM	1	1mM	94 °C 30 sec
dNTPs	10 mM	2	0.2 mM	50 °C 30 sec
primer Fw	10 µm	2	0.4 µm	68 °C 40 sec
primer Rv	10 µm	2	0.4 µm	68 °C 7 min
H <sub>2</sub> O		27.8	-	CYCLES 30
TaqPol		0.2		
Sample	H <sub>2</sub> O	10	100 ng DNA	

Vf = 50 µl

**1.2.3. Detection of presence of the insert cloned in pBIG2i**

Primers:

Name	Sequence (5' → 3')	Annealing T (°C)	Amplified fragment (bp)
T7	TAA TAC GAC TCA CTA TAG GC	55	Depends on the size of the insert
T3	ATT AAC CCT CAC TAA AG	55	

Enzyme:

Ecotaq Ecogen Ref.: ETAQ-500

Reaction:

Reagent	Co	Vo (µl)	Cf	
Buffer	10X	2.5	1x	94 °C 5 min
MgCl <sub>2</sub>	50 mM	1.75	3.5 mM	94 °C 30 sec
dNTPs	10 mM	2	0.8 mM	55 °C 30 sec
primer Fw	10 µm	2.5	1 µm	72 °C 30 sec
primer Rv	10 µm	2.5	1 µm	72 °C 5 min
H <sub>2</sub> O		0	-	CYCLES 30
TaqPol		0.25		
Sample	H <sub>2</sub> O	13.5	50 ng DNA	

Vf = 25 µl

**1.2.4. DNA Sequencing**

*Sequencing PCR:*



Primers:

The primers used depended on the fragment desired to sequence, the PCR process is always the same.

Reagents:

Applied Biosystems ABI PRISM® Big Dye® Terminator v1.1 Cycle sequencing kit, part. no. 4336778.

Reaction:

Reagent	Co	Vo	Cf		
Big Dye buffer	5x	4	1x	94 °C	3 min
Primer	5 µM	1	0.25 µM	96 °C	10 sec
BigDye Terminator ready reaction mix	10x	2	1x	55 °C	5 sec
H <sub>2</sub> O		9		60 °C	4 min
DNA		5 µl	900 ng	CYCLES	25

Vf = 20 µl

*Precipitation of sequencing PCR products:*

The amplification products were EtOH 100% (v/v) precipitated for 10-15 min at room temperature, centrifuged at maximum speed for 20 min, washed with 250 µl 70% EtOH and dried by letting stand the open tubes on the bench for 30 min (approximately).

*Sequencing process:*

This step was carried out in the Automatic Sequencing Service of the STSU (Scientific Technical Support Unit of VHIR). The DNA sequencing was based on Sanger technology, through Applied Biosystems ABI PRISM 3100 Genetic analyzer.

### 1.2.5. PCR product checking on agarose gel

The PCR product was analyzed using an agarose (Ecogen, Agarose standard media, EEO-A3 0220) electrophoresis gel, the agarose percentage of which depends on the size (bp) of the fragment to analyze. The PCR product samples were treated with BioLine loading buffer stop solution (cat. n° BIO-37045). The gels were stained with 5 µg/ml EtBr solution Applichem 1%, 25 ml (A1152.0025). The samples were loaded in the wells as well as a molecular weight marker BioLine Hyperladder I, 100 lanes (cat. n° BIO-33024) and run under an electrophoresis source Bio Rad Power PAC 300 at 90-100 V.

Gels were read in a Bio-Rad Universal Hood II (S/N 765/02847) under ultraviolet light, and the image was processed and save using Gel Doc XR software.

### 1.3. Purification and ligation of DNA bands from agarose gels

#### *Purification:*

In order to recover the amplified fragment all the PCR product was electrophoresed through a 1% agarose gel stained with EtBr 5 µg/ml, optimum conditions to be able to separate the DNA band from the gel. DNA was purified from the bands using GE Healthcare: Illustra™ GFX™ PCR DNA and Gel Band Purification kit (Product No. 28-9034-71), a UV light lamp (LKB Bromma 2011 Macrovue Transilluminator cat. no. 2001-002) and an appropriate mask to work under UV light (Pulsafe Clearways Model CV83P D 166 1-B3), following the manufacturer's instructions.

#### *Ligation:*

Using Invitrogen TOPO TA-cloning® kit pCR® 2.1-TOPO® Vector (Part no. 45-0641) and ROCHE Rapid DNA ligation kit ref.: 11 635 379 001. This kit works for purified PCR product bands from agarose gels (Illustra™ GFX™ PCR DNA and Gel Band Purification Kit GE Healthcare ref.: 28-9034-71). The process took place following the manufacturer's instructions.

## 2. Expression analysis techniques

### 2.1. RNA preparation

#### 2.1.1. RNA isolation

Total RNA was isolated both from cell pellets and tissue samples using QIAGEN RNeasy Mini Kit (ref. 74104). RNA from cell pellet samples (using half a pellet from a 10 mm culture plate), kidney and liver (30 mg/sample) was extracted according to the manufacturer's instructions and always treated with Qiagen RNase-free DNase Set (cat. no. 79254). RNA from inguinal white adipose tissue (100 mg) was also isolated with this kit, but samples were pre-treated with organic solvents in order to remove lipid residues that could interfere with the outcome of further techniques.

#### 2.1.2. Quantitative analysis of RNA

The RNA concentration was determined by spectrophotometry using a Nucliber NanoDrop Technologies ND-1000 spectrophotometer and adding 1.5 µl of sample. The purity of RNA was assessed by absorbance ratios 260/280 nm (1.9-2.1) and 230/260 nm (1.8-2) obtained by spectrophotometry.

#### 2.1.3. Qualitative analysis of RNA

The RNA quality was assessed by 2 different methods, the latter confirming as well the RNA concentration:

#### *Agarose gel:*

The state of degradation of RNA was verified by the presence of ribosomal RNA by electrophoretic separation at 100 mV for 30 min in a 1.5% agarose gel with 50 ml TAE buffer and stained with 5 µg/ml EtBr. The gel was read in a BioRad UV hood Universal Hood II.

Intact total RNA run on a denaturing gel will have sharp, clear 28S and 18S rRNA bands in eukaryotic samples. The 28S rRNA band should be approximately thrice as intense as the 18S rRNA band (3:1) (fig. 5, lane 3).

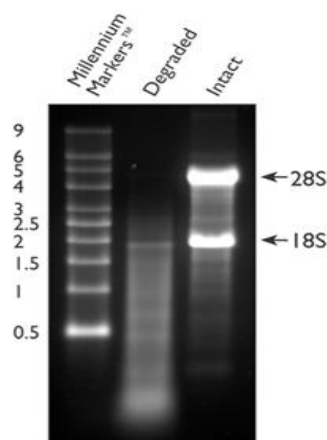


**Figure 5.** Intact vs. degraded RNA. 2  $\mu$ g of degraded total RNA and intact total RNA were run as well as Ambion's RNA Millennium Markers™ on a 1.5% agarose gel. The 18S and 28S ribosomal RNA bands are visible in the intact RNA lane while degraded RNA appears as a lower molecular weight smear.

Picture obtained from [www.invitrogen.com/site/us/en/home.html](http://www.invitrogen.com/site/us/en/home.html)

#### *Agilent 2100 Bioanalyzer:*

The Agilent 2100 bioanalyzer uses a combination of microfluidics, capillary electrophoresis, and fluorescent dye that binds to nucleic acid to evaluate both RNA concentration and integrity. An RNA reference standard (the RNA 6000 Ladder cat# 7152; Ambion) and a microfluidics chip (The RNA Lab Chip; Agilent Technologies) are also required.

### **2.2. RT-PCR**

Reverse-transcription Polymerase Chain Reactions (RT-PCRs) using RNA from cultured cell pellets and from several animal solid organs in order to obtain cDNA for gene expression assays were performed under standard conditions using the following different kits for the different purposes:

#### **2.2.1. RNA from animal solid tissue for endogenous genes checking for microfluidic cards**

400 ng RNA were retrotranscribed using Applied Biosystems High Capacity cDNA Reverse Transcription Kit, Part. Number 4368814, following the manufacturer's instructions.

#### **2.2.2. RNA from animal solid tissue for microfluidic cards**

1  $\mu$ g RNA was retrotranscribed using Applied Biosystems High Capacity RNA-to-cDNA Master Mix (50 rxn), Part. Number 4390777, following the manufacturer's instructions.

#### **2.2.3. RNA from cell pellets for NF $\kappa$ B RT-PCR profiler**

RNA from half a pellet of 100 mm cell culture plates was retrotranscribed to cDNA using SABiosciences™ RT<sup>2</sup> First Strand Kit cat. no. 330401 following the manufacturer's instructions.

### **2.3. Real Time PCR**

Real time quantitative PCR was used to amplify a certain cDNA (coming from RNA RT-PCR) target region allowing to view the increase in the amount of RNA (being inversely equivalent to the expression levels) of this target region in the different samples as it was

amplified. The template standard was used either with the Taqman probe based method or the SYBR Green method depending on the purpose of the Real Time PCR. Real Time PCR was performed under standard procedure and took place in an Applied Biosystem, 7500 Real Time, PCR system, using Applied Biosystems MicroAmp™ Optical 96-Well Reaction Plate with Barcode (code 128), Part. No 4306737, and Applied Biosystems transparent film, part. n° 4311971, for Real Time.

All Real Time PCR results were analysed with 7500 SDS software according to the  $2^{(-\Delta\Delta Ct)}$  method to determine the relative change/fold difference of a mRNA target in a test sample relative to that in the calibrator sample. This method uses the values of Ct or crossing points of each transcript for the mathematical analysis. The Ct or threshold cycle is defined as the point at which the fluorescence of the fluorescent cDNA significantly exceeds the background signal. Assuming 100% PCR efficiency, the number of amplicons doubles with every PCR cycle. Thus the difference of 1 Ct equals to 2-fold difference in copies:

$$\text{Fold change} = 2^{-\Delta\Delta Ct}$$

$$\Delta Ct = (Ct_{\text{gene of interest}} - Ct_{\text{reference gene}})$$

$$\Delta\Delta Ct = (\Delta Ct_{\text{condition of interest}} - \Delta Ct_{\text{basal condition}})$$

### 2.3.1. Search of best endogenous (housekeeping) genes for the microfluidic cards

For the study of endogenous genes for the microfluidic cards assay Real-Time PCR reactions were performed using Applied Biosystems SYBR® Green PCR Master Mix (Part. Number 4309155) by diluting 1/50 the cDNA obtained from the retrotranscription of 400 ng of RNA, since preliminary tests had shown that this was the best concentration of samples for these assays. The sequence of the primers that were tested (18S, CypA (also known as Ppia), β-actin, lamin, and GAPDHs 36B4) is shown in the table below. To conduct these preliminary tests the cDNA of half the kidney and liver hfd experiment samples were used (n = 15).

	Gene	5'-3' Sequence
Fw	PPIA (CypA)	CAAGACTGAATGGCTGGATG
Rv	PPIA (CypA)	ATGGGGTAGGGACGCTCTCC
Fw	GAPDH	TCAACGGGAAGCCCATCA
Rv	GAPDH	CTCGTGGTTCACACCCATCA
Fw	B-actin	GGTCATCACTATTGGCAACGAG
Rv	B-actin	GTCAGCAATGCCTGGGTACA
Fw	36B4 (Rplp0)	CTGTGCCAGCTCAGAACACTG
Rv	36B4 (Rplp0)	TGATCAGCCCGAAGGAGAAG
Fw	18S	AGGGTTCGATTCCGGAGAGG
Rv	18S	CAACTTTAATATACGCTATTGG
Fw	LaminA	GTGTGGCGGTAGAGGAAGTCG
Rv	LaminA	AGTCAGTAGGGGGGCTATGGG

The reagents were loaded as shown below:

RT Reagents	V ( $\mu$ l/reaction)	Cf
10x SYBR <sup>®</sup> Green Master Mix	10	1x
10 mM primer F	1	1 mM
10 mM primer R	1	1 mM
RNase free H <sub>2</sub> O	6	-
cDNA/well	2	-
Vf	20 $\mu$ l	-

The reactions were carried out in an Applied Biosystems 7500 Real Time PCR System in the following conditions:

		40 x		
50 °C	95 °C	95 °C	60 °C	72 °C (*)
2 min	10 min	20 sec	20 sec	34 sec

A phase of separation to check that there were no contaminating DNA primer dimers was also added (15 sec at 95 °C, 1 min at 60 °C and 15 sec at 95 °C). After the reaction had ended, the results were analyzed with 7500 SDS Software.

### 2.3.2. Real Time qPCR

Differential expression assays by Real Time PCR using a conventional TaqMan probe for Lamin A gene (Mm00497783\_m1, 18 mM to 5 mM and the primer for the probe) pre-test were conducted to confirm that all samples had similar Ct to this housekeeping gene, and to check that the fact of having used a different reaction kit to search for the endogenous did not vary the results. Real Time PCR reactions were prepared using Applied Biosystems TaqMan Universal<sup>®</sup> PCR Master Mix, Part. Number 4304437, reagents were loaded according to the manufacturer's instructions as shown in the table below:

Real Time reagents	V ( $\mu$ l/reaction)	Cf
5x Master Mix	10	1x
Lamin A Taqman Probe	1	-
RNase free H <sub>2</sub> O	5	-
Sample cDNA	4	50 ng
Vf	20	

Master mix was prepared and distributed in 96-well plate MicroAmp <sup>™</sup> Optical 96-Well Reaction Plate with Barcode from Applied Biosystems (Part No. 4306737) 16  $\mu$ l per well, and 4  $\mu$ l from each cDNA sample (50 ng) were added per well. The reaction was conducted in the Applied Biosystems 7500 Real Time PCR System according to the following conditions:

Step	UDG incubation	Ampli Tag Gold	PCR	
	Hold	Hold	40 CICLES	
Time	2 min	10 min	Denaturing	Extension
Temperature (°C)	50	95	15 sec	1 min
			95	60

Real Time PCR results were analysed with 7500 SDS software according to the  $2^{(-\Delta\Delta Ct)}$  method.

**2.4. Microfluidic cards**

Microfluidic cards are 384 wells cards that enable to perform Real time quantitative PCR to amplify a certain cDNA (coming from RNA RT-PCR) target region allowing to view the increase in the amount of RNA (being inversely equivalent to the expression levels) of this target region in the different samples as it is amplified (fig. 6). The reference of the cards used in this study is Applied Biosystems Taqman® Low Density Array, format 32, Part. N 434799G. Each well is preloaded with different Taqman probes, allowing the analysis of the expression of 32 genes at the same time in 4 sample cDNA per card by very sensitive Real Time PCR reactions.

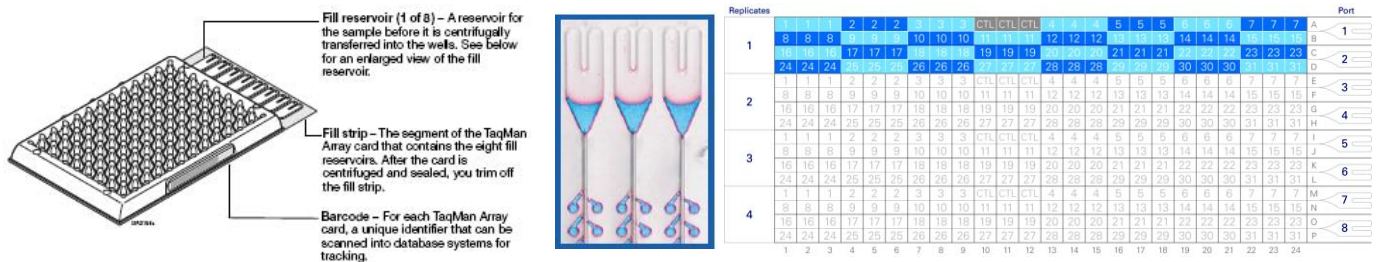


**Figure 6.** Schematic view of a microfluidic card (left), the loading port (middle) and the distribution of the genes (right).

Housekeeping Taqman® probes commercially loaded in certain wells in order to be able to normalise RNA expression results with reference genes’ expression and compare quantity and quality of RNA of each sample. These are the genes known as endogenous genes, their identification comes from the previously detailed study (search of endogenous genes) and their expression should not vary among the different samples.

- Loading and development of the cards: the loading of the different samples was randomised among the cards in order to ensure that no samples from one same experimental group were loaded in the same card or in the same position of a different card. Cards were loaded and centrifuged in a Heraus Multifuge 3L (2 times during 1 min at 1200 rpm). After centrifuging, cards were sealed with a special sealer for microfluidic cards and they were processed in an Applied Biosystems 7900HT Real-Time PCR System (were the reactions took place).

- Analysis of results: the microfluidic cards results were analysed by the  $2^{(-\Delta\Delta Ct)}$  relative quantification method.

The best endogenous genes were sought among those included commercially in the cards using DataAssist™ software v. 2.0, so that the data were corrected using the geometric mean of the more stable endogenous genes (GAPDHs, CypA and  $\beta$ -actin).

### 2.5. RT-PCR Profiler

RT<sup>2</sup> Profiler PCR Array Systems from SA Biosciences analyse expression of a panel of genes associated with a certain biological pathway. They are primer assays comprised of qRT-PCR primer sets for genes of different genomes. These qPCR primer assays are ready-to-use for gene-by-gene expression analysis, microarray data validation, biomarker discovery and siRNA knock-down verification. RT<sup>2</sup> qPCR assay uses an instrument-specific PCR master mix and an optimised first strand synthesis kit. The system combines SYBR® Green detection real-time quantitative PCR with microarray multiple gene profiling.

The PCR array is a 384-well plate containing RT<sup>2</sup> qPCR primer assays for a set of 84 related genes, five housekeeping genes and three different controls, each arranged as 4 replicates.

The Mouse NF $\kappa$ B Signalling Pathway RT<sup>2</sup> Profiler™ PCR Array profiles the expression of 84 key genes related to NF $\kappa$ B-mediated signal transduction. The array includes genes that encode members of the Rel, NF $\kappa$ B, and I $\kappa$ B families, NF $\kappa$ B-responsive genes, extracellular ligands and receptors that activate the pathway, and kinases and transcription factors that propagate the signal. NF $\kappa$ B-mediated signal transduction has been implicated in the regulation of viral replication, autoimmune diseases, the inflammatory response, tumorigenesis and apoptosis.

Material required:

- Qiagen RNeasy Mini Kit cat. no. 74104: for RNA purification from cell pellets, and Qiagen RNase-Free DNase Set cat. no. 79254 for DNase digestion recommended during RNA purification.
- SA Biosciences™ RT<sup>2</sup> First Strand Kit cat. no. 330401: for first strand cDNA synthesis.
- SA Biosciences™ RT<sup>2</sup> Profiler™ PCR Array Mouse NF $\kappa$ B Signalling Pathway Cat. No. PAMM-025E-4 primers preloaded plates.
- SA Biosciences RT<sup>2</sup> SYBER Green / ROX qPCR Master Mix Cat. No. PA-012-12

The experimental procedure overview is the following (fig. 7):

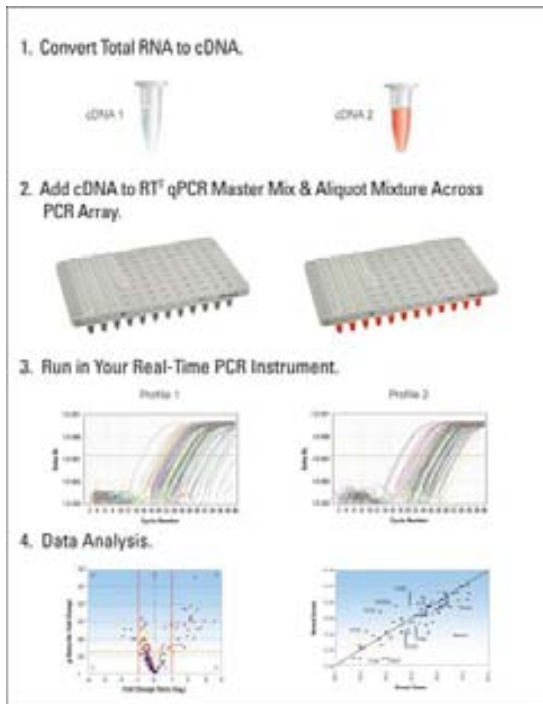


**Figure 7.** Schematic view of the steps followed to carry out RT-PCR profiler assay. Scheme obtained from [www.sabiosciences.com](http://www.sabiosciences.com)

- Loading and development of the plates: the loading of the 4 plates was carried out distributing each one of the replicates of the 4 different experimental samples into one of each of the 4 plates, so that every plate carried one of the 4 replicates of each experimental sample. Plates were loaded and sealed with a special sealer for 384-wells RT-PCR profiler plates. They were centrifuged in a Du Pont Sorvall® RT 6000D Multifuge (during 1 min at 1200 rpm). After centrifuging, plates were processed in an Applied Biosystems 7900HT Real-Time PCR System (where the reactions took place).

- Analysis of results: the RT-PCR profiler plates results were analysed by the  $2^{-\Delta\Delta Ct}$  relative quantification method.

The best endogenous genes were sought among those included commercially in the cards using DataAssist™ software v. 2.0, so that the data were corrected using the geometric mean of the more stable endogenous genes (GAPDHs, CypA and  $\beta$ -actin).

### 3. Protein analysis and proteomic techniques

#### 3.1. Protein isolation

##### 3.1.1. Protein isolation from cell pellets

Protein isolation was performed using RIPA buffer in a final volume of 50  $\mu$ l for 24 wells plates pellets, 100  $\mu$ l for 6 wells plates pellets and 500  $\mu$ l for half a pellet of 10 cm plates using the following procedure:



*RIPA BUFFER PROTEIN ISOLATION*

**Reagents:**

- RIPA Lysis Buffer:  
 - 50 mM Tris-Cl pH 7.5  
 - 150 mM NaCl  
 - 1 mM EDTA  
 - 1% NP40  
 - 0.5% Sodium deoxycholate  
 - 0.1% SDS

Before use add:

- 1 mM PMSF or 0.5 mg / ml Pefabloc SC (Roche, Cat. No. 11 429 868 001).
- Protease inhibitor cocktail (Sigma, Cat. No. P8340) (dilution according to what is stated by the manufacturer).

**Procedure:**

1. Resuspend cell pellet with a micropipette.
2. Lyse extracts using insulin syringes; pull the extracts about 5 times through the syringes being careful not to produce foam.
3. Incubate for 30 min on ice.
4. Centrifuge 30 min at 4 °C at maximum speed.
5. Recover the supernatant and transfer to a new eppendorf.
6. Short term storage: -20 °C, long term storage: -80 °C.

**3.1.2. Protein isolation from animal solid organs**

Protein isolation from animal solid tissue (kidneys) was carried out through the use of the urea/CHAPS buffer in order to quantify the levels of KAP in the animals' kidneys.

*UREA/CHAPS BUFFER PROTEIN ISOLATION*

Before starting, the following considerations must be taken into account:

- Keep the sample at -80 °C until processed.
- All steps with the lysis buffer UREA-Chaps are carried out at room temperature (RT).

**Reagents and materials:**

- Plunger homogenizer or blue sticks
- 1 ml syringes, 27Gs needles
- Sonicator (Heat Systems Microson TM Ultrasonic cell disruptor XL 2005, series no. Serie M1390) and headphones
- Lysis buffer Urea-Chaps:

Urea	8 M
Chaps (*)	4 %
Tris Base	40 mM

(\*) Sigma-Aldrich Chaps, Sigma Ultra, minimum 98% TLC (ref.: c5070-5G).  
 Buffer may be aliquoted and stored at -20 °C.

**Procedure:**

1. Add 1 ml to 50 mg tissue, usually this is half a kidney.  
 Either, a) Mix the kidney with the lysis buffer using a plunger homogenizer.  
 Transfer the sample to a new eppendorf.  
 Or, b) mix the kidney in 1 ml of lysis buffer in the same eppendorf with blue sticks and then pull the samples several times through the syringes until they look homogenized.
2. Sonicate at an approximate power of 17, this step is done in ICE, sonicate samples for 6 pulses of 3 sec 10 sec of rest between pulses.
3. Incubate for 1 hour at RT.
4. Centrifuge at 14000 rpm 1 hour at 20 °C.
5. Transfer the supernatant to a new eppendorf (the pellets will not move much).
6. Aliquote samples.
7. Short term storage: -20 °C, long term storage: -80 °C.

### 3.1.3. Protein quantitative analysis

The protein quantification was performed using two methods in order to ensure accuracy on the concentration estimation:

- The BioRad spectrophotometer SmartSpec™ Plus by Lowry method, BioRad kit (ref: # 500-0114), performed following manufacturer's instructions.
- The BCA method, Thermo Scientific Pierce® BCA Protein Assay Kit (Cat. No. 23225), based on the use of bicinchoninic acid (BCA) for colourimetric detection and quantification of total protein, was performed according to manufacturer's instructions.

### 3.2. Sample concentration

Urine proteins were concentrated in order to be able to detect low molecular weight proteins using 3 kDa pore Amicon filters, Millipore UFC500396, under standard conditions following the manufacturer's instructions.

### 3.3. Immunoblotting or Western blot analysis

This technique allows analysing proteins in a three steps procedure where, proteins are first separated according to their molecular weight on an SDS-PAGE where they are denatured in order to easily migrate through the polyacrylamide under an electric field; on second place, proteins are transferred, also under an electric field, to a PVDF membrane where they may be finally detected through the use of specific antibodies.

Protein extracts both from cells and solid tissue were electrophoresed on SDS-PAGE 10% or 12% acrylamide (depending on the molecular weight of the protein of interest) gel and then transferred to PVDF membranes (Whatmman Westram, Item No.: 10413096, Pore size: 0.2 microns). These membranes were blocked and probed following the conditions detailed in antibodies table at the end of this procedure. The immunoblotting was performed following the steps below:

#### *PROTEIN ANALYSIS THROUGH SDS-PAGE AND WESTERN BLOT*

##### **1st. Polyacrylamide gel electrophoresis (PAGE):**

- Preparation of the protein samples: at the desired concentration in 3x Laemli sample buffer or 5x TMR buffer; in either cases, the final concentration of buffer will be 1x.

3x Sample (Laemli) buffer:  
 10 ml  
 0.5 M Tris-HCl pH 6.8    3.76 ml  
 SDS                            0.6 g  
 Glycerol                      3 ml  
 2-BMercaptoEtOH        1.5 ml  
 mQ H<sub>2</sub>O                      1.74 ml

For 5 ml buffer, add 30 µl bromophenol blue 1%

5x TMR buffer:  
 Sucrose 0.5 M  
 SDS 10%  
 Tris/HCl 312.5 mM  
 EDTA 10 mM  
 DTT 250 mM  
 Bromofenol Blue 0.05 %

##### **- Procedure:**

1. Prepare 5x SDS electrophoresis buffer:  
 1 l

## MATERIALS AND METHODS

Tris base 15.1 g  
Glycine 72 g  
SDS 5 g  
mQ H<sub>2</sub>O up to 1 l  
Dilute with mQ H<sub>2</sub>O 1:5 to reach concentration of use. 2 gels = 0.5 l.

2. Prepare polyacrylamide gels according to the table below. Prepare 2 different types of gels: first separating or running (in which the acrylamide concentration will vary depending on the size of the protein of interest), and second, stacking or concentrating.

Separating gel:

	Acrylamide Cf (%)	
Stock solutions	10	12
H <sub>2</sub> O ml	6.25	5.25
4X Tris/SDS pH 8.8 ml	3.75	3.75
30% acryl/0.8% bis ml	5	6
10% PA $\mu$ l	50	50
TEMED $\mu$ l	10	10

Stacking gel:

H <sub>2</sub> O	3.05 ml
4x Tris-HCl/SDS pH 6.8	1.25 ml
30% acryl/ 0.8% bis	0.65 ml
10% PA	25 $\mu$ l
TEMED	10 $\mu$ l

3. Arrange the electrophoresis assembly.

4. Cover gels with 1x electrophoresis buffer.

5. Denaturing of the protein samples:

Depending on the buffer used to isolate the proteins, denaturing process will take place according to the following conditions:

- 5 min at 100 °C (e.g.: RIPA buffer)

- 2-3 h at RT (e.g.: Urea/Chaps).

6. Load samples to the wells of the acrylamide gel.

7. Run the gels at 20 mA/gel and RT using BIO RAD Power PAC 300 electrophoresis source until the blue front reaches the lower end of the gels.

### **2nd. Electroransference:**

**- Procedure:**

1. Prepare transference buffer:

	2 l	Cf
Tris base	45.81 g	50 mM
Glycine	217.5 g	386 mM
SDS 20 %	37.5 ml	0.1%
mQ H <sub>2</sub> O up to	2 l	

Dilute with mQ H<sub>2</sub>O 1:3 to reach concentration of use. 2 gels = 1 l.

Add 20% of MetOH to the final solution.

2. Activate PVDF Westran® S (Item No.: 10413096 Whatman™) membrane sinking it in MetOH during 5-10 sec.

3. Wash membranes with distilled H<sub>2</sub>O 3 times.

4. Balance membrane in transference buffer.

5. Arrange the transference “sandwich” following the scheme below:

10. TRANSPARENT SIDE (top)

9. Sponge

8. Whatmman paper

7. Whatmman paper

6. Membrane

5. Gel

4. Whatmman paper

3. Whatmman paper

2. Sponge

1. BLACK SIDE (bottom)

6. Cover with MetOH-transference buffer 1x and place cubette on a shaker.

7. Transfer using a BIO RAD Power PAC 300 electrophoresis source (fig. 12) at the following conditions:

Shaker: intermediate power.

Transference: 1h30min 400 mA at RT

o/n at 70 mA at 4 °C

### **3rd Immunoblotting of the membranes with antibodies:**

1. Block the membranes to avoid unspecific unions of the antibodies and according to the specific conditions required by each primary antibody.

2. Dilute primary antibody in blocking solution and incubate at temperature and for time specifically required by this antibody.

3. Wash 3 times with PBS1x tween 0.1% 10-15 min/wash depending on the efficiency of the primary antibody.

4. Dilute secondary antibody in blocking solution and incubate at temperature and for time specifically required by this antibody.

5. Wash 3 times with PBS1x tween0.1% 10-15 min/wash.

6. Develop through the use of ECL (Amersham-Pharmacia, Cat: RPN 2106) or more sensitive ECL Plus (Amersham-Pharmacia, Cat: RPN 2132) detection system following the manufacturer's instructions. Films:  
Blue films (AGFA, AGFA Medical X-RAY FILM BLUE, Ref.: EA78W), less sensitive  
Grey films (Amersham, Amersham Hyperfilm™ ECL, Product code 28906836), more sensitive.

7. Scan the films with a GS-800 Calibrated Densitometer and analyse them with Quantity One software.

8. Dehybridation (or stripping) of the PVDF membranes:  
- Incubate with abundant NaOH 1 m for 1 min.  
- Wash the membrane with PBS1x Tween 0.1%.

Antibodies used in this study and their corresponding working conditions:

	ANTIBODY	ORIGIN (mono/policlonal)	SUPPLIER REFERENCE	WESTERN BLOT CONDITIONS		
				Blocking solution	Working concentration	Incubation
<b>PRIMARY</b>	Anti-KAP1/2	Rabbit (policlonal)	Non commercial	PBS1xTween 0.1%+1% milk	1/250	o/n at 4°C
	Anti-MAPK	Rabbit (policlonal)	Upstate 08-182	PBS1xTween 0.1%+1% milk	1/1000	o/n at 4°C or 1 h at RT
	Anti-actin	Rabbit (policlonal)	Santa Cruz Biotechnology	PBS1xTween 0.1%+1% milk	1/1000	o/n at 4°C or 1 h at RT
	Anti-HA	Rat (policlonal)	Santa Cruz Biotechnology	PBS1xTween 0.1%+1% BSA	1/500	o/n at 4°C or 1 h at RT
<b>SECONDARY</b>	Anti-rabbit*	Goat (policlonal)	DAKO P0448	-	1/5000	1 h RT
	Anti-rat*	Goat (policlonal)	SIGMA A9037	-	1/5000	2 h RT
	*Peroxidase conjugated					

### 3.4. Two dimensional (2D) analysis

Bidimensional or two dimensional electrophoresis or 2D is the most used technique to analyse complex mixture of proteins from animal tissues, cell cultures or biological samples. It comprises two stages: the first one is based on an isoelectric proteomic separation and the second one is based on SDS-PAGE molecular weight separation. Proteins are identified through mass spectrometry.

Proteomics analysis was carried out to 5 h morning fasted animal serum pulls through bidimensional electrophoresis (2D) using an IPGphor system.

Collection of the samples:

Serum samples were obtained from living animals, after a morning 5 h fasting. Total blood was collected in BD Microtainer® SST™ Amber Tubes (ref. 365979). After serum separation, samples were pulled to reach a final volume of 100 µl per experimental group and frozen at -20 °C.

*BIDIMENSIONAL ELECTROPHORESIS USING AN IPGPHOR SYSTEM*

**1<sup>st</sup> First dimension: IEF in IPGphor**

Isoelectric focusing is based on the migration of proteins through a pH gradient when connecting to an electric source. Proteins will migrate to the isoelectric point which is equal to their own pH.

**Reagents:**

- 24 cm pH strips
- Rehydration solution:

Reagent	Cf
Urea	8.5 M
Chaps	2 %
IPG buffer (of same pH range as the strip)	0.5 % (IPGphor system)
SDS Bromophenol blue	0.002 %
mQ H <sub>2</sub> O	

- DTT

**Procedure:**

1. Add DTT (0.28%) to the rehydration solution.
2. Prepare protein samples by diluting them in rehydration solution: add to the 500µl of rehydration solution 2D2 the quantity of sample in lysis solution necessary to obtain the desired protein concentration: 50 µg of protein for ordinary silver, silver 150 µg for masses and for 500-1000 µg coomassie.
3. Load the sample in the center of the strip holder.
4. Carefully place the strip on the proteic suspension with the barcode (anodic +) at the pointed end of the strip holder and the gel face to face with the bottom of the strip holder, move it forward and backward to impregnate the gel and place the strip into the receptacle.
5. Add several drops of IPG Cover Fluid on the strip until it is completely covered (to prevent evaporation). Cover the strip holders with the corresponding lids.
6. Place the sarcophagi on IPGphor as indicated in the diagram drawn in the apparatus. Isoelectric focusing conditions vary depending on the strip length, for linear strip pH3-10 are as follows (program: L 24 cm strip std). The IEF conditions are:

Steps	Voltage	Time	Ramp
1	Rehydration 500	10+ x h 1 h	step gradient gradient step
2	1000	1 h	
3	8000	3 h	
4	8000	7 h	

Total: 22h+x

Arrange 50 µA per strip and 20 °C for both IEF and rehydration.

Rehydration time will be 10h minimum, but it can be increased to 18h according to the needs (press Edit button to edit and modify with arrows).

7. After the IEF, SDS-PAGE can be performed immediately or strips may be frozen to -80 °C in closed tubes, placing the plastic side against the tube wall.

**2<sup>nd</sup> Second dimension: SDS-PAGE**

**Reagents:**

- Balancing solution:

Reagent	Cf
Tris 1.5M pH 8.8	50 mM
Urea	6 M
Glycerol (87 %)	30 %
SDS	2 %
Bromophenol blue	0.002 %
Deionised H <sub>2</sub> O	

- 30% acrylamide/0.8% bisacrylamide (Bio-Rad)

- Gelification buffer:

Reagent	Cf
Tris	1.5 M
Deionised H <sub>2</sub> O	

- APS

- 10% SDS

- Electrophoresis buffer:

Reagent	Concentration 10x
Tris base	250 mM
Glycine	1.92 M
SDS	1%
Deionised H <sub>2</sub> O	

- Sealling solution:

Reagent	Cf
1x Electrophoresis buffer	-
Agarose	0.5 %
SD6 Bromophenol blue	0.002 %

**Procedure:**

1. Prepare the gels according to the table below:

Reagents	12.5 % gel		
PAGE1	187.5 ml	145.8ml	104.2ml
PAGE2	112.5 ml	84.5ml	62.5ml
H <sub>2</sub> O	145.5 ml	113.5ml	80.8ml
SDS 10%	4.5ml	3.5ml	2.5ml
PAGE5	225mg	175mg	125mg
TEMED	225µl	175µl	125µl
Vol.	450 (6 gels)	350 (4)	250 (2)

Incubate under mild shaking and degassing under vacuum for 15 min.

While still shaking, add the catalysts: APS and TEMED. Shake for 30 sec and use immediately. Carefully add 1 ml H<sub>2</sub>O saturated isobutanol to each glass. Once polymerized (at least 1 h), remove i-butanol and the excess of acrylamide and wash 3 times with PAGE2 buffer diluted 1:4 with H<sub>2</sub>O.

2. After IEF, balance the strips: add DTT (100 mg per 10 ml of solution) to to half of the aliquots of Amersham balancing tubes: balancing solution (reductive solution), and iodoacetamide alkylant solution (400 mg per 10 ml) to the remaining half of aliquots. Shake. The strips are balanced with 5 ml of solution.

3. Place each strip in an Amersham balancing tube for 24 cm, with 5 ml of reductive balancing solution, and cover. Place the tubes in a horizontal position on the orbital shaker for 15 min. Change reductive balancing solution for 5 ml of the alkylant balancing solution. Shake for 15 min more.

4. Wash the strips with electrophoresis buffer (in a balancing tube) and place on the SDS-PAGE gel, so that the face of the IEF strip without gel sticks to the rear glass and IEF gel looks to the operator. Place the strip anode (barcode) to the left of the operator and touching the spacer.

5. With the help of a flat spatula, press down the strip so that the strip gel and the SDS-PAGE gel are in contact.

6. Seal the system with 60 °C pre-warmed agarose.

#### 4. Histochemistry and other tissue methods

##### 4.1. Tissue extraction and conservation

Animals were anaesthetised with ABBOTT Forane®, isoflurane 250 ml (ref.: 880393.4) and sacrificed by pleural scission. Fresh tissues were removed from the animals and immediately placed in histology cassettes (biopsy processing / Embedding cassettes Simport M499 - Histosette® I) and sunk in formalin (Sigma F-8775) 4% PBS 1x for fixing.

7. Preparation of the EttanDALT six tray: Add 450 ml of 10x electrophoresis buffer and 4 l of H<sub>2</sub>O to the LBC. Start pump and thermostat and let it mix. Assemble cassettes in the electrophoresis cubette. Place the upper buffer chamber (UBC). Add 0.8 l of 2x electrophoresis buffer to UBC (160 ml 10x electrophoresis buffer and 640ml H<sub>2</sub>O). Add 1x buffer to LBC to match UBC and LBC levels.

8. Electrical conditions for EttanDalt6: 2.5 W / gel 30 min + total 100W until shortly before the blue leaves the gel (6 gels take about 4 h). The Multitemp must be at 10 °C.

9. After the electrophoresis is finished, remove the cassettes from the cubette and stain either with colloidal Coomassie blue as follows.

#### **3<sup>rd</sup> Colloidal Coomassie blue staining:**

##### **Reagents:**

1. Colloidal Coomassie fixative solution
  - 500 ml EtOH
  - 30 ml 85% orthophosphoric acid
  - MQ H<sub>2</sub>O up to 1 l
2. “Blue silver” colloidal Coomassie Candiano, Electrophoresis 2004,25,1327
  - To 100 ml of mQ H<sub>2</sub>O add under shaking, sequentially and until complete dissolution each of the following components:
    - 100 ml orthophosphoric acid
    - 100 g ammonium sulphate
    - 1.2 g of Coomassie Brilliant Blue G-250
    - Add up to 800 ml MQ H<sub>2</sub>O.
    - While still shaking, add 200 ml of MetOH. A greenish solution will appear that is stable for more than 6 months at RT.

##### **Procedure:**

- Fix from 1 h to o/n with coomassie fixative solution.
- Wash 3x 20 min with H<sub>2</sub>O.
- Stain with bluesilver for 3-4 days.
- Fade with H<sub>2</sub>O 3x 20 min or until disappearance of background.

Samples were kept in 4% formalin 4 °C for 24–48 h, time after which they were washed 3 times with tap H<sub>2</sub>O and kept in PBS 1x 4 °C for no longer than 2 weeks.

### **4.2. Paraffin blocks**

Formalin-fixed tissue samples were embedded in paraffin (Klinipath, Ref. 2079 A Paraclean) after going through a dehydrating process. Dehydration and paraffin embedding took place in a Leica TP 1020 tissue automatic processor.

After this step, samples were included in paraffin blocks using a Leica EG 1150C tissue inclusions, aluminum casts, 62 °C paraffin and a cold (-4 °C) plate. Paraffin embedded tissues were shaped with the aluminum casts while paraffin was melted and let solidify on the cold plate. Once paraffin blocks were solidified, casts were removed and samples were stored at RT.

### **4.3. Paraffin-embedded tissue sections**

Sections were performed using an ultramicrotome. Histology sections were cut at 4 µm slices, treated on a 37 °C distilled H<sub>2</sub>O with jelly (Sigma, 300 bloom) bath and placed on the slides to dry up.

Slides were stored at RT until histochemical staining was performed.

### **4.4. Tissue staining**

Paraffin-embedded tissue section slides were stained with Eosin-Hematoxylin, Masson's trichrome and periodic acid-Schiff according to standard procedures to be able to assess morphological and structural changes in the animal's tissues.

#### *Eosin-Haematoxylin:*

Cytoplasmic and nuclear staining most commonly used for studying the general structure of tissues, in our study: kidney, liver and adipose tissues. Besides, it is the best for observing hypercellularity of the glomerulus, interstitial infiltrate no matter the cell type (mesangial, inflammatory, etc) and is also useful for observing mitochondrial proliferation in the proximal tubule. Reagents used were Harris hematoxylin (Dako ref. S2020) and Eosin (Sigma No. E4382).

#### *Masson's trichrome:*

This staining is used in the study of connective tissue, muscle and collagen fibres, therefore, ideal for viewing sclerosing glomerular damage in kidney and interstitial fibrosis in kidney and liver. Reagents used were:

- Bouin's solution: 71% saturated picric acid solution (Applichem, Darmstadt, Germany) + 24% formaldehyde + 5% acetic acid.
- Weigert's Iron Hematoxylin working solution (Accustain® Trichrome Stains (Masson) Procedure No. HT15, Sigma-Aldrich).

- Phosphotungstic / phosphomolybdic acid working solution (Accustain® Trichrome Stains (Masson). Procedure No. HT15, Sigma-Aldrich).
- Biebrich scarlet-acid fuchsin (Accustain® Trichrome Stains (Masson). Procedure No. HT15, Sigma-Aldrich).
- Aniline blue solution (Accustain® Trichrome Stains (Masson). Procedure No. HT15, Sigma-Aldrich).

### *Periodic acid-Schiff:*

This staining is used for the evidencing of lymphocytes and mucopolysaccharides. In kidney sections it is excellent for detecting tubular damage which deprives the tubular cells from the integrity and continuity of the brush border. Reagents used were periodic acid solution (periodic acid-Schiff (PAS) Staining System. Procedure No. 395, Sigma-Aldrich), Schiff's reagent (periodic acid-Schiff (PAS) Staining System. Procedure No. 395, Sigma-Aldrich), Haematoxylin solution (periodic acid-Schiff (PAS) Staining System. Procedure No. 395, Sigma-Aldrich).

### **4.5. Assembly**

The assembly of the stained slides took place using DPX Mountant for histology (Fluka, BioChemika. Ref. 4458) following standard procedures.

### **4.6. Microscopy observation and image acquiring**

Observation of the sections was carried out by light microscopy using an Olympus microscope BX61 and photography taking using the DP Controller software.

### **4.7. Lipid extraction from frozen liver**

Lipid fraction was separated from mice livers in order to be able to quantify the percentage of lipids in this tissue. This procedure is based on the method described by Folch et al. (Folch J, Lees M, Sloane S GH, J. Biol. Chem.1957 May;226(1):497-509.), using aluminium weighing dishes (Cole-Parmer Cat. No. RZ-01017-41).

## **5. In bacteria methods**

### **5.1. Bacteria cultures**

Bacteria cultures took place both in liquid and solid agar medium. Solid medium cultures were incubated o/n in an appropriate still incubator at 37 °C. Liquid medium cultures were incubated in a Comecta shaker (WY model 100) under medium shaking (200 rpm) and at 37 °C.

### **5.2. Bacteria transformation**

#### **5.2.1. Transformation of competent bacteria from DH5 $\alpha$ TM strain**

The DH5 $\alpha$ TM strain (Invitrogen, cat. no. K4520-01) is not commercially competent; it is made competent in the laboratory.



*TRANSFORMATION OF BACTERIA FROM DH5 $\alpha$ TM STRAIN*

This transformation is done by thermal shock.

**Procedure:**

1. Thaw 100  $\mu$ l bacteria aliquot on ICE, stored at -80 °C.
2. Add 1  $\mu$ l of plasmid solution.
3. Incubate for 30 min on ICE.
4. THERMAL SHOCK: Incubate the bacteria in a Thermbloc at 42 °C for 1 min.
5. V E R Y Q U I C K L Y transfer bacteria vial to ICE.

From here on, it is mandatory to work near a Bunsen burner flame.

6. Add 250  $\mu$ l of SOC medium, which is stored at 4 °C. It should be taken out of the fridge a

while before using it in order to warm it up a bit. If there is no SOC available, standard liquid LB without ampicillin can be used.

7. Incubate for 1h at 37 °C in a Comecta shaker (WY model 100) under medium shaking (200 rpm).
8. Seed on standard LB-ampicillin 10 cm plates: 10  $\mu$ l of bacteria liquid culture per plate by massive seeding. Diluted first in 40  $\mu$ l (approximately) of SOC or standard L B without ampicillin to improve seeding.

Colonies are picked from the 10 cm plate for bacterial growth in Luria-Broth (LB)-agar with **ampicillin 50  $\mu$ g/ml used to seed the product of the transformation and seeded in 5 ml of liquid Luria-Broth (LB)-ampicillin 50  $\mu$ g/ml. Liquid cultures are incubated in a Comecta shaker (WY model 100) at 37 °C and 200 rpm shaking o/n.**

**5.2.2. Transformation of competent bacteria from One-Shot® TOP10 strain**

The product of the DNA purified from a agarose bands ligation product is used to transform bacteria One-Shot® TOP10 strain Invitrogen (44-0301).

*TRANSFORMATION OF COMPETENT BACTERIA FROM TOP10 STRAIN*

After performing the ligation reaction:

**Procedure:**

1. Thaw an aliquot of competent bacterial strain One-Shot® TOP10 in standard ICE, stored at -80 °C.
2. Add 2  $\mu$ l of the ligation product to the aliquot of competent bacteria and mix SLOWLY with the pipette.
3. Incubate for 30 min in carbonic ice (dry ice). This is a minimum time range; the incubation may last for a little longer.
4. THERMAL SHOCK: Incubate the bacteria in a Thermbloc at 42 °C for 30 sec.
5. V E R Y Q U I C K L Y transfer bacteria vial to ICE.

From here on, it is mandatory to work near a Bunsen burner flame.

6. Add 400  $\mu$ l of SOC medium (similar to LB) which is stored at 4 °C. It should be taken out of the fridge a while before using it to warm it up a bit.
7. Incubate for 1h at 37 °C in a Comecta shaker (WY model 100) under medium shaking (200 rpm).
8. Seed on standard LB-ampicillin 10 cm plates. Around 100 -250  $\mu$ l of the transformation products should be sufficient. Antibiotic selection of transformed colonies takes place due to the resistance to this antibiotic contained in the pCR 2.1TOPO plasmid.
9. Incubate at 37 °C O/N.

The following day, colonies that appear are those that have been transformed with the plasmid.

To verify that the transformed colonies contain the insert the most representative ones are selected, harvested and seeded in 5 ml of LB-

ampicillin 50 mg/ml. Liquid cultures are incubated in a Comecta shaker (WY model 100) at 37 °C and 200 rpm shaking o/n.

The presence of the insert is checked by PCR using the universal primers M13-F and M13-R.

## 6. In cell methods

### 6.1. Cell cultures

All cell lines used in this study were kept in a culture incubator (IGO 150 Cell Life, Jouan Thermo Electro Corporation) at 37 °C, 5% CO<sub>2</sub> and saturated atmosphere, and cultured in rich medium containing the essential nutrients needed for cell growth and proliferation while not involved in assays. Cells were seeded in polystyrene multywell plates, Petri dishes or flasks coated for optimal cell growth according to the purpose of the culture.

Medium was renewed every two days, when cells reached confluence they were trypsinized and a fraction was transferred to a new cell culture plate. If the assay was to be performed maintaining confluent cultures for several days, the medium was changed every day.

All material used for cell cultures was either commercially sterile or autoclaved and, liquid reagents used for cell cultures were always pre-warmed at 37 °C.

Chart of recommended volumes according to the plate used for cultures:

	Industry	Cat. No.	Growth surface (cm <sup>2</sup> )	Medium (ml)	1x PBS (ml)	Trypsin (ml)
<b>96 well plate</b>	Sigma-Aldrich	TPP 92096	0.335	0.1	0.1	0.05
<b>24 well plate</b>	IWAKI	1820-024	1.862	1	0.5	0.2
<b>6 well plate</b>	Nunc®	145380	8.962	2	1.5	1
<b>60 mm dish</b>	Nunc®	01930-32	22.1	4	2.5	2
<b>T25 flask</b>	IWAKI	3102-025	25	5	3	2
<b>T75flask</b>	Nunc®	130190	75	9	7	4
<b>100 mm dish</b>	Sigma-Aldrich	TPP 93100	60.1	10	8	6

### 6.2. Cell thawing

Cellular growths are stored in liquid nitrogen containers while not being used and are thawed when assays are to be started.

#### *CELL THAWING FROM LIQUID NITROGEN*

Before bringing the cells from liquid nitrogen, the following material must be prepared.

#### **Materials:**

- A tube with 9 ml of culture medium kept in ICE
- A T25 cell growth flask with 4 ml of culture medium

- Table centrifuge at 4 °C
- H<sub>2</sub>O bath at 37 °C

#### **Procedure:**

1. Take the 2 ml cryovial (Nunc® Cryo Tubes™, Cat. No. 363401) containing the cells

## MATERIALS AND METHODS

from liquid nitrogen and transported to the cell culture room in carbonic ice (dry ice).

2. Thaw the cryovial of cells in a 37 °C bath. Remove from the bath when only a small ball (pea size) of frozen cells is left.

3. Add 1 ml from the 9 which are standing in ice.

4. Resuspend gently with a micropipette to avoid breaking the cells until they have completely thawed.

From here on no ice is necessary.

5. Transfer the thawed cells to the tube containing 8 ml of medium.

6. Centrifuge at 1500 rpm 4 °C 5 min.

7. Discard supernatant.

8. Resuspend pellet in 1 ml of culture medium.

9. Seed the cells in the T25 flask that should be prepared with 4 ml of medium and mix with the pipette.

10. Observe the cells under an optic microscope to check that cells are well separated from each other and homogeneously distributed.

11. Keep cells in a culture incubator (IGO 150 Cell Life, Jouan Thermo Electro Corporation) at 37 °C, 5% CO<sub>2</sub> and saturated atmosphere.

12. Renew the medium the following day.

### 6.3. Trypsinization

When cell cultures reached confluence, cells were trypsinised in order to be reseeded on a new culture plate.

#### *TRYPsinIZATION OF CELLS*

The cell culture must be confluent, otherwise it is very difficult for most cell lines detach from the culture plates.

#### **Material:**

- Standard culture medium for the cells to be trypsinised
- Trypsin-EDTA Solution C vol. 500 ml, Biological Industries Cat. 03-053-1A
- Sterile 1x PBS
- H<sub>2</sub>O bath at 37 °C
- All reagents have to be pre-heated 37 °C

#### **Procedure:**

1. Remove the medium of the plate using a vacuum pump.
2. Wash briefly with sterile 1x PBS.
3. Vacuum the PBS.
4. Add trypsin to cover the cells at the bottom of the plate.
5. Incubate for 2-3 min in the culture incubator (IGO 150 Cell Life, Jouan Thermo Electro Corporation) at 37 °C, 5% CO<sub>2</sub> and saturated atmosphere.

6. Tap the plate gently to help the cells detach from the bottom.

7. Resuspend the cells in the trypsin and transfer to a new 12 ml tube.

8. Add the same volume of standard culture medium of cells to the tube with trypsin and cells. Dilution of trypsin decreases its effect and the foetal bovine serum contained in the culture medium inactivates trypsin.

9. Centrifuge at 1500 rpm 4 °C for 5 min.

10. Vacuum the supernatant and keep the pellet.

11. Resuspend the pellet in a small volume of culture medium.

12. Seed a fraction of this volume in a new culture plate and add the volume of culture medium required depending on the size of the plate.

13. Mix with the pipette.

14. Keep the plates in the incubator (IGO 150 Cell Life, Jouan Thermo Electro Corporation) at 37 °C, 5% CO<sub>2</sub> and saturated atmosphere.

### 6.4. Cell counting

Cultured cells are counted in order to be able to seed a determined number of them in a certain plate.

#### CELL COUNTING

##### Procedure:

Preparation of the samples:

1. Trypsinize cells.
2. Centrifuge them.
3. Discard the supernatant and keep the pellet.
4. Resuspend the pellet adding the volume of medium that is considered appropriate (recommended: 2 or 3 ml for a confluent T25).
5. In a 1.5 ml eppendorf add 90  $\mu$ l of trypan blue + 10 $\mu$ l of resuspended cells (dilution 1:10).
6. Load the two chambers (top and bottom) with trypan blue + cells with a micropipette by inserting a volume of trypan blue + cells between the slide that contains the chamber and the glass cover, the volume enters by capillarity.
7. Count cells using an optic microscope:  
Dark blue colour cells are dead, and bright/shiny light blue are alive (alive cells reject the trypan blue staining).  
The Neubauer chamber has characteristic dimensions to help the estimation of the concentration of cells in the culture (fig. 8).

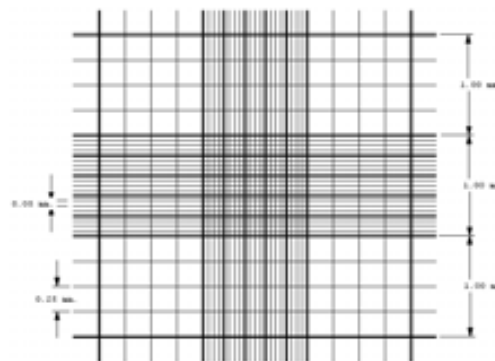


**Figure 8.** Detail of one of the Neubauer's chambers.

(Cells in field 1 + cells in field 2 + cells in field 3 + cells in field 4) / 4 = X

X = mean number of cells in the camera

Conversion factor:

1 mm • 1 mm • 0.1 mm = chamber dimensions  
1/10 dilution performed with trypan blue

(1 mm • 1 mm • 0.1 mm) • (1 dm<sup>3</sup> / 10<sup>6</sup> mm<sup>3</sup>) • (1 l / 1 dm<sup>3</sup>) • (10<sup>3</sup> ml / 1 l) = 10<sup>-4</sup> ml

10<sup>-4</sup> ml = 0.1  $\mu$ l

(X cells /  $\mu$ l 0.1) • 1 / 10 = Cells /  $\mu$ l

### 6.5. Cell freezing

Cells were kept frozen in liquid nitrogen containers for long term storage until further studies. The following procedure needs to be carried out in a laminar flow hood.

#### CELL FREEZING

##### Materials:

- 2 ml Nunc® Cryo Tubes™, Cat. No. 363401
- DMSO (Roth Art. No. 3949)
- A T25 or T75 cell growth flask
- Standard 4 °C cell culture antibiotic-free medium

- Trypsin-EDTA Solution C vol. 500 ml, Biological Industries Cat. 03-053-1A
- Sterile 1x PBS
- Table centrifuge at 4 °C
- Ice

##### Procedure:

1. Add 100  $\mu$ l of DMSO to each 2 ml cryovial (Nunc® Cryo Tubes™, Cat. No. 363401), prepare as many cryovials as needed to freeze the entire cell growth. For small diameter cells, it is recommended to divide 1 T75 flask into 5 cryovials and 1 T25 flask into 2 or 3 cryovials. For large diameter cells, it should be 1 T75 flask into 3 cryotubes and 1 T25 flask into no more than 2 cryotubes.

2. Keep all cryotubes in ice.

3. Trypsinise the cells.

4. Add the suitable cool cell culture medium volume to the cell pellet according to the following list:

Small diameter cells:

T75 flask = 4500  $\mu$ l

T25 flask = 3600  $\mu$ l

Large diameter cells:

T75 = 3600  $\mu$ l

T25 flask = 1800  $\mu$ l

5. Resuspend gently with a micropipette to avoid breaking the cells.

6. Transfer 900  $\mu$ l of cells to the cryotube containing 100  $\mu$ l of DMSO and return the cryotube to the ice.

7. When all cryotubes have been filled, resuspend the frozen DMSO by tapping gently on the side of cryotube.

8. Place the cryotubes on a grid and put the grid into the freezer until liquid is completely frozen (4-8 h).

9. Transfer the grid to -80 °C freezer and keep the cells there for not less than 32 h and no more than 5 days.

10. Finally, transfer all cryotubes to the liquid nitrogen container.

### 6.6. Stable transfection of cells

PCT3 cells were stably transfected either with pBIG2i-KAP vector or pBIG2i empty vector. Transfected clones were selected thanks to the resistance to hygromycin antibiotic of pBIG2i vector.

Cells were kept in a culture incubator (IGO 150 Cell Life, Jouan Thermo Electro Corporation) at 37 °C, 5% CO<sub>2</sub> and saturated atmosphere, and cultured in rich medium for PCT3 detailed above.

Medium was renewed every two days, until the cells reached confluence, when they were trypsinised and a fraction was transferred to a new cell culture plate.

The transfection process was carried out during five days on the following weekly schedule:

Day 1 (Monday):

Three 10 cm plates were seeded with PCT3 cell at passes p101 for the empty vector and p115 for KAP functional variant. Cells were counted as described above:

Plate A: 1.5 x 10<sup>6</sup> cells

Plate B: 2 x 10<sup>6</sup> cells

Plate C: 2.5 x 10<sup>6</sup> cells

Complete medium for PCT3 cells was used in this step.

Day 2 (Tuesday):

The plate that had reached 60% confluence was selected in order to perform the transfection itself using Invitrogen LipofectAMINE™ Reagent (Cat. No.: 18324-020) and Plus™ Reagent (Cat. No.: 10964-021).

12 µg of DNA maxi-preps product of the functional variant of KAP cloned in pBIG2i and the empty vector were transfected respectively, using 30 µl of 20 µl LipofectAMINETM and PlusTM transfected per plate, which are the amounts stipulated by the manufacturer to transfect 10 cm plates cultures as detailed in the procedure below.

Day 3 (Wednesday):

The 10 cm plates were already confluent; they were trypsinised and expanded into four separate 10 cm plates each, seeding the same number of cells on each new plate.

Day 4 (Thursday):

PCT3 rich medium was changed for PCT3 rich medium with the selection antibiotic hygromycin B 400 µg/ml.

Day 5 (Friday):

All non-transfected cells had died, each plate was washed with 1x PBS and the medium was renewed. From this point the culture medium used always contained the selection antibiotic at concentration previously described.

#### *STABLE TRANSFECTION*

##### **Reagents:**

- LipofectAMINETM Reagent (Invitrogen Cat. No. 18324-020) stored at 4 °C
- PlusTM Reagent (Invitrogen Cat. No. 10964-021) stored at 4 °C
- Opti-MEM medium (Gibco) stored at 4 °C
- 1X PBS stored at 4 °C

Prewarm 1x PBS and Opti-MEM in a bath at 37 °C.

##### **Procedure:**

1. Seed an appropriate number of cells in 10 cm culture plates the day before transfection is planned so that the next day they are at 60% confluence.

Transfection day:

2. Prepare A solution:

Dilute DNA in appropriate volume of Opti-MEM (up to 750 µl) and add the appropriate amount of PlusTM reagent (see chart for quantities).

VORTEX

Incubate for 15 min at RT.

3. Prepare B solution:

Dilute LipofectAMINETM reagent in Opti-MEM.

VORTEX.

4. Mix DNA-PlusTM reagent (A solution) with LipofectAMINETM from step 3 (B solution). Incubate for 15 min at RT.

5. Wash the cells with 1x PBS prewarmed at 37 °C.

6. Add the final transfection mixture (A+B) in the necessary volume of Opti-MEM to reach the final volume of transfection.

Distribute the mixture homogeneously across the bottom of the plate.

7. Incubate cells with the complex DNA/lipid (A+B) for 3h in the culture incubator at 37 °C, 5% CO<sub>2</sub> and saturated atmosphere.

8. Remove the transfection solution and wash with 1x PBS.

9. Add normal culture medium: rich PCT3 medium without selection antibiotic.

10. Return plates to the culture incubator.

Chart of volumes according to the plate used for transfection:

Plate	DNA (µg)	PLUS™ (µl)	LipofectAMINE™ (µl)	Vol. A+B sl. (µl)	Vf transfection (µl)
96 well	0.1	1	0.5	10+10	0.07
24 well	0.4	4	1	25+25	0.25
6 well	2	6	4	100+100	1.0
60 mm	5	8	12	250+250	2.5
T25	5	10	15	250+250	2.5
100 mm	12	20	30	750+750	6

### 6.7. Cell clones picking

About 15 days after transfection clones begin to appear and they must be transferred to wells of 96-wells culture plates (see procedure below), then to wells of 24-well plates, then to wells of 6-well plates and finally to T25 flask. When the latter is confluent, cells are separated for testing of the clone, for freezing a portion and for seeding a new maintenance T25 flask.

In this set of experiments aliquots of each cell pass were separated for freezing with the usual culture medium and DMSO (Roth Art. No. 3949) diluted 1/10.

#### *PICKING CELL CLONES USING THE MICROSCOPE*

##### **Procedure:**

1. Locate the clone to pick under a microscope.
2. Change the medium of the plate for serum-free medium.
3. In a 96-well plate, load 50 µl of trypsin to as many wells as clones to pick.
4. Put the microscope inside the hood and place the plate containing the clone to be picked in the hood. Locate this clone under the microscope.
5. Adjust a micropipette to 100 µl, locate the tip by looking through the microscope and place near the clone.
6. Scrape the clone with the pipette tip, pressing the plunger, until all the cells detach, pipette the clone and the medium with the pipette releasing the plunger slowly.
7. Transfer the 100 µl of medium with the cells of the clone to the wells of the 96-well plate loaded with trypsin and resuspend with the pipette.
8. Add 50 µl to this same well of medium used routinely for culturing the cells. This 50 µl must be supplemented with 10 % serum.
9. Remove the medium from the original plate from which the clone was picked, wash 2 times with sterile 1x PBS and add the usual culture medium.
10. Return all plates to the culture incubator at 37 °C, 5% CO<sub>2</sub> and saturated atmosphere.
11. Renew the medium the next day using the usual cell culture medium.

### 6.8. Toxicity assays

The toxicity of both prokaryotic and eukaryotic recombinant KAP on all isolated cell culture models was evaluated using a cytotoxicity detection kit based on the secretion of lactate dehydrogenase (LDH) to the culture medium Roche Cytotoxicity detection kitplus (LDH) (Cat. No. 04744926001) following the manufacturer's recommendations.

### 6.9. Viability assays

The viability and proliferation of all cells used in this work when treated with both prokaryotic and eukaryotic recombinant KAP was also evaluated using a non-reactive quantification but colourimetric quantification assay based on tetrazolium salt XTT ROCHE Cell Proliferation Kit II (XTT) (Cat. No. 11465015001) following the manufacturer's recommendations.

### 6.10. Hoechst staining

This staining evidences cell nuclei and has been used in this work to estimate cell density in cell culture plates.

#### *HOECHST STAINING*

##### **Materials:**

- Hoechst (stock 2 mg/ml)
- Formalin
- 100% MetOH
- 50 mM NH<sub>4</sub>Cl
- 1x PBS

##### **Procedure:**

There is no need to work in a laminar flow hood.

1. Wash with 4 °C 1x PBS 3 times.
2. Fix with 4% formalin in 1x PBS for 20 min.
3. Wash with 1x PBS for 5 min 3 times.
4. Incubate with 50 mM NH<sub>4</sub>Cl in 1x PBS at RT for 30 min.
5. Wash with 1x PBS for 5 min 3 times.
6. Permeabilise with 4 °C absolute MetOH at 4 °C for 10 min.
7. Wash with 1x PBS for 5 min 3 times.
8. Add Hoechst 1:1000 in 1x PBS at RT for 10 min.
9. Wash with 1x PBS for 5 min 3 times.
10. View under a fluorescence microscope using DAPI filter. Nuclei will appear blue.

### 6.11. Oil red o staining

Oil red o staining was used for lipid and fat identification on HepG2 cell cultures.

#### *OIL RED O STAINING*

##### **Materials:**

- Oil Red O (Sigma, catalogue Number: O 0625-25G)
- 25 % glutaraldehyd (Sigma G-6257)
- 1x PBS
- 60 % isopropanol
- dH<sub>2</sub>O
- Tap H<sub>2</sub>O
- Whatman filters or 0.45 µm pore filters

##### **Procedure:**

There is no need to work in a laminar flow hood.

1. Preparing stock solution (Oil Red O 0.5% in isopropanol):
  - Add 500 mg of Oil Red O powder to 100 ml of 99% isopropanol.
2. Cell fixing:
  - Prepare the fixative solution: 0.05% glutaraldehyd in 1x PBS (24 µl of 25% glutaraldehyd in 12 ml of 1x PBS).
  - Discard culture medium and add fixative solution.
  - Incubate at room temperature for 10 min.
3. Cell Staining:
  - Discard fixative and wash with PBS two times:



- Staining solution:
- Mix 3 parts (6 ml) of Oil Red O stock solution with 2 parts (4ml) of deionised H<sub>2</sub>O (the working solution is not stable for more than 2 hours).
- Allow to sit for at least 10 min. at room temperature.
- Filter solution on Whatman or on a 0.45µm filter.

- Add 60% isopropanol to cover cells.
- Discard Isopropanol and add staining solution. Let it stand for 5 min.
- Rinse three times with tap H<sub>2</sub>O.

View the plates on a phase contrast microscope. Lipids will appear red.

### 6.12. "In cell" experiments

#### 6.12.1. Production of mouse proximal tubule cell systems with controlled expression of KAP

Cell clones containing pBIG2i empty vector or pBIG2i-KAPwt were produced following these steps:

- Amplification KAPwt construct:

The KAPwt construct cloned in pHA-CMV resulting in clones pBIG2i-KAP was amplified by PCR and checked in 1% agarose gel in TAE buffer stained with EtBr 5 µg/ml.

- DNA Extraction: mini-preps

DNA was extracted using a plasmid DNA mini-preps kit GE Healthcare MiniSpin plasmidPrep Illustrat<sup>TM</sup> Kit (28-9042-70) from the bacterial culture that was not used to verify the presence of the insert.

The total concentration of DNA was determined by absorbance spectrophotometry. The product of the mini-prep was sequenced to make sure that the construct was intact using M13 (Fw and Rv) universal primers for the end point PCR.

- Cloning of the insert in TOPO plasmid: KAPwt construct amplified from pHA-CMV-KAPwt plasmid was cloned in TOPO plasmid in order to add the two restriction enzyme targets at both ends of the insert so that it could be further cloned in pBIG2i.

- Digestion of plasmid DNA:

Both pBIG2i and the construct cloned into TOPO (KAPwt) containing the intact insert and the targets for restriction enzymes Nhe I and Spe I (both from Roche) were digested

Digestion:

Reagent	Volume	Cf
plasmid	13 $\mu\text{g}$	
Nhe I	1.5 $\mu\text{l}$	
Spe I	1.5 $\mu\text{l}$	
Buffer M 10x	5 $\mu\text{l}$	1x
H <sub>2</sub> O	Up to 50 $\mu\text{l}$	
Vf = 50 $\mu\text{l}$		

Digest o/n at 37 °C.

Digestion was checked on 1% agarose gel in TAE buffer stained with EtBr 5  $\mu\text{g}/\text{ml}$  and loading 4  $\mu\text{l}$  of each digestion product per well.

- DNA purification:

The remaining digestion product (46  $\mu\text{l}$ ) was run in 1% agarose gel in TAE buffer stained with EtBr 5  $\mu\text{g}/\text{ml}$ .

- The bands corresponding to the desired fragments were separated from the agarose gel as described in the protocol. pBIG2i was separated on one side and KAPwt on the other.

The DNA bands were purified using a kit GE Healthcare.

The total concentration of DNA was determined by absorbance spectrometry.

Purification of DNA was checked in 1% agarose gel in TAE buffer stained with EtBr 5  $\mu\text{g}/\text{ml}$  and loading 1 ml of each purification per well.

- Dephosphorylation:

Before ligation it was essential to dephosphorylate both ends of empty linearised pBIG2i because the enzymes that were used to digest the plasmid left compatible ends in the plasmid so that the plasmid was able to recircle, which is not what was desired to happen. To avoid recircling, these ends must be dephosphorylated using alkaline phosphatase:

Reagent	Co	Vo in $\mu\text{l}$	Cf
Alkaline phosphatase	20U/ $\mu\text{l}$	0.55	2 U/ $\mu\text{l}$
buffer	10x	5.5	1x
plasmid		46	
Vf = 55 $\mu\text{l}$			

Incubate for 2 h at 37 °C.

- pBIG2i ligation with KAPwt construct:

Using Rapid DNA Ligation Kit from Roche (ref: 11635379001), ligation took place as described in the ligation protocol.

### - Transformation of competent TOP 10 strain bacteria:

The ligation product was used to transform bacteria from the One-Shot TOP10 strain. 100 µl of the transformation product were seeded in LB- agar with 50 µg/ml ampicillin 10 cm plates for bacterial growth.

The plates were incubated o/n at 37 °C.

The next day, colonies transformed with the plasmid appeared.

To verify that the transformed colonies contain the insert, the most representative were selected, harvested and seeded in 5 ml of LB-ampicillin 50 µg/ml. Liquid cultures were incubated o/n in a shaker at 200 rpm and 37 °C.

The presence of insert was checked by end point PCR using universal primers M13-Fw and M13-Rv as described above.

The correct orientation of the insert regarding the plasmid was also checked by end point PCR. If the insert is cloned in the correct direction a band was be observed when the PCR product was checked in a 1% agarose gel in TAE buffer and stained with EtBr 5 µg/ml.

### - DNA Extraction: maxi-preps

In case of confirmation of the presence of the insert and insertion in the correct direction, the culture that was not used for the PCR test was seeded in 100 ml LB-ampicillin 50 µg/ml and incubated in o/n in a shaker at 200 rpm and 37 °C.

Plasmid DNA was extracted using a kit from Qiagen maxi preps.

The total concentration of DNA was determined by absorbance spectrometry.

The product of the maxi-prep was sequenced to make sure the construct was intact using T7 universal primer for the end point PCR.

### - PCT3 cells transfection:

Cells were transfected by the use of the LipofectAMINE™ Plus™ reagents as described above. After transfection they were kept in a culture incubator (IGO 150 Cell Life, Jouan Thermo Electro Corporation) at 37 °C and 5% CO<sub>2</sub>, and cultured in rich medium for PCT3 routinely used in the laboratory that contains the essential nutrients needed for growth and proliferation. See medium composition above.

Medium was renewed every two days, when the cells reached confluence they were trypsinised (see protocol in above) and a fraction was transferred to a new cell culture plate.

Clones were selected by adding 400 µg/ml of the antibiotic hygromycin B, which killed all non-transfected cells.

15 days after transfection, clones began to appear. They were transferred to wells of 96-well plates, then to 24-well plates, then to 6-well plates and finally to a T25 flask. When the latter

was confluent cells were split to check clone, to freeze a fraction and to seed a new maintenance T25.

Checking the inducibility of the expression of KAP with doxycycline antibiotic:

- *Cell cultures*: two wells per clone were seeded in a 24-well plate, 20 000 cells per well and grown in PCT3 cells rich culture medium and selected with Hygromycin B antibiotic at the concentration described above. Medium was renewed every two days until the cells reached pre-confluence.
- *24 h treatment at fixed dose of doxycycline 2 µg/ml*: when reaching pre-confluence, one of the wells of each clone was treated at time and doxycycline dose defined. After treatment media were collected (two per clone: untreated and treated) and stored at -20 °C for further analyses, as well as cell pellets (two per clone: untreated and treated) which were stored at -80 °C until extraction of protein.

The defined treatment time and doxycycline dose are those commonly performed.

#### **6.12.2. Stably transfected KAP**

- Characterization of the model: dose-response and time-response assays

Doxycycline dose- or time-dependent regulation of the expression of KAP was checked through these assays.

- Two KAPwt clones were selected and only one empty vector based on the results of checking inducibility. Those clones which showed evident expression of KAP when adding doxycycline and showed no leaking expression in the presence of the antibiotic were selected for these assays.

- Cell cultures: 24 wells were seeded in 24-well plates per clone, 20.000 cells per well, grown in PCT3 cells rich culture medium and selected with the hygromycin B at the concentration described above. Medium was renewed every two days until the cells reached pre-confluence.

- 24 h treatment at different doses of doxycycline: in this case there were two dose-response experiments (fixed time: 24 h) with both KAPwt clones that were found to be inducible by doxycycline. Triplicates were arranged for each experimental dose.

Dose-Response 1: doses 200, 20, 2 µg/ml, 200, 20, 2 ng/ml, 200, 20, 2 pg/ml and 0 doxycycline.

Dose-response 2: dose 0, 10, 20, 40, 80, 160 ng / ml, 1, 2, 5, 10, 20 µg/ml.

According to the obtained results, the experimental treatment time was set to 24 h.

- 2 µg/ml treatment at different times of doxycycline: in this case there were two time-response experiments (2µg/ml dose) with both KAPwt clones that were found to be inducible by doxycycline. Triplicates were arranged for each experimental dose.

Time-response 1: times 1, 2 and 3 days.

Time-response 2: times 6, 8, 12, 24, 48 h.

According to the obtained results, the experimental treatment dose was set to 2 µg/ml.

- Characterization of the model: toxicity and viability assays

In order to check toxicity of eukaryotic recombinant KAP in isolated cell cultures, LDH assays were conducted in standard procedures following the steps described in the LDH protocol.

### 6.12.2.1. NFκB in PCT3 cells

The relationship between KAP and NFκB inflammatory pathway was tested by the use of pBIG2i-KAPwt stably transfected PCT3 cell clones and through RT-PCR profiler assays-

#### **Materials:**

- PCT3 clones: V01 p101+17 and KAPwt2 p21
- 10 cm plates, 4 biological replicates per experimental situation
- Treatment: + / - Doxycycline 1 µg/ml 24 h
- Protein extraction from cell pellet for WB
- RNA extraction from cell pellet for:  
RT PCR, and Real Time Profiler

#### **Procedure:**

- Treatments: according to the results obtained when characterizing the cell model, treatments were set at a time of 24 h and a dose of 1 µg/ml. This experiment was designed following the time line detailed below:

Friday:

- Seeding: one confluent T75 was trypsinized, diluted 1/10 and reseeded in 16 10 cm culture plates

Saturday and Tuesday:

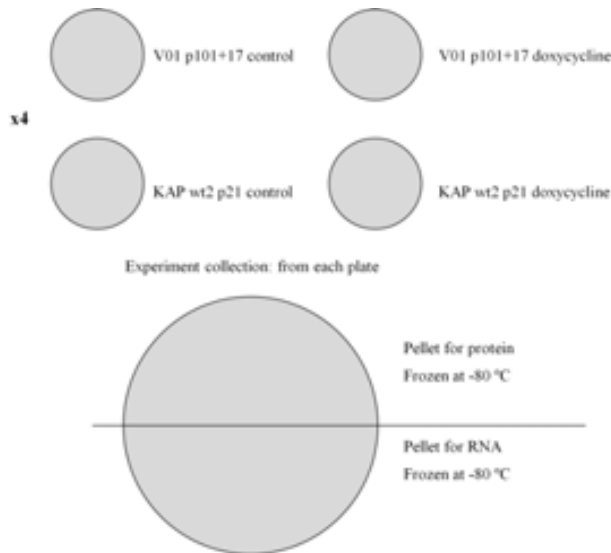
- Renew media.

Thursday:

- Add doxycycline treatment. Quadruplicates were arranged for every experimental situation.

Friday:

Experiment collection in the following manner:



- Protein:

Protein samples were extracted in RIPA buffer,  $V_f = 200 \mu\text{l}$ .

Quantified by Lowry method.

Stored in reductant 5x TMR buffer at  $-80 \text{ }^\circ\text{C}$ .

WB conditions:

Load:  $10 \mu\text{g}$  protein/well

Acrylamide gel electrophoresis 12%, run for 1 h 15 min at 20 mA/gel and RT.

Transference for 1 h 30 min at 400 mA and  $4 \text{ }^\circ\text{C}$ .

anti-HA primary antibody dil. 1/500, incubated o/n at  $4 \text{ }^\circ\text{C}$ .

anti-Actin (housekeeping) primary antibody dil. 1/1000, incubated for 1 h at RT.

- RNA:

RNA samples were extracted using Qiagen RNeasy® Mini Kit Catalogue # 74104.

Quantification by absorbance spectrophotometry.

RNA quality checking on 1.5% agarose gel: in all cases  $s_{28} = 3x s_{18}$

Quantification in bioanalyzer: these concentrations were taken into account for RTs (very good RIN in all cases)

RT PCR test: to verify RNA and manipulation procedures

Real Time PCR test: to check quality of cDNA (RT efficiency) and pipetting efficiency. Only one gene: CypA (not very good results were obtained but they served as endogenous to detect differences between technical triplicates).

Dil. cDNA = 1/50

Ultimate RT PCR.

RT profiler PCR assay: 4 384-wells assay plates were used for this experiment. Biological replicates were distributed one per plate.

#### 6.12.2.2. Secretion of eukaryotic recombinant KAP

In order to define whether eukaryotic recombinant KAP expressed in PCT3-pBIG3i-KAPwt clones is released through the apical or basal membrane of the cells, transwell assays were conducted with KAPwt clone 2.

Cell cultures:

Friday:

- Cell cultures: one 6-transwells plate was seeded, 20 000 cells per well, grown in PCT3 cells rich culture medium and selected with the hygromycin B at the concentration described above. Medium was renewed every two days until the cells reached pre-confluence.

Tuesday:

- Doxycycline dose was fixed at 1 µg/ml and treatment time was fixed at 24 h. Triplicates were arranged for every one of the two experimental conditions.

Wednesday:

- Experiment was collected by freezing cell pellets at -80 °C (obtained by scraping the transwell membrane, resuspending in 4 °C 1x PBS, transferring pellets to an eppendorf for each sample, centrifuging for 5 min at 4 °C and 1500 rpm and freezing at -80 °C) and freezing medias in reductant 1x TMR sample buffer (obtained by centrifuging each medium for 5 min at 4 °C and 1500 rpm, transferred each one to new eppendorfs and freezing at -20 °C).

- WB assays were conducted using apical and basal media from both experimental conditions, wce (protein extracted on RIPA buffer and quantified by BCA method) and both human and murine serum and urine. Urine proteins were concentrated by the use Amicon filters.

Load: 10 µg protein/well

Acrylamide gel electrophoresis 12%, run for 1 h 15 min at 20 mA/gel and RT.

Transference for 1 h 30 min at 400 mA and 4 °C.

anti-KAP primary antibody dil. 1/250, incubated o/n at 4 °C.

anti-KAP primary antibody dil. 1/250 + KAP-peptide 1/25, incubated o/n at 4 °C.

#### 6.12.3. Prokaryotic recombinant KAP: Oleic acid + recombinant prokaryotic KAP in HepG2 cells

• Characterization of the model: dose-response and time-response assays

Prokaryotic recombinant KAP crossed dose- time-response assays were carried out to observe the effects of this protein on hepatic human cell cultures (HepG2).

- Characterisation of the model: dose-response and time-response assays

Prokaryotic recombinant KAP dose- or time-response assays were carried out to observe the effects of this protein on proximal tubule cell cultures both murine (PCT3) and human (HK2). Duplicates were arranged for each experimental condition.

- 48, 72 h treatment.
- Oleate doses: 0.5 mM, 1 mM and 2 mM
- Prokaryotic recombinant KAP dose: 10 µg/ml

- Characterisation of the model: toxicity and viability assays

In order to check toxicity of prokaryotic recombinant KAP in isolated cell cultures, XTT and LDH assays were conducted in standard procedures following the steps described in the XTT and LDH protocols.

Lipid storage in human hepatocytes (HepG2) cells and the influence of prokaryotic recombinant KAP in this process was tested following the steps detailed below:

### **Materials:**

- Sodium oleate Sigma O7501-1G
- Albumin, from bovine serum, free fatty acid Essentially A6003-10G
- Rich Medium for HepG2 cells (10% foetal bovine serum)
- Medium for HepG2 cells without foetal bovine serum

### **Procedure:**

a) Conjugation of oleic acid with BSA (fatty acid free):

- In an eppendorf dissolve sodium oleate in 1 ml of absolute EtOH (approximately), applying vigorous shaking. It takes about 45 min to dissolve.
- Dry oleate in a speed-vac at RT. 1ml takes about 2 h to dry.
- Prepare HepG2 medium with 1.5% fatty acid free BSA. Stir briefly to dissolve.
- Resuspend oleate in 1ml of 1.5% BSA medium, applying vigorous stirring. It takes about 30 min.
- Add to the 1 ml BSA-conjugated oleate to the required volume of 1.5% BSA medium to reach the desired concentration of oleate.
- Store at 4 ° C, maximum for 2 days.



b) Preparation of cells following this time line:

Friday:

- Trypsinise cells from a confluent T75.
- Resuspend in 10-ml of complete medium and diluted 1/10.
- In 24-well plate, seed 1 ml per well from the final 1/100dilution.

Monday:

72h post seeding cells will have achieved 60-70% of confluence.

- wash 2 times with 1x PBS
- add HepG2 serum free medium

Tuesday:

96h post seeding change cells medium to serum free medium with 1.5% fatty acid free BSA and the desired concentration of oleic and prokaryotic recombinant KAP.

- Treatment time was fixed at 60 h.
- Oleate doses: 0.5 mM, 1 mM and 2 mM.
- Prokaryotic recombinant KAP doses: 10 µg/ml, 25 µg/ml.

Three different situations were designed according to the time at which prokaryotic recombinant KAP and oleate were added:

- 1) KAP and oleate both at the same time
- 2) 1<sup>st</sup> KAP and 24h later, oleate
- 3) 1<sup>st</sup> oleate and 24h later, KAP

6 replicates were arranged per experimental condition.

		mM oleate			
		0	0,5	1	2
µg/ml KAP	0	6	6	6	6
	10	6	6	6	6
	25	6	6	6	6

Friday:

60h post treatment harvest experiment:

- Oil Red O staining for lipid visualizing (3 replicates)
- Hoechst staining for nuclei visualizing (3 replicates)
- LDH (3 replicates) and XTT (8 replicates) assays.

## 7. In vivo methods

All studies were carried out in compliance with the laws of the European Union and the US Department of Health and Human Services Guide for the Care and Use of Laboratory Animals. All procedures were approved by the author's Institutional Review Board on Animal Health: Comitè Ètic d'Experimentació Animal (CEEA) Hospital Universitari Vall d'Hebron. Permit Number FIS PI08/1351.

### 7.1. Animal weighing

Mice were weighed awake and always using the same Ohaus Adventurer™ Pro AV4101 precision balance. All the animals of the study were weighed weekly on the same day of the week (Tuesday) and following the same order so that each animal was weighed approximately at the same time of the day (first animal at 0900, last animal at 0930).

Animal welfare and ensuring reliability of data:

Guaranteeing mice's comfort and welfare also ensures obtaining reliable and reproducible data.

- The weight measurements were taken first thing in the morning to reduce the stress that diurnal manipulations have on this species the activity of which takes place during the night, since stress seems to have a dramatic effect on the weight of the mice.
- End-of-test conditions were not considered during the weight measurements.

### 7.2. Food and H<sub>2</sub>O intake register

In order to register the food and H<sub>2</sub>O intake, animals were isolated in couples belonging to the same experimental group. Both food and H<sub>2</sub>O were weighed always using the same Ohaus Adventurer™ Pro AV4101 precision balance before providing the animals with both of them, animals were provided with more than enough food and drink for one week nourishment. One week is a maximum time period for not renewing the animals' food and drink. The same day of the following week remaining food and H<sub>2</sub>O was weighed again.

Animal welfare and ensuring reliability of data:

- The weight measurements were taken first thing in the morning, as explained before.
- The "isolation" of the animals was not strictly such, since they were grouped in couples to avoid the stress that actual isolation may produce to this species of social nature.
- Food and H<sub>2</sub>O was renewed ensuring that the amount of both was the approximately the same as the first day. The amount of food may vary the intake since small amounts of food make it more difficult for the animals to gnaw it, causing the animals to reduce their intake.
- Weighing took place always on the same day of the week (Tuesday), at the same time of the day, following the same cage order and mandatorily carried out by the same person. This same person was also in charge of the cleaning of the cages. During this procedure, no one but this only person was allowed to touch, move, clean or refill the cages.
- End-of-test conditions were not considered during the weight measurements.

Calculations:

H<sub>2</sub>O intake was calculated as the difference of the initial weight minus the final weight, the balance was always tared with the bottle belonging to the cage in study. Food intake was calculated subtracting initial weight minus final weight and normalised by kcal per gram of each diet type.

### **7.3. Glucose tolerance test (GTT)**

Glucose tolerance tests took place after 12 h o/n fasting. The following day, glucose solution was prepared fresh by weighing glucose (Glucose anhydrous, Sigma G-7021) using an Ohaus Adventurer™ SL Adventurer Pro AS 1502 precision balance and mixing with sterile injection H<sub>2</sub>O to achieve a stock solution of 0.2 g/ml. Insulin syringes (1 ml, with needle attached and sterile plunger) were charged with glucose solution after numbering them, weighing the animals on an OHAUS Adventurer™ Pro AV4101 precision balance and calculated the appropriate volume to inject to each mice a bolus of 2 g glucose/kg animal. A small incision was performed at the end of the tail of the animal in order to measure basal fasting blood glucose (pre-injection) using a glucose-meter (Bayer's Ascensia Elite™ Glucometer®). Mice were next given an intraperitoneal glucose bolus and glucose measurements were taken at 15, 30, 60, 90 and 120 min post-injection always using the same glucose-meter (Bayer's Ascensia Elite™ Glucometer®). One single drop of blood was collected from the tail incision for each measurement by spiral massaging the animal's tail; after the drop was obtained, haemostasia was performed by gently pressing the end of the tail to stop the bleeding. During the test animals were allowed H<sub>2</sub>O "ad libitum" but not food. GTT always took place in the same day of the week (Friday).

Animal welfare and ensuring reliability of data:

- Injection volumes were calculated according to the recommendations of the Federation of European Laboratory Animal Science Associations (FELASA), and stocks solutions were built up based on these injection volumes.
- Haemostasia was performed to each animal after every glucose measurement.
- Animals were kept in their own cages with their cage mates during the whole procedure.
- End-of-test conditions were not considered during GTT.

### **7.4. Insulin tolerance test (ITT)**

Insulin tolerance tests took place after 5 h, over morning (0930-1430), fasting. After 4.5 h, insulin solution was prepared fresh by weighing insulin (Insulin, Sigma I-6634 50 mg) using an Ohaus Adventurer™ SL Adventurer Pro AS 1502 precision balance and mixing with sterile injection H<sub>2</sub>O to achieve a stock solution of (0.075 U/ml). Insulin syringes (1 ml, with needle attached and sterile plunger) were charged with insulin solution after numbering them, weighing the animals on an Ohaus Adventurer™ Pro AV4101 precision balance and calculated the appropriate volume to inject each mice a bolus of 0.75 U / kg animal. A small incision was

performed at the end of the tail of the animal in order to measure basal fasting blood glucose (pre-injection) using a glucose-meter (Bayer's Ascensia Elite™ Glucometer®). Mice were next given an intraperitoneal insulin bolus and glucose measurements were at 15, 30, 60, 90 and 120 min post-injection always using the same glucose-meter (Bayer's Ascensia Elite™ Glucometer®). One single drop of blood was collected from the tail incision for each measurement by spiral massaging the animal's tail; after the drop was obtained, haemostasia was performed by gently pressing the end of the tail to stop the bleeding. During the test animals were allowed H<sub>2</sub>O "ad libitum" but not food. ITT always took place in the same day of the week (Monday before GTT).

Animal welfare and ensuring reliability of data:

- Injection volumes were calculated according to the recommendations of the Federation of European Laboratory Animal Science Associations (FELASA), and stocks solutions were built up based on these injection volumes.
- Haemostasia was performed to each animal after every glucose measurement.
- Animals were kept in their own cages with their cage mates during the whole procedure.
- End-of-test conditions: mice were checked for hypoglycaemic coma signs such as lethargy, dark circles around the eyes and/or asthenia or lack of movement, as well as pain signs such as exacerbated curvature of the back and snuggling in a corner of the cage. If any of these signs were detected on any animal, this animal was immediately excluded from this test and was given a bolus of 2 g intraperitoneal glucose per animal kg. During the animal's recovery, it was checked for improvement of its pain signs, and if recovery did not take place, the animal was intended to be sacrificed by cervical dislocation (however, few mice reached this situation during the procedure and all of them recovered successfully so that there was no need to sacrifice them).

### **7.5. Collection of blood samples**

Blood collection from periorbital plexus took place after 5 h, over morning (0930-1430), fasting. Animals were fasted sequentially and the blood collection took place in the same fasting order to ensure that all of them fasted for 5 h.

Blood was collected in BD Microtainer® SST™ Amber Tubes (ref. 365979) for serum separation.

Serum was stored at -20 °C for short term storage and moved to -80 °C for long term storage. It was used for proteomics analysis, Milliplex assays and insulin and lipid determination.

*BLOOD COLLECTION FROM PERIORBITAL PLEXUS*

**Anaesthesia:** Required (Abbott Forane®, isoflurane 250 ml ref.: 880393.4 recommended).

**Materials:**

- Short tip glass Pasteur pipettes (treated or not with anticoagulant: EDTA, heparin ...)
  - Surgical gauzes
  - Vitulia physiological serum (0.9 % sodium chloride injectable solution), or 1x PBS
  - Ophthalmic pomade (Lubrifilm) (optional)
- Extraction volume: See table below.

**Procedure:**

- Anesthetize the mouse and make sure that it has reached the surgical level.
- With one hand, hold the mouse decubitus prone and gently stretch the skin of the neck slightly back to open the eye making sure not to interfere the animal's breathing.
- With the other hand, insert pipette tip into the corner of the eye (2 mm approx) and rotate slowly until the blood flows through it (fig. 9). Do not press the pipette against the animal's eye since severe damage could be caused.



**Figure 9.** Immobilization and inserting of the capillary into the mouse's eye.

- Remove the capillary from the eye and collect the sample in a suitable vial. The blood should flow continuously from the pipette, if this is not so, the sample is likely to be coagulating.
- Press gently puncture site with a gauze or absorbent paper impregnated with saline or 1x

PBS to stop the bleeding and clean any traces of blood.

Anoint ophthalmic pomade (Lubrifilm) around the eye (optional).

Check that the recovery from anaesthesia occurs adequately providing the measures considered necessary (for example, heat providing).

Observe the animal several days after bleeding looking for possible complications such as protrusion of tissue adjacent to the eye, infection, bleeding...

Collection volumes referred to Vc (circulating volume):

Single collection		Multiple collections	
%Vc collected	Recovery period	%Vc collected in 24h	Recovery period
7.5 %	1 week	7.5 %	1 weeks
10 %	2 weeks	10 %	2 weeks
15 %	4 weeks	15 %	3 weeks

Vc: circulating volume  
 Vc mouse: 72 ml/kg  
 Vc rat: 68 ml/kg

Collection volumes referred to Vt (total volume):

	Blood collection				
	Vt (ml)	7.5 % (ml)	10 % (ml)	15 % (ml)	20 % (ml)
Mouse (25g)	1.8	0.1	0.2	0.3	0.4
Rat (250g)	16	1.2	1.6	2.4	3.2

Vt: total volume approx. 6% of body weight (in ml)

Animal welfare and ensuring reliability of data:

- Haemostasia was performed to each animal before returning them to their cages.
- Extraction volumes were calculated according to the recommendations of the Federation of European Laboratory Animal Science Associations (FELASA), and stocks solutions were built up based on these injection volumes.
- Animals were kept on a warm blanket during the immediate recovery of this procedure.
- End-of-test conditions: mice were checked for complications such as protrusion of tissue adjacent to the eye, infection or bleeding. If any of these signs appeared, veterinary advice was requested to take recommended actions.

### **7.6. Blood pressure measurement**

Blood pressure measurement was performed by the tail-cuff method, by which measurements were taken to awaken immobilized animals, in darkness conditions and using a heating tunnel to improve blood flow in the animal's tail and avoid animal's hypothermia caused by immobilization. This method avoids acute or chronic invasive characterisation. It is based on sphygmomanometry, the same mechanism for measuring blood pressure in humans, using a transducer/cuff and a built-in air pump that ensures automated cuff inflation/deflation at a constant rate. The air pump is controlled by a storage pressure meter that records blood pressure values. Animal's heart rate, pulse and blood pressure are visualized on a computer screen through data-acquisition software. The material required is the following:

- Transducer/cuff (for all sizes of mouse) LE 5160-M Panlab ref.:76-0012
- Data analyzer: LE 5007 Storage Pressure Meter Programable System Panlab Harvard apparatus ref.:76-0175
- Data acquisition system: AD Instruments Powerlab 8/30 Panlab Technologies for Bioresearch
- Chart 5<sup>TM</sup> data acquisition software
- Restrainer LE 5016 90 x 30 mm (restrainer for mice of 35 g), LE 5018 100 x 34 mm (restrainer for mice of 50 g) Panlab Technology for Bioresearch, refs.: 76-5016 and 76-5018 respectively
- Heating tunnel: LE 5610 Panlab Technology for Bioresearch heater for one animal ref.: 76-0178, temperature adjustable from room temperature to 38 °C
- Lap top, preferably PC

This test always took place during one same week and in the same time range of the morning (0830-1130) or afternoon (1500-1800). Time of the day: as happens in human beings, blood pressure changes from day to night time; opposite to what happens in human beings, blood pressure is higher in rodents during night time [97]. In order to asses HT not dependent on the time range, BP was measured in the afternoon during a first experiment and in the morning during the second experiment. Habituation of the animals took place during the first morning or afternoon of the round. BP measurements took place during the following four. Mice were

picked up randomly every day, following no definite order but making sure that each animal was tested at least twice during these four days in order to avoid day of the week and time of the day's influence in blood pressure.

Animal welfare and ensuring of reliability of data:

BP measurement by tail-cuff method is generally a difficult process since the values measured are erratic and slightly higher than the base measurements. To optimize immobilization time of the mice it is recommended to:

- Leave from 1 to 3 min in between each measurement to allow the arteries go back to their initial shape and size since the cuff pressure squeezes them.

During this process, rodents must be in a state of relaxation:

- Induce a moderate dilatation of the blood vessels by subjecting them to a slight rise in temperature produced in the heating tunnel which also keeps the mouse from an external view and environmental noises, uncontrolled and significant sources of stress (anxiety).

The stress must also be minimized by:

- Minimizing the time during which the animal is subjected to this process. Keeping the animal in the restrainer for longer than 15 min is not recommended if the aim is to both reduce anguish and obtain accurate results.

- Taking the BP measurements in darkness conditions.

- Several environmental factors may produce variance in the data obtained from one round to another and it is recommended to take them into account when comparing the data. These factors include: time of the day, season of the year, age and others.

- Habituation of the animals:

Since it is not possible to explain to the animals the process to which they are going to go through, it is recommended to slowly habituate the mice to this method so that they feel comfortable and calmed when it comes to taking the actual measurements. The best way to do this is to subject each mouse to 2 or 3 measurements a couple of days before the real measurement. No longer than 5 min in the restrainer and no more than 3 measurements.

### **7.7. Animal sacrifice and tissue collection**

Once reaching the sixth and a half month of experiment, animals were sacrificed by pleural scission under isoflourane anaesthesia (Abbott Forane®, isoflourane 250 ml ref.: 880393.4) in order to collect the organs to weigh them for a comparative organ size study and keep them either frozen at -80 °C or fixed with formalin (Sigma F-8775) 4% PBS 1x for further studies.

Animals were sacrificed always during the same time period in the morning (0930-1200), about 8 animals per day during about 4 days.

The organs collected for further studies were: kidneys, liver, brain, heart, gastrocnemius muscle, brown adipose tissue, inguinal and epididymal white adipose tissue.

Autoclaved Eppendorf tubes were appropriately labelled and pierced with a 21G needle to prepare them for tissue storage. Immediately after extraction, these organs were weighed using an OHAUS Adventurer™ SL Adventurer Pro AS 1502 precision balance. Tissues were immediately placed in histology cassettes (Biopsy processing / Embedding cassettes Simport M499 - Histosette® I) and sunken in formalin (Sigma F-8775) 4% PBS 1x fixing solution (for histology assays) or frozen in liquid N<sub>2</sub> (for protein or RNA extraction). Tube piercing helps N<sub>2</sub> entering the tube and faster freezing the tissue as well as preventing from bursting when they are transferred to a -80 °C storage box due to quick change of gas pressure in the tube since it expands when warmed. The purpose of each tissue is detailed in the table below:

		Liquid N <sub>2</sub>	Formalin
Kidney	Left (2 longitudinal halves)	x	
	Right		x
Liver	Left lobe		x
	Median lobe (2 halves)	x	
Brain	Left hemisphere (2 halves)	x	
	Right hemisphere		x
Heart	Left	x	
	Right		x
BAT	Left (only one half for RNA)	x	
	Right		x
ING WAT	Left (2 halves)	x	
	Right		x
GON WAT	Left (2 halves)	x	
	Right		x

Kidneys were de-capsulated and renal pelvis was removed before weighing. Bile bladder was removed from liver before processing. Adipose tissues were appropriately cleared from other tissues remains.

### 7.8. High fat diet assays

Three equal or similar sets of experiments were designed (hfd1, hfd2 and hfd3). The mice used to carry out this work were male mice, heterozygous for the KAP transgene and their corresponding control littermates, and they were fed either on a standard diet or hfd.

The experimental N was calculated based on the variances obtained from the pilot study.

The hfd assays were designed upon a time line where t=0 represents the birth of the mice as follows:

t= -5 weeks → Selection of parental couples.

t= -4 weeks → Mating of parental couples.

t= -3 weeks → Sacrifice of reproductive males.

t= -2 weeks → Separation of pregnant females in individual cages.

t=0 → Birth of mice.



t= +2 week → Mice genotyping.

t= +2.5 weeks → Groups designing.

t= +3 weeks → Mice weaning and grouping as follows:

Hfd 1 and 2: four experimental groups: c chow, Tg chow, c hfd and Tg hfd; 8 animals per group; 4 animals per cage separated by Tg line: L49 (2 c and 2 Tg) and L59 (2 c and 2 Tg).

Total: 32 animals.

Weekly body weight measurement.

t= +1, 3, 5 months: no tests performed

t= +2, 4, 6 months: week 1 → blood pressure measurement training

week 2 → blood pressure measurement

week 3 → hfd group: ITT on Monday, GTT on Friday

chow group: 5h fasting serum collection on Tuesday

week 4 → chow group: ITT on Monday, GTT on Friday

hfd group: 5h fasting serum collection on Thursday

t= +6.5 months: animal sacrifice

organs dissection

organs weighing

organs collection: frozen at -80 °C for further molecular analyses or fixed in 4 % formalin for further HQ analyses.

Hfd 3: four experimental groups: c chow, Tg chow, c hfd and Tg hfd; 8 animals per group; 2 animals per cage separated by Tg line: L49 (2 c and 2 Tg) and L59 (2 c and 2 Tg). Total: 32 animals.

Weekly body weight measurement.

Weekly food and H<sub>2</sub>O intake measurement.

t= +6 months: week 1 → blood pressure measurement training

week 2 → blood pressure measurement

week 3 → hfd group: ITT on Monday, GTT on Friday

chow group: 5h fasting serum collection on Tuesday

week 4 → chow group: ITT on Monday, GTT on Friday

hfd group: 5h fasting serum collection on Thursday

t= +6.5 months: animal sacrifice

organs dissection

organs weighing

organs collection: frozen at -80 °C for further molecular analyses and fixed in 4 % PFA for further HQ analyses.

## 8. Data treatment, statistical analyses and calculation of the N for experiments on live animals

### 8.1. Statistical analysis

Comparison of the different data from the four groups of each experiment was carried out in pairs for all measured parameters. Statistical analyses of the data took place through standard Student's t-test not assuming equal variances by means of Microsoft Office Excel 2007 in all cases: both for animals' and cells' data. Statistical significance was considered when p-value was equal or below 0.05.

Equal conditions t-tests were performed prior to the hfd data analysis comparing same parameter between transgenic lines (L49 and L59) and between different experiments (hfd1, hfd2 and hfd3) in order to ensure that differences found in these two comparisons were not statistically significant.

Microfluidic cards differential expression assays data were also analyzed by the Unitat d'Estadística i Bioinformàtica Vall d'Hebron Institut de Recerca. The statistical methods followed in this study were based mainly based on Hellemans et al.2007 publication. Data were checked using the DataAssist Software (ABI) in order to detect and remove outliers among the triplicate measurements of each gene. The selection of differentially expressed genes has been based on unadjusted p-values under 0.05 obtained through t-tests using R analysis.

### 8.2. Calculation of the N for experiments on live animals

In order to minimize the use of experimental animals, a pilot study was designed to calculate the most appropriate experimental sample size (n) for our animal model. An arbitrary number (decided upon what is described in other publications) of 8 animals per group distributed in the following way:

Group 1. Cotrols: 4 L49 mice + 4 L59 mice

Group 2. Tg: 4 L49 mice + 4 L59 mice

All of them were fed on the described hfd from weaning. BP measurement, GTT, ITT and weight measurements were performed at 1<sup>st</sup>, 3<sup>rd</sup> and 5<sup>th</sup> months of life of the animals. Lipid profile was studied at 3<sup>rd</sup> and 5<sup>th</sup> months of life. Differences were detected from the 5<sup>th</sup> month of life and these data were used to calculate the sample size with the formula:

$$n = \frac{Z^2 \cdot \sigma^2}{c^2}$$

Where:

Z = 95% confidence level (standard value 1.96)

$\sigma$  = population standard deviation obtained empirically through the measurements described

c = confidence interval or margin of error (standard value of 0.05)

## MATERIALS AND METHODS

Finally, sample size was determined as the mean of the individual calculations for each measurement and was fixed in  $n=8$ . Since no significant differences were found between L49 and L59, both Tg lines were used and treated in the same way for the experiment.

## **RESULTS**

---

# RESULTS

## 1. Phenotype of the animal experimental models:

Both control (c) and transgenic (Tg) animals were fed either on a chow or high fat diet (hfd) from weaning until sacrifice at almost seventh month of age. During the “in vivo” step of the experiment several physiological parameters were measured. After sacrifice, certain selected organs were extracted and appropriately treated for further molecular analyses.

### 1.1. Blood pressure measurements

Bimonthly blood pressure measurements were taken during the afternoon period in a first experiment and during the morning period in a second experiment in order to prove that the trend is equal among the groups no matter the time of the day.

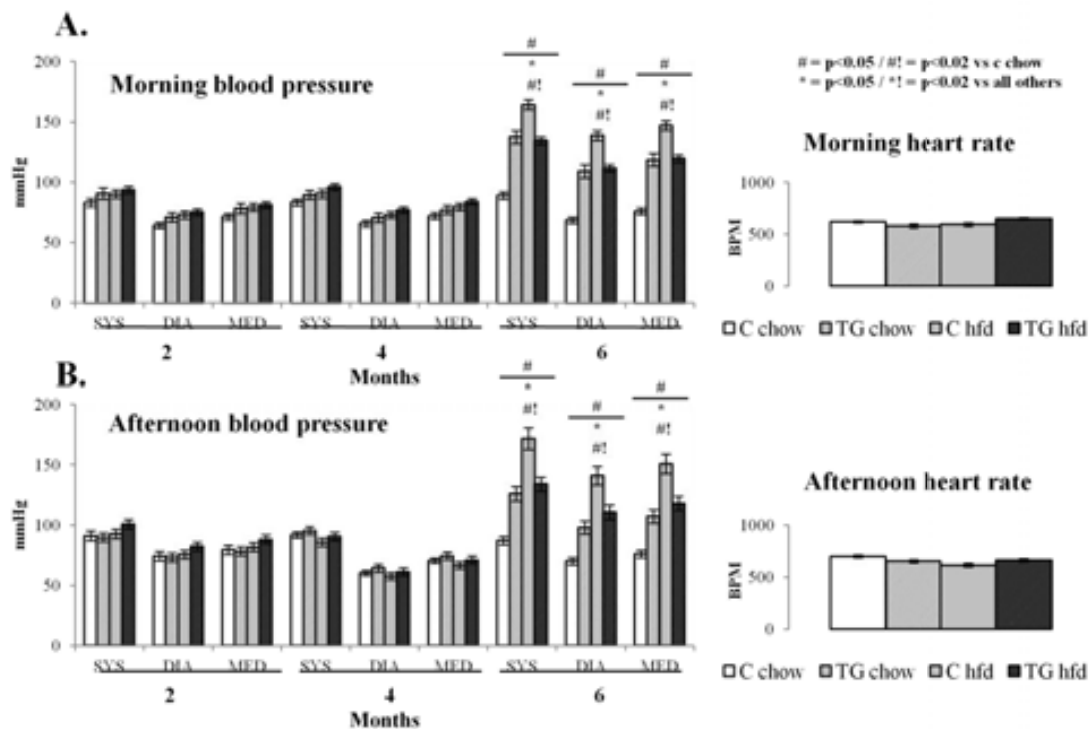


**Figure 1. Blood pressure.** Mice blood pressure (mmHg) measurements taken by the tail cuff method at 2<sup>nd</sup>, 4<sup>th</sup> and 6<sup>th</sup> month of life during the morning period (experiment 2) (A) and afternoon period (experiment 1) (B). Measurements were taken between 0830 and 12 h, or 1430 h and 18h, during one same week. Animals were accustomed before first measurement. They were immobilized and awake. Measurements were taken in darkness conditions and T > RT. Systolic, diastolic and median blood pressure are indicated in order to show that both systolic and diastolic pressures followed one same pattern among the groups, and median blood pressure is recorded as a more accurate value of these data. Blood pressure data were analyzed separating the two Tg lines (L49 and L59) finding slight but no significant differences between them and always assessing one same pattern among the groups of both lines. Heart rate in beats per minute (BPM), also evaluated both during the morning period (experiment 2) and afternoon period (experiment 1) shows that the differences in blood pressure among the groups is not due to alterations in this parameter. N=8. Statistical analysis performed through t-test.

These measurements demonstrated that hfd induced hypertension in 6-months-old adult mice in a more dramatic manner than overdosing of KAP in Tg animals (fig. 1). However, addition of both factors, Tg and hfd, did not induce animals to be more hypertensive than the transgene alone. Blood pressure was measured both in the morning (fig. 1A) and in the afternoon (fig. 1B), and, although as expected blood pressure was higher in the morning than in the afternoon, the pattern among the groups was the same. Measurements included systolic, diastolic and mean blood pressure; all of them appeared altered in the described way, even mean blood pressure, confirming variation among groups in systolic and diastolic pressure. No differences were found in the heart rate among the different experimental groups, not between the morning and afternoon measurements either.

### 1.2. Evaluation of glucose metabolism

Glucose metabolism was evaluated through glucose tolerance test (GTT) by fasting the animals during 12 h, giving them an i/p glucose bolus and following their blood glucose levels during a time line and through insulin tolerance tests (ITT) by fasting them during 5 h, giving them an i/p insulin bolus and following their blood glucose levels.

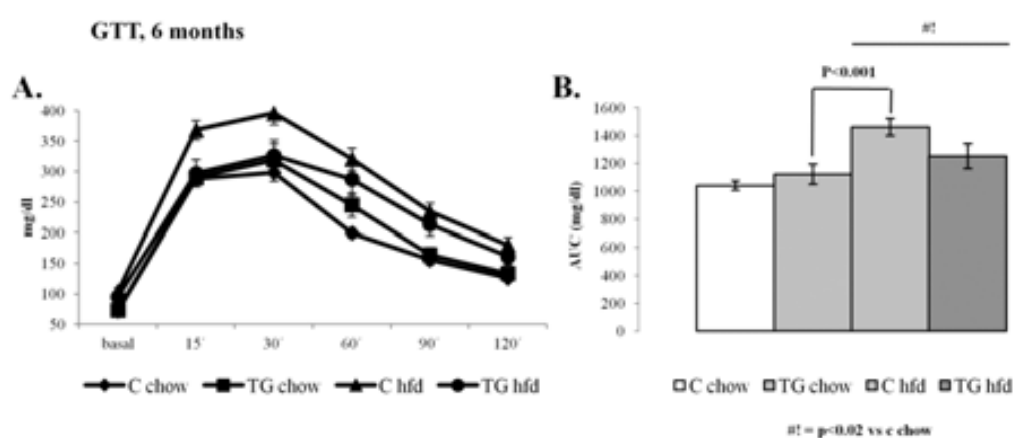


**Figure 2. Glucose tolerance test (GTT).** GTT performed after 12 h o/n fasting. Always carried out during the morning and in awoken animals. Glucose bolus: i/p 2 g/kg, given to half-asleep mice. Glucose was measured with a glucometer in basal conditions (before glucose bolus) and after glucose bolus, every 15, 30, 60, 90 and 120 min. Results are given in absolute values (mg/dl) (A) and in area under the curve (B). GTT data were analyzed separating the two Tg lines (L49 and L59) finding slight but no significant differences between them and always assessing one same pattern among the groups of both lines. N=24. Statistical analysis performed on area under the curve (AUC) data through t-test.

Glucose tolerance tests demonstrated that there were no differences in the basal glucose after 12 h o/n fasting and that controls fed on a hfd showed problems in metabolizing glucose (fig. 2). Basal glucose was measured after a 5 h fasting and before starting the insulin tolerance tests.

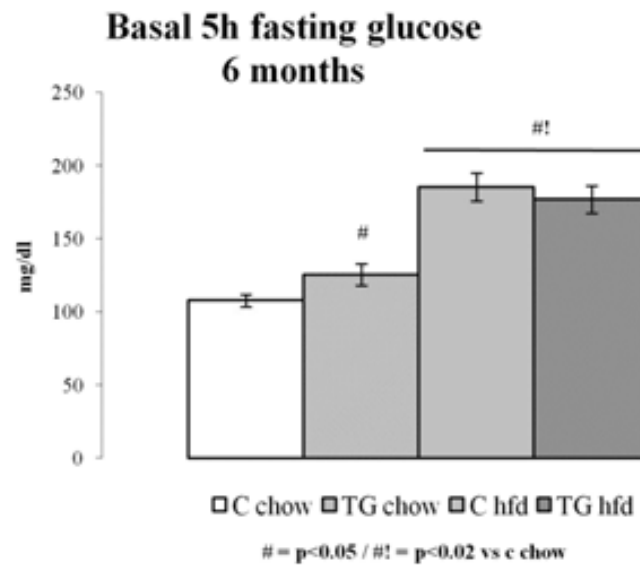


**Figure 3 . Basal glucose.** Measurements taken after 5 h over morning fasting in a waken animals. Glucose was measured with a glucometer. Results are given in absolute values (mg/dl). Glucose data were analyzed separating the two Tg lines (L49 and L59) finding slight but no significant differences between them and always assessing one same pattern among the groups of both lines. N=24. Statistical analysis performed through t-test.

Basal glucose measurements demonstrated that animals fed on a hfd showed a higher basal blood glucose after 5 h over morning fasting. Basal glucose was already significantly different in the presence of the transgene alone (fig. 3).

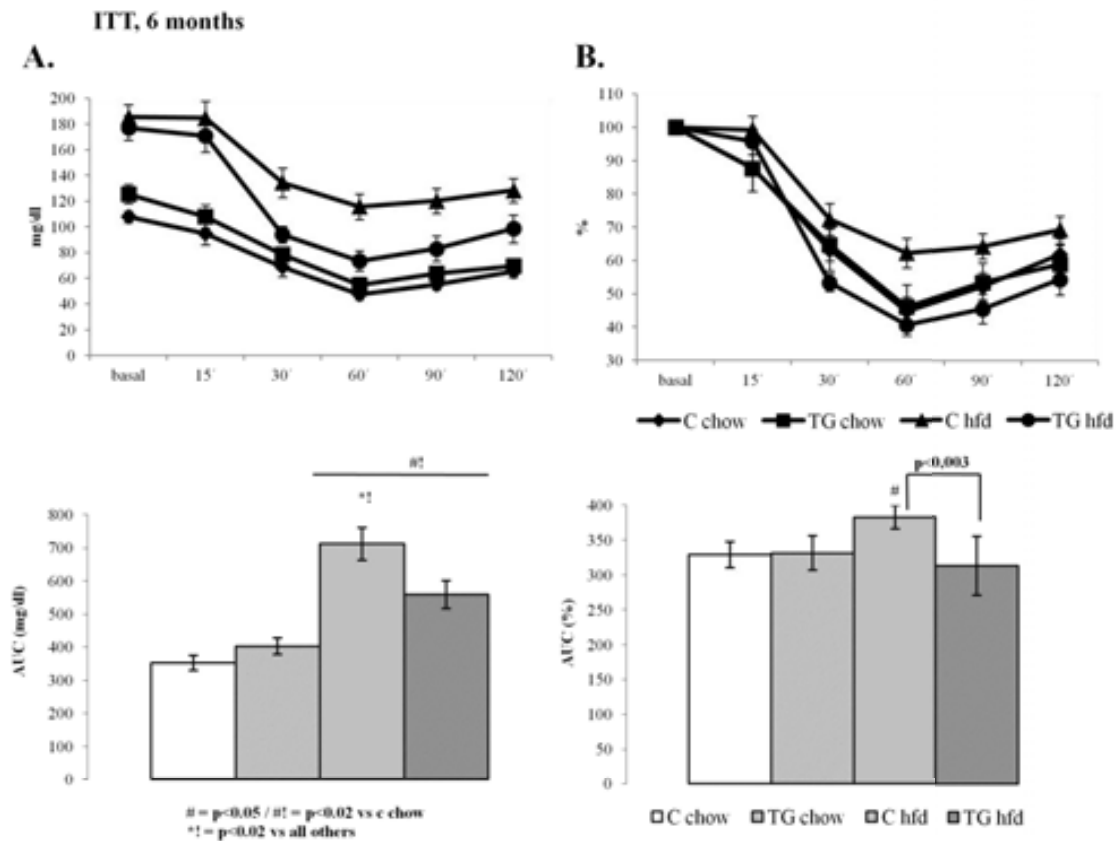


**Figure 4. Insulin tolerance test (ITT).** ITT performed after 5 h fasting. Always carried out during the afternoon and in awoken animals. Insulin bolus: *i/p* 0.75 u/kg, given to half-asleep mice. Glucose was measured with a glucometer in basal conditions (before insulin bolus) and after insulin bolus, every 15, 30, 60, 90 and 120 min. **A.** Results are given in absolute values (mg/dl) and **B.** in percentage ratio over basal glucose. ITT data were analyzed separating the two Tg lines (L49 and L59) finding slight but no significant differences between them and always assessing one same pattern among the groups of both lines. N=24. Statistical analysis performed on area under the curve (AUC) data through t-test.

Controls fed on a hfd showed resistance to insulin compared to all other groups (fig. 4A), while Tg hfd did not and behaved in the same way as both c and Tg fed on a chow diet (fig. 4B).

Insulin levels were evaluated in these mice through the use of a mouse serum adipokine milliplex assay.

Insulin serum levels were measured through a mouse serum adipokine milliplex assay in order to search for a correlation between observations in ITT and a possible rise in insulin levels.



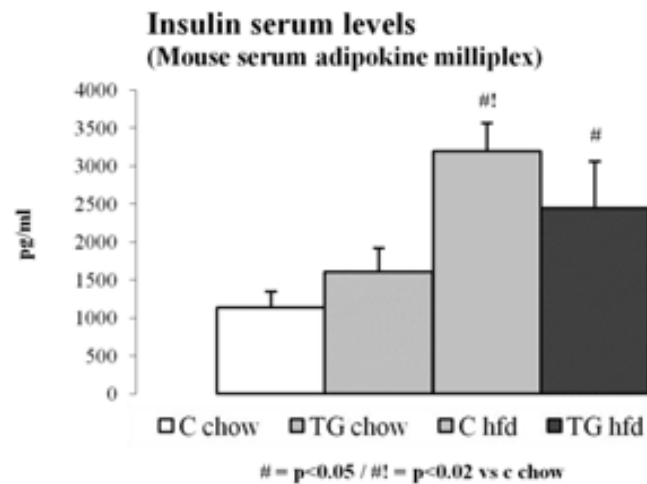


**Figure 5. Insulin serum levels.** Insulin was measured in 6-month old 5 h fasted animals by Mouse serum adipokine milliplex kit. N=16. Statistical analysis performed through t-test.

Both hfd diet groups demonstrated statistically significant compensatory hyperinsulinemia, and this was significantly higher in c hfd than Tg hfd (fig. 5).

### 1.3. Body weight

Mice were weighed once a week during the 7 months experiments in order to evaluate their weight gain along the study period.

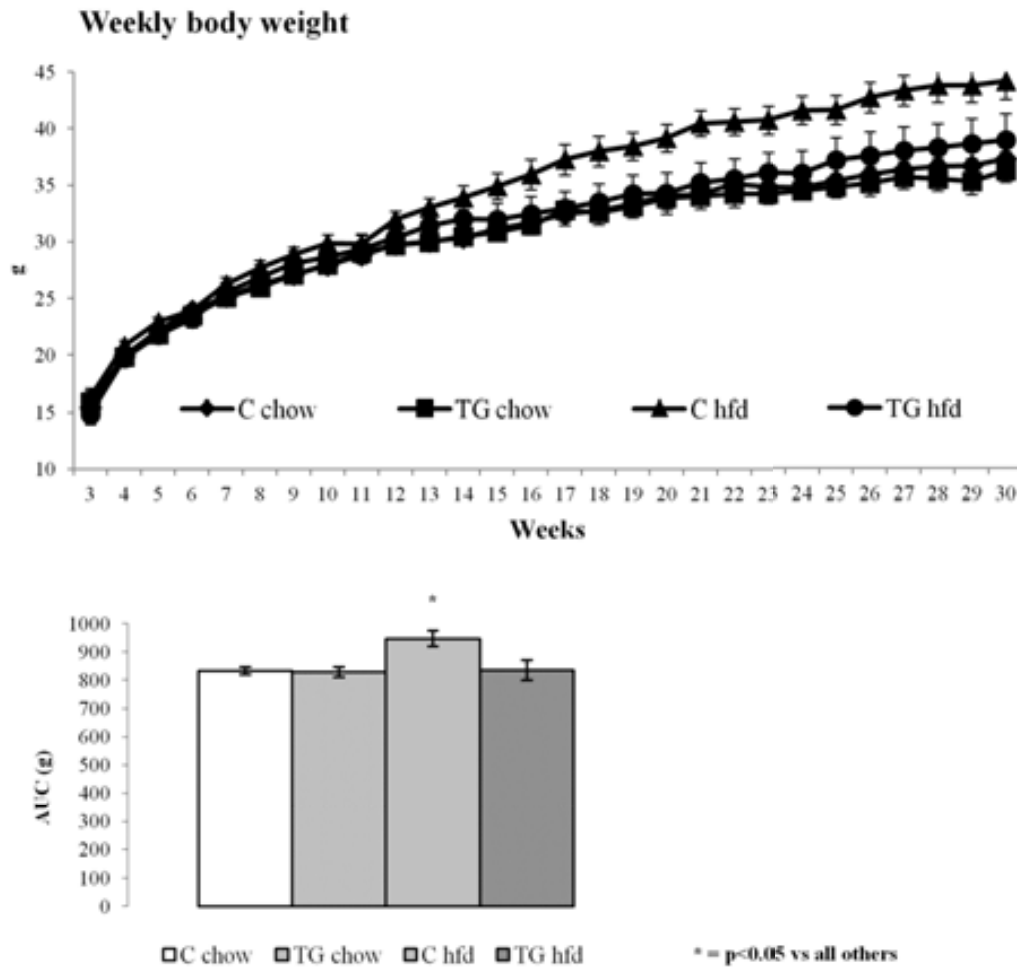


**Figure 6. Weekly body weight.** Mice weekly body weight taken in awoken, free animals, from 09 a.m. to 0930 a.m. Body weight data were analyzed separating the two Tg lines (L49 and L59) finding slight but no significant differences between them and always assessing one same pattern among the groups of both lines. N=16. Statistical analysis performed on area under the curve (AUC) data through t-test.

Animals' growth curves revealed that the c hfd group gained much more weekly weight than all others, including Tg hfd which behaved in a very similar manner to those fed on a chow diet (fig. 6).

With the aim of assessing whether these differences in the gain of weight were due to a differential food intake among the groups and, at the same time evaluate the water intake in the search of DM sign polydipsia, food and water intake were followed during 6 months on a weekly basis.

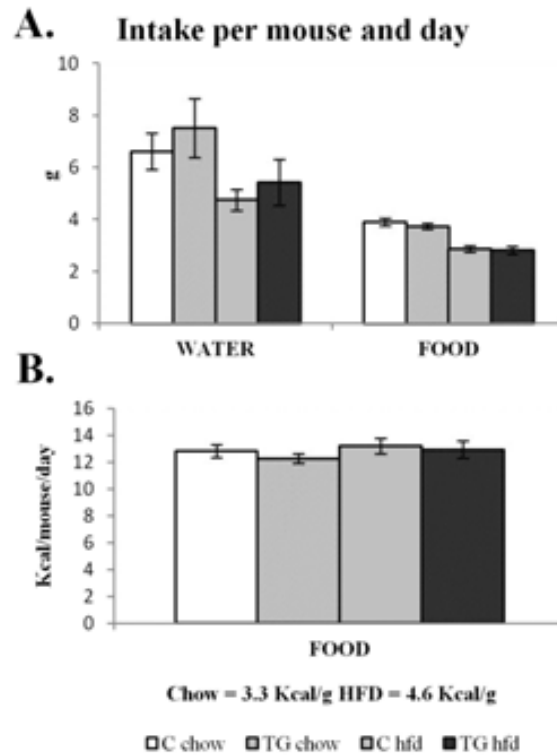


**Figure 7. Food and water intake.** **A.** Mean water and food intake (both in grams) calculated upon measurements taken on weekly basis and **B.** mean kcal intake calculated upon food intake in grams and each type of diet's caloric value. N=8. Data were analyzed separating the two Tg lines (L49 and L59) finding slight but no significant differences between them and always assessing one same pattern among the groups of both lines. Statistical analysis performed through t-test.

Yet both water and food intake were lower in the hfd groups, no significant differences were found between c and Tg fed on one same diet, even in the case of water intake where there seemed to be a slight increase in the intake of Tg compared to c fed with both diets (fig. 7A). No differences were found among the 4 groups regarding the calories intake (fig. 7B). Leptin serum levels were measured as a satiety indicator using a mouse serum adipokine multiplex assay to compare the results with those obtained measuring the food intake.

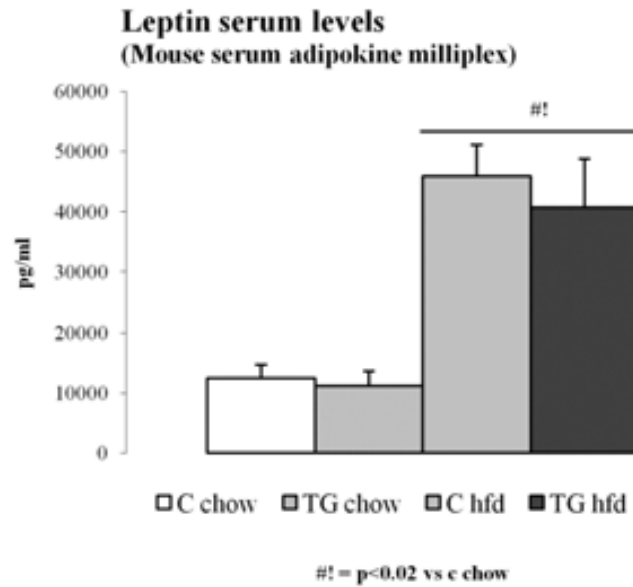


**Figure 8. Leptin serum levels.** Leptin was measured in 6-month old 5 h fasted animals by Mouse serum adipokine milliplex kit. N=16. Data were analyzed separating the two Tg lines (L49 and L59) finding slight but no significant differences between them and always assessing one same pattern among the groups of both lines. Statistical analysis performed through t-test.

Although, both hfd groups exhibited a dramatic increase in the serum leptin satiety hormone, no differences appeared between c and Tg fed on one same diet (fig. 8). The difference in the weight increase between c hfd and all other groups was not justified by a difference in the ingestion.

#### 1.4. Lipid profile

The lipidic profile of these animals was studied in serum samples obtained after a 5 h fasting.

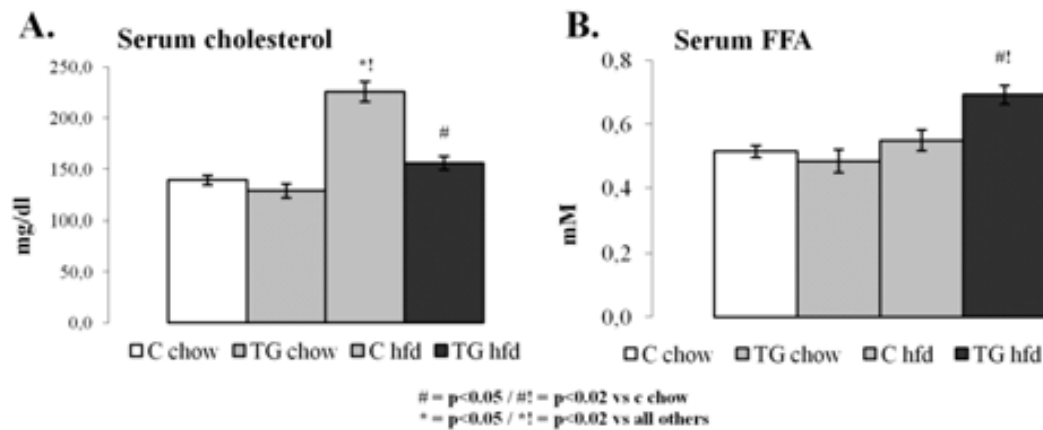


**Figure 9. Lipidic profile.** **A.** Serum cholesterol quantification performed in 6-month old 5 h fasted animals by FAR Cholesterol liquid ELISA-like kit Ref.: 7050 under manufacturer's recommendations. Results are given in mg/dl. N=16. Statistical analysis performed through t-test. **B.** Serum FFA quantification performed in 6-month old 5 h fasted animals by FFA Wako NEFA standard ELISA-like kit Ref.: 270-77000 under manufacturer's recommendations. N=16.

Serum cholesterol was found increased in both groups fed on hfd, however much more significantly in c than Tg suggesting a saturation of the cholesterol storage and processing in these groups (fig. 9A).

Serum free fatty acids (FFA) were only raised in Tg hfd animals (fig. 9B).

### 1.5. Effect of KAP and hfd on inflammation

The effects of the transgene, hfd or both at the same time were also tested on inflammatory pathways through mouse serum adipokine multiplex assays.

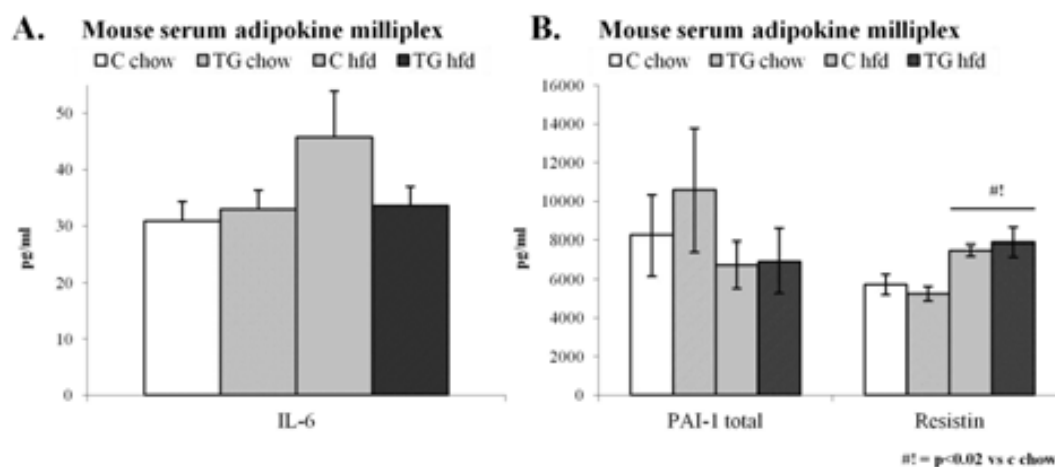


**Figure 10. Adipokines serum level.** Serum IL-6, PAI-1 and resistin measured in 6-month old 5 h fasted animals through Mouse serum adipokine multiplex kit. N=16. Statistical analysis performed through t-test.

IL-6 (interleukin 6) levels, which is an interleukin that acts as both a pro-inflammatory and anti-inflammatory cytokine, were only increased in c hfd animals, while surprisingly it was not increased in the presence of both hfd and Tg at the same time (fig. 10A). IL-6 is secreted by T cells and macrophages to stimulate immune response, during tissue damage leading to inflammation as well as in fighting infection. IL-6's role as an anti-inflammatory cytokine is mediated through its inhibitory effects on TNF- $\alpha$  and IL-1, and activation of IL-1ra and IL-10. It is one of the most important mediators of the acute phase response. IL-6 produced by adipocytes is thought to be a reason why obese individuals have higher endogenous levels of CRP (C-reactive protein). In muscle and fatty tissue, IL-6 stimulates energy mobilization. IL-6 is relevant to many diseases such as diabetes and atherosclerosis.

Serum PAI-1 (plasminogen activator inhibitor-1) is a serine protease inhibitor (serpin) that functions as the principal inhibitor of tissue plasminogen activator (tPA) and urokinase (uPA), the activators of plasminogen and hence fibrinolysis (the physiological breakdown of blood clots). This serpine levels were found risen only in the presence of the transgene, but not hfd or Tg plus hfd (fig. 10B). PAI-1 is present in increased levels in several diseases such as a number of forms of cancer, as well as in obesity and the metabolic syndrome.

Resistin, also known as adipose tissue-specific secretor factor (ADSF) or C/EBP-epsilon-regulated myeloid-specific secreted cysteine-rich protein (XCP1) is a cysteine-rich protein is secreted by adipose tissue in rodents. Its levels in serum were higher in hfd fed animals than chow fed independently of the genetic background (Tg or c) (fig. 10B). Resistin increases the production of LDL in human liver cells and also degrades LDL liver receptors. It also participates in the inflammatory response and has been shown to increase transcriptional events, leading to an increased expression of several pro-inflammatory cytokines including (but not limited to) interleukin-1 (IL-1), interleukin-6 (IL-6), interleukin-12 (IL-12), and tumour necrosis factor- $\alpha$  (TNF- $\alpha$ ) in an NF- $\kappa$ B-mediated fashion. There seems to be a strong correlation between resistin and obesity, serum resistin levels increase with increased adiposity and diminish with decreased adiposity. Specifically, central obesity (waistline adipose tissue in humans and epydidymal white adipose tissue in mice) seems to be the region of adipose tissue most actively contributing to rising levels of serum resistin. This fact takes on significant implications linking central obesity and insulin resistance.

### 1.6. Proteomic assays

A proteomic 2D assay was conducted in order to search for differential presence of proteins in serum among the experimental groups.

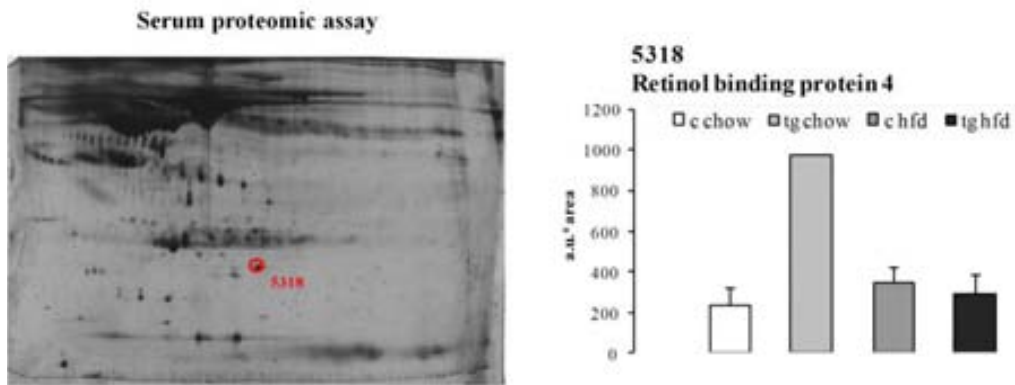


**Figure 11. Serum proteomic assay.** 2d assay carried out on 6-month old 5 h fasted animals serum pulls in order to reach appropriate sample volume. Differential protein presence among the four groups was analysed in Silver stained gels with the help of BioRad's PDQuest software. Differentially present proteins were identified by MALDI-TOFF. N=4. Statistical analysis performed through t-test.

This assay manifested a rise in Rbp4 (retinol binding protein 4) in Tg chow compared to all other 3 groups (fig. 11). Rbp4 is usually used as a nutritional indicator since it is a short half life protein, so that when nutrition is not adequate, the aminoacid input is diminished and Rbp blood levels decrease. When nutrition is adequate, Rbp4 blood level will rise.

### 1.7. Effect of stably transfected KAP on NFκB inflammation pathway in PCT3 clones

#### 1.7.1. PCT3-pBIG2i clones: doxycycline dose and time response effects of stably transfected KAP

Before carrying out the evaluation of the NFκB pathway, PCT3-pBIG2i-KAPwt transfected clones were characterized in order to assess inducibility of the expression of eukaryotic recombinant KAP according to the dose of doxycycline. Cells were treated in the way described in materials and methods, when they reached confluence at doxycycline recommended dose of 2 µg/ml during, 24, 48 and 72 hours.

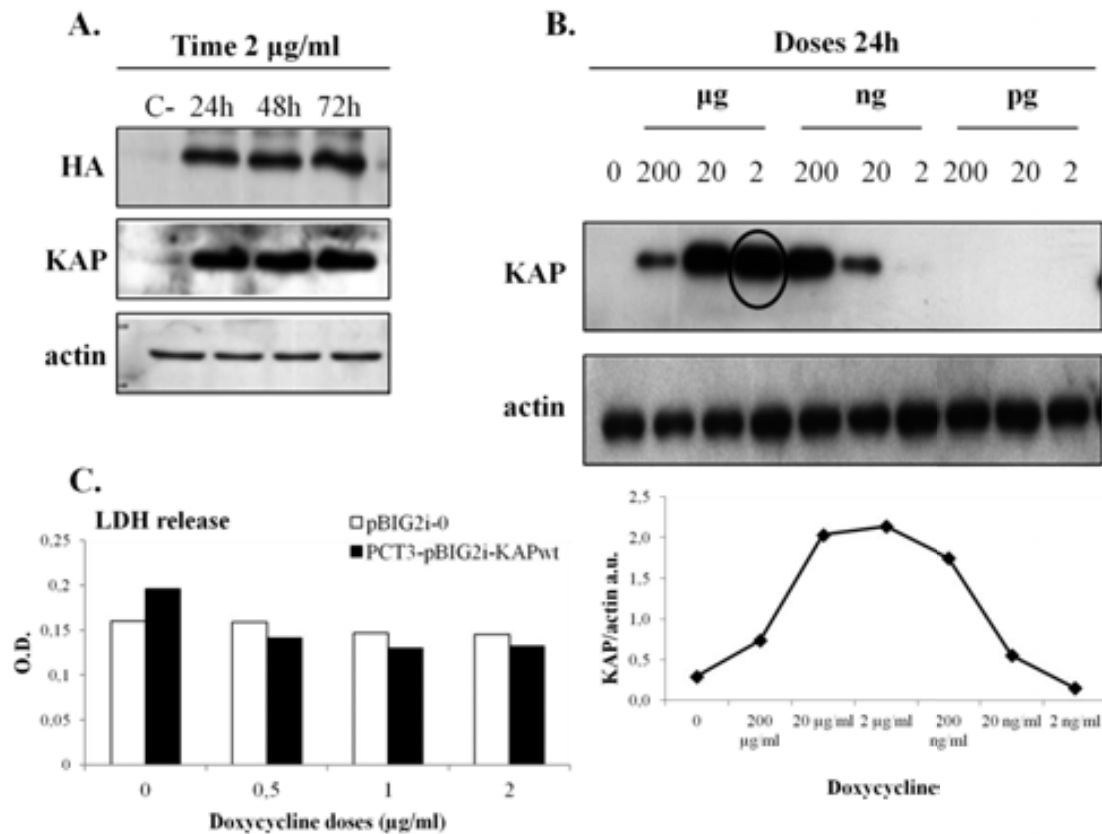


**Figure 12. Characterization of PCT3-pBIG2i-KAPwt transfected clones in the presence of doxycycline.** Cells were cultured in standard conditions (as described in Materials and Methods) and treated with doxycycline when they reached confluence. At the end of each experiment, cells were collected for further protein extraction using RIPA buffer. WB performed using whole cell protein extract and hybridized. Images acquired with a GS-800 C calibrated Densitometer and analysed with Quantity One software. **A.** Time-response assay with a determined dose of doxycycline. Membranes were hybridized both with anti-HA commercial antibody and anti-KAP lab made antibody in order to determine whether results of both antibodies correlated. Actin was used as housekeeping. **B.** Dose-response assay during a determined period of time. Membranes were hybridized with anti-HA antibody once confirmed that results are the same as with anti-KAP antibody. Results are given in HA/actin ratio arbitrary (densitometry) units. Actin was used as housekeeping. **C.** Media were collected in order to perform LDH release quantification as says which was quantified through colorimetric methods (as described in Materials and Methods) and read using an ELISA-plate reader. Results are given in optic density (O.D.) arbitrary units. N=3 biological replicates and 3 technical replicates. PCT3 transfected with the empty pBIG2i are used as a toxicity control for doxycycline.

No differences were found in the expression of the insert (KAPwt) (fig. 12A).

An in depth dose-response experiment proved that transfected cell clones expressed the insert (KAPwt) in a doxycycline dose dependent manner, demonstrating that the optimum dose for maximum expression is 2 µg/ml of doxycycline (fig. 12B).

Toxicity assays (evaluation of toxicity by quantifying LDH released to the culture medium) were carried out in order to check whether eukaryotic recombinant KAP is increases cell mortality. Cells were cultured and treated at confluence with 0, 0.5, 1, 2 µg/ml doses during 24 h to find out that doxycycline is not toxic for the cells and that eukaryotic recombinant KAP reduces slightly ldh release to the medium (fig. 12C).



### 1.7.2. Effect of stably transfected KAP on NFκB inflammation pathway

Since NFκB induces proinflammatory IL-6 and this was found increased when feeding control animals with hfd but not in the presence of the transgene alone or in the interaction of both, RT<sup>2</sup> Profiler PCR Array Systems differential gene expression assay (qReal Time SYBR® Green labelled probes PCR) was performed in order to validate activation of this inflammatory signalling pathway in proximal tubule cells with controlled expression of KAP.

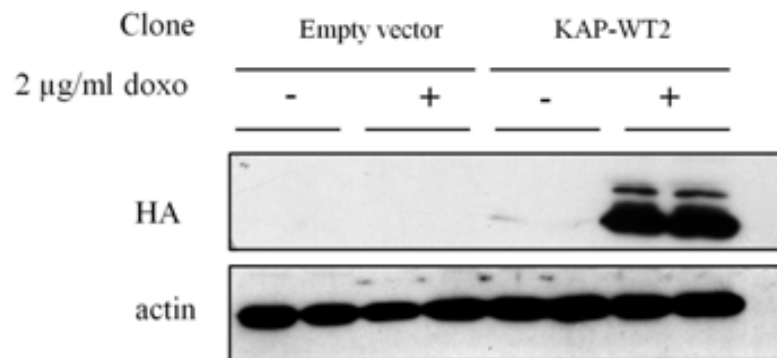
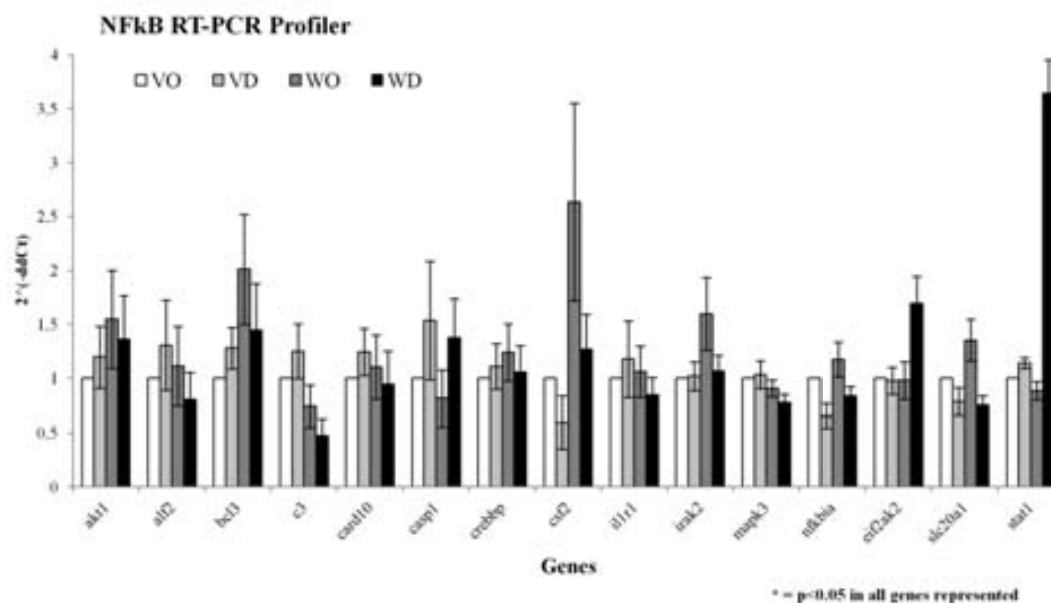


**Figure 13. Immunodetection of KAP in PCT3-pBIG2i clones.** WB performed using whole cell protein extract from PCT3-pBIG2i transfected clones, both empty plasmid and KAP wt, treated and not treated with 2 µg/ml doxycycline during 24 h. The four experimental groups, empty vector +/- doxycycline and KAPwt +/- doxycycline, shown in the figure were analysed in order to select the best negative control for the target study group KAPwt + doxycycline. Image acquired with a GS-800 Calibrated Densitometer and analysed with Quantity One software. Results are given in HA/actin ratio arbitrary (densitometry) units. N=4.

PCT3-pBIG2i-KAPwt and PCT3-pBIG2i (as a negative control) confluent cell cultures were treated with a single dose of 2 µg/ml doxycycline during 24h (fig. 13).



$2^{-(\Delta\Delta C_t)}$ WD-WO	akt1	akt2	bcl3	c3	casp10	casp1	crebbp	csf2	il1r1	irak2	mapk3	nfkb1a	nfkb2	slc20a1	stat1
MEAN	0.88	0.74	0.69	0.60	0.83	1.77	0.85	0.58	0.81	0.69	0.85	0.72	1.79	0.58	4.14
SEM	0.024	0.062	0.075	0.081	0.050	0.200	0.027	0.119	0.024	0.069	0.016	0.036	0.176	0.081	0.158
p-value	0.0154	0.0237	0.0257	0.0158	0.0441	0.0307	0.0113	0.0398	0.0045	0.0203	0.0025	0.0046	0.0208	0.0139	0.0003

**Figure 14. RT<sup>2</sup> P profiler PCR Array Systems differential gene expression assay** (q Real Time SYBR® Green labelled probes PCR) performed with whole cell RNA extract from PCT3-pBIG2i transfected clones, both empty plasmid and KAP wt, treated and not treated with 2 µg/ml doxycycline during 24h. Gene expressions given in fold change (FC)  $2^{(-\Delta\Delta C_t)}$  and calculated normalizing by a mean of GAPDH and actin as endogenous gene and since no calibrator sample was used for this assay, FC was calculated upon the ratio KAPwt+doxycycline vs KAPwt-doxycycline. N =4. Statistical analysis performed through t-test.

Only genes that showed no significant differences due to insertional effect or to doxycycline itself were taken into account for further statistical analysis. Genes represented above are those showing a p-value under 0.05.

Pro-inflammatory genes found down-regulated are detailed below (fig. 14):

**AKT1:** (serine-threonine protein kinase) and the related AKT2 are activated by platelet-derived growth factor. Activation occurs through phosphatidylinositol 3-kinase. Mice lacking Akt1 display a 25% reduction in body mass, indicating that Akt1 is critical in transmission of growth promoting signals, most likely via the IGF1 receptor.

**BCL3:** (B-cell lymphoma 3-encoded protein) is a proto-oncogene candidate. This protein works as a transcriptional co-activator that activates through its association with NFκB homodimers. The expression of this gene can be induced by NFκB, which forms a part of the autoregulatory loop that controls the nuclear residence of p50 NFκB. Bcl3 has been shown to interact with pparγ and NFκB2, among others.

C3: (complement component 3) plays a central role in the complement system and contributes to innate immunity activating complement system. Its activation is required for both classical and alternative complement activation pathways. Cross-sectional studies in humans have correlated C3 and obesity; there is also a linkage relationship of the insulin receptor gene with the complement component 3.

CARD10: (caspase recruitment domain-containing protein 10) is an enzyme that participates in apoptosis signalling through highly specific protein-protein homophilic interactions. CARDs induce NF $\kappa$ B activity through the IKK complex.

CREBBP: (CREB-binding protein) is a protein that carries out its function by activating transcription, where interaction with transcription factors is managed by one or more CREB domains. This gene is expressed ubiquitously and is involved in the transcriptional co-activation of many different transcription factors. Recent results suggest that novel CBP-mediated post-translational N-glycosylation activity alters the conformation of CBP-interacting proteins, leading to regulation of gene expression, cell growth and differentiation.

CSF2: colony stimulating factor 2 (granulocyte-macrophage) encodes for a cytokine that controls the production, differentiation, and function of granulocytes and macrophages.

IL1R1: interleukin 1 receptor type 1 encodes for a cytokine receptor that belongs to the interleukin 1 receptor family. This protein is a receptor for interleukin alpha (IL1A), interleukin beta (IL1B), and interleukin 1 receptor, type I (IL1R1/IL1RA). It is an important mediator involved in many cytokine induced immune and inflammatory responses.

IRAK2: (interleukin-1 receptor-associated kinase-like 2) encodes for an interleukin-1 receptor-associated kinase 2, one of two putative serine/threonine kinases that become associated with the interleukin-1 receptor (IL1R) upon stimulation. IRAK2 is reported to participate in the IL1-induced upregulation of NF $\kappa$ B.

MAPK3: (mitogen-activated protein kinase 3) encodes for an enzyme member of the MAP kinase family. MAP kinases, also known as extracellular signal-regulated kinases (ERKs), act in a signalling cascade that regulates several cellular processes including proliferation, differentiation, and cell cycle progression in response to a variety of extracellular signals. This kinase is activated by upstream kinases, resulting in its translocation to the nucleus where it phosphorylates nuclear targets. Alternatively spliced transcript variants encoding different protein isoforms have been described.

NFKB1: (nuclear factor NF $\kappa$ B p105 subunit) encodes a protein which can undergo cotranslational processing by the 26S proteasome to produce NF- $\kappa$ B protein complex. NF- $\kappa$ B is activated by various intra- and extra-cellular stimuli such as cytokines, oxidant-free radicals, ultraviolet irradiation, and bacterial or viral products. Activated NF- $\kappa$ B translocates into the nucleus and stimulates the gene expression. Inappropriate activation of NF- $\kappa$ B has been

associated with a number of inflammatory diseases while persistent inhibition of NF- $\kappa$ B leads to inappropriate immune cell development or delayed cell growth.

SLC20A1: (sodium-dependent phosphate transporter 1) the protein encoded by this gene is a sodium-phosphate symporter that absorbs phosphate from interstitial fluid for use in cellular functions such as metabolism, signal transduction, and nucleic acid and lipid synthesis. The encoded protein is also a retroviral receptor, causing human cells to be susceptible to infection by gibbon ape leukemia virus, simian sarcoma-associated virus, feline leukemia virus subgroup B, and 10A1 murine leukemia virus.

The following anti-inflammatory genes were found up-regulated:

CASP1: (caspase 1/interleukin-1 converting enzyme) is an enzyme that proteolytically cleaves other proteins, such as the precursor forms of the inflammatory cytokines interleukin 1- $\beta$  and interleukin 18, into active mature peptides. Caspase 1 has demonstrated to induce cell necrosis or pyroptosis and may function in various developmental stages.

EIF2AK2: (eukaryotic translation initiation factor 2-alpha kinase 2) also known as protein kinase RNA-activated or protein kinase R (PKR). PKR is activated by double-stranded RNA (dsRNA), the synthesis of which is caused virally, activating its pro-apoptotic (cell-killing) functions. Once active, PKR is able to phosphorylate the eukaryotic translation initiation factor EIF2A. This inhibits further cellular mRNA translation, preventing viral protein synthesis. Active PKR is also able to mediate the activation of the transcription factor NF $\kappa$ B, by phosphorylating its inhibitory subunit, I $\kappa$ B. Activated NF $\kappa$ B up-regulates the expression of interferon cytokines, which work to spread the antiviral signal locally. Active PKR is also able to activate tumour suppressor PP2A which regulates the cell cycle and the metabolism. Through complex mechanisms, active PKR is also able to induce cellular apoptosis, to prevent further viral spread.

STAT1: Signal Transducer And Activator Of Transcription 1 is a signal transducer and transcription activator that mediates cellular responses to interferons (IFNs), cytokine KITLG/SCF and other cytokines and growth factors.

## **2. Studies in isolated organs:**

### **2.1. Organs' weight**

The difference in the body weight gain between c hfd and all other 3 groups seemed to depend on the increase in size of epididymal and inguinal white adipose tissues, and liver. Brown adipose tissue also appeared slightly larger in c hfd (fig. 15), however, since it represents a small tissue compared to the whole body size, it was not involved in the difference in the body weight.

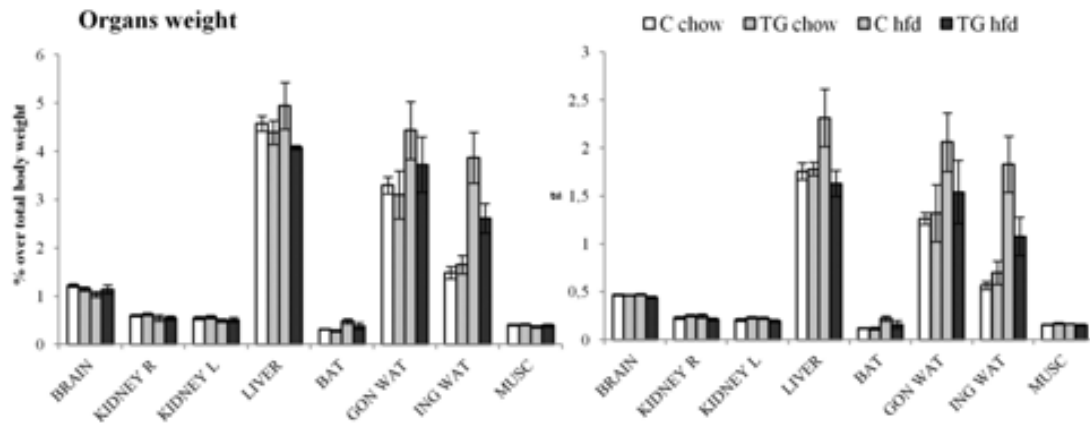


**Figure 15. Organs weight.** Organs weights measured after extraction at the time of animals' sacrifice at their 6.5 months of life. Data are given in absolute numbers (grams) and in percentage over total body weight. Data were analyzed separating the two tg lines (L49 and L59) finding slight but no significant differences between them and always assessing one same pattern among the groups of both lines. N=16. Statistical analysis performed through t-test.

## 2.2. Adipose tissues histology

Histochemical analyses (eosin-haematoxylin) in three adipose tissue types: brown, epididymal and inguinal white, showed larger adipocytes in both Tg groups vs c chow and even bigger in c hfd, no apparent differences were found between sizes of Tg chow and hfd (fig. 16).

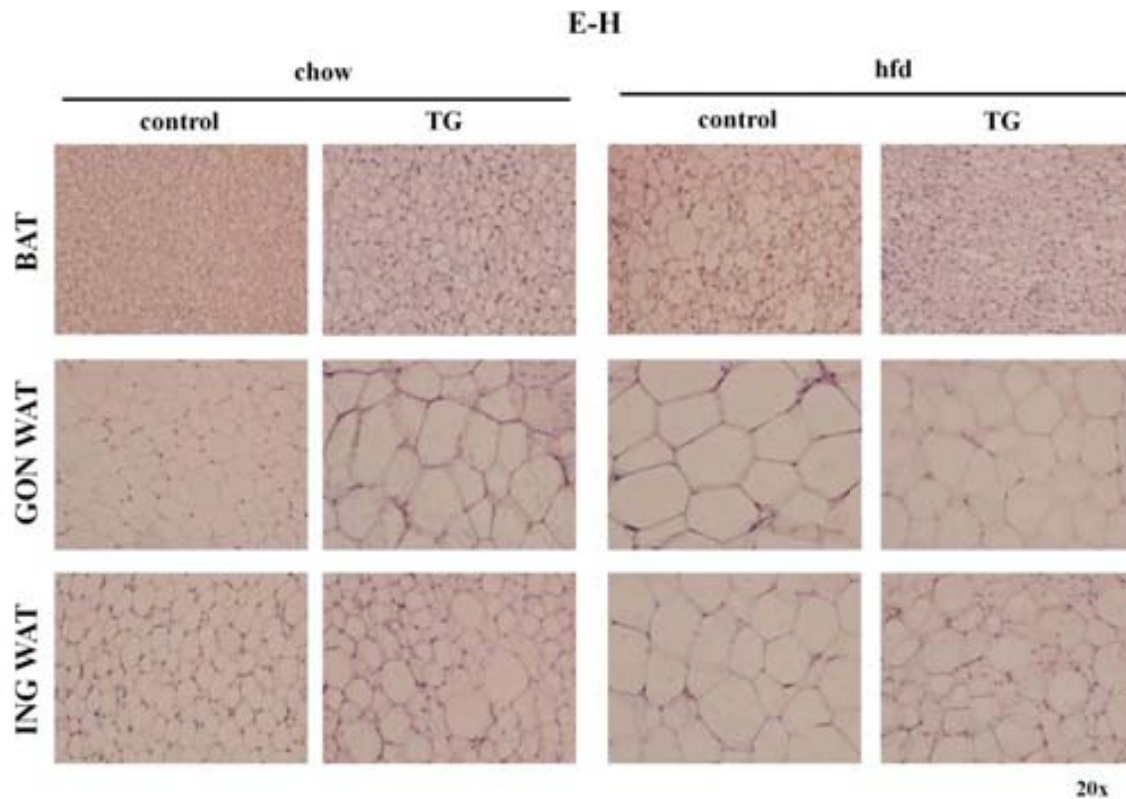


**Figure 1 6. Adipose tissues histochemistry.** Histochemical analysis of paraffin imbedded animals' adipose tissues: brown, and inguinal and gonadal (epididymal) white extracted and fixed at animals' sacrifice at their 6.5 months of life by eosin-haematoxylin (E-H) staining in tissue slides performed with the help of Haizea Lekuona. N=8.

### 2.3. Liver histology

Further histochemical analyses (eosin-haematoxylin and Masson's trichrome) in mice's livers showed no evident differences between c chow and Tg chow 6-months-old animals. Livers of animals fed on a hfd showed hepatic steatosis which was milder in Tg than in c (fig. 17A). This fact was verified by lipid quantification techniques in liver that confirmed statistically significant differences between the quantities of lipids in liver of animals fed on hfd vs chow diet as well as between c and Tg animals fed on hfd (fig. 17B).

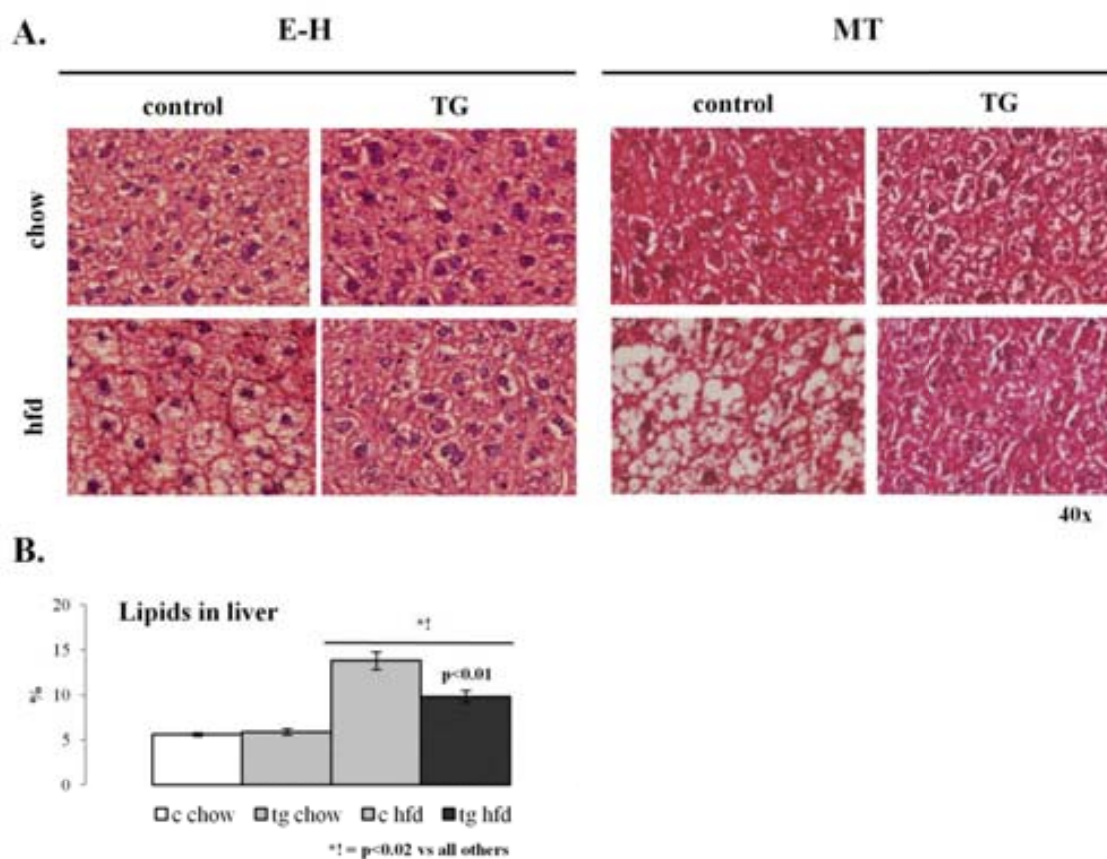


**Figure 1 7. Liver h istochemistry.** **A.** Histochemical analysis of paraffin imbedded animals' livers extracted and fixed at animals' sacrifice at their 6.5 months of life by eosin-haematoxylin (E-H), and Masson's trichrome (MT) staining in tissue slides performed with the help of Cristina Suarez and Andrea Caballero. N=8. **B.** Lipid quantification in liver was measured by separating the lipids from the rest of the tissue, measuring lipid weight and calculating the ratio over total liver weight for each animal. Assay performed with the help of Ayleen de la Rivera. Results are given in percentage. N=8. Statistical analysis performed through t-test.

#### 2.4. Effect of prokaryotic recombinant KAP on lipid storage in HepG2 cells

With the aim of evaluating whether KAP affects lipidic content in human hepatoma cell line (HepG2) and given that the over-expression of KAP in our in vivo model influenced lipid storage in liver, the influence of KAP in hepatocyte lipid accumulation was studied in HepG2 by culturing these cells with prokaryotic recombinant KAP and oleic acid.

##### 2.4.1. HepG2: dose-response effects of prokaryotic recombinant KAP

On a first study, cells were cultured in 1.5 % FFA free BSA medium with different doses of oleate, one single KAP dose and one KAP+oleate crossed dose during either 48 or 72h. In order to visualise lipids in-cell, cultures were stained with oil red o lipid staining, and this revealed that the amount of lipid found inside the cell is directly related to the dose of oleate added to the medium: the more oleate in the medium, the more lipid found inside the cell. However, 2 mM oleate maximum dose appeared to be toxic for the cells. The presence of prokaryotic

recombinant KAP alone did not seem to have an effect on the intra-cell accumulated lipid compared to non treated cultures, although, when treating cells with both KAP and 1 mM oleate, the amount of lipid accumulated in the cells seemed to be less than in 1mM oleate treated cells (fig. 18).



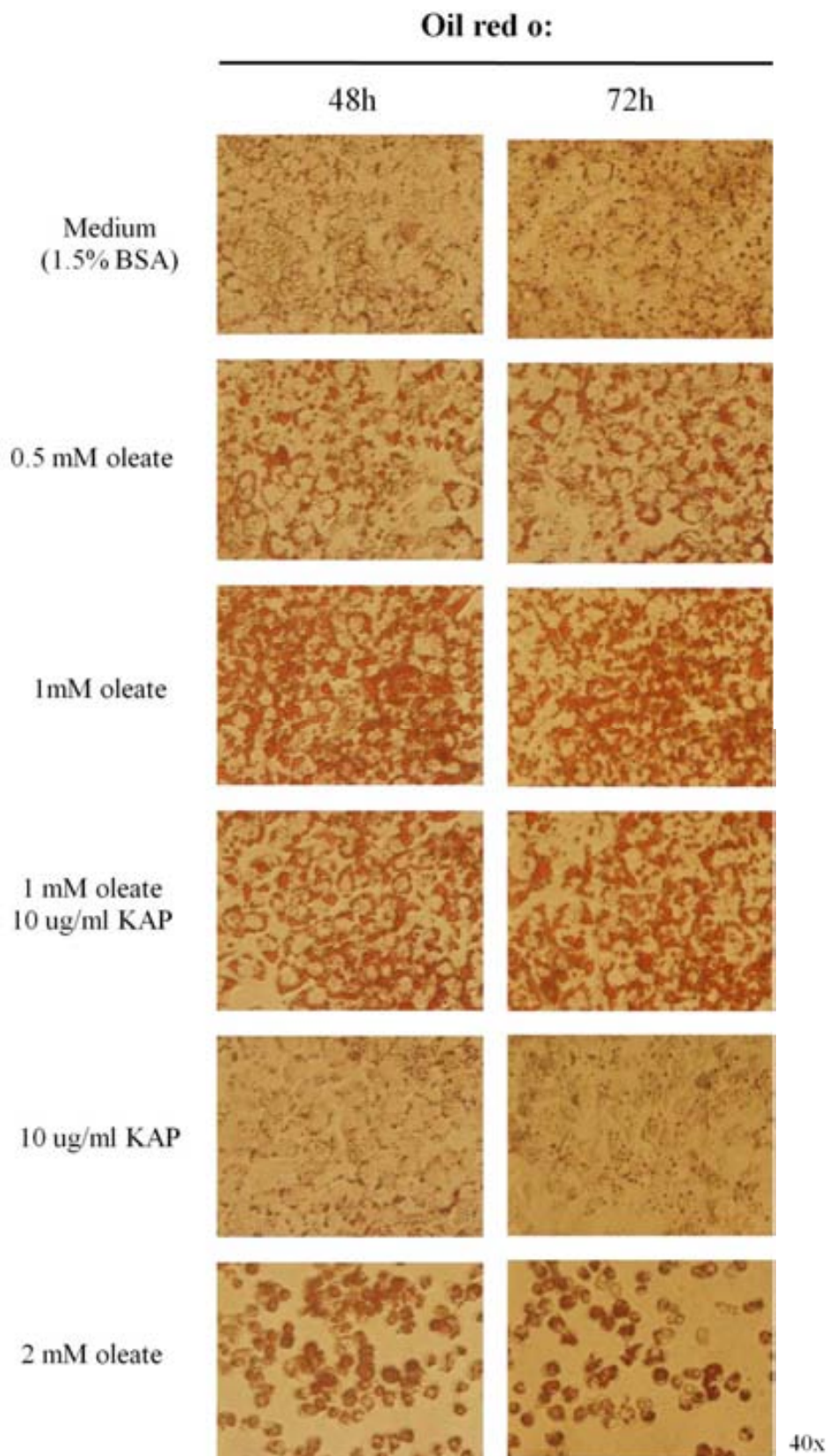


**Figure 18. Oil red o (ORO) staining of oleate and KAP treated HepG2 cells.** ORO lipid staining of HepG2 human liver cells cultures cultured in 1.5 % FFA free BSA medium and treated with 0, 0.5, 1 and 2 mM oleate or with 10 u g/ml prokaryotic recombinant KAP (produced by Antonio Cuevas) and 10 ug/ml prokaryotic recombinant KAP + 1 mM oleate, all of the after 24 h of deprivation when cells reached 60-70 % of confluence. Treatments performed during 48h and 72 h. N=3.

In order to evaluate whether prokaryotic recombinant KAP and/or oleate were toxic or could influence viability of human liver isolated cell cultures, LDH (for toxicity) and XTT (for viability) assays were performed.

LDH assays showed that oleate was significantly toxic ( $p < 0.01$ ) for the cells no matter the dose or preconditioning, except for cells preconditioned with KAP, where oleate is more toxic than in all other cases (fig. 19).

These same assays demonstrated that KAP acts significantly against oleate toxicity when:

- both were added at the same time at 0.5 mM oleate and 25  $\mu\text{g/ml}$  KAP doses (fig. 19A)
- cells were preconditioned with oleate at 2 mM oleate and 10  $\mu\text{g/ml}$  KAP (fig. 19B)
- cells were preconditioned with KAP at 0 mM oleate and 10  $\mu\text{g/ml}$  KAP, 0 mM oleate and 25  $\mu\text{g/ml}$  KAP, and 2 mM oleate and 25  $\mu\text{g/ml}$  KAP (fig. 19C).

However, KAP worked significantly pro-toxicity when:

- cells were preconditioned with oleate at 0 mM oleate and 25  $\mu\text{g/ml}$  KAP, 0.5 mM oleate and 10  $\mu\text{g/ml}$  KAP, and 1 mM oleate and 10  $\mu\text{g/ml}$  KAP.

In general terms, KAP seemed to be toxic for the cells when these were preconditioned with oleate, but protected against oleate toxicity when cells were preconditioned with KAP and less strongly when KAP and oleate were added at the same time.

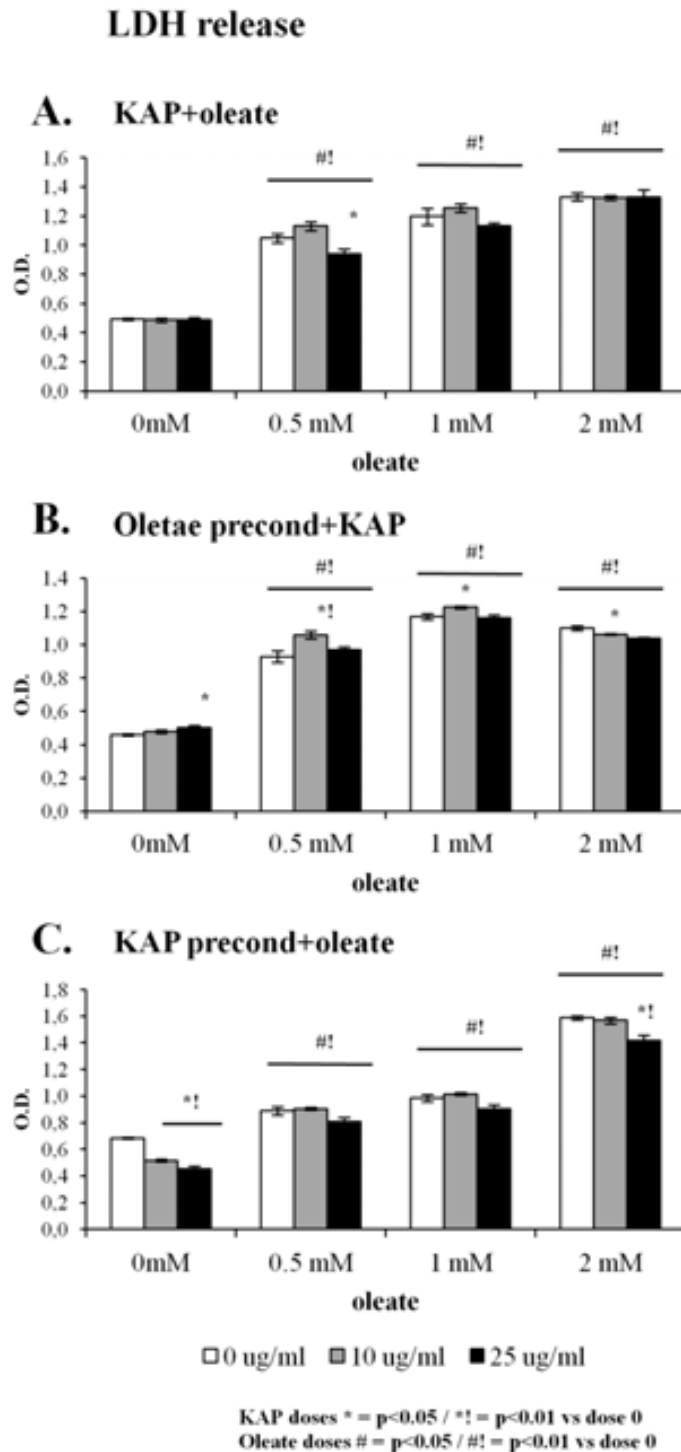


**Figure 19. LDH release analysis of oleate and KAP treated HepG2 cells.** Crossed doses of prokaryotic recombinant (produced by Antonio Cuevas) KAP (0, 10, 25 ug/ml) and oleate (0, 0.5, 1, 2 mM) treated HepG2 cultures after 24 h of deprivation when cells reached 60-70 % of confluence in three treatment groups: **A.** KAP and oleate are added at the same time and cells are cultured during 72h. N=3. **B.** HepG2 are preconditioned with oleate for 24h and then treated with KAP+oleate for 48h. N=3. **C.** HepG2 are preconditioned with KAP for 24h and then treated with KAP+oleate for 48h. N=3. Media were collected in order to perform LDH release quantification assays which was quantified through colorimetric methods (as described in Materials and Methods) and read using an ELISA-plate reader. Results are given in optical density (O.D.) arbitrary units. N=3 biological replicates and 3 technical replicates. Statistical analysis performed through t-test.

XTT viability assays showed that oleate enhanced viability at 0.5 mM and 1 mM doses. KAP was another viability enhancing factor when added at the same time with oleate at 0 mM oleate and 25 µg/ml KAP, 1 mM oleate and 10 µg/ml KAP, and 1 mM oleate and 25 µg/ml KAP doses. However, viability decreased at 2 mM oleate dose, independently of the preconditioning. When cells were preconditioned either with oleate or KAP, viability was unaffected by the presence of KAP.

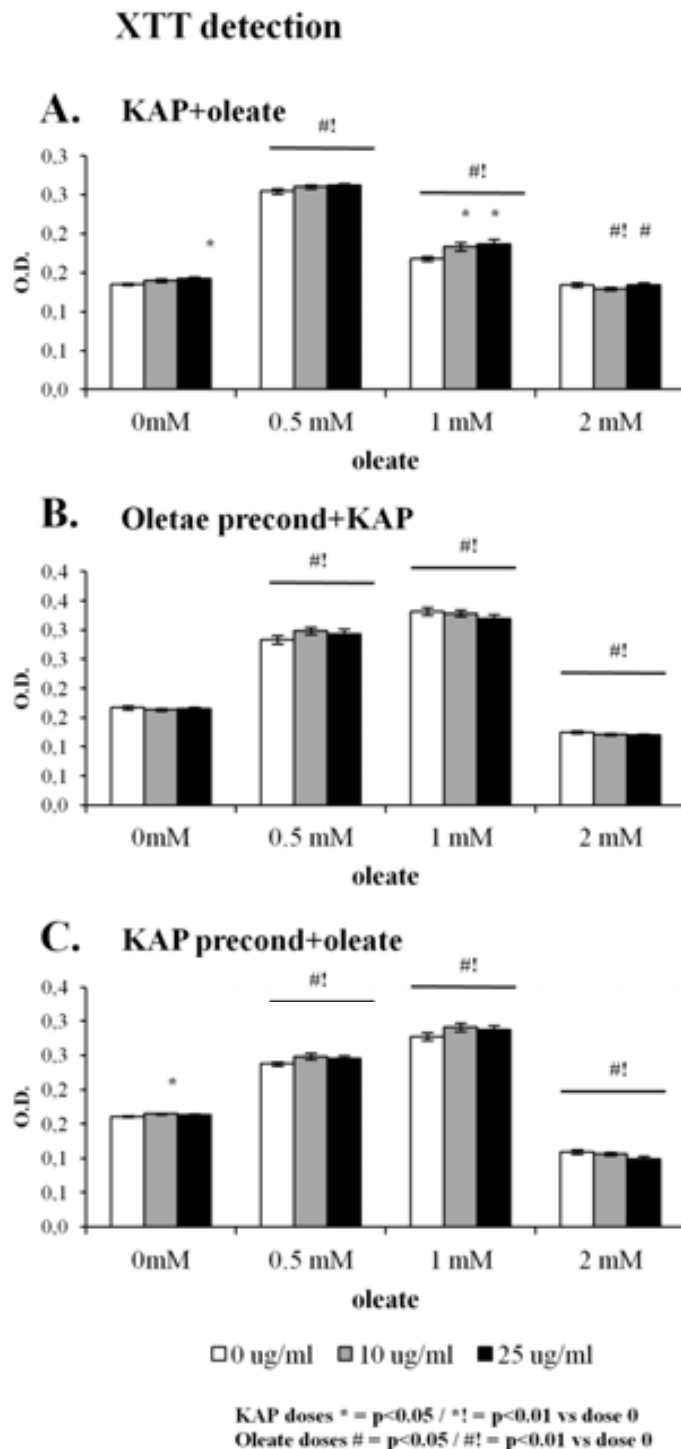


**Figure 20. XTT release analysis of oleate and KAP treated HepG2 cells.** Crossed doses of prokaryotic recombinant (produced by Antonio Cuevas) KAP (0, 10, 25 ug/ml) and oleate (0, 0.5, 1, 2 mM) treated HepG2 cultures after 24 h of deprivation when cells reached 60-70 % of confluence in three treatment groups: **A.** KAP and oleate are added at the same time and cells are cultured during 72h. N=3. **B.** HepG2 are preconditioned with oleate for 24h and then treated with KAP+oleate for 48h. N=3. **C.** HepG2 are preconditioned with KAP for 24h and then treated with KAP+oleate for 48h. N=3. Cells were cultured in 96-wells plates in order to perform XTT quantification as says which was quantified through colorimetric methods (as described in Materials and Methods) and read using an ELISA-plate reader. Results are given in optic density (O.D.) arbitrary units. N=8. Statistical analysis performed through t-test.

### 2.4.2 Effect of prokaryotic recombinant KAP on lipid storage in human liver cells

A second step experiment, involving the quantification of oil red o by fading it with isopropanol, confirmed this fact in the following way: cells were cultured and treated in three different ways with KAP+oleate crossed-over doses. Lipid amount (in optic density (O.D.) arbitrary units) was normalized by the total cell density, quantified by staining the cells with nuclei staining Hoescht, taking pictures of several fields of each plate well and quantifying the amount of blue using ImageJ software.

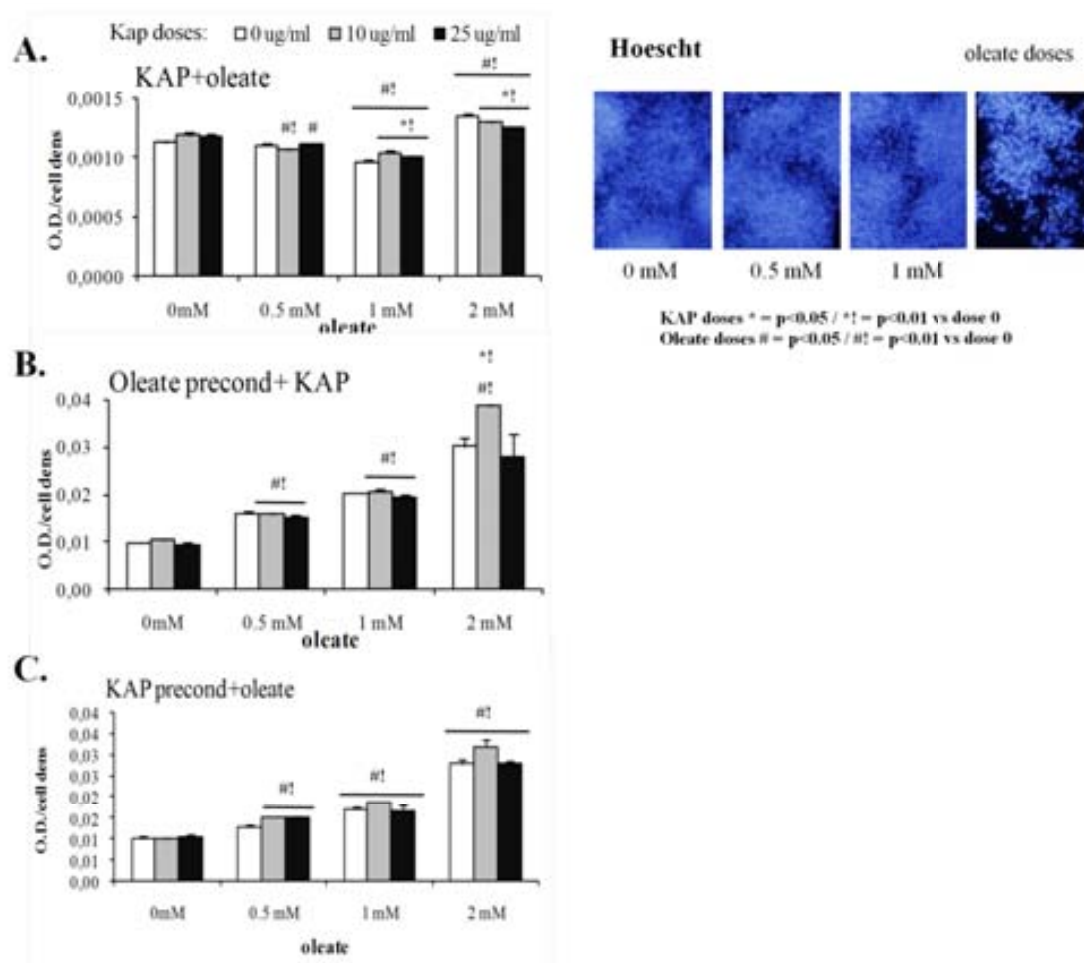


**Figure 21. Lipid quantification in oleate and KAP treated HepG2 cells.** Crossed doses of prokaryotic recombinant KAP produced by Antonio Cuevas (0, 10, 25 ug/ml) and oleate (0, 0.5, 1, 2 mM) treated HepG2 cultures after 24 h of deprivation when cells reached 60-70 % of confluence in three treatment groups: **A.** KAP and oleate are added at the same time and cells are cultured during 72h. N=3. **B.** HepG2 are preconditioned with oleate for 24h and then treated with KAP+oleate for 48h. N=3. **C.** HepG2 are preconditioned with KAP for 24h and then treated with KAP+oleate for 48h. N=3. Cultures were stained with oil red o in order to visualize lipids inside them. Oil red o was removed from the cells by fading them with isopropanol and amount of oil red o (in proportion to intra cell lipids) was quantified using an ELISA-plate reader. Statistical analysis performed through t-test.

On the first place, KAP and oleate were added at the same time, showing no difference in the cells lipid content until 2 mM oleate, were all three cultures treated with KAP showed an increase in the amount of lipids vs all other lower oleate doses, however the lipid content decreased with the increase in the KAP doses in this group (fig. 21A).

Secondly, cells were first preconditioned with oleate and then treated with both KAP and oleate. In this case, an increase in intra-cell lipid levels did show when increasing oleate doses. Moreover, when adding 25 µg/ml dose, intra-cell lipid accumulation seemed to decrease compared to 0 and 10 µg/ml of KAP in one same oleate dose (fig. 21B).

And third, cells were preconditioned with KAP and then treated with KAP and oleate together. Cells behaved in a similar way as formerly described, but the effect shown by 25 µg/ml dose was evident only from 1 mM oleate dose and further (fig. 21C).

### **2.5. Kidney histology**

In additional histochemical analyses (eosin-haematoxylin, Masson's trichrome and periodic acid-Schiff stains) of the mice's kidneys no evident differences were found between c chow and Tg chow 6-months-old kidneys. Kidneys of animals fed on hfd showed tubular damage and vacuolisation from a lipidic origin in tubular cells, being these more evident in Tg than c. Tg's glomeruli seemed more collapsed than c's (fig. 22).

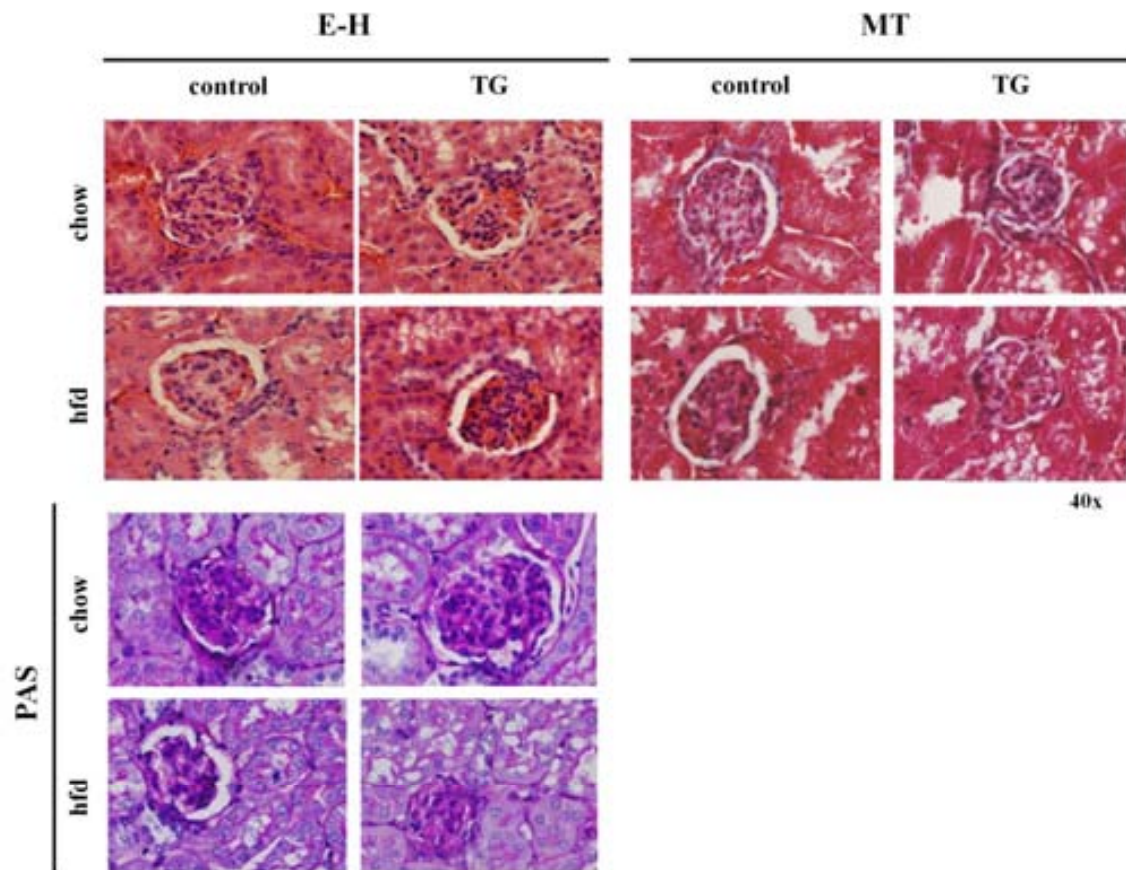


**Figure 22. Kidney histochemistry.** Histochemical analysis of paraffin-embedded animals' kidneys extracted and fixed at animals' sacrifice at their 6.5 months of life by eosin-haematoxylin (E-H), Masson's trichrome (MT) and Periodic acid-Schiff (PAS) staining in tissue slides performed with the help of Cristina Suarez and Andrea Caballero. N=8.

The expression of KAP (protein) was analysed in kidney protein extracts by immunoblotting demonstrating to be not affected by hfd alone, Tg mice exhibited higher expression of KAP vs c and in the case of Tg, hfd did enhance the expression of Kap (fig. 23).



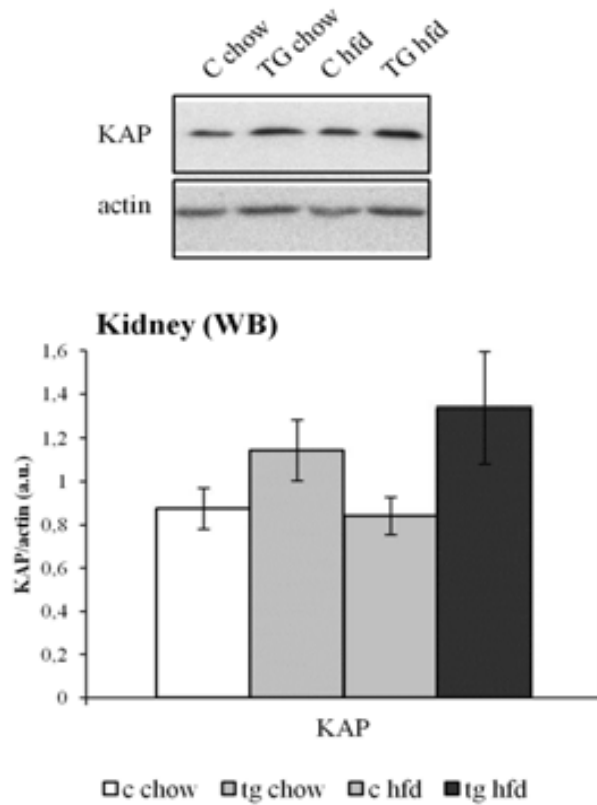


**Figure 23. Immunoblotting of KAP in mice's kidneys.** WB analysis of whole kidney protein extract hybridised with antiKAP antibody and normalised with actin. N=8. Image acquired with a GS-800 Calibrated Densitometer and analysed with Quantity One software. Results are given in KAP/actin ratio arbitrary (densitometry) units. Statistical analysis performed through t-test.

## 2.6. Study of the secretion of KAP

Since KAP (protein) proved to have an action not only in kidney but also on distal tissues such as liver and adipose tissues, and, given that, KAP has been found located in Golgi apparatus and endoplasmic reticulum secretory pathway as well as secreted to the cell culture medium, the arrival mean to the tissues was analysed by immunoblotting.

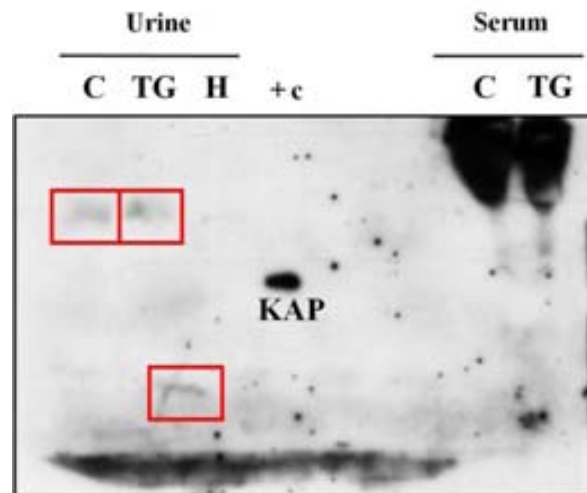


**Figure 24. Immunoblotting of KAP in mice's serum and urine.** WB performed using serum from a KAP tg mouse and from a c littermate, as well urine from both these mice and human (h) urine. Kidney protein extract from a c mouse was used as an antibody positive control. Membrane was hybridised with antiKAP antibody. Images acquired with a GS-800 Calibrated Densitometer and analysed with Quantity

Through the use of serum from a KAP Tg mouse and from a c littermate, as well urine from both these mice and human (h) urine. The samples were analysed by SDS-PAGE immunoblotting and demonstrated the presence of encouraging bands in c, Tg and human urine lanes, however not with the appropriate molecular weight (fig. 24).

The samples used for the following step were the same as in the previous, adding one more: human serum, and concentrating all urine samples with Amicon filters. In this case, each sample was analysed twice by SDS-PAGE immunoblotting, the first duplicated was hybridised with antiKAP antibody and the second duplicate with antiKAP antibody plus 25x KAP's peptide in order to be able to detect unspecific bindings of the antibody.

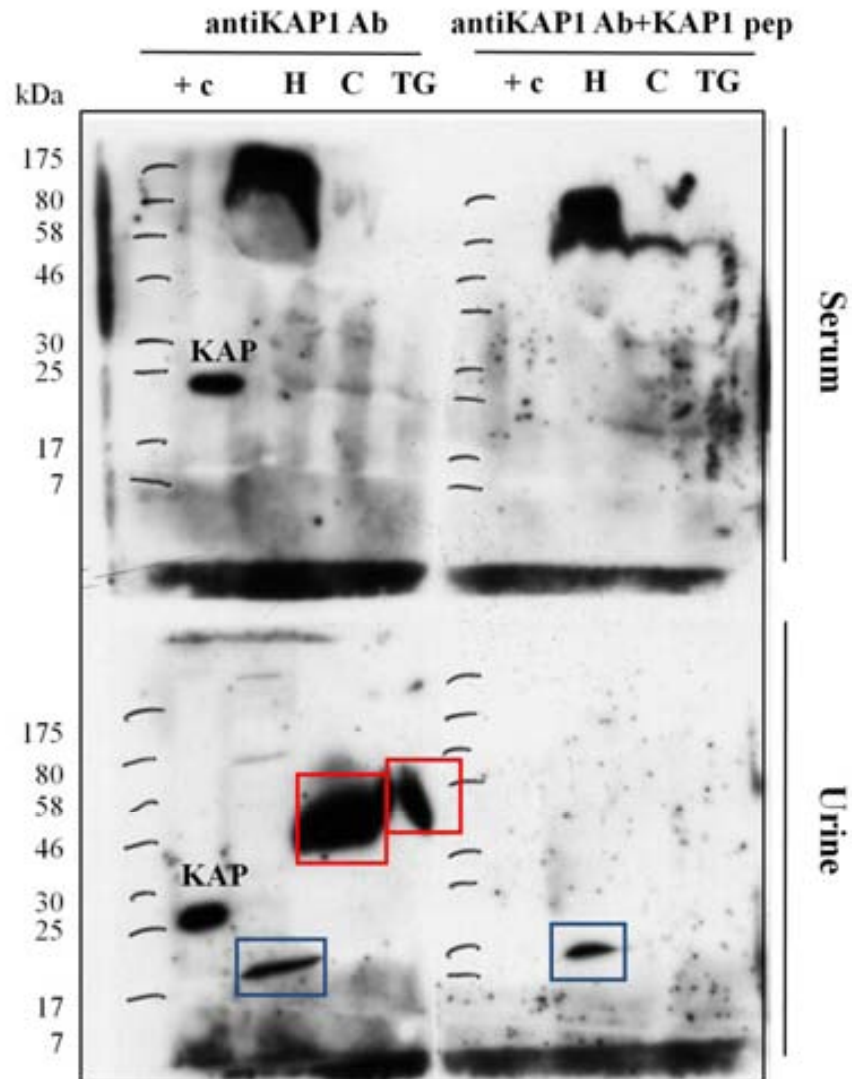


**Figure 25. Immunoblotting of KAP in mice's serum and urine.** WB performed by running each of the former samples twice in SDS-PAGE gels, the first duplicated was hybridised with antiKAP antibody and the second duplicate with antiKAP antibody+25x KAP's peptide in order to be able to detect unspecific bindings of the antibody. Bands which mean unspecific bindings should disappear when the peptide is added. Image acquired with a GS-800 Calibrated Densitometer and analysed with Quantity One software.

Results obtained in serum samples were not conclusive since new bands appeared in this last step (never seen in step two) and these did not vanish when hybridised with antibody's peptide. Nevertheless, interesting results were obtained in urine samples. When hybridising with antiKAP antibody bands were detected on all samples lanes: human, c and Tg, still not at the appropriate molecular weight. When hybridising with antiKAP+peptide, the band in the human sample lane remained, confirming an unspecific binding of the antibody. But the bands in c and Tg samples lanes disappeared confirming specific binding of the antibody and, although not at the appropriate molecular weight, identifying these bands as KAP (fig. 25).

PCT3 clones transfected with wt KAP cDNA in P BIG2i doxycycline inducible plasmid and clones transfected with P BIG2i empty plasmid (used as a negative control) were cultured on standard conditions in transwell culture plates and treated with doxycycline 2 µg/ml for 24h.

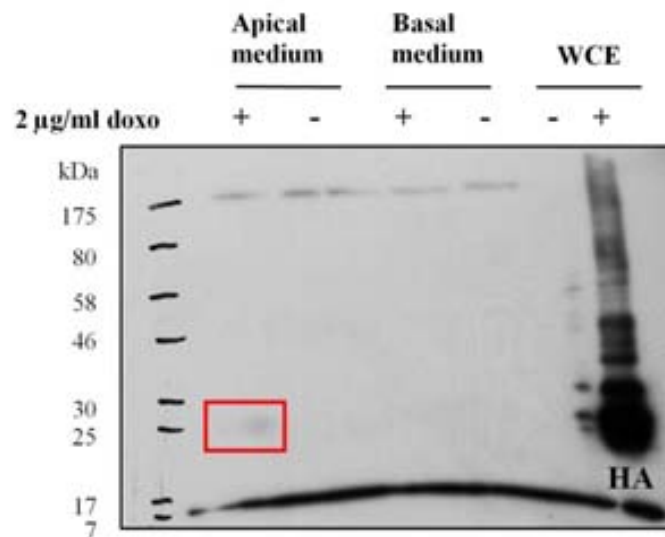


**Figure 26. Immunoblotting of KAP in PCT3-pBIG2i clones' culture media.** WB performed using both media and whole cell protein extract from PCT3-pBIG2i-KAPwt transfected clones treated and not treated with 2 µg/ml doxycycline during 24 h. Cells were cultured in transwell plates in order to distinguish apical medium from basal medium and, therefore, be able to evaluate whether KAP is released to one or the other, or both. WCE was used as an antibody positive control. Membrane was hybridised with antiHA antibody. Images acquired with a GS-800 Calibrated Densitometer and analysed

Apical and basal media as well as whole cell protein extract (wce) as an antibody positive control were analysed by SDS-PAGE immunoblotting showing that cells treated with doxycycline (activating the expression of KAP) released KAP to the apical medium that corresponds to the urinary space in renal tubules (fig. 26).

### 3. Differential gene expression assays in adipose tissue, liver and kidney:

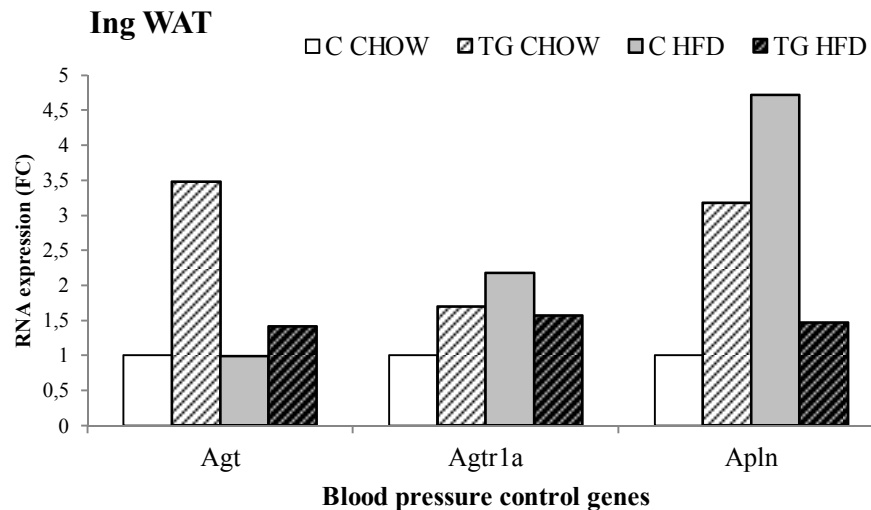
Differential gene expression assays were performed on our study target organs and tissues with the aim of finding a molecular correlation with physiological observations. Genes were selected basing the decision on previous RNA microarray assays as well as in published genes related to metabolic syndrome in these three organs.

#### 3.1. Differentially expressed genes in inguinal white adipose tissue (WAT)

Differential gene expression assays in inguinal white adipose tissue evidenced that AGT (angiotensin II) is significantly up-regulated in t g chow vs c c how animals, and AGTR1a (angiotensin II receptor, type 1a) was up-regulated in the presence of the transgene alone, and its expression was increased even more in c hf d vs c c how ( fig. 27 ). AGTR1a, binds to

angiotensin II and this latter contributes to blood pressure control by enhancing vasoconstriction and inhibiting the excretion of water by the kidneys.

APLN (a pelin) is a cell surface peptide involved in blood pressure control by activating the release of hypotensive vasodilator NO, the expression of which was significantly increased in tg chow and c hfd vs c chow, and diminished in tg hfd vs c hfd (fig. 27).



TG CHOW vs WT CHOW				
GENE ID	TG_CHOW	WT_CHOW (basal condition)	logFC	p-value
-0,76089	-0,00116	-0,76089	0,75972	0,00485
Agt	0,54110	-1,25544	1,79654	0,01196
Aplin	-0,13194	-1,79714	1,66521	0,03084

WT HFD vs WT CHOW				
GENE ID	WT_HFD	WT_CHOW (basal condition)	logFC	p-value
Agtr1a	0,36355	-0,76089	1,12444	0,00008
Aplin	0,44061	-1,79714	2,23776	0,00465

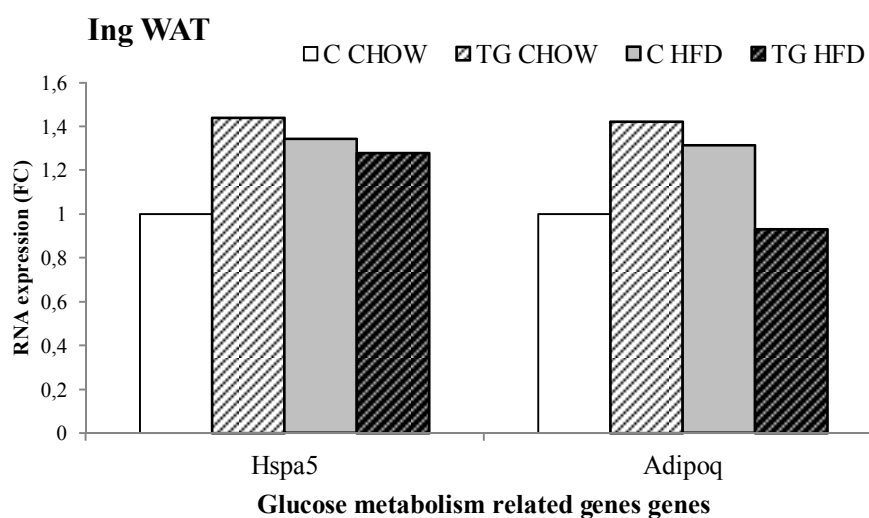
TG HFD vs WT_HFD				
GENE ID	TG_HFD	WT_HFD (basal condition)	logFC	p-value
Aplin	-1,24616	0,44061	-1,68677	0,02887

TGvsWT HFDvsCHOW		
GENE ID	logFC	p-value
Agtr1a	-1,23969	0,00140
Aplin	-3,35198	0,00290

**Figure 27. Differential gene expression analysis in WAT.** Microfluidic cards differential gene expression assay (q Real Time TaqMan probes PCR) from inguinal WAT RNA extracted from frozen tissue after animals' sacrifice at their 6.5 months of life performed by Haizea Lekuona. Gene expression given in fold change (FC)  $2^{-\Delta\Delta Ct}$  and calculated normalizing by Ppia as endogenous gene and one same c chow mouse sample as calibrator sample. N=8. Statistical analysis performed through t-test.

This same assay also showed differential expression of genes involved in glucose metabolism such as a slight raise in the expression of HSPA5 in tg chow and c hfd vs c chow (fig 28). HSPA5 encodes for binding immunoglobulin protein (BiP) also known as 78 kDa glucose-regulated protein (GRP-78) or heat shock 70 kDa protein 5 which is found to decrease when cells are glucose-starved. When starved of glucose, the synthesis of these so called glucose-regulated proteins (GRPs), is markedly increased, such as HSPA5, which is involved in the folding and assembly of proteins in the endoplasmic reticulum (ER). The level of HSPA5 is strongly correlated with the amount of secretor proteins within the ER. Like many stress and heat shock proteins, BiP/GRP78 has potent immunological activity when released from the internal environment of the cell into the extracellular space. Specifically, it feeds anti-inflammatory and pro-resolatory signals into immune pathways.

Adicytokine ADIPOQ appeared up-regulated in the presence of either the transgene or the hfd, but not in the presence of both (fig. 28).



TG CHOW vs C CHOW				
GENE ID	TG_CHOW	C_CHOW (basal condition)	logFC	p-value
Hspa5	0,81975	0,29516	0,52459	0,01661

C HFD vs C CHOW				
GENE ID	C_HFD	C_CHOW (basal condition)	logFC	p-value
Hspa5	0,72104	0,29516	0,42588	0,04868

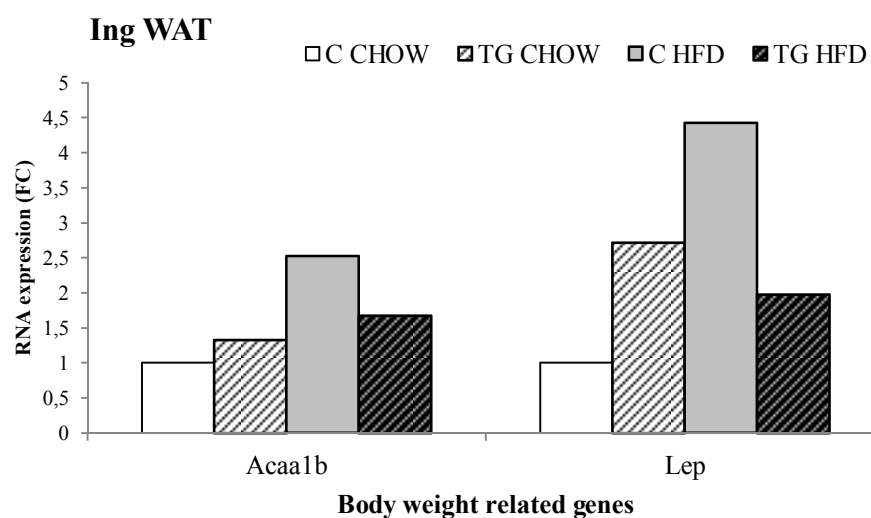
TGvsC HFDvsCHOW		
GENE ID	logFC	p-value
Adipoq	-1,00196	0,01752

**Figure 2 8. Differential gene expression analysis in WAT.** Microfluidic cards differential gene expression assay (q Real Time TaqMan probes PCR) from inguinal WAT RNA extracted from frozen tissue after animals' sacrifice at their 6.5 months of life performed by Haizea Lekuona. Gene expression given in fold change (FC)  $2^{-\Delta\Delta Ct}$  and calculated normalizing by Ppia as endogenous gene and one same c chow mouse sample as calibrator sample. N=8. Statistical analysis performed through t-test.

Genes involved in lipid storage ACAA1B and LEP (leptin) also showed significant differences in their expression (fig. 29).

ACAA1b, involved in lipid and fatty acid metabolism and cholesterol biosynthesis and storage, was significantly up-regulated in c hfd involving more lipid storage in this experimental group and justifying the larger size of their adipocytes.

LEP (leptin) encodes for a hormone involved in the regulation of body weight by controlling appetite and metabolism. It is secreted by adipocytes acting as an adiposity marker and as a satiety signal by travelling to hypothalamus inhibiting appetite counteracting with Y-peptide. The expression of this hormone in adipose tissue gives an idea of the amount of lipid stored in this tissue. Leptin's expression was significantly increased in all experimental groups vs c chow. Leptin's gene expression pattern matches the histological findings.



TG CHOW vs WT CHOW				
GENE ID	TG_CHOW	WT_CHOW (basal condition)	logFC	p-value
Lep	0,49942	-0,94493	1,44435	0,00862

WT HFD vs WT CHOW				
GENE ID	WT_HFD	WT_CHOW (basal condition)	logFC	p-value
Lep	1,20101	-0,94493	2,14594	0,00021
Acaa1b	0,74139	-0,59569	1,33707	0,00050

TG HFD vs WT HFD				
GENE ID	TG_HFD	WT_HFD (basal condition)	logFC	p-value
Lep	0,03904	1,20101	-1,16197	0,03162

TGvsWT HFDvsCHOW		
GENE ID	logFC	p-value
Lep	-2,60632	0,00112

**Figure 29. Differential gene expression analysis in WAT.** Microfluidic cards differential gene expression assay (q Real Time TaqMan probes PCR) from inguinal WAT RNA extracted from frozen tissue after animals' sacrifice at their 6.5 months of life performed by Haizea Lekuona. Gene expression given in fold change (FC)  $2^{-\Delta\Delta Ct}$  and calculated normalizing by Ppia as endogenous gene and one same c chow mouse sample as calibrator sample. N=8. Statistical analysis performed through t-test.

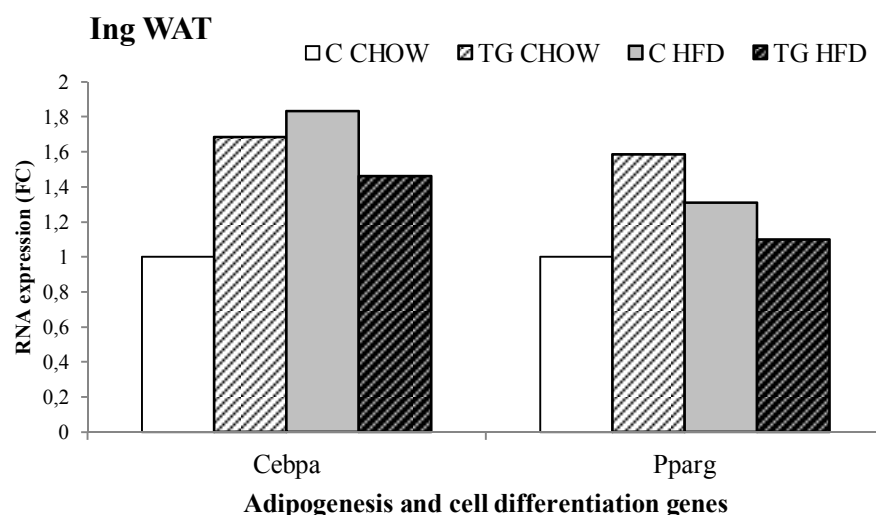
Genes involved in adipogenesis and cell differentiation C/EBPA and PPAR $\gamma$ 2 showed a same expression pattern among the four experimental groups as that shown by histochemistry (fig. 30).

C/EBPA, CCAAT/enhancer-binding protein alpha, has been shown to bind to the promoter and modulate the expression of the gene encoding leptin, which plays an important role in body weight homeostasis. This protein can also interact with CDK2 and CDK4, thereby inhibiting these kinases and causing growth arrest in cultured cells. C/EBPA is involved in the first step of



adipocyte differentiation, and appeared significantly up-regulated in all experimental groups vs c chow.

PPAR $\gamma$ 2 is involved in adipocyte differentiation and expandability; the genes activated by PPAR $\gamma$  stimulate lipid uptake and adipogenesis by adipocytes. PPAR $\gamma$  knockout mice fail to generate adipose tissue when fed a high-fat diet. This gene was slightly up-regulated in hfd groups and significantly up-regulated in tg chow vs c chow.



TG_CHOW vs WT_CHOW				
GENE ID	TG_CHOW	WT_CHOW (basal condition)	logFC	p-value
Cebpa	-0,02709	-0,77669	0,74960	0,00518
Pparg	-0,03945	-0,70373	0,66428	0,01460

WT_HFD vs WT_CHOW				
GENE ID	WT_HFD	WT_CHOW (basal condition)	logFC	p-value
Cebpa	0,09767	-0,77669	0,87436	0,00137

TGvsWT_HFDvsCHOW		
GENE ID	logFC	p-value
Cebpa	-1,07802	0,00454
Pparg	-0,91909	0,01670

**Figure 30. Differential gene expression analysis in WAT.** Microfluidic cards differential gene expression assay (q Real Time TaqMan probes PCR) from inguinal WAT RNA extracted from frozen tissue after animals' sacrifice at their 6.5 months of life performed by Haizea Lekuona. Gene expression given in fold change (FC)  $2^{-\Delta\Delta Ct}$  and calculated normalizing by Ppia as endogenous gene and one same c chow mouse sample as calibrator sample. N=8. Statistical analysis performed through t-test.

Genes involved in lipolysis also manifested a differential expression pattern (fig. 31):

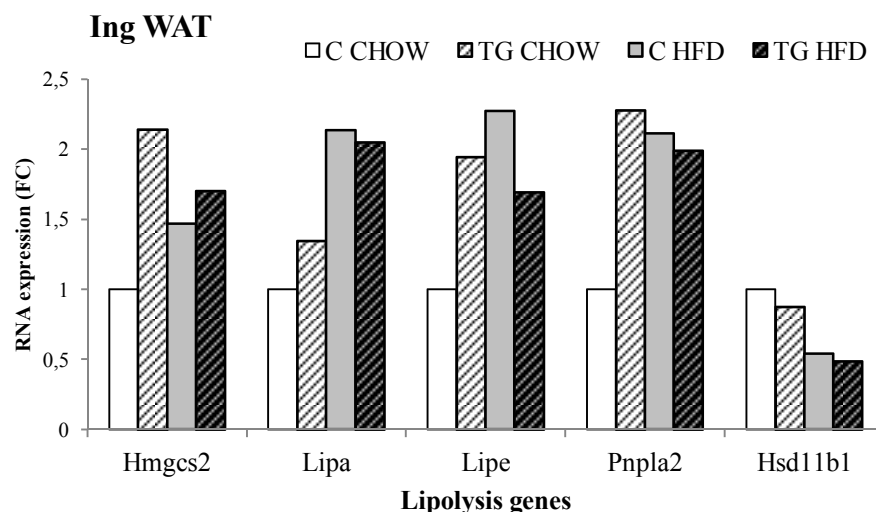
HMGCS2, catalyzing the first reaction of ketogenesis, a metabolic pathway providing lipid-derived energy for various organs during times of carbohydrate deprivation, was up-regulated in all three experimental groups vs c chow, yet only significantly in tg chow.

LIPA (lipase A), encodes for the lysosomal acid lipase (also known as cholesterol ester hydrolase). This enzyme is crucial for the intracellular hydrolysis of cholesterol esters and triglycerides that have been internalized via receptor-mediated endocytosis of lipoprotein particles in the lysosome. Mutations in this gene can result in Wolman disease and cholesterol ester storage disease. LIPA expression was increased in control animals hfd fed vs chow fed (fig. 31).

LIPE (hormone-sensitive lipase), the protein encoded by this gene has a long and a short form, generated by use of alternative translational start codons. The long form is expressed in steroidogenic tissues such as testis, where it converts cholesterol esters to free cholesterol for steroid hormone production. The short form is expressed in adipose tissue, among others, where it hydrolyzes stored triglycerides to free fatty acids. This hormone was found significantly risen in all three experimental groups vs c chow (fig. 31).

PNPLA2 (patatin-Like Pphospholipase Domain Containing Protein), encodes an enzyme which catalyzes the first step in the hydrolysis of triglycerides in adipose tissue. Mutations in this gene are associated with neutral lipid storage disease with myopathy. The expression of this gene appeared up-regulated in all experimental groups vs c chow (fig. 31).

HSD11b1 gene expression was significantly diminished in c hfd vs c chow (fig. 31).



TG CHOW vs WT CHOW				
GENE ID	TG_CHOW	WT_CHOW (basal condition)	logFC	p-value
Lipe	0,03217	-0,92661	0,95879	0,00220
Pnpla2	0,17619	-1,00947	1,18566	0,00267
Hmgcs2	0,43109	-0,66700	1,09809	0,00496

WT HFD vs WT CHOW				
GENE ID	WT_HFD	WT_CHOW (basal condition)	logFC	p-value
Lipe	0,25822	-0,92661	1,18484	0,00024
Pnpla2	0,06895	-1,00947	1,07842	0,00578
Hsd11b1	-0,85094	0,04044	-0,89138	0,00615
Lipa	1,18395	0,09063	1,09332	0,00736

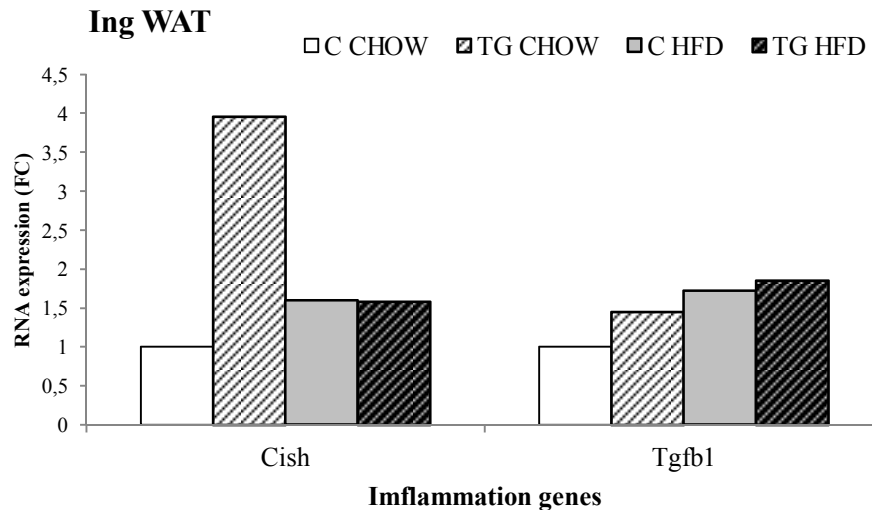
TGvsWT HFDvsCHOW		
GENE ID	logFC	p-value
Lipe	-1,38651	0,00180
Pnpla2	-1,27358	0,01919

**Figure 3 1. Differential gene expression analysis in WAT.** Microfluidic cards differential gene expression assay (q Real Time TaqMan probes PCR) from inguinal WAT RNA extracted from frozen tissue after animals' sacrifice at their 6.5 months of life performed by Haizea Lekuona. Gene expression given in fold change (FC)  $2^{-\Delta\Delta Ct}$  and calculated normalizing by Ppia as endogenous gene and one same chow mouse sample as calibrator sample. N=8. Statistical analysis performed through t-test.

As regards to immune response genes, CISH gene expression showed to be slightly up-regulated in both hfd groups vs c chow, and significantly up-regulated in tg chow (fig. 32). CISH encodes for cytokine-inducible SH2-containing protein that controls interleukin-2 signalling. The protein belongs to the cytokine-induced STAT inhibitor (CIS), also known as suppressor of cytokine signalling (SOCS) or STAT-induced STAT inhibitor (SSI), protein family. CIS family members are known to be cytokine-inducible negative regulators of cytokine signalling. Low CISH expression levels would therefore mean more inflammation.

TGFB gene encodes a member of the transforming growth factor beta (TGF $\beta$ ) family of cytokines, which are multifunctional peptides that regulate proliferation, differentiation,

adhesion, migration, and other functions in many cell types. Many cells have TGF $\beta$  receptors, and the protein positively and negatively regulates many other growth factors. The expression of TGF $\beta$  was significantly increased in c hfd vs c chow (fig. 32).



TG_CHOW vs WT_CHOW				
GENE ID	TG_CHOW	WT_CHOW (basal condition)	logFC	p-value
Cish	2,10803	0,12219	1,98584	0,00694

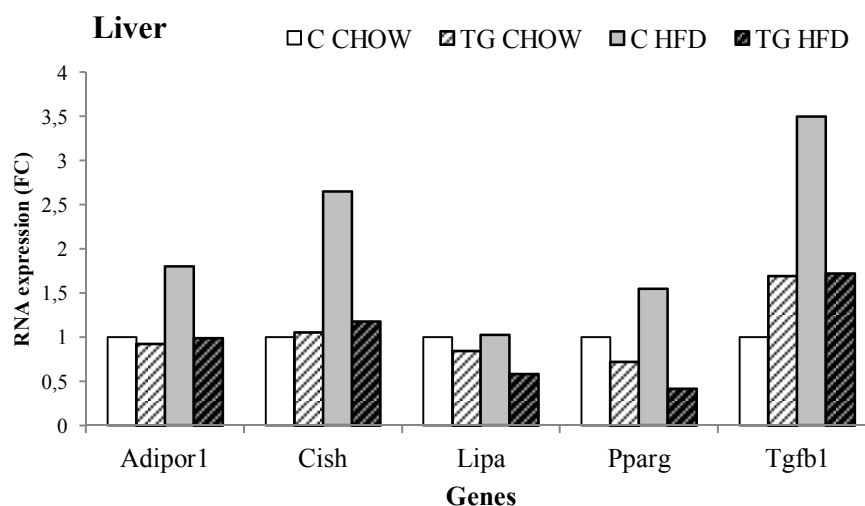
WT_HFD vs WT_CHOW				
GENE ID	WT_HFD	WT_CHOW (basal condition)	logFC	p-value
Tgfb1	0,76105	-0,02400	0,78505	0,00622

TGvsWT_HFDvsCHOW		
GENE ID	logFC	p-value
Cish	-2,00125	0,04852

**Figure 32. Differential gene expression analysis in WAT.** Microfluidic cards differential gene expression assay (q Real Time TaqMan probes PCR) from inguinal WAT RNA extracted from frozen tissue after animals' sacrifice at their 6.5 months of life performed by Haizea Lekuona. Gene expression given in fold change (FC)  $2^{-\Delta\Delta Ct}$  and calculated normalizing by Ppia as endogenous gene and one same c chow mouse sample as calibrator sample. N=8. Statistical analysis performed through t-test.

### 3.2. Differentially expressed genes in liver

Microfluidic cards differential expression assays demonstrated that liver also showed differentially expressed genes among the different experimental groups.



TG_HFD vs C_HFD				
GENE ID	TG_HFD	C_HFD (basal condition)	logFC	p-value
Pparg	-0,27353	1,61780	-1,89133	0,00886
Adipor1	0,04908	0,91226	-0,86318	0,03361
Lipa	-0,27585	0,52977	-0,80562	0,04159

C_HFD vs C_CHOW				
GENE ID	C_HFD	C_CHOW (basal condition)	logFC	p-value
Tgfb1	0,96801	-0,83899	1,80700	0,00079
Cish	1,36550	-0,04100	1,40650	0,02716
Adipor1	0,91226	0,06410	0,84816	0,03076

TGvsC_HFDvsCHOW		
GENE ID	logFC	p-value
Tgfb1	-1,78017	0,02476

**Figure 33. Differential gene expression analysis in liver.** Microfluidic cards differential gene expression assays (q Real Time TaqMan probes PCR) from liver RNA extracted from frozen tissue after animals' sacrifice at their 6.5 months of life performed by Cristina Suarez. Gene expression given in fold change (FC)  $2^{-\Delta\Delta Ct}$  and calculated normalizing by GAPDH and Ppia as endogenous reference gene and one same c chow mouse sample as calibrator sample. N=8. Statistical analysis performed through t-test.

Liver analysis showed a significant increase in the expression of ADIPOR1 in c hfd vs c chow and vs tg hfd (fig. 33). This gene encodes a protein which acts as a receptor for adiponectin, a hormone secreted by adipocytes which regulates fatty acid catabolism and glucose levels. Binding of adiponectin to the encoded protein results in activation of an AMP-activated kinase signalling pathway which affects levels of fatty acid oxidation and insulin sensitivity, so that diminished levels of this protein would mean higher risk to overweight and/or insulin resistance.

This same analysis in liver showed that CISH gene's expression was significantly increased in c hfd vs c chow, and increased vs all others (fig. 33).

The expression LIPA (lipolysis related gene) was increased in c hfd fed animals vs tg hfd (fig. 33).

PPAR $\gamma$  (peroxisome proliferator-activated receptor gamma, ppar- $\gamma$ ) is a nuclear receptor manifesting two isoforms both in human and in mouse: Ppar- $\gamma$ 1 (found in nearly all tissues except muscle) and ppar- $\gamma$ 2 (mostly found in adipose tissue and the intestine). Ppar $\gamma$  regulates fatty acid storage and glucose metabolism and its transcript is regulated by food intake. Fasting inhibits transcription of PPAR $\gamma$ 2. In a positive energy input situation, PPAR $\gamma$ 2 is ectopically expressed in liver in order to balance the excess of energy by promoting the storage of extra energy in the shape of triglyceride depots. This gene was significantly over expressed both in c hfd animals vs tg hfd (fig. 33).

TGF $\beta$ 1 was another gene showing differential expression in this tissue, manifesting a statistically significant increase in the presence of the hfd in c animals, but not in the presence of both at the same time (fig. 33).

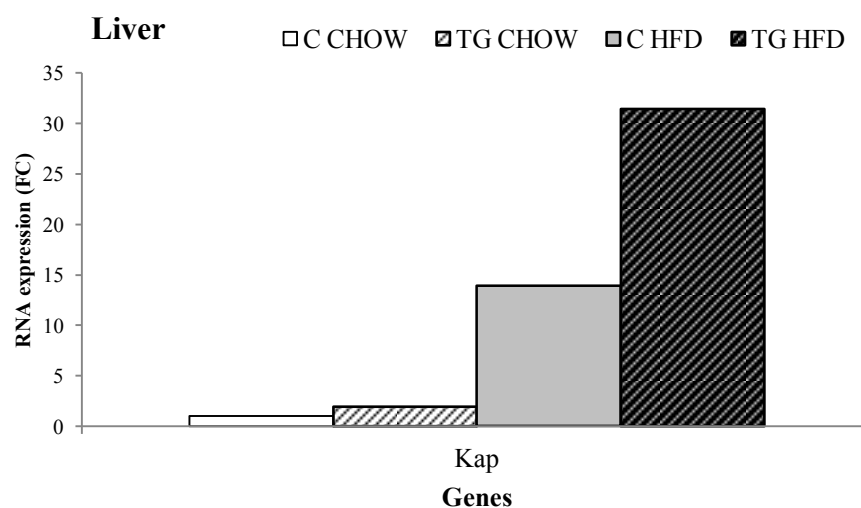


**Figure 34. Differential gene expression analysis in liver.** Microfluidic cards differential gene expression assays (q Real Time TaqMan probes PCR) from liver RNA extracted from frozen tissue after animals' sacrifice at their 6.5 months of life performed by Cristina Suarez. Gene expression given in fold change (FC)  $2^{-\Delta\Delta C_t}$  and calculated normalizing by GAPDH and Ppia as endogenous reference gene and one same c chow mouse sample as calibrator sample. N=8. Statistical analysis performed through t-test.

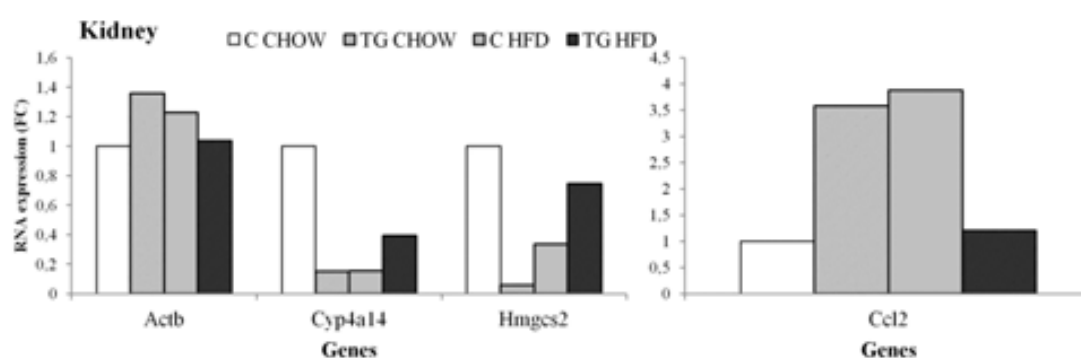
Surprisingly, both tg groups and c hfd showed a slight ectopic yet not statistically significant expression of KAP (RNA) in liver, lower in c hfd than both tg suggesting a relationship between expression of KAP and positive energy input (fig. 34).

### 3.3. Differentially expressed genes in kidney

Differential gene expression assays in kidney, showed a significant rise in the expression of actin (ACTb) in tg chow vs c chow (fig. 35).

CYP4A14 (cytochrome P 450, family 4, subfamily a, polypeptide 14), the cytochrome P 450 proteins are monooxygenases which catalyze many reactions involved in drug metabolism and synthesis of cholesterol, steroids and other lipids. Cyp4a family is involved in 20-HETE (20-hydroxyeicosatetraenoic acid) production in kidney which causes blood pressure to rise. CYP4A14 was found significantly decreased in the presence of either the transgene or hfd.

HMGCS2 gene expression was significantly down-regulated in tg chow vs c chow (fig. 35).



TG_CHOW vs C_CHOW				
GENE ID	TG_CHOW	C_CHOW (basal condition)	logFC	p-value
Hmgcs2	1.18363	5.26983	-4.08620	0.01587
Cyp4a14	0.57629	3.31738	-2.74109	0.01993
Actb	0.07763	-0.36191	0.43954	0.03037

C_HFD vs C_CHOW				
GENE ID	C_HFD	C_CHOW (basal condition)	logFC	p-value
Cyp4a14	0.63063	3.31738	-2.68675	0.01849
Ccl2	0.13991	-1.81711	1.95702	0.03252

**Figure 35. Differential gene expression analysis in kidney.** Microfluidic cards differential gene expression assays (q Real Time TaqMan probes PCR) from kidney RNA extracted from frozen tissue after animals' sacrifice at their 6.5 months of life performed by Cristina Suarez. Gene expression given in fold change (FC)  $2^{-\Delta\Delta C_t}$  and calculated normalizing by GAPDH and Ppia as endogenous reference gene and one same c chow mouse sample as calibrator sample. N=8. Statistical analysis performed through t-test.

#### 4. Other metabolic syndrome models:

Other metabolic syndrome mouse models, such as ob/ob spontaneously leptin deficient mice, ppar $\gamma$  knock-out mice and poky mice as a result of ob/ob and ppar $\gamma$  ko mating, were also analyzed in this study all compared to control wild type mice.

#### 4.1. Characterization of the phenotype

Upon data provided by Dr. Antonio Vidal Puig's research group: *Metabolic Research Laboratories. Institute of Metabolic Science. Addenbrooke's Hospital. University of Cambridge* animals' body weight, urine and blood glucose and water intake were described in order to characterize these animal models in our laboratory: ob/ob mice showed a significantly higher weight at their fifth month of life compared to all other groups showing no differences among them. Glucose metabolism was affected by the lack of leptin and ppary together, glucose levels were significantly increased in poko mice both in urine during 22 h of fasting and in blood before and after fasting. Ppary ko mice showed slightly decreased levels in urine and both ob/ob and ppary ko mice showed higher glucose levels in blood after 22 h fasting vs wt animals. Water intake during 22 h of fasting was significantly lower in this OB/OB group vs all others.

Histological analyses (eosin-haematoxylin) in these animals' livers revealed a strong steatosis in the lack of leptin (ob/ob) and a milder steatosis in the lack of both leptin and ppary together (fig. 36).

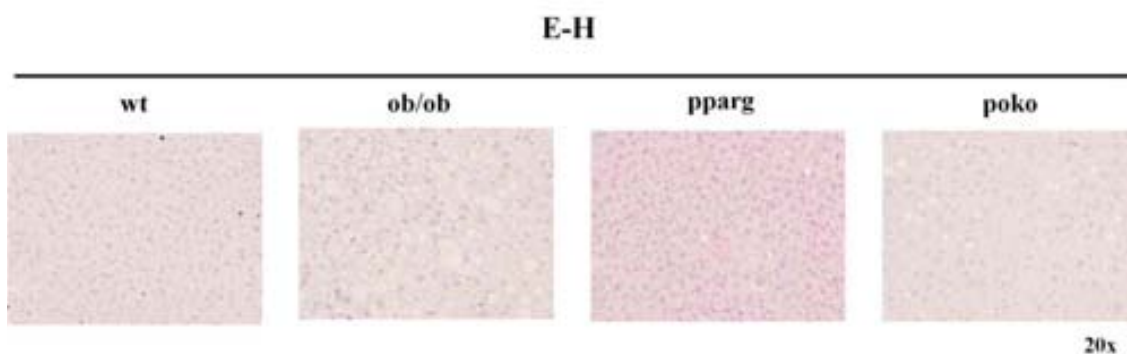


**Figure 36. Liver histochemistry.** Histochemical analysis of paraffin imbibed animals' livers extracted and fixed at animals' sacrifice at their 5.5 months of life by eosin-haematoxylin (E-H) staining in tissue slides performed with the help of Andrea Cabllero. Histochemistry performed upon 4% formalin fixed provided by Dr. Antonio Vidal Puig's research group: *Metabolic Research Laboratories. Institute of Metabolic Science. Addenbrooke's Hospital. University of Cambridge. UK. N=7.*

#### 4.2. Characterization of the kidney

Kidney function was also studied in these groups by measuring creatinine and urea blood levels. Creatinine is a breakdown product of creatine, which is an important part of muscle. It is removed from the body entirely by the kidneys. If kidney function is abnormal, creatinine levels will increase in the blood since less creatinine is released through urine. Creatinine blood levels were not affected by the lack of leptin, slightly affected by the lack of ppary and significantly affected by the lack of both vs wt involving worst kidney function in poko mice (fig. 37). Urea is the final result of protein metabolism; it is synthesized in liver from protein catabolism.



Increased urea levels in blood indicate a strong kidney failure. There were no significant differences in urea blood levels among the groups, meaning milder kidney damage (fig. 37).

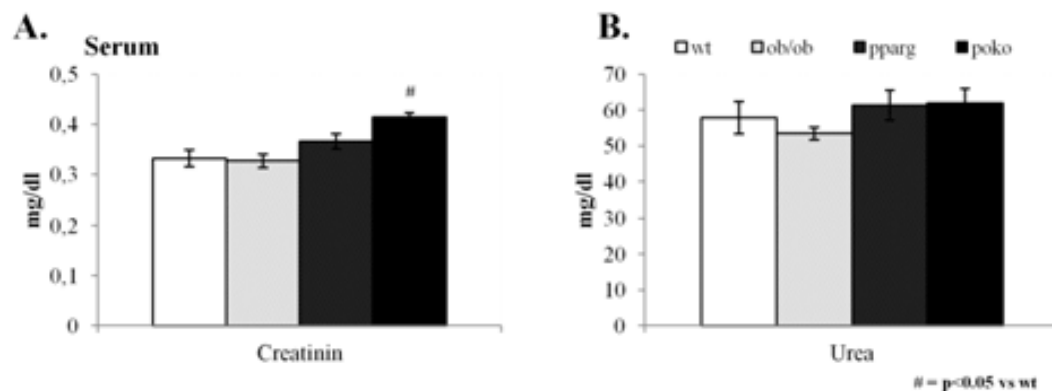


**Figure 37. Kidney function analysis.** Creatinine and urea serum levels were measured in Universitat Autònoma de Barcelona Veterinary Faculty. Measurements performed upon frozen serum provided by Dr. Antonio Vidal Puig's research group: Metabolic Research Laboratories. *Institute of Metabolic Science, Addenbrooke's Hospital, University of Cambridge, UK.* Results are given in mg/dl. N=7. Statistical analysis performed through t-test.

Histological analyses (eosin-haematoxylin) in these animals' kidneys demonstrated none concluding differences between the four experimental groups (fig. 38).

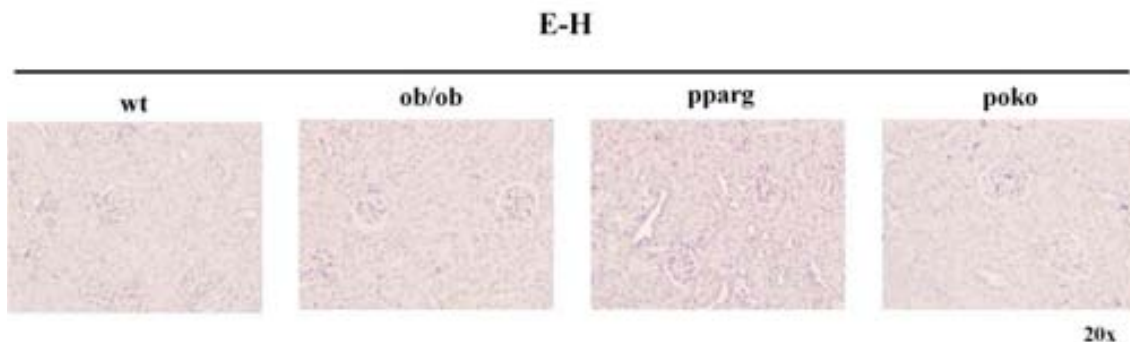


**Figure 38. Kidney histology.** Histochemical analysis of paraffin imbedded animals' kidneys extracted and 4% formalin fixed at animals' sacrifice at their 5.5 months of life by eosin-haematoxylin (E-H) staining in tissue slides performed with the help of Andrea Caballero. Histochemistry performed upon 4% formalin fixed tissue provided by Dr. Antonio Vidal Puig's research group: Metabolic Research Laboratories. *Institute of Metabolic Science, Addenbrooke's Hospital, University of Cambridge, UK.* N=7.

The expression of KAP (protein), was analysed by immunoblotting and showed a dramatic (statistically significant) decrease in leptin deficient mice both ob/ob and poko and a slight increase in pparγ ko mice (fig. 39A). The expression of KAP (RNA) analysed by microfluidic cards differential gene expression assays in kidney showed a correspondence between protein and RNA levels (fig. 39B).

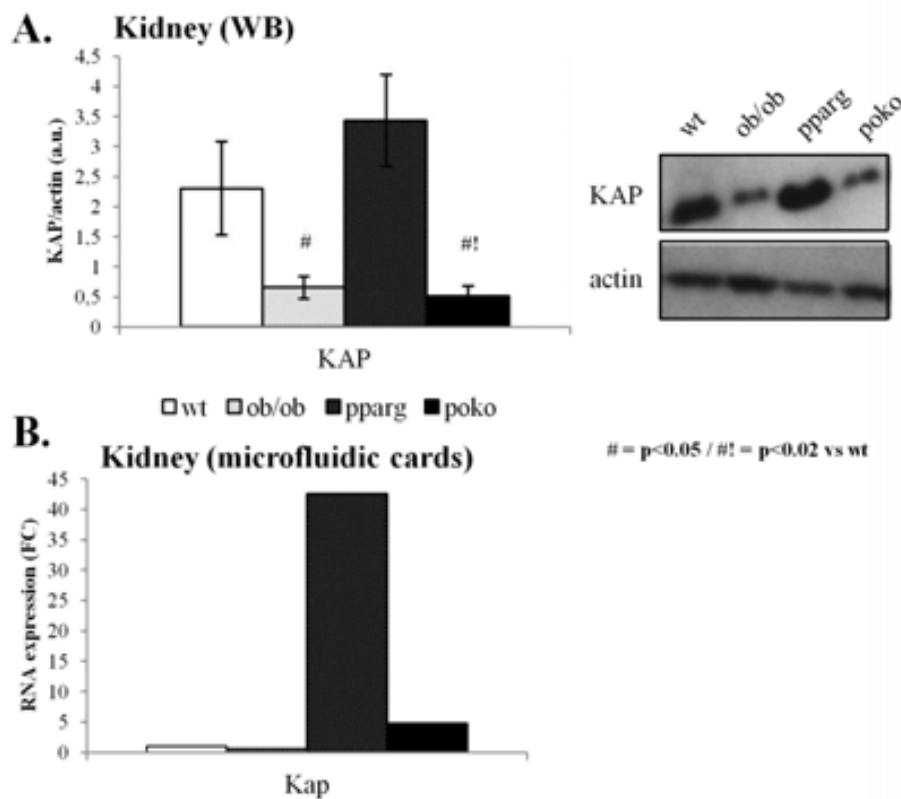


**Figure 39. Detection of KAP in mice's kidneys.** **A.** WB analysis of whole kidney protein extract hybridised with antiKAP antibody and normalised with actin performed with the help of Ayate Alloul. Assay performed upon frozen tissue provided by Dr. Antonio Vidal Puig's research group: Metabolic Research Laboratories. *Institute of Metabolic Science. Addenbrooke's Hospital. University of Cambridge. UK.* Image acquired with a GS-800 Calibrated Densitometer and analysed with Quantity One software. Results are given in KAP/actin ratio arbitrary (densitometric) units. N=7. **B.** Microfluidic cards differential gene expression assays (qRT-PCR) from kidney RNA extracted from frozen tissue after animals' sacrifice at their 5.5 months of life performed by Cristina Suarez with the help of Sonia Díez. Assay performed upon frozen tissue provided by Dr. Antonio Vidal Puig's research group: Metabolic Research Laboratories. *Institute of Metabolic Science. Addenbrooke's Hospital. University of Cambridge. UK.* Gene expression given in fold change (FC)  $2^{-\Delta\Delta Ct}$  and calculated normalizing by GAPDH and Ppia as endogenous gene and one same c chow mouse sample as calibrator sample. N=7. Statistical analysis performed through t-test.

As performed in c/Tg fed on c haw o r h fd, selected genes expression was analysed by microfluidic cards differential gene expression assays in kidney of these groups.

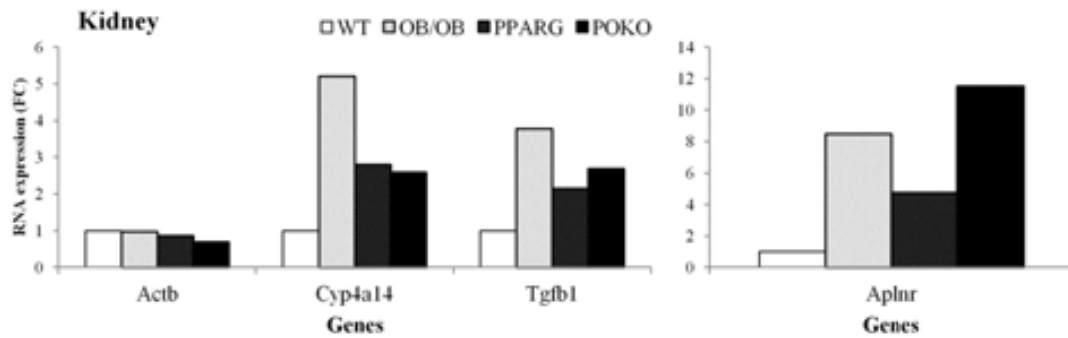
The expression of actin was down-regulated in the absence of leptin and ppary together (POKO mice) (fig. 40).

CYP4A14 was also affected in these animal groups being significantly up-regulated in OB/OB animals (fig. 40).

TGFβ1 also showed differential expression in this tissue, manifesting a statistically significant increase in the absence of leptin (ob/ob), and in the absence of leptin and ppary together (fig.

40), demonstrating that kidneys of these groups were also differentially affected by inflammation.

Apelin receptor was found significantly risen in POKO mice (lacking both leptin and PPAR $\gamma$ ) (fig. 40).



OBOB vs WT				
GENE ID	OBOB	WT (basal condition)	logFC	p-value
Tgfb1	0.74518	-1.17109	1.91628	0.00134
Cyp4a14	1.71854	-0.66193	2.38047	0.05119

POKO vs WT				
GENE ID	POKO	WT (basal condition)	logFC	p-value
Actb	-0.24509	0.27137	-0.51646	0.01213
Tgfb1	0.25106	-1.17109	1.42216	0.01323
Aplnr	-0.14152	-3.66773	3.52620	0.05099

**Figure 40. Differential gene expression analysis in kidney.** Microfluidic cards differential gene expression assays (q Real Time TaqMan probes PCR) from kidney RNA extracted from frozen tissue after animals' sacrifice at their 5.5 months of life performed by Cristina Suarez with the help of Sonia Diez. Assay performed upon frozen tissue provided by Dr. Antonio Vidal Puig's research group: Metabolic Research Laboratories. *Institute of Metabolic Science. Addenbrooke's Hospital. University of Cambridge. U.K.* Gene expression given in fold change (FC)  $2^{-\Delta\Delta C_t}$  and calculated normalizing by LaminA as endogenous gene and one same chow mouse sample as calibrator sample. N=7. Statistical analysis performed through t-test.

## **DISCUSSION**

---

## DISCUSSION

The exact cause of the metabolic syndrome in humans is not yet known, but the factors that might contribute to it include genetic predisposition, body fat excess (especially abdominal) and physical inactivity. The main parameters taken into account for the diagnosis of metabolic syndrome are impaired glucose regulation, insulin resistance, hypertension, dyslipidemia and obesity.

Many evidences obtained from previous studies have shown that the kidney androgen-regulated protein is involved in several physiological processes. It has been proven that the over-expression of KAP induces some pathophysiological mechanisms leading to hypertension, oxidative stress or kidney damage and regulates the expression of genes involved in glucose and lipid metabolisms [67]. Therefore, the KAP Tg mouse has demonstrated to be a useful model for studying physiological processes in which this protein would be involved.

In our laboratory, it has been previously suggested that, according to obtained results, KAP could be inducing responses that were classically attributed to androgens, exerting its action, perhaps, somewhere in-between the secretion of androgens and the subsequent response [67]. This theory became stronger when studies were published on genes the expression of which is modified by increasing androgen levels. By means of microarray assays and quantitative RT-PCR it was found that KAP Tg mice showed modified expression of some of these genes in the same manner, as happens in the case of CYP4A14 [63], which is down-regulated both in the increase of androgens and the over-expression of KAP in Tg.

Androgens are synthesized in testis and travel to peripheral organs where, depending on the presence of aromatase or 5- $\alpha$ -reductase enzymes, they are metabolized to estrogens or dihydrotestosterone (DHT) respectively. DHT cannot be metabolized to estrogens, and only works in the presence of active androgen receptor. Organs such as white adipose tissue or kidney contain high levels of aromatase.

Increase in the production of testosterone in intra-abdominal adipose tissue may have important metabolic consequences either on the actual local adipose tissue or on liver where androgens can be drained through the portal system. Both adipose tissue [95, 96] and liver [97, 98] express high affinity androgen receptors, becoming potential targets for the action of androgens. Testosterone increases  $\beta$ -adrenergic receptors in adipocytes [99, 100], which may result in an increased lipolysis and release of fatty acids [101]. If over-expression of KAP was involved in the increased production of androgens, this might explain the observations on lipid metabolism in our experiments. Increased free fatty acid distribution reduces insulin clearance and produces dyslipidemia associated with central obesity [102]. An increase of androgenicity in intra-

abdominal adipose tissue depots in women may influence lipid turnover in this tissue, with adverse consequences for lipid and insulin liver metabolism. In women, non insulin-dependent diabetes mellitus, often develops when visceral obesity and hyperinsulinemia are associated with hyperandrogenization [103].

Regarding the other metabolic syndrome models studied in this work, many authors have studied the sterility of ob/ob mice and tested the hypothesis that leptin has effects on their reproductive system. When administrating leptin to ob/ob mice of both sexes, females displayed an increase in LH, and in the ovarian and uterine weight, and in males increased FSH, testicular weight, seminal vesicles and spermatozoid number. Therefore, leptin stimulates the reproductive endocrine system in ob/ob mouse in both sexes and its action seems to occur by stimulation of estrogens in females and testosterone in males. It has been demonstrated the presence of leptin receptors in testis and ovaries. The sterility of the leptin deficient mice is due to low levels of LH and FSH and sex steroids [104]. We have demonstrated that KAP protein levels are altered in all three models: ob/ob, ppar $\gamma$ 2 KO and poko, being significantly decreased in ob/ob and poko leptin deficient models, which makes sense since KAP is regulated by androgens meaning that if the androgen axis is low due to the lack of leptin, KAP levels should be found decreased. However, the fact that the low KAP levels are due to the lack of leptin per sé and independently of androgens should not be dismissed.

The role of ppar $\gamma$ 2 in adipose tissue expandability has been widely carried out by Dr. Vidal Puig's research group who has focused this research on characterizing the ppar $\gamma$ 2 knockout mice also analysed in this study. These ppar $\gamma$ 2 deficient animals in balanced energy conditions (standard diet) display a regular body weight, food intake and energy expenditure. In this situation the number and size of adipocytes are normal. Switching to a high fat diet, the weight remains normal but they show adipocyte hypertrophy. In these conditions, analyzing by microarray the signalling pathways profile it was demonstrated that male ppar $\gamma$ 2KO display a slightly diabetic phenotype [105].

Through the mating of ppar $\gamma$ 2KO and ob/ob animals poko mice were obtained (PPAR $\gamma$ 2<sup>-/-</sup> Lep<sup>-/-</sup>). Under positive energy balance conditions these animals have a limitation on the expansion of adipose tissue. At their 16 weeks post birth, poko animals are hyperphagic as ob/ob, but water intake is higher than in ob/ob, they show a slight overweight compared to wt and ppar $\gamma$ 2KO but they are not obese as ob/ob. They also have a slightly larger amount of body fat than the wt and ppar $\gamma$ 2KO mice but much less than ob/ob, showing a larger liver than wt and ppar $\gamma$ 2KO, and blood glucose levels higher than in ob/ob. They also manifest reduced movement compared to wt and ppar $\gamma$ 2KO.

The imbalance between a large energy availability and the limitation on the expansion of adipose tissue leads to a severe metabolic disorders in poko mice. When comparing young animals (6 weeks of life, when the ob/ob animals are not yet metabolically compromised) it was

demonstrated that pokko animals have insulin blood levels, glucose and triglyceride levels above ob/ob, and they are insulin resistant [105].

Given that these three metabolic syndrome models have shown altered KAP levels and that our own animal model manifests hypertension, enhanced immune response and apparent predisposition to impaired glucose and lipid metabolism, we aimed to study the MS features in our model and decided to try to induce SM by feeding it with a high fat diet since there seems to be a relationship between KAP and energy balance.

In order to study the role of KAP in blood pressure and weight control, glucose and lipid metabolism and immune response activation, the mice in this study were fed with high fat diet intending to induce some of the symptoms already described that define the metabolic syndrome using control mice fed on a high fat diet as a metabolic syndrome model (positive control) and compare the obtained results with those observed in Tg fed on standard diet and Tg fed on the same high fat diet. Control and experimental diets were given to the corresponding experimental group at weaning. Starting the high fat diet straight from weaning or after a few months of being fed on a standard diet may lead to metabolic differences, since at the moment of weaning the digestive system is still immature in rodents. It has been described that rat pups fed on high fat diet showed alterations in the regulation of some of the enzymes involved in the oxidation of fatty acids between 16 and 21 days from weaning to be found up-regulated in the renal cortex but not in medulla. Further studies following this line demonstrated that pups fed with regular diet that was switched to high fat diet for one day also showed these alterations, moreover it was demonstrated that the up-regulation of the cortical expression of  $\beta$ -oxidation enzymes is initiated 6h after starting the lipid intake [106]. Based on other groups' published results, it was decided that the optimum moment to start feeding the mice with hfd was at weaning.

When feeding animals on a high-fat diet, used to induce type 2 diabetes, obesity and metabolic syndrome, Tg mice displayed lower glucose plasma levels, less hypertension and gained less weight than controls demonstrating that KAP is somehow involved in these processes. Experiments in ob/ob (leptin deficient) mice and other animal models in which glucose and lipid metabolism are affected, such as pary2 knock out and pokko, show differential expression of KAP in these animals' kidneys, which reinforces the above hypothesis that this protein must be involved in the control of blood pressure, glucose and lipid metabolism. Ppary displays two isoforms: ppary1 and ppary2; there is a described a mutation in PPAR $\gamma$ 2 gene in mouse that is associated with insulin resistance [105], although it has not been established a direct link between ppary and glucose metabolism. In humans, some allelic variants and characterized mutations in the PPAR- $\gamma$  gene have been associated with hypertension and obesity [107] and [108].

In the present work physiological observations were correlated with differential gene expression assays, since it has been proven that KAP induces regulation of several already described genes, in order to try to find the molecular origin of these physiological effects.

### **1. Animals' body weight is controlled in a multigenic and multitissular manner independently of the over-expression of KAP**

When feeding control animals with hfd, weight gain near obesity was expected. Controls fed on hfd did gain more weight than all others, although not as dramatically as expected. It would be possible to understand the behaviour of mice in the study regarding the hfd as an effect of their genetic background. If the genetic background is important in the response, it is possible that this is the reason why obesity like weight increase is not observed as evident in the controls hfd which should be the positive control to the experiment. As an example of this hypothesis, Db gene (encoding for the leptin receptor) related to diabetes may display a recessive mutation that causes obesity in mice and is capable of producing diabetes only by modifying the interaction of indefinite related genetic background of certain strains. Modifier genes dependent on the genetic background interact deleteriously with this mutation so that this obesity-related gene would by altering the regulation of these genes [109].

Although effects of hfd in control mice were not as dramatic as expected, these animals still gained significantly much more weight than all other groups, meaning that the over-expression of KAP does not enhance animals' weight gain and when fed on a high fat diet, the over-expression of KAP inhibits the diet-effect.

These differences in the weight gain between controls and Tg both fed on hfd did not account for an increase in the calories intake, fact that was confirmed by analysing serum leptin levels. No differences in the satiety signalling were found between these two experimental groups indicating that Tg hfd do not gain less weight than controls due to a lower calorie intake driven by higher leptin levels. Leptin serum levels were not affected by the transgene independently of the diet.

The differences in the weight gain were justified by an increase in the major adipose tissues (gonadal and inguinal) and liver, which are the three tissues most influenced by high calorie intake.

When comparing our data to ob/ob, ppar $\gamma$ 2 KO and poko, it was observed that the lack of leptin is a stronger factor generating over-weight than the lack of PPAR $\gamma$ 2, however, when lacking both together; the effect of deleting PPARG2 is stronger than the effect of deleting leptin, so that poko animals do not show a significant increase in body weight.

The differences on final animal weight among our experimental models seemed to account for a differential weight distribution in liver and white adipose tissue. Although there are no reported significant differences in the ratio of visceral white adipose tissue and body weight between Tg



and control animals both fed on a hfd, there is a trend that indicates a higher ratio in c hfd vs Tg hfd. In a study in male mouse model susceptible to obesity and insulin resistance induced by a high fat diet (KK/Ta), it was found that, when comparing animals fed on control standard diet and a rich in fat diet, the ratio of visceral (gonadal in the case of the mice in our study) white adipose tissue and animal's body weight was greater in mice fed on a high fat diet. The white adipose tissue increase precedes the development of insulin resistance, which is associated with the infiltration of fat and TNF- $\alpha$  expression in liver. Thus, visceral white adipose tissue and its products are involved in the development of metabolic syndrome [110].

Brown adipose (heat generating) tissue's weight was analysed, finding that controls hfd display an increase in the weight of this tissue compared to all other groups. Since this is a very small piece of tissue, its weight does not contribute to the total body weight. The function of brown adipose tissue is to transfer energy from food into heat (thermogenesis). Heat production is activated when the organism needs extra heat and the rate of thermogenesis is centrally controlled via a pathway initiated in the hypothalamus. Feeding as such also results in activation of brown adipose tissue; a series of diets, apparently all characterized by being low in protein, result in a leptin-dependent recruitment of the tissue. When the tissue is active, high amounts of lipids and glucose are combusted in this same tissue [111].

Target tissues were analysed after sacrificing the animals in order to find which of them are affected by the over-expression of KAP, hfd, or both at the same time.

Regarding the liver histological sections, the fact that the mice fed on the high fat diet displayed an almost normal liver suggests a role of the protein KAP in lipid metabolism at a liver histological level. Liver histological findings were correlated with serum cholesterol levels. These were found increased in both groups fed on hfd, although much more significantly in controls than Tg. This suggests that the saturation of cholesterol storage and processing is higher in c than Tg. Serum cholesterol levels appeared unaltered in the presence of the transgene alone, significantly risen in c hfd vs all other groups and only risen in Tg hfd vs c chow matching all histological observations.

Ppar $\gamma$ 2 (Peroxisome proliferator activated receptor gamma) transcription factor involved in adipocyte differentiation and expandibility, is ectopically expressed in liver in the presence of a positive energy unbalance in order to enhance lipid catabolism. The expression of this gene varies differently in liver of Tg mice than in controls. In Tg animals its expression decreases with the hfd, whereas in the control animals it increases with hfd compared to standard diet, as expected. In the presence of the transgene, PPAR $\gamma$ 2 expression decreases slightly but not significantly vs c when fed on a chow diet, and decreases significantly in Tg vs c when fed on a hfd. This result matches observations on ppar $\gamma$  KO mice that showed increased KAP levels, suggesting a bidirectional interaction between KAP and ppar $\gamma$ . Induction of PPAR  $\gamma$  2 in adipose tissues should be considered as a physiological adaptation to prevent the toxic effects of

excess nutrients [89] enabling lipid storage in adipocytes. In addition, mice heterozygously deficient for PPAR  $\gamma$  show increased insulin sensitivity and are protected against obesity induced by intake of a high fat diet [112]. Therefore, this transcription factor may be induced by high fat diet while protecting from the harmful effects of it. The fact that ppar $\gamma$ 2 decreased in liver of Tg hfd animals vs c hfd, and c hfd increase the expression of ppar $\gamma$ 2 vs c chow could indicate that there might be a mechanism of adjusting and compensating for the harmful effects of this diet. Apparently Tg activate this mechanism in a different way, since over-expression of KAP seems to down-regulate ppar $\gamma$  and animals would already be protected from the effects of high fat diet.

The influence of KAP was also studied in human liver derived cell line HepG2. The aim of this assay was to determine whether the effect of prokaryotic recombinant KAP in HepG2 cells was somehow similar to the effect of the transgene in mouse liver regarding lipid accumulation in hepatocytes. In order to simulate hfd intake in mice, cells were treated with oleic acid and prokaryotic recombinant KAP, to find out that an excess of lipid is toxic for hepatocytes and that, although similar, the effects of KAP+oleate are more evident when cells are pre-treated with oleate than when they are pre-treated with KAP. This might be due to the fact that the first option is closer to a physiologic situation, since when mice are born and they are still breast feeding they are already taking lipids, while they will not express KAP until puberty. Unfortunately, after a promising pilot study, results on this field ended up not being satisfactory conclusive.

As regards to adipose tissue histology sections, brown adipose tissue, inguinal and gonadal white adipose tissue, each experimental group follows a similar behaviour.

Brown adipose tissue is not a clear model in the study of obesity since the tissue varies depending on the increase or decrease of thermogenesis. Thermogenesis may be a mean to dissipate the triglycerides in the form of energy and therefore reduce lipid depots. Still, this tissue is characterized by multiple small lipid droplets as observed in the histologies of all experimental groups. These droplets are larger in all experimental groups compared to control chow, being largest in the c hfd group.

In the case of gonadal white adipose tissue, androgens sensitive and metabolically most active adipose tissue, Tg hfd displayed slightly larger sized adipocytes than controls chow diet and seem to be more spherical. Whereas, when fed on a high fat diet, controls show much larger adipocytes than Tg. These results partially correlate serum free fatty acids levels which are not increased in the presence of the transgene or hfd alone or the hfd, but when both factors converge, serum FFA levels rise significantly, indicating that Tg hfd animals have a more active lipolysis than all others and are mobilizing a larger amount of lipids from adipose tissue to liver where they will be  $\beta$ -oxidized. In obese patients, higher lipolytic activity under basal conditions

has been described, showing levels of circulating fatty acids or free fatty acids (FFA) above than in normal individuals [32, 113].

Inguinal white adipose tissue proved to be highly representative of the effect of high-lipid diet and over-expression of KAP. Adipocytes of control mice fed on the high-fat diet are the largest in size due to increased hypertrophic growth, excessive increase in the size of fat cells observed in histological slides is mainly due to the accumulation of lipids, or an increase of adipocytes (hyperplastic growth), both singularities always present in obese animals. Thanks to the differential gene expression study, it was confirmed that these control mice exhibited the most hyperplastic growth supported by CEBP $\alpha$  over-expression, gene that is involved in adipogenesis. This same phenotype is observed in the Tg chow group suggesting that over-expression of KAP has harmful effects similar to those produced by the high-fat diet but on a smaller scale. The effect of the transgene does not seem to sum up to the hfd effects.

Focusing on the Tg hfd group, their adipose cells are not as large as those of the controls hfd and not so different from the controls chow diet. They also display significant differences in expression of genes related to adipogenesis and lipolysis by decreasing their expressions compared to Tg with the standard diet and the controls hfd, seeming to be protected against the effects of the high fat diet.

Adipose tissue histologies showed a similar pattern among them and similar to what was shown in gene expression: the transgene increases the size of adipocytes, the high-fat diet increases the size even more, but when adding the two factors an additive effect is not observed, they behave similarly to Tg chow diet.

Genes involved in adipogenesis and cell differentiation in inguinal WAT C/EBP $\alpha$  and PPARG2 showed a same expression pattern among the four experimental groups as that shown by histochemistry.

The CCAAT/enhancer-binding protein alpha (CEBP  $\alpha$ ) is a transcription factor which appears to be essential and critical in the final stages of adipogenesis, a process in which this factor is found up-regulated [114]. CEBP  $\alpha$  expression precedes ppar  $\gamma$  in the induction of the cascade of events leading to adipogenesis sharing a positive correlation between them. It has been shown that the protein encoded by this gene binds to the promoter of leptin, negatively modulating its expression and displaying high levels CEBP  $\alpha$  in obese individuals. Moreover, an interaction between this protein and KAP has already been demonstrated [115].

These data suggest that both the controls fed on hfd and Tg fed on standard diet, having CEBP  $\alpha$  over-expressed are likely to manifest obese phenotype unlike controls fed on the standard diet.

Peroxisome proliferator activated receptor gamma (ppar  $\gamma$ ) is a nuclear receptor presenting two isoforms that are predominantly expressed in white adipose tissue. The most studied function with which it relates is one in which it regulates the differentiation of adipocyte precursor cells in adipogenesis process [116]. Ppar $\gamma$ 2 is involved in adipocyte differentiation and expandability;

ppary2 knockout mice fail to generate adipose tissue when fed a high-fat diet. It is also involved in the uptake of FA, lipogenesis, GLUT-4 (liver glucose facilitated transporter) synthesis and secretion of cytokines. Given its crucial role in the differentiation and function of adipocytes, the participation of ppary in the development of obesity has been widely suggested. On one side, its activator thiazolidinedione an antidiabetic drug, reduces leptin levels (see table below) [117], consequently, stimulates appetite and therefore food intake increasing the lipid depots.

---

Consequences of thiazolidinedione

---

Decrease in insulin resistance  
 Adipocyte differentiation  
 Angiogenesis inhibition  
 Decrease in leptin levels  
 Increase in adiponectin levels

On the other hand, it has been determined that the body mass index is proportional to the ratio of the two isomers, Ppary 2/Ppary 1 demonstrating that obese animal models display high levels of ppary2 mRNA in adipose tissue. Several studies performed in heterozygous mice deficient in this protein manifested increased insulin sensitivity and were protected against induced obesity by hyperlipidic dietary intake [117].

In the present study, Tg mice fed on the chow diet displayed differences from controls in the same conditions, having increased RNA levels of ppar  $\gamma$  gene. By contrast, both groups fed on the high-fat diet displayed lower levels compared to Tg fed standard diet, and lower in Tg hfd vs c hfd. It is worth highlighting that Tg fed on hfd showed ppar  $\gamma$  levels similar to controls. Both ppary2 and CEBP $\alpha$  expression give an idea of adipocytes' size and match histological findings.

Since we have demonstrated that KAP (protein) has an action not only in kidney but also on distal tissues such as liver and adipose tissues, the way in which this protein arrives to these tissues has also been analysed. Our data demonstrated that, in mouse and human blood and urine samples KAP is not found in human blood or urine, but it is released to mouse urine and it is not found in mouse blood. This fact was confirmed in cultured PCT3-pBIG2i-KAPwt clones that express the protein in the presence of doxycycline antibiotic where KAP is released to the apical medium of the cell culture which is equivalent to urinary space in whole tubule.

The reason why KAP was not found in mouse blood when it is evident that it travels at least to adipose tissues to exert effects on them, but not as evident that it travels to liver since KAP RNA expression has been detected in this tissue in Tg and hfd conditions, could be that it travels at a very low concentration in this body fluid and/or that it has very short half life. KAP could have also suffered post release modifications that could make it difficult to detect with our current antibodies.

KAP protein found in mouse urine does not appear at the expected molecular weight in SDS-PAGE gels meaning that KAP could probably be released to urine as a complex with itself or another molecule. KAP could probably be excreted to urine to be further modified and then reabsorbed further on in the proximal tubule. In order to gain insight in why KAP is released to urine both in control and Tg animals further studies are needed.

To coordinate adipocyte differentiation a large number of transcription factors are needed.

Genes involved in lipid storage and body weight in inguinal WAT ACAA1B (Acetyl-Coenzyme A acyltransferase 1  $\beta$ ) and LEP (leptin) also manifested significant differences in their expression. Excess of cholesterol is stored as cholesterol esters in lipid droplets. This enzyme is responsible for catalyzing the conversion of cholesterol into cholesteryl esters [118]. Proper regulation of this process is essential since high cholesterol levels are associated with cardiovascular disease and early atherosclerosis in animals [119]. Several studies in animals suggest that ACAA1 $\beta$  inhibitors can reduce cholesterol ester content as well as reducing and stabilizing atherosclerosis plates in rabbits. Certain KAP peptides have demonstrated to be present in the urine proteome of ApoE<sup>-/-</sup> atherosclerotic mice matching our own results identifying the presence of KAP in urine, moreover, these peptides were also identified in highly expressed in atherosclerotic plates of these mice when fed on high fat diet [120] indicating a possible role of KAP in atherosclerosis. According to our results, control mice fed on hfd show significantly up-regulated the expression of ACAA1B vs controls fed on chow diet. Since this enzyme is associated with cholesterol metabolism and the development of atherosclerosis, the expression of this gene in controls would indicate more lipid storage and increased likelihood of atherosclerosis induced by high-fat diet. Tg animals also display slight up-regulation of this gene, although not significant, however demonstrating a similar over expression patten as blood pressure measurements and genes.

Enzymes Acaa1 and 2 (Acetyl-coenzyme A acyltransferase 1 and 2) participate in the storage of cholesterol esters as "lipid droplets", in the absorption of dietary cholesterol and provide of cholesterol esters to the lipid core for the synthesis and assembly of lipoprotein [121]. The process of storage of cholesterol esters as cytoplasmic lipid droplets is very important for the body, since high levels of plasma cholesterol are associated with cardiovascular disease. Inhibition of ACAA also prevents the conversion of macrophages into foam cells in artery walls, a fact critical to the development of atherosclerosis [122]. Acaa1 and 2 are related to atherosclerosis and cholesterol metabolism.

Our results show that control mice fed on high-fat diet have increased expression of leptin vs controls fed on standard diet, a finding that correlates with the fact that these mice have greatly increased lipid depots and adipocyte size in relation to the controls fed with standard diet. By contrast, both Tg groups display similar leptin levels between them but have lower leptin mRNA expression compared to the controls hfd, indicating perhaps that although Tg mice over

express leptin vs controls chow, hfd is not able to enhance the expression of these gene in the presence of the transgene, which would explain the smaller size of adipocytes and adipose tissue weight.

Leptin (Lep) is the ob gene product that is synthesized mainly in the adipose tissue and its expression is proportional to the body fat. The quantity of triglycerides stored in the adipocyte is proportional to the amount of leptin produced by these cell type, larger adipocytes produce more leptin. Leptin travels through blood and its hypothalamic action informs the central nervous system about the size of adipose tissue and acts as a satiety factor and as intake regulator. Various published studies suggest the possibility that leptin inhibits the synthesis and secretion of the neuropeptide Y (NPY), a potent orexigenic it acts on the regulation of appetite with another hormone. It has also been thought that leptin has a role in glucose metabolism, inhibiting the secretion of insulin by pancreatic B-cells, and stimulating glucose utilization [123]. As regards to lipid metabolism, leptin induces lipolysis in adipocytes, stimulates thermogenesis and is capable of increasing fatty acid synthesis in the liver. It also promotes angiogenesis by stimulating endothelial cell proliferation [124]. In ob/ob mice (that show a spontaneous mutation in the gene encoding for leptin making them leptin-deficient) the amount of NPY RNA is high causing an increase in appetite and body weight [125]. In sight of these data and the fact that leptin synthesis is proportional to body weight giving information on the amount of lipid stored inside the adipocytes, control mice with hfd, as well as Tg mice with chow diet would show larger adipocytes than Tg fed on the chow diet. Once again, our histological observations match differential gene expression findings.

To sum up, the over-expression of KAP in mice seems to be activating ppar $\gamma$  and leptin mediated mechanisms related to an energy imbalance (over nutrition) that in the presence of chow diet only manifest in the shape of hypertension. However, when adding a rich in fat diet to the over-expression of KAP (Tg mice), energy imbalance effects are not as strong as expected since these mechanisms were apparently already activated at a gene expression level. Moreover, some of the effects observed in organs extracted from the animals demonstrated to occur directly on these certain tissues through cell culture studies, even when using human cells, fact that could support the prospect of using KAP to interact with metabolic syndrome symptoms in human beings.

## **2. Interaction of the transgene with the high fat diet diminishes the deleterious effects produced by these separately on lipid metabolism**

Differential expression assays in inguinal white adipose tissue and liver showed altered lipolysis activation in all three experimental groups. All of them display an enhanced lipolysis in WAT compared to c chow, which would be explained mainly by the over-expression of the Lipe and Lipa enzymes in WAT, although other genes related to lipolysis also showed differential

expression in both tissues. This phenotype (enhanced lipolysis) is observed in the Tg standard group suggesting that over-expression of KAP leads to harmful effects similar to those produced by the high-fat diet.

The Hmgcs2 (3-hydroxy-3-methylglutaryl-CoA synthase) is a mitochondrial enzyme involved in the first step of ketogenesis, the condensation of acetyl-CoA with acetoacetyl-CoA to generate HMG-CoA and CoA in mitochondria. This reaction provides energy derived from lipids to the brain, kidney and other organs during fasting. It is known that fatty acids regulate HMGCS2 gene through the ppar transcription factor [126]. The mRNA levels vary rapidly depending on the amount of cAMP, insulin, dexamethasone, and increase greatly in response to fasting, high fat diet, diabetes and early neonatal period. It has been shown that insulin inhibits transcriptional activity of the gene Hmgcs2. Thus, this enzyme has been proposed as a key control point in the pathway of ketogenesis, which produces ketones which can be used as a metabolic fuel during catabolic states such as fasting and diabetes [127]. The fact that the transgenic mice fed on a standard diet over-express this gene compared to controls fed on the same diet in WAT, may indicate that the transgene factor stimulates the production of ketonic bodies and thereby obtain energy from lipids. It could be assumed that these animals have low glucose levels, being even hypoglycaemic, complication that appears due to an inadequate control of diabetes mellitus, disease that these animals do not display clearly, although they have proved to manifest certain features that might lead to DM. High fat diet also enhances the expression of this gene both in c and Tg vs c chow, but at a lower scale than Tg chow. Once again, it is observed that over-expression of KAP and hfd not only do not manifest synergic effects, but keep harmful effects at the lowest generated by one or the other.

The cholesterol esterase lipase A (Lipa) is an enzyme found in the lysosome connecting extracellular with intracellular lipid metabolisms through low density lipoproteins (LDL). It is in charge of hydrolyzing triglycerides (TG) and cholesterol esters, generating fatty acids and cholesterol. Lipa mRNA deficiency causes significant changes in the fatty acid mobilization, adipocyte differentiation, and insulin sensitivity in particular to TG and cholesterol esters mass storage [128]. The higher the expression of LIPA, the more increased activity of the enzyme and therefore less accumulation of lipids in general. According to our data, hfd fed animals show similar expression levels of this gene independently of the transgenic background in WAT, but higher than controls fed on chow diet. Tg chow animals display a slight increase in this gene's levels vs c chow, although not statistically significant. Since we have demonstrated that our experimental models on a hfd displayed high cholesterol serum levels, the over-expression of Lipa enzyme in both groups could be explained by this increase in its substrate. The expression of LIPA is also altered in liver of these animals, where it is significantly decreased in Tg hfd vs c hfd demonstrating antagonistic effects and perhaps justifying higher free fatty acid (FFA) levels serum levels in the Tg hfd group vs all others.

The Hormone sensitive lipase (Lipe) degrades the diglycerides obtained in the catalysis of adipose triglyceride lipase (patatin-like phospholipase domain containing 2, pnpla2) in monoacylglycerol and fatty acids and is activated by protein kinase A controlled phosphorylation, which is activated via the cyclic AMP (cAMP). Thus, the reaction is stimulated by hormones that cause stimulation of adenylate cyclase, a lyase that is involved in cAMP synthesis [129]. Oppositely, it will be inhibited by those hormones which receptor is associated with adenylate cyclase, leading to a lower production of cAMP and consequently lower Lipe activation. Insulin is an inhibitor of this hydrolytic enzyme since it stimulates the inactivating enzyme of cAMP and adenylate cyclase. Furthermore, it has been shown that in the absence of Lipe or ablation of Pnpla2 mice are obese and do not display a remarkable resistance to the development of obesity after long term exposure to a high-fat diet [130-132], also suggesting a decrease in lipolysis that improve glucose tolerance and insulin sensitivity. All experimental groups showed increased expression of LIPE in WAT vs c chow in a similar pattern as hypertension. PNPLA2 expression is increased in a similar manner in all experimental groups (WAT). In this sense, the control mice fed on hfd would be the obese animal model (our positive control) displaying an increase on LIPE and PNPLA2 genes expression compared to control mice that were fed a regular diet and therefore an increased lipolysis. Besides, according to the results obtained in control and Tg animals both treated with standard diet, it is observed that the transgene could also have an effect similar to the high fat diet and that could influence the development of obesity in these Tg animals. The addition of both factors also enhances the expression of these genes however at a lower scale than separately.

The hydroxysteroid-11- $\beta$ -dehydrogenase type 1 enzyme (HSD11B1) is a reductase that catalyzes the conversion of inactive 11-dehydrocorticosterone to its active form, corticosterone [133]. Studies have demonstrated that obesity is associated with increased activity of this protein in murine adipose tissue, it has been found that hsd11- $\beta$ -1 is over-expressed in mice that develop obesity and other features of the metabolic syndrome, including insulin resistance [134, 135]. This event may be due both to increase of lipolysis and lipoprotein lipase (Lipa), which promotes storage of triglycerides in adipose tissue. It has been proven that knockout mice for this same gene are less prone to diet-induced obesity and exhibit improved insulin sensitization [136, 137]. Both controls and transgenics fed on a high-fat diet have a lower expression compared with mice fed the standard diet. It is evident that the deficiency in this enzyme represents a reaction against the effects of the hfd leading to the metabolic syndrome, however no differences were detected between c and Tg fed on one same diet, in other words, the expression of this gene was not affected by the over-expression of KAP.

Adipose tissue volume is in active balance, depending on the relationship between lipogenesis (triglyceride synthesis) and lipolysis (breakdown of triglycerides). Depots of fatty acids (FA) in



the form of triglycerides represent its primary source of energy. In periods of high energy demand, triglycerides are hydrolyzed releasing fatty acids into the circulation. Lipolysis, hormone sensitive lipase and adipose triglyceride lipase are required for this reaction.

All lipolysis genes analyzed in inguinal white adipose tissue point to enhanced lipolysis processes in all experimental groups (Tg chow, c hfd and Tg hfd) that is only shown in FFA serum levels in Tg hfd involving more lipid release from WAT to liver to be processed.

So far our results have shown that the presence of the transgene modifies the expression of certain genes involved in lipid metabolism, moreover when being fed on a diet rich in fat, Tg animals gain less weight than their respective controls, display higher serum free fatty acids levels and lower serum cholesterol levels, demonstrating an influence of the transgene in lipid metabolism. An increase in liver fatty acid oxidation and ketogenesis would drain fatty acids from blood and extra-hepatic tissues and contribute significantly to the beneficial effects of the accumulation of fat mass and enhance the peripheral insulin sensitivity. This may be related ultimately to hypolipidemia, anti-adiposity and improved insulin sensitivity [138]. This could be partially the reason for observed less altered glucose curves in Tg vs controls fed on a high-fat diet.

It has been widely described by means of non-quantitative RT-PCR, Northern blot, in situ hybridising and immunoblotting that KAP expression is restricted to the kidney [66]. However, when using microfluidic cards, which is much more sensitive and quantitative technique, it was found that there was a low expression of KAP in the liver, and yet differences in this expression were observed between Tg and control animals. There seems to be a slight expression of KAP in the presence of the transgene or the hfd alone in liver. In addition, expression in Tg mice is much more pronounced when fed on a high fat diet. Although their mRNA levels remain way much lower than in the kidney, it could be hypothesized that KAP produced in Tg animal liver could have effects on changes in the expression of certain described genes. Alternatively, one could hypothesize that KAP (protein localized to the secretory pathway in proximal tubule) was secreted and have endocrine effects on the liver by modulating the expression of these genes.

### **3. The high fat diet but not the over-expression of KAP demonstrates an evident role in the development of impaired glucose metabolism**

Glucose metabolism was also analysed at a physiological and genetic levels. Response to glucose bolus after a 12 h fasting only appeared altered in controls fed on a high fat diet, suggesting that over-expression of KAP alone might not affect glucose metabolism as suspected. Moreover, over-expression of KAP seemed to be hindering the hfd effects.

When analysing insulin resistance in these animals it was found that environmental factors, in our study, high fat diet, were stronger than genes in altering glucose metabolism. Tg chow animals displayed a 5 h basal glucose significantly higher than c chow supporting our initial

hypothesis that KAP Tg mice might show a certain predisposition to altered glucose metabolism and/or insulin resistance, but when animals were fed on hfd both groups (c and Tg) showed a dramatic increase in basal glucose compared to c chow no matter the transgenic phenotype. Although Tg hfd mice started with a 5 h fasting basal glucose at the same level as controls hfd, the formers decreased their glucose levels after an insulin bolus almost to a chow diet levels. This fact correlates with the analysis of insulin levels in serum, which were slightly higher in Tg chow and significantly higher in both groups fed on hfd, but much more in controls than Tg.

There seemed to be a slight (not statistically significant) increase in the water intake of Tg (manifesting lower adipocytic leptin levels) compared to c, suggesting a predisposition to insulin resistance (one of the symptoms of which is polydipsia) in Tg independently of the diet they are fed on. The increase in water intake in all chow groups vs hfd groups shown in our results accounts for the diet type, since chow diet is much drier than hfd and therefore enhances water intake.

In leptin deficient animals manifesting low KAP levels, water intake, as a marker on unpaired glucose metabolism, is significantly lower than in wild type mice.

Muscle is the main glucose consumer tissue; on this tissue insulin exerts a protein anabolic effect, “in vitro” studies have confirmed a stimulatory effect of insulin on muscle protein synthesis. Certain studies suggest that the response of muscle protein synthesis to insulin is dose dependent, and that only supra-physiological dose of insulin stimulates this protein synthesis. On the other hand, some studies show a stimulatory effect of insulin at low doses. The effects of insulin, according to the results from various experiments, are expressed in the context of the availability of amino acids: insulin stimulates muscle protein synthesis when intramuscular amino acid availability is maintained or increased regardless of the dose of insulin, however, it is ineffective in stimulating muscle protein synthesis when amino acid availability is allowed to drop, again independently of the dose of insulin [139]. Amino acid availability seems to be diet-dependent, since under-nutrition in animals alters protein anabolism. These insulin effects serve to encourage the synthesis of carbohydrate, fat and protein, therefore, insulin can be considered to be an anabolic hormone [140].

Insulin's direct effects on the liver are different to those observed in muscle or adipose tissue, where it acts as an anabolic hormone. In liver, insulin controls glucose production. Insulin inhibits glucose production through both direct and indirect effects on the liver. Studies using somatostatin and portal vein infusions of insulin and glucagon to clamp the pancreatic hormones at basal levels in non-diabetic dogs showed that, the arterial insulin levels were doubled and the hepatic sinusoidal insulin level was reduced to half. Arterial plasma FFA level and net hepatic FFA uptake fell by 40-50%, and net hepatic glucose output increased more than 2-fold. When studying the effect of a 4-fold rise in brain insulin on hepatic glucose production during peripheral hyperinsulinemia and hepatic insulin deficiency this studies demonstrated that

sensitivity of the liver was not enhanced by increased insulin delivery to the brain, demonstrating that the direct effects of insulin dominate the acute regulation of hepatic glucose production [141].

The retinol binding protein 4 (RBP4) has been described as a nutritional indicator being a short half life protein, so that in not adequate nutrition conditions, the amino acid input is diminished and Rbp blood levels decrease [142]. This protein functions as a nutritional marker when found diminished in serum and as a DM marker when found increased in serum [143]. When performing proteomic assays in serum of the four experimental groups in the search of differential presence of proteins in them, Rbp4 appeared in larger amount in the serum of Tg animals fed on chow diet, suggesting that the over-expression of KAP might be involved in activating mechanisms related to DM signalling. This finding matches 5 h fasting basal glucose levels were Tg chow had increased basal glucose vs c chow and could justify increased Rbo4 serum levels in Tg chow. [144].

Rbp, synthesized in liver and adipose tissue, has recently been described as an adipocytokine involved in regulation of glucose metabolism and the development of insulin resistance [145]. Studies in transgenic mice that over-expressed RBP4 supported the development of insulin resistance in these animals, whereas the lack of it in knockout mice improved insulin sensitivity [146]. Thus, we would expect insulin sensitivity worsened in Tg fed on the hfd, compared to c hfd and Tg chow diet, however interaction of transgene and hfd appear to normalize Rbp4 serum levels.

The glucose-regulated protein Hspa5, a glucose metabolism related gene, belongs to the set of heat shock proteins that are produced in response to any type of stress. It resides in the endoplasmic reticulum (ER) and is a key to the control of this organelle homeostasis. It acts as chaperone molecule helping to obtain a proper folding of newly synthesized proteins, marking unfolded proteins for degradation and controlling activation of stress sensors present in the ER membrane [147]. In order to study the role of this gene in detail a mouse model was created with decreased Hspa5 expression [148.], and found that a diet high in lipid content minimized its effects on obesity and insulin resistance, and improved energy consumption and high glucose uptake in insulin-stimulated white adipose tissue of these animals [148]. Inflammation in adipose tissue linked with obesity is associated with insulin resistance [149]. Consequently, the adipose tissue of mice with partial expression Hspa5 showed greatly reduced inflammation. Therefore, the fact that control mice fed on the hfd displayed an up-regulated expression of this gene unlike the controls that were fed on the chow diet indicate that the intake of the hfd diet promotes the development of obesity and diabetes in these animals based on an inflammatory process. This same effect was observed in Tg fed on chow diet showing over-expression of Hspa5 versus controls fed on the same diet matching 5 h fasting basal glucose results, in this case disorders would be driven by the presence of the transgene indicating once again that this

experimental group should display certain predisposition to altered glucose metabolism. Nevertheless, once again there is no synergic effect of transgene and hfd.

Adiponectin (ADIPOQ), hormone that modulates metabolic processes such as lipid catabolism, shows decreased mRNA levels in obese animals. It is secreted by adipocytes and regulates glucose and lipid metabolism, low levels of its receptor adiponectin receptor 1 (Adipor1) seems to be related to overweight or resistance to insulin. Adiponectin is a hormone that protects against obesity, and due to its anti-inflammatory properties it may have beneficial effects on cardiovascular and metabolic disorders such as atherosclerosis and insulin resistance [150]. There is a product resulting from increased fatty acid oxidation ADIPOQ proteolytic reaction that causes weight loss in mice consuming a rich in fat diet [151]. Similarly, several studies claim that its down-regulation is capable of promoting insulin resistance that often results as a consequence diabetes, inflammation, increased free fatty acid and atherosclerosis [152, 153]. Adiponectin was increased in the presence of the transgene or the hfd in WAT vs c chow, reinforcing the hypothesis that transgene and hfd should be leading to same pathological effects. Adiponectin levels are enhanced as a protective mechanism against hfd and transgene. The fact that the expression in Tg fed on the hfd decreased vs both transgenic fed on standard diet and controls fed on high fat diet, suggests that due to agonistic effects of transgene and hfd, there is no need to over-express adiponectin.

ADIPOR1 (adiponectin receptor 1) expression manifested significant differences among the experimental groups' livers, the expression of which only showed differential expression levels in control animals fed on hfd. AdipoR1A is down-regulated in liver of control animals that eat hfd compared with standard diet, confirming that these animals are likely to manifest obesity; this would be a factor causing the observed weight gain. Accordingly, when fed on a high fat diet, control mice should display overweight and insulin resistance, which they do. This gene is only over-expressed in the presence of the hfd, thus, standard levels of this protein in Tg hfd mice could suggest that there are KAP-mediated mechanisms going on in these animals to counteract with hfd's effects.

According to these results, the Tg mice seem to manifest a slight predisposition to insulin resistance, DM and consequent obesity, but when trying to induce and enhance Dm and obesity through the use of the high fat diet, opposite effects to those expected are observed.

#### **4. The over-expression of KAP, high fat diet and interaction of both are differentially involved in the development of inflammation in the different animals' tissues**

Given that it has been demonstrated that unpaired lipidic and glucidic metabolisms trigger inflammatory processes, activation of inflammatory pathways were also studied in these animals both at a serum and tissue levels.

Serum pro inflammatory IL-6 (that stimulates energy mobilization in muscle and adipose tissue and is involved in diabetes and atherosclerosis) levels were only increased in the presence of the hfd but not of the Tg alone or Tg+hfd, demonstrating once more antagonistic effects of transgene and hfd. The over-expression of KAP inhibiting the effects of hfd on IL-6 serum levels matches the fact that adipose TNF $\alpha$  producter tissue activates NF $\kappa$ B pathway in order to produce IL-6. Lager adipose tissue means more TNF $\alpha$  to activate NF $\kappa$ B and increase IL-6 levels, matching as well histological results in WAT.

Resistin levels in serum were increased in the presence of hfd vs chow independently of the presence of the transgene. Resistin increases LDL liver production and degrades LDL liver receptors so that the liver is less able to clear LDL cholesterol from the body accelerating the accumulation of LDL in arteries. It also participates in the inflammatory response increasing transcriptional events leading to increased expression of pro-inflammatory cytokines such as IL-6 and TNF- $\alpha$  mediated by NF- $\kappa$ B. A correlation between resistin and obesity has been demonstrated where serum resistin levels increase with increased adiposity; when adiposity decreases serum resistin levels diminish. There seems to be no influence from the transgene on the levels of serum resistin, not even interference of the transgene on hfd effects on resistin.

There is a hypothesis that states that elevated levels of PAI-1 form the link between obesity, insulin resistance, and the risk of cardiovascular events [154]. PAI-1 serum levels were found risen only in the presence of the transgene, but not hfd or Tg plus hfd indicating that Tg could show a certain predisposition to these alterations that are invalidated with the hfd, perhaps due to a genetic origin of the high PAI-1 serum levels. PAI-1 serum levels behave in the same way as Rbp4 serum levels, enhanced in the presence of the transgene but not by the high fat diet and decreased in the presence of both.

Differential expression assays demonstrated that target study tissues were also differentially affected by inflammation.

RNA expression of CISH (Cytokine-inducible SH2-containing protein) in liver also manifested differences among the groups. CISH protein belongs to the family of the inhibitor of STAT signalling (CIS) [155]. It also inhibits cyclin D1 through STAT 5; therefore, CISH inhibits cell proliferation. The CISH gene expression is increased significantly in the liver of c hfd mice compared to all other groups, so that these animals would show decreased several cytokines through the JAK/STAT signalling pathway. The fact that Cish has highly significant increased expression in inguinal adipose tissue of Tg compared to controls both fed with chow standard diet, would mean that the transgene factor causes an increase in the inactivation signalling of various cytokines at this level. Both groups fed on a high fat diet display less significantly increased CISH levels vs c chow and not manifesting differences between them, perhaps indicating that hfd and transgene counteract between them hindering each other's effects. Antagonistic effects of transgene and hfd are seen in the expression of CISH both in liver (were

hfd enhances CISH expression) and in WAT (where transgene enhances CISH expression), in both tissues, cish levels are decreased in the interaction of both factors.

The cytokine Transforming growth factor  $\beta 1$  (Tgf  $\beta 1$ ), to which many functions are attributed such as cell proliferation and differentiation, has a key role in controlling the immune system releasing pro-inflammatory factors. In studies performed using obese mice models such as ob/ob mRNA levels of Tgf  $\beta 1$  were 5 times higher compared to wild type mice. Similarly, there are evidences of a relationship between obesity and presence of pro-inflammatory factors [156-158]. Chronic inflammation accompanying obesity occurs when there is an increase of the classic inflammation markers such as tumour necrosis factor alpha (TNF $\alpha$ ). Furthermore, it has been shown that TNF  $\alpha$  contributes to increased expression of TGF  $\beta 1$  in adipocytes [159]. Thus, the expression of TGF $\beta 1$  in WAT of controls fed on the hfd and Tg fed on a hfd diet is up-regulated versus controls chow. This suggests that these groups are animal models with a potentially obese phenotype and would support the theory that obesity could be a chronic inflammatory process [159].

Despite what has been observed in TGF $\beta 1$  expression and although in some of the analyzed features we do find effects when adding hfd to Tg, the effect of the hfd is manifested more mildly in the presence of the transgene.

#### **5. Blood pressure is more affected by a high fat diet than by the over-expression of KAP**

In all hypertensive groups (these are Tg chow, c hfd and Tg hfd) hypertension appeared simultaneously at their 6<sup>th</sup> month of life, showing a stronger effect of the hfd vs the transgene when acting separately, although, when acting together hypertension remained at transgene levels, not reaching hfd levels. These results indicate that in terms of hypertension, high fat diet action is worst than over-expression of KAP.

The results obtained during this first physiological study of the experiment demonstrate that hypertension is influenced both by genetic and environmental factors, although environmental factors seem to be stronger in our mice than genetics. Genetic hypertension background was studied through differential gene expression assays in these mice.

In the same way as in human beings, blood pressure follows circadian changes in mice [97], this was tested in our experiments by taking blood pressure measurements in two different experiments on the first one during the afternoon and on the second one during the morning; confirming that blood pressure was significantly lower in the afternoon than in the morning, but always following the same pattern along a time line and among the four different groups, demonstrating that hypertension was an intrinsic fact in the mice and not dependent on the time of the day or the external influences that a different day time might carry.

Recent studies on the control of blood pressure and proteinuria by specific inhibition of the renin-angiotensin-aldosterone system (RAAS) have been performed by using angiotensinogen

converting enzyme inhibitors (ACE) or angiotensin receptor blocking Ang II to halt the progression of diabetic nephropathy [160]. In the early stages of this disease, there is an unpaired self-regulation of the afferent arteriole tone due to the complex interaction of several mediators such as prostanoids, nitric oxide, reactive oxygen species (ROS), lipids, vascular endothelial growth factor (VEGF), transforming growth factor-beta 1 (TGF- $\beta$ 1), high glucose and renin-angiotensin-aldosterone system, specifically angiotensin II (Ang II). In our experimental models, the only group displaying high angiotensin II levels in inguinal white adipose tissue is Tg chow which already showed increased Ang II circulating levels [161], suggesting a possible predisposition in this group to diabetic nephropathy. Tgf-b1 in this same tissue shows an increasing level pattern among the groups, where Tg chow Tgf-b1 levels are higher than c chow, c hfd are higher than Tg chow, and Tg hfd are higher than c hfd, suggesting a additive effect of factors. However, Tgf-b1 expression in liver shows the same pattern as blood pressure measurements. In addition, promoting depletion of the glomerular angiotensin II also seems to have other actions that promote the development of proteinuria. In fact, it has been demonstrated that angiotensin II is involved in almost every pathophysiological process related to the development of diabetic nephropathy. Therefore the interruption of the renin-angiotensin-aldosterone pathway through inhibition of Ang II is essential for the treatment of patients with diabetic kidney disease [160].

In this regard, animal models have been generated using rats that over-expressed angiotensin II type 1 receptor (Angt1R), so that these rats developed albuminuria, defects in podocytes, progressive fibrosis, resulting in focal segmental glomerulosclerosis. These effects were reversed when Ang II was blocked [162]. Therefore, the fact that in the inguinal white adipose tissue of Tg mice eating high-fat diet expression levels of AgtR1A decreased significantly compared to control hfd animals, and remained the same in Tg hfd fed compared to Tg chow diet fed but higher than c chow mice following the same pattern as blood pressure measurements. This may indicate that the transgene might be inhibiting the harmful effects caused by high-fat diet in terms of blood pressure regarding the down regulation of this receptor in Tg. It is not yet clear whether down-regulation of AgtR1A by KAP is due to a direct effect of KAP on this receptor or indirectly as a result of circulating AngII.

At a physiological level, apelin (vasodilator NO release enhancing molecule) is one of the most potent molecules that improves cardiac contractility and is also involved in regulating the amount of water and food intake as well as the immune system [163, 164]. The apelin receptor (AplnR) is a membrane receptor which has a significant structural homology with angiotensin II receptor. Recently the apelin system has been described in liver, it has been observed that blocking apelin receptor in cirrhotic rats, produces a decrease in fibrosis and angiogenesis, as well as an improvement in cardiovascular function and renal disease. These effects point to this system as a new therapeutic target for liver disease [165]. The fact that apelin is down-regulated

in inguinal WAT of Tg mice compared to controls both fed on hfd to reach almost control chow levels, may indicate that the decrease of apelin allows these animals to prevent cardiovascular and liver disease induced by the high-fat diet. Apelin levels among groups also follow the opposite pattern observed in blood pressure measurements given that low apelin levels mean higher blood pressure. In this case, Tg chow are more affected than in Tg hfd. This is a peptide highly expressed in endothelial cells and vascular structures. Adipose tissue is highly vascularized and increased fat mass during the development of obesity is accompanied by an increase in size of microcirculation [166]. This protein is key to control of the cardiovascular system, modulating blood pressure and blood flow by releasing a potent vasodilator such as nitric oxide [167]. In studies where mice have been treated with apelin, it has been shown to increase blood pressure and tachycardia [168]. Similarly, several studies showed that the expression of apelin was up-regulated in obese hyperinsulinemic models, showing a significant positive correlation between mRNA levels of insulin and adipocyte apelin. This is due to insulin regulating the production mechanism of this peptide [169].

Cyp4A14 (cytochrome P450, family 4, subfamily A, polypeptide 14) decreases its expression in kidney of Tg chow mice, already published [67], it also decreases in all mice groups fed on a diet rich in fat compared to controls fed on a standard diet, pointing to a similar effect produced by Tg and hfd separately which is milder when these two factors act together. Cyp4a14 genes encode for enzymes of the CYP4A subfamily. They are involved in lipid metabolism since they perform the  $\omega$ -hydroxylation of fatty acids and related compounds. This reaction facilitates the degradation of long-chain fatty acids. The CYP4A groups are capable of  $\omega$ -hydroxylate arachidonic acid to produce 20-HETE that plays an important role in the regulation of renal vascular and tubular function. In addition, the altered expression of CYP4A is associated with hypertension [63, 170]. The Cyp4A12A gene is  $\omega$ -hydroxylase arachidonic acid predominant in mouse kidney and its expression levels determine the specific differences of sex and strain on the renal production of 20-HETE, a potent vasoconstrictor. An increased production of 20-HETE has been associated with increased oxidative stress, through activation of NADPH oxidase induced by 20-HETE [67]. Animal models with disruption of Cyp4A14 gene display increased  $\omega$ -hydroxylase arachidonic acid activity causing hypertension in male mice, meaning that the lack of Cyp4A14 leads to hypertension. The mechanism appears to involve increased plasma levels of androgens followed by an up-regulation of Cyp4A12 induced by androgens [170]. However, differences in the expression of CYP4A12 gene were not significant among our current experimental groups, as well as in previous studies from our group. This is probably due to Cyp4A12 not being involved directly in the process.

These data demonstrate that it is a combination of differential expression of several genes involved in hypertension what is giving the hypertension pattern observed among the four experimental groups.



As regards to these genes analysed in ob/ob, ppar $\gamma$ 2 KO and poko, CYP4A14 gene shows an increased expression in both experimental groups lacking ppar $\gamma$ 2 (ppar $\gamma$ 2 KO and poko) and this happens in a more pronounced manner in ob/ob animals lacking leptin. In leptin deficient animals showing low KAP levels Cyp4A14 is significantly increased. TGF-B1 is up-regulated in the lack of leptin, PPAR $\gamma$ 2 and both as happens with APLNR (apelin receptor) gene that shows a similar expression pattern as TGF-B1. Studies on transgenic mice over-expressing leptin in liver demonstrated an increase in blood pressure in these animals [171]. Therefore, these studies suggest that leptin deficiency would be beneficial in terms of hypertension probably due to low KAP levels and high Cyp4A14. According to our results, the ob/ob animals would be more protected from cardiovascular disease than poko mice, although the results of several studies in deficient in leptin mice (ob/ob) indicate that these develop cardiac hypertrophy, and this is reversible if leptin is administered exogenously [172]. Other studies confirmed that PPAR $\gamma$ 2 KO mice suffer hypertension associated with cardiac fibrosis [173].

#### **6. Kidneys are more affected by high fat diet than by over-expression of KAP**

Kidneys were analyzed both at histological and differential gene expression levels in both experimental groups' sets: c/Tg with chow/hfd and wt, ob/ob, ppar $\gamma$ 2 and poko.

Vacuolisation observed in kidney slides of animals fed on a hfd might suggest that this finding could be affected by the high-fat diet. This requires a more in-depth study and analysis on the urine of transgenic animals to determine the presence of elevated levels of lipids. In this study line, we did not observe kidney damage described in previous publications on these Tg mice [67].

When analysing KAP protein levels in these animals' kidneys, no significant differences among the kidneys of the four experimental groups were observed. However, there was an interesting trend showing an expected rise in the levels of Tg chow vs c chow. KAP levels did not seem to be affected by hfd alone, but they seemed to rise over Tg chow levels in the case of Tg hfd animals, suggesting that the expression of these protein is enhanced by hfd in Tg mice.

Differential gene expression assays did confirm results already published [67] and gave new ones.

The HMGCS2 is involved in the first step of ketogenesis to provide energy derived from lipids to the brain, kidney and other organs during fasting at it has already been commented. HMGCS2 is significantly under-expressed in kidney of Tg fed on chow diet vs c chow (as expected). When fed on a hfd this pattern changes, control mice show lower levels than Tg. The pattern observed is no longer new, this gene's levels are altered by the presence of the transgene and the hfd separately, but go back to almost standards when adding both factors together.

CCL2 (chemokine (C-C motif) ligand 2), also referred to as monocyte chemoattractant protein-1 (MCP-1), is a small cytokine that recruits monocytes, memory T cells, and dendritic cells to the sites of inflammation produced by both tissue injury and infection. This gene appeared up-regulated either in the presence of the transgene or the hfd vs c chow animals; however, levels were unaltered in the interaction of both factors. CCL2 is also involved in pathogenesis of several diseases characterized by monocytic infiltrates, such as atherosclerosis. Hypomethylation of CpG sites within the CCL2 promoter region is affected by high levels of blood glucose and triglycerides, which increase CCL2 levels in the blood serum. The latter plays an important role in the vascular complications of type 2 diabetes. CCL2 induces amylin expression through ERK1/ERK2/JNK-AP1 and NF- $\kappa$ B related signalling pathways independent of CCR2. Amylin upregulation by CCL2 contributes to the elevation of the plasma amylin and insulin resistance in obesity. Adipocytes secrete several adipokines that may be involved in the negative cross-talk between adipose tissue and skeletal muscle. CCL2 impairs insulin signalling in skeletal muscle cells via ERK1/2 activation, but does not involve activation of the NF- $\kappa$ B pathway.

ACTB (beta-actin) gene encodes for one of six different actin proteins. Actins are highly conserved proteins that are involved in cell motility, structure, and integrity. This actin is a major constituent of the contractile apparatus and one of the two non-muscle cytoskeletal actins. B-actin is found significantly up-regulated in Tg vs c both fed on chow diet and slightly in c hfd, indicating that actin is altered by hfd or the transgene but not by the interaction of both.

A histopathologic characterization of ob/ob, ppar $\gamma$ , poko kidneys was carried out in order to confirm what was observed in the analysis of kidney function, creatinine levels were only significantly raised in poko mice vs wt, and determine if alterations were similar to those observed in the KAP transgenic. Although these analyses were not conclusive, since no differences could be visualised in the slides, the differential lipid metabolism gene expression assays in kidney suggested that lipid metabolism could be altered in this organ.

Studies examining pathological phenotypes related to diabetes such as diabetic nephropathy demonstrated that PPAR $\gamma$  gene wt allele carriers manifested fewer complications, suggesting that the presence of wt PPAR $\gamma$  is associated with a certain protection against the onset of nephropathy (need for dialysis, proteinuria, creatinine over 2 mg/dl). This would mean that ppar $\gamma$ -KO mice may suffer from renal disorders. Kidney function (serum creatinine and urea) analysed in these four experimental groups appeared intact in ob/ob mice, slightly unpaired in ppar $\gamma$ -KO and significantly altered in poko mice, suggesting that lack of PPARG2 and its relationship with KAP are indeed important to renal function, apparently through disorders of glucose metabolism, but when lack of PPARG2 and lack of leptin combine, the negative effect on kidney function is much more dramatic. This is probably due to a more dramatic effect on glucose metabolism of deletion of leptin and Ppar $\gamma$  together.

Through microfluidic card assays, significant differences were detected in the expression of ACTB gene manifesting a slight decrease in the absence of ppar $\gamma$ 2 and a significant decrease in poko animals compared with wt. This may be because the combined deficiency of leptin and ppar $\gamma$ 2 produces more pronounced effects than in ppar $\gamma$ 2 KO. Nevertheless, these results could not be correlated with KAP levels.

The lack of leptin, ppar $\gamma$ 2 or both showed to affect inflammatory pathways at a gene expression level. Ob/ob Mice display an increased in TGF- $\beta$  1 gene expression compared with wt mice, which may be indicative of involvement of the immune system in obesity suffered by ob/ob mice, and therefore, would support the theory that obesity is caused by chronic inflammation.

Expression of KAP was also analyzed at protein and RNA level in kidney homogenates of these animals to find out that in the lack of leptin (both in ob/ob and poko mice), KAP levels decrease significantly vs wt animals, and in ppar $\gamma$ 2 KO mice KAP levels appear increased. This suggests a correlation between the presence of ppar $\gamma$ 2 and/or leptin and the expression of KAP.

It is interesting to note that in the studies of Dr Vidal Puig group differences were observed between the behaviour between females and males in relation to glucose metabolism. According to the observed relationship between leptin, ppar $\gamma$ 2 and KAP and since KAP, but not ppar $\gamma$ 2, is regulated by androgens, moreover leptin is involved in the regulation of androgen levels, it is suggestive think that leptin could be interacting with KAP and KAP could be interfering in the effects observed in animals ppar $\gamma$ 2KO.

Based on the observed results, it would be interesting to determine the levels of PPAR $\gamma$ 2 in our transgenic model KAP.

Inflammatory response observed in mice kidney and described above was studied through differential gene expression assays in PCT3-pBIG2i-KAPwt doxycycline treated clones by evaluating NF- $\kappa$ B signalling pathway in order to verify whether effects observed in animal tissue were caused by the over-expression of KAP directly or secondarily. NF $\kappa$ B controls the expression of many genes including angiotensinogen, endothelin (vasoconstrictor), PAI-1, neuropeptide Y receptor, aromatase promoter, androgen receptor, IL-6 or STAT5.

Many of the pro-inflammatory genes evaluated in the pathway were found up-regulated, indicating that doxycycline induced expression of KAP acted straight on tubular cells and inflammation shown in kidney sample was a consequence of KAP's over-expression primary action. Moreover, some interesting genes appeared altered such as AKT1; in this case, its expression appeared down-regulated in the presence of KAP suggesting a role of the increase of KAP in insulin signalling pathway alterations. Akt is activated by phosphorylation through the action of PI3K when insulin reaches its receptor in cell membrane.

Another interesting gene that appeared differently regulated is caspase 1 involved in cell apoptosis promotion, which increases its expression when clones express KAP.

EIF2A2 or PKR was found up-regulated in the expression of KAP; PKR induces apoptosis as a response to stress, inhibiting cell growth and enhancing stress responses that lead to apoptosis [174].

SLC20A1, a sodium-phosphate symporter that absorbs phosphate from interstitial fluid to be used in cellular functions such as metabolism, signal transduction, and nucleic acid and lipid synthesis, appeared down-regulated in doxycycline treated clones. Up-regulation in the expression of this gene may promote apoptosis and mineralization through the regulation of Akt1 (which was also altered in this condition) [175].

It has been published that EIF2A2 up-regulation induces nephrotoxicity in CsA treated PCT3 cells through the interaction with PI3K. As a consequence Akt and NF $\kappa$ B produce cycle arrest and apoptosis blockade, PI3K induces apoptosis straight away, as well as through oxidative stress and mitochondrial damage enhancement. Finally apoptosis is induced and further necrosis through the action of caspases [176]. In this study, inhibition of MAPK, diminished in our current study when activating expression of KAP, inhibition of PI3K or inhibition of CK2 prevented from nephrotoxicity produced by CsA. It has been described that CypB intracellular receptor of CsA [76] interacts with KAP [177]. Based on the interaction between KAP and CypB, the effects of CsA on KAP in the kidney include a decrease of the protein, concomitantly with an increase of its mRNA. KAP over-expression increases resistance to CsA toxicity in PCT3 cells [177]. The loss of KAP in the presence CsA is due to a slight increase in the secretion of the protein into the extracellular medium but mainly to the degradation that occurs in the presence of the immunosuppressant. Effects occur preferentially when the protein is phosphorylated by CK2 in well identified residues and located in a PEST sequence present in KAP [80]. It is suggestive to think that the over-expression of KAP in doxycycline induced clones leads to similar effects to those already described in PCT3 CsA treated cells in which expression of EIF2A2 is enhanced by the apparition of ER stress (in which over-expression of KAP has also been suggested to be involved). Moreover, these could explain physiological damage observed in kidney of KAP Tg mice [67].

These results together with those obtained through CsA treatments studies in control and Tg mice, suggest that KAP might be an element interfering in renal toxicity and possibly hindering metabolic syndrome.

To sum up, among all analysed data, there are three patterns observed that end in the same way:

- 1) Effects are enhanced by the presence of the transgene but not by the high fat diet, and are normalized or diminished in the interaction of both.
- 2) Effects are enhanced by the high fat diet but not by the transgene, and are normalized or diminished in the interaction of both.

3) Effects are enhanced by the high fat diet as well as by the transgene, and are normalized or diminished in the interaction of both.

In all cases the sum up of both factors does not show a synergic effect.

Our current data demonstrate a key role of KAP in the regulation of extra-renal responses and connect the function of KAP, through the action of leptin, ppar $\gamma$ 2 and androgens, with processes involved in developing hypertension, glucose and lipid metabolism alterations and immune response activation. These results could shed some light on the molecular mechanisms underlying the metabolic syndrome, an increasingly prevalent disease in developed countries suggesting that KAP could be a possible target for therapeutic interventions.

## **CONCLUSIONS**

---

## CONCLUSIONS

The over expression of KAP, though producing similar alterations to those defined in the MS by itself, seems to prevent from the damage induced by a HFD.

KAP has its action not only on kidney but also on distal tissues such as liver and both brown and white adipose tissues.

Blood pressure is more affected by a high fat diet than by the over-expression of KAP.

The high fat diet but not the over-expression of KAP demonstrates a role in the development of impaired glucose metabolism.

Animals' body weight and appetite is not affected by the over-expression of KAP independently of the diet.

KAP is expressed in liver in the presence of high fat diet.

In the majority of the assays, the over-expression of KAP proves to have a similar effect to high fat diet in the development of impaired lipid metabolism.

The over-expression of KAP, high fat diet and interaction of both are differentially involved in the development of inflammation in the different animals' tissues.

Kidneys are more affected by high fat diet than by over-expression of KAP.

KAP is released to the urinary space.

The over expression of KAP, though producing similar alterations to those defined in the MS by itself, seems to prevent from the damage induced by a high fat diet.

## **REFERENCES**

---



## REFERENCES

- 1 Revista de Posgrado Vía Cátedra de Medicina. N° 174-Oct 2007
- 2 <http://www.nlm.nih.gov>
- 3 Carlos Lorenzo, MD, Ken Williams, MS, Kelly J. Hunt, PHD and Steven M. Haffner, MD. The National Cholesterol Education Program–Adult Treatment Panel III, International Diabetes Federation, and World Health Organization Definitions of the Metabolic Syndrome as Predictors of Incident Cardiovascular Disease and Diabetes. doi: 10.2337/dc06-1414 *Diabetes Care* January 2007 vol. 30 no. 1 8-13
- 4 Neda Rasouli and Philip A. Kern; Adipocytokines and the Metabolic Complications of Obesity; *Clin Endocrinol Metab.* 2008 November; 93(11 Suppl 1): S64–S73.
- 5 <http://medical-dictionary.thefreedictionary.com>
- 6 Scott M. Grundy, MD, PhD; H. Bryan Brewer Jr, MD; James I. Cleeman, MD; Sidney C. Smith Jr, MD; Claude Lenfant, MD; for the Conference Participants. Definition of Metabolic Syndrome. Report of the National Heart, Lung, and Blood Institute/American Heart Association Conference on Scientific Issues Related to Definition. *Circulation.* 2004; 109: 433-438 doi: 10.1161/01.CIR.0000111245.75752.C6
- 7 Grundy SM, Cleeman JI, Daniels SR, Donato KA, Eckel RH, Franklin BA, Gordon DJ, Krauss RM, Savage PJ, Smith SC Jr, Spertus JA, Costa F: Diagnosis and management of the metabolic syndrome: an American Heart Association/National Heart, Lung, and Blood Institute Scientific Statement. *Circulation* 112:2735–2752, 2005
- 8 Alberti KG, Zimmet P, Shaw J, the IDF Epidemiology Task Force Consensus Group: The metabolic syndrome: a new worldwide definition. *Lancet* 366:1059–1062, 2005
- 9 World Health Organization: Definition, Diagnosis and Classification of Diabetes Mellitus and Its Complications: Report of a WHO Consultation. Geneva, World Health Org., 1999
- 10 <https://www.clinicalkey.com>
- 11 Daniel Fernández-Bergés, Antonio Cabrera de León, Héctor Sanz, Roberto Elosua, María J. Guembe, Maite Alzamora, Tomás Vega-Alonso, Francisco J. Félix-Redondo, Honorato Ortiz-Marrón, Fernando Rigo, Carmen Lama, Diana Gavrilá, Antonio Segura-Fragoso, Luis Lozano, Jaume Marrugat. Síndrome metabólico en España: prevalencia y riesgo coronario asociado a la definición armonizada y a la propuesta por la OMS. *Estudio DARIOS. Rev Esp Cardiol.* 2012;65:241-8.
- 12 <http://medical-dictionary.thefreedictionary.com>
- 13 <http://www.xortx.com>
- 14 Roberto Corti, MD; John C. Burnett Jr, MD; Jean L. Rouleau, MD; Frank Ruschitzka, MD; Thomas F. Lüscher, MD. Cardiovascular Drugs. Vasopeptidase Inhibitors. A New Therapeutic Concept in Cardiovascular Disease? *Circulation* October 9, 2001 vol. 104 no. 15 1856-1862
- 15 Volpe M, Tocci G, Pagannone E. [Activation of the renin-angiotensin-aldosterone system in heart failure]. *Ital Heart J.* 2005 May;6 Suppl 1:16S-23S.
- 16 Shahriar Iravanian1 and Samuel C. Dudley, Jr. The Renin-Angiotensin-Aldosterone System (RAAS) and Cardiac Arrhythmias. *Heart Rhythm.* Author manuscript; available in PMC 2009 June 1. Published in final edited form as: *Heart Rhythm.* 2008 June; 5(6 Supplement 1): s12–s17. doi: 10.1016/j.hrthm.2008.02.025 PMID: PMC2600881 NIHMSID: NIHMS54305
- 17 <http://www.kidney.org>
- 18 <http://www.cdc.gov>
- 19 <http://www.themetaboliccenter.com>
- 20 Unwin N, Shaw J, Zimmet P, Alberti KG. Impaired glucose tolerance and impaired fasting glycaemia: the current status on definition and intervention. *Diabet Med.* 2002 Sep;19(9):708-23.
- 21 <http://science.howstuffworks.com>
- 22 Wisse BE. The inflammatory syndrome: the role of adipose tissue cytokines in metabolic disorders linked to obesity. *J Am Soc Nephrol.* 2004 Nov;15(11):2792-800.

## REFERENCES

- 23 Antonino De Lorenzo, Vera Del Gobbo, Maria Grazia Premrov, Mario Bigioni, Fabio Galvano, and Laura Di Renzo. Normal-weight obese syndrome: early inflammation? 2007 American Society for Clinical Nutrition
- 24 Satoshi Nishimura. Adipose Tissue Inflammation in Obesity and Metabolic Syndrome. *Discovery Medicine*. Published on September 22, 2009
- 25 Klok MD, Jakobsdottir S, Drent ML .The role of leptin and ghrelin in the regulation of food intake and body weight in humans: a review. *Obes Rev*. 2007 Jan;8(1):21-34.
- 26 Lihn AS, Pedersen SB, Richelsen B. Adiponectin: action, regulation and association to insulin sensitivity. *Obes Rev*. 2005 Feb;6(1):13-21.
- 27 Jamaluddin MS, Weakley SM, Yao Q, Chen C. Resistin: functional roles and therapeutic considerations for cardiovascular disease. *Br J Pharmacol*. 2012 Feb;165(3):622-32. doi: 10.1111/j.1476-5381.2011.01369.x.
- 28 <https://www.meducation.net>
- 29 Vaughan DE. PAI-1 and atherothrombosis. *J Thromb Haemost*. 2005 Aug;3(8):1879-83.
- 30 M.J. Moreno, J.A. Martines. El tejido adiposo: órgano de almacenamiento y órgano secretor. *ANALES Sis San Navarra* 2002;
- 31 M. Mohsen Ibrahim. Subcutaneous and visceral adipose tissue: structural and functional differences. *Etiology and Pathophysiology*. doi: 10.1111/j.1467-789X.2009.00623.x
- 32 Marta Garaulet, Maria Puy, Francisca Pérez Llamas, Carmen Cuadrado, Rosaura Leis, Maria Jesús Moreno. Obesidad y ciclos de vida del adulto. *Rev Esp Nutr Comunitaria* 2008;14(3):150-155
- 33 Christiane Koch, Rachael A. Augustine, Juliane Steger, Goutham K. Ganjam, Jonas Benzler, Corinna Pracht, Chrishanthi Lowe, Michael W. Schwartz, Peter R. Shepherd, Greg M. Anderson, David R. Grattan, and Alexander Tups. Leptin Rapidly Improves Glucose Homeostasis in Obese Mice by Increasing Hypothalamic Insulin Sensitivity. *The Journal of Neuroscience*, 1 December 2010, 30(48): 16180-16187; doi: 10.1523/JNEUROSCI.3202-10.2010
- 34 Frederico G.S. Toledo, MD1, Allan D. Sniderman, MD2 and David E. Kelley, MD1. Influence of Hepatic Steatosis (Fatty Liver) on Severity and Composition of Dyslipidemia in Type 2 Diabetes. doi: 10.2337/dc06-0455 *Diabetes Care* August 2006 vol. 29 no. 8 1845-1850
- 35 Speliotes EK, Massaro JM, Hoffmann U, Vasan RS, Meigs JB, Sahani DV, Hirschhorn JN, O'Donnell CJ, Fox CS. Fatty liver is associated with dyslipidemia and dysglycemia independent of visceral fat: the Framingham Heart Study. *Hepatology*. 2010 Jun;51(6):1979-87. doi: 10.1002/hep.23593.
- 36 Adiels M, Taskinen MR, Borén J. Fatty liver, insulin resistance, and dyslipidemia. *Curr Diab Rep*. 2008 Feb;8(1):60-4.
- 37 Nguyen P, Leray V, Diez M, Serisier S, Le Bloc'h J, Siliart B, Dumon H. Liver lipid metabolism. *J Anim Physiol Anim Nutr (Berl)*. 2008 Jun;92(3):272-83. doi: 10.1111/j.1439-0396.2007.00752.x.
- 38 José R. Banegas, Fernando Villar, Auxiliadora Graciani y Fernando Rodríguez-Artalejo. Epidemiología de las enfermedades cardiovasculares en España. *Rev Esp Cardiol Supl*. 2006;6:3G-12G
- 39 <http://www.fundaciondiabetes.org>
- 40 Special Problems in Hemodialysis Patients, Edited by Maria Goretti Penido. p. cm. ISBN 978-953-307-396-5. First published November, 2011. Printed in Croatia
- 41 <http://www.news-medical.net>
- 42 <http://www.kidney.org>
- 43 <http://www.news-medical.net>
- 44 Andrew S Levey, Josef Coresh Chronic kidney disease. *Lancet* 2012; 379: 165–80. DOI:10.1016/S0140-6736(11)60178-5
- 45 Evans, R. M. (1988) *Science* 240, 889-895
- 46 Beato, M. (1989) *Cell* 56, 335-344
- 47 Aranda, A., Pascual, A. (2001) *Physiol. Rev.* 81, 1269-1304
- 48 Ikonen, T. J., Palvimo J. J., Kallio, P. J., Reinikainen, P., Janne, OA. (1994) *Endocrinol* 135, 1359-1366

- 49 Catterall JF, Meseguer A, Niu EM. *Ann N Y Acad Sci.* (1991);626:92-100.
- 50 Ralph D, McClelland, Welsh J (1993). *Proc Natl Acad Sci USA* 90:10710-10714
- 51 Hubank M, Schatz D G (1994). *Nucleic Acids Res* 22:5640-5648
- 52 Meliá M.J., Bofill N., Hubank M., Meseguer A. *Endocrinology* (1998). 139:2, 688-695
- 53 Isern J, Meseguer A. (2003). *Biochem. Biophys. Res. Commun.*; 307: 139-147.
- 54 C. Aresté, M. J. Meliá, J. Isern, J. L. Tovar and A. Meseguer (2004). *J. of Endocrinology.* 183, 101-104
- 55 Isern J., Hagenbuch B., Stieger B., Meier P., Meseguer A. (2001). *Biochim et Biophys Acta.*; 1518. 73-78.
- 56 Nakata K, Tanaka Y, Nakano T, Adachi T, Tanaka H, Kaminuma T, Ishikawa T. (2006) *Drug Metab Pharmacokinet*;21(6):437-57.
- 57 Metcalfe PD, Meldrum KK (2006) *J Urol.* Jul;176(1):15-21.
- 58 Pechere-Bertschi A, Burnier M.(2007) *Curr Opin Nephrol Hypertens.* 16(1):16-21
- 59 Quan A, Chakravarty S, Chen JK, Chen JC, Loleh S, Saini N, Harris RC, Capdevila J (2004) *Am J*
- 60 Dammanahalli KJ, Sun Z (2008) *Clin Exp Pharmacol Physiol.* Jan;35(1):2-6.
- 61 Lamas S, Lowenstein CJ, Michel T. (2007) *Cardiovasc Res.* 15;75(2):207-9.
- 62 McGuire BB, Watson RW, Pérez-Barriocanal F, Fitzpatrick JM, Docherty NG. (2007) *Kidney Blood Press*
- 63 Capdevila JH (2007) *Curr Opin Nephrol Hypertens.* 16(5):465-70.
- 64 Verzola D, Gandolfo MT, Salvatore F, Villaggio B, Gianiorio F, Traverso P, Deferrari G, Garibotto G.
- 65 Gandolfo MT, Verzola D, Salvatore F, Gianiorio G, Procopio V, Romagnoli A, Giannoni M, Garibotto G.
- 66 Toole J. J., Hastie N. D., and Held W. A. An abundant androgen-regulated mRNA in the mouse kidney. *Cell* (1979) 17, 441-448.
- 67 Tornavaca O., Pascual G., Barreiro M. L., Grande M. T., Carretero A., Riera M., Garcia-Arumi E., Bardaji B., González-Núñez M., Montero M.A., López-Novoa J.M. i Meseguer A. *Kidney Androgen-Regulated Protein Transgenic Mice Show Hypertension and Renal Alterations Mediated by Oxidative Stress.* *Circulation* (2009) 119; 1908-1917.
- 68 Meseguer A., Y Catterall J.F. (1987). Mouse kidney androgen-regulated protein messenger ribonucleic acid is expressed in the proximal convoluted tubules. *Mol Endocrinol*, 1(8): 535-541.
- 69 Meseguer A, Catterall JF (1990). *Mol. Endocr.* 4: 1240
- 70 Meseguer A, Catterall JF.(1992). *Mol. Cell Endocrinol*; 89: 153-162
- 71 Solé E, Calvo R, Obregón MJ, Meseguer A. (1994) *Endocrinology*; 135: 2120-2129
- 72 Meseguer A, Watson CS, Catterall JF.(1989) *Mol. Endocr*; 3: 962
- 73 Solé E, Calvo R., Obregón M.J., Meseguer A. (1996). *Mol and Cell Endocrinol* 119:147-159.
- 74 Teixidó N., Soler M., Rivera, N., Bernués J, Meseguer A. (2006). *Mol Endocrinol.*; 20: 389-404.
- 75 Cebrián C., Aresté C., Nicolás A., Olivé P., Carceller A., Piulats J., Y Meseguer A. (2001). *Kidney Androgen-regulated Protein Interacts with Cyclophilin B and Reduces Cyclosporine A-mediated Toxicity in Proximal Tubule Cells.* *The Journal of Biological chemistry*, 276(31): 29410–29419.
- 76 Carpentier M, Allain F, Haendler B, Slomianny MC, Spik G (2000). *ProteinSci.*;9(12):2386-93.
- 77 González-Santiago L, López-Ongil S, Lamas S, Quereda C, Rodríguez-Puyol M, Rodríguez-Puyol D.
- 78 Puigmulé M, López-Hellin J, Suñé G, Tornavaca O, Camaño S, Tejedor A, Meseguer A. *Nephrology Dialysis Transplantation.* 2009; doi: 10.1093/ndt/gfp149
- 79 Sarró E, Tornavaca O, Plana M, Meseguer A, Itarte E (2008). *Kidney International.* Jan;73(1):77-85.
- 80 Tornavaca O., Sarró E., Itarte E., Meseguer, A. *Calpain-mediated degradation of the kidney androgen- regulated protein (KAP) is regulated by protein kinase CK2 phosphorylation (manuscrito sometido)*
- 81 Tornavaca O, Sarró E, Pascual G, Bardaji B, Montero MA, Salcedo MT, Plana M, López-

- Hellin J, Itarte E, Meseguer A. KAP degradation by calpain is associated with CK2 phosphorylation and provides a novel mechanism for cyclosporine A-induced proximal tubule injury. *PLoS One*. 2011;6(9):e25746. doi: 10.1371/journal.pone.0025746. Epub 2011 Sep 28
- 82 Malstrom S.E., Purchio, A.F., Tornavaca O., Meseguer A., West D.B. (2004). *Toxicological Sciences*.79(2):266-77. Epub 2004 Mar 31.
- 83 Muller DN, Schmidt C, Barbosa-Sicard E, Wellner M, Gross V, Hercule H, Markovic M, Honeck H, Luft
- 84 Holla VR, Adas F, Imig JD, Zhao X, Price E Jr, Olsen N, Kovacs WJ, Magnuson MA, Keeney DS, Breyer
- 85 Masuda E.S, Imamura R, Amasaki Y, Arai K, Arai N: Signalling into the T-cell nucleus: NFAT regulation. *Cell Signal* 10: 599-611, 1998.
- 86 Jackson Lab web: <http://jaxmice.jax.org/strain/000632.html>
- 87 Lau D., Dhillon B., Yan H., Szmitko P., and Verma S. Adipokines: molecular links between obesity and atherosclerosis. *American Journal of Physiol Heart and Circulatory Physiology* (2005) 288: H2031–H2041.
- 88 Kis A., Murdoch C, Zhang M. et. al. Defective peroxisomal proliferators activated receptor gamma activity due to dominant-negative mutation synergizes with hypertension to accelerate cardiac fibrosis in mice. *European Journal of Heart Failure* (2009) 11, 533-541.
- 89 Medina-Gomez G, Gray SL, Yetukuri L, Shimomura K, Virtue S, et al. PPAR gamma 2 prevents lipotoxicity by controlling adipose tissue expandability and peripheral lipid metabolism. *PLoS Genet* (2007) 3(4): e64.
- 90 Cartier N. et al., 1993
- 91 Lacave R, Bens M, Cartier N, Vallet V, Robine S, Pringault E, Kahn A, Vandewalle A. Functional properties of proximal tubule cell lines derived from transgenic mice harboring L-pyruvate kinase-SV40 (T) antigen hybrid gene. *J Cell Sci*. 1993 Mar;104 ( Pt 3):705-12.
- 92 Soler M, Tornavaca O, Solé E, Menoyo A, Hardy D, Catterall JF, Vandewalle A, Meseguer A.. Hormone-specific regulation of the kidney androgen-regulated gene promoter in cultured mouse renal proximal-tubule cells. *Biochem J*. 2002 Sep 15;366(Pt 3):757-66.
- 93 Guo L, Song L, Wang Z, Zhao W, Mao W, Yin M. Panaxydol inhibits the proliferation and induces the differentiation of human hepatocarcinoma cell line HepG2. *Chem Biol Interact*. 2009 Sep 14;181(1):138-43. doi: 10.1016/j.cbi.2009.04.015. Epub 2009 May 18.
- 94 Strathdee CA et al. *Gene*. 1999 Mar 18;229(1-2):21-9
- 95 Miller LK, Kral JG, Strain GW, Zumoff B. Androgen binding to ammonium sulfate precipitates of human adipose tissue cytosols. *Steroids* 1990; 55: 410-415.
- 96 Pedersen, S. B.; Fuglsig, S.; Sjogren, P.; Richelsen, B. Identification of steroid receptors in human adipose tissue. *Eur J Clin Invest* 1996; 26: 1051-1056.
- 97 Eagon P K; Elm M S; Stafford E A; Porter L E. Androgen receptor in human liver: characterization and quantitation in normal and diseased liver. *Hepatology* 1994. 19:92-100.
- 98 C.Cohen, D.Lawson, P.DeRose. Sex and androgenic steroid receptor expression in hepatic adenomas. *Hum Patol* 1998; 29: 1428-1432.
- 99 Xu X, De Pergola G, Björntorp P. The effects of androgens on the regulation of lipolysis in adipose precursor cells. *Endocrinology*. 1990 Feb;126(2):1229-34
- 100 Xu X, De Pergola G, Björntorp P. Testosterone Increases Lipolysis and the Number of  $\beta$ -Adrenoceptors in Male Rat Adipocytes. *Endocrinology* 1991; 128: 379-382.
- 101 F Lönnqvist, A Thöme, K Nilsell, J Hoffstedt, and P Arner. A pathogenic role of visceral fat beta 3-adrenoceptors in obesity. *J Clin Invest*. 1995 March; 95(3): 1109–1116.
- 102 Björntorp P. "Portal" adipose tissue as a generator of risk factors for cardiovascular disease and diabetes. *Arteriosclerosis*. 1990 Jul-Aug;10(4):493-6.
- 103 *J Clin Invest*. 1994 May;93(5):2007-13.
- 104 Cunningham MJ, Clifton DK, Steiner RA. Leptin's actions on the reproductive axis: perspectives and mechanisms. *Biol Reprod*. 1999 Feb;60(2):216-22.
- 105 Medina-Gomez G, Gray SL, Yetukuri L, Shimomura K, Virtue S, et al. PPAR gamma 2 prevents lipotoxicity by controlling adipose tissue expandability and peripheral lipid metabolism. *PLoS Genet* (2007) 3(4): e64.
- 106 F. Ouali, F. Djouadi, C. Merlet-Bénichou, and J. Bastin. Dietary lipids regulate beta-oxidation

- enzyme gene expression in the developing rat kidney. *Am J Physiol Renal Physiol* 275: F777-F784, 1998.
- 107 Blur I et al., 1999
  - 108 Stefanski A, Majkowska L, Ciechanowicz A, Frankow M, Safranow K, Parczewski M, Pilarska K.. Lack of association between the Pro12Ala polymorphism in PPAR-gamma2 gene and body weight changes, insulin resistance and chronic diabetic complications in obese patients with type 2 diabetes. *Arch Med Res.* 2006 Aug;37(6):736-43.
  - 109 E H Leiter and H D Chapman. Obesity-induced diabetes (diabesity) in C57BL/KsJ mice produces aberrant trans-regulation of sex steroid sulfotransferase genes. *J Clin Invest.* 1994 May; 93(5): 2007–2013.
  - 110 Satomi Akagiri, Yuji Naito, Hiroshi Ichikawa, Katsura Mizushima, Tomohisa Takagi, Osamu Handa, Satoshi Kokura, and Toshikazu Yoshikawa. A Mouse Model of Metabolic Syndrome; Increase in Visceral Adipose Tissue Precedes the Development of Fatty Liver and Insulin Resistance in High-Fat Diet-Fed Male KK/Ta Mice. *J Clin Biochem Nutr.* 2008 March; 42(2): 150–157.
  - 111 Cannon B, Nedergaard J. *Physiol Rev.* 2004 Jan;84(1):277-359.
  - 112 Freedman B., Lee E., Park Y. and Jameson L. A dominant negative peroxisome proliferator-activated receptor-gamma knock-in mouse exhibits features of the metabolic syndrome. *The Journal of Biological Chemistry* (2005). Vol. 280. No. 17, pp 17118-17125.
  - 113 Adipose Triglyceride Lipase and Hormone-sensitive Lipase Are the Major Enzymes in Adipose Tissue Triacylglycerol Catabolism
  - 114 Linn Ft, Lane Md. CCAAT/enhancer binding protein alpha is sufficient to initiate the 3T3L1 adipocyte differentiation program. *Proc Natl Acad Sci USA* 1994;91:8757-8761
  - 115 Teixidó N., Soler M., Rivera, N., Bernués J, Meseguer A. (2006). *Mol Endocrinol.*; 20: 389-404.
  - 116 Gregoire F, Smas C, Sook Sul H. Understanding adipocyte differentiation. *Physiol Reviews*, 1998; 78: 783-809.
  - 117 De Vos P, Lefevre A, Miller S, Guerre-Millo M, Wong K, Saladin R. Thiazolidinediones repress ob gene expression in rodents via activation of peroxisome proliferator-activated receptor. *J Clin Invest*, 1996; 198: 1004-9.
  - 118 Chang TY, Chang CC, Lin S, Yu C, Li BL, Miyazaki A. Roles of acyl-coenzyme A:cholesterol acyltransferase-1 and -2. *Curr Opin Lipidol* (2001)12:289±296.
  - 119 Acyl-coenzyme A:cholesterol acyltransferases, Ta-Yuan Chang, Bo-Liang Li, Catherine C. Y. Chang and Yasuomi Urano *Am J Physiol Endocrinol Metab* 297:E1-E9, 2009. First published 13 January 2009; doi:10.1152/ajpendo.90926.2008
  - 120 von zur Muhlen C, Schiffer E, Sackmann C, Zürgbig P, Neudorfer I, Zirlik A, Htun N, Iphöfer A, Jänsch L, Mischak H, Bode C, Chen YC, Peter K. Urine proteome analysis reflects atherosclerotic disease in an ApoE<sup>-/-</sup> mouse model and allows the discovery of new candidate biomarkers in mouse and human atherosclerosis. *Mol Cell Proteomics.* 2012 Jul;11(7):M111.013847. doi: 10.1074/mcp.M111.013847. Epub 2012 Feb 27.
  - 121 Chang TY, Chang CC, Lin S, Yu C, Li BL, Miyazaki A. Roles of acyl-coenzyme A:cholesterol acyltransferase-1 and -2. *Curr Opin Lipidol* (2001)12:289±296.
  - 122 Leon C, Hill JS, Wasan KM. Potential role of acyl-coenzyme A:cholesterol transferase (ACAT) inhibitors as hypolipidemic and antiatherosclerosis drugs. *Pharm Res.* (2005) Oct;22(10):1578-88.
  - 123 Darlington GJ, Wang N, Hanson RW: C/EBP alpha: a critical regulator of genes governing integrative metabolic processes. *Curr Opin Genet Dev* 1995, 5:565-570. PubMed Abstract |
  - 124 Martínez JA, Frühbeck G. Regulation of energy balance and adiposity: a model with new approaches. *J Physiol Biochem* 1996; 52: 255-258.
  - 125 Flier JS, Maratos-Flier E. Obesity and the hypothalamus: novel peptides for new pathways. *Cell* 1998; 92: 437-440.
  - 126 Rodríguez J., Gil-Gómez G., Hegardt F. And Haro D. Peroxisome proliferator-activated receptor mediates induction of the mitochondrial 3-hydroxy-3-methylglutaryl-CoA synthase gene. *The Journal of Biological Chemistry* (1994).nVol. 269, No. 29, pp. 18767-18772.
  - 127 Nadal A., Marrero P. and Haro D. Down-regulation of the mitochondrial 3-hydroxy-3-

- methylglutaryl-CoA synthase gene by insulin: the role of the forkhead transcription factor FKHRL1. *Biochem. J.* (2002) 366, 289±297.
- 128** Lysosomal acid lipase-deficient mice: depletion of white and brown fat, severe hepatosplenomegaly, and shortened life span Hong Du, 1, \* Martin Heur,\* Ming Duanmu, 2, \* Gregory A. Grabowski,\* David Y. Hui, § David P. Witte, † and Jaya Mishra\* *Journal of Lipid Research* Volume 42, 2001
- 129** 31. Jeroen de Meijer. Hormone sensitive lipase: structure, function and regulation.
- 130** Strom K, Hansson O, Lucas S, Nevsten P, Fernandez C, et al. (2008) Attainment of brown adipocyte features in white adipocytes of hormone sensitive lipase null mice. *PLoS One* 3: e1793.
- 131** Harada K, Shen WJ, Patel S, Natu V, Wang J, et al. (2003) Resistance to highfat diet-induced obesity and altered expression of adipose-specific genes in HSL deficient mice. *Am J Physiol Endocrinol Metab* 285: E1182–1195.
- 132** Haemmerle, G., Lass, A., Zimmermann, R., Gorkiewicz, G., Meyer, C., Rozman, J., Heldmaier, G., Maier, R., Theussl, C., Eder, S., Kratky, D., Wagner, E. F., Klingenspor, M., Hoefler, G., and Zechner, R. (2006) *Science* 312, 734–737
- 133** Stewart PM, Krozowski ZS 1999 11-Hydroxysteroid dehydrogenase. *Vitam Horm* 57:249–324
- 134** Masuzaki H, Paterson J, Shinyama H, Morton NM, Mullins JJ, Seckl JR, Flier JS: A transgenic model of visceral obesity and the metabolic syndrome. *Science* 2001, 294:2166–2170.
- 135** Masuzaki H, Paterson J, Shinyama H, Morton NM, Mullins JJ, Seckl JR, Flier JS 2001 A transgenic model of visceral obesity and the metabolic syndrome. *Science* 294:2166–2170
- 136** Morton N, Paterson J, Masuzaki H, Holmes MC, staels B, Fievet C, Walker B, Flier J, Mullins J, Seckl : Reduced 11-Hydroxysteroid dehydrogenase type 1-mediated intra-adipose glucocorticoid regeneration: a novel protective adaptation to and treatment for the metabolic syndrome. Program & Abstracts of the 85th Annual Meeting of the Endocrine Society, 2003, June 19-22, abstract OR39-5 114. 4. Williams LJ, Lyons V, MaLeod
- 137** Alberts P, Nilsson C, Selen G, Engblom LO, Edling NH, Norling S, Klingstrom G, Larsson C, Forsgren M, Ashkzari M, Nilsson CE, Fiedler M, Bergqvist E, Ohman B, Björkstrand E, Abrahamson LB 2003 Selective inhibition of 11-hydroxysteroid dehydrogenase type 1 improves hepatic insulin sensitivity in hyperglycemic mice strains. *Endocrinology* 144:4755–4762
- 138** Berge R K; Tronstad K J; Berge K; Rost T H; Wergedahl H; Gudbrandsen O A; Skorve J. The metabolic syndrome and the hepatic fatty acid drainage hypothesis. *Biochimie* 2005;87(1):15–20.
- 139** Wolfe RR. *Curr Opin Clin Nutr Metab Care.* 2000 Jan;3(1):67-71.
- 140** Dimitriadis G, Mitrou P, Lambadiari V, Maratou E, Raptis SA. *Diabetes Res Clin Pract.* 2011 Aug;93 Suppl 1:S52-9. doi: 10.1016/S0168-8227(11)70014-6.
- 141** Edgerton DS, Lautz M, Scott M, Everett CA, Stettler KM, Neal DW, Chu CA, Cherrington AD. *J Clin Invest.* 2006 Feb;116(2):521-7.
- 142** *J Clin Endocrinol Metab.* 2007 Mar;92(3):1168-71. Epub 2006 Dec 12.
- 143** <http://www.medicalnewstoday.com>
- 144** Yang Q, Graham TE, Mody N, Preitner F, Peroni OD, Zabolotny JM, Kotani K, Quadro L, Kahn BB. Serum retinol binding protein 4 contributes to insulin resistance in obesity and type 2 diabetes. *Nature.* 2005 Jul 21;436(7049):356-62.
- 145** Erikstrup Ch., Mortensen Oh, Pedersen Bk: Retinol-binding protein 4 and insulin resistance. *N Engl J Med* 355: 1393-1394, 2006.
- 146** Graham Te, Yang Q, Bluher M, Hammarstedt A, Ciaraldi Tp, Henry Rr, Wason Cj ,et al: Retinol-binding protein 4 and insulin resistance in lean, obese, and diabetic subjects. *N Engl J Med* 354: 2552-2563, 2006.
- 147** Lee AS. The glucose-regulated proteins: stress induction and clinical applications. *Trends Biochem Sci* 2001;26:504–510
- 148** Risheng Ye,<sup>1</sup> Dae Young Jung,<sup>2</sup> John Y. Jun,<sup>2</sup> Jianze Li,<sup>1</sup> Shengzhan Luo,<sup>1</sup> Hwi Jin Ko,<sup>2</sup> Jason K. Kim,<sup>2</sup> and Amy S. Lee<sup>1</sup> Grp78 Heterozygosity Promotes Adaptive Unfolded Protein Response and Attenuates Diet-Induced Obesity and Insulin Resistance *DIABETES*, VOL. 59, JANUARY 2010

- 149 Wellen KE, Hotamisligil GS. Inflammation, stress, and diabetes. *J Clin Invest* 2005;115:1111–1119
- 150 Ouchi N., Walsh K., Adiponectin as an anti-inflammatory factor. *Clin Chim Acta* (2007). 380(1-2): 24–30.
- 151 Fruebis J, Tsao Javarschi S, Ebbets Reed D, Erickson Mr, Yen Ft et al. Proteolytic cleavage product of 30-kDa adipocyte complement-related protein increases fatty acid oxidation in muscle and causes weight loss in mice. *Proc Natl Acad Sci USA* 2001; 98;2005-2010
- 152 K. Sharma, S. RdraRao, G. Qiu et al., “Adiponectin regulates albuminuria and podocyte function in mice,” *Journal of Clinical Investigation*, vol. 118, no.5, pp.11645 1656, 2008
- 153 Ouchi N., Walsh K., Adiponectin as an anti-inflammatory factor. *Clin Chim Acta* (2007). 380(1-2): 24–30.
- 154 Paul J. Declerck, PharmD, PhD Ann Gils, PharmD, PhD. *Semin Thromb Hemost* 2013;39:356–364.
- 155 <http://www.genecards.org/cgi-bin/carddisp.pl?gene=CISH&search=cish>
- 156 Ogston D, McAndrew GM. Fibrinolysis in obesity. *Lancet* 1964; 285: 1205-7.
- 157 Elevated Expression of Transforming Growth Factor- $\beta_3$  in Adipose Tissue from Obese Mice Fahumiya Samad, Koji Yamamoto, Manjula Pandey, and David J. Loskutoff The Scripps Research Institute, Department of Vascular Biology, La Jolla, California, U.S.A. *Molecular Medicine*, Volume 3, Number 1, January 1997 37-48
- 158 Papel del tejido adiposo en la inflamación asociada a la obesidad Javier Gómez-Ambrosi<sup>1,2</sup>, Amaia Rodríguez<sup>1,2</sup>, Victoria Catalán<sup>1,2</sup>, Gema Frühbeck<sup>1-3</sup> 1 Laboratorio de Investigación Metabólica. Clínica Universitaria de Navarra. Universidad de Navarra. Pamplona 2 CIBER de Fisiopatología de la Obesidad y Nutrición (CIBEROBN). Instituto de Salud Carlos III. Madrid 3 Departamento de Endocrinología. Clínica Universitaria de Navarra. Universidad de Navarra. Pamplona *Revista Española de Obesidad* • Vol. 6 • Núm. 5 • Septiembre-octubre 2008 (264-279)
- 159 Kees Meijer, Marcel de Vries, Saad Al-Lahham, Marcel Bruinenberg, Desiree Weenin, Farhard Rezaee, Human Primary Adipocytes Exhibit Immune Cell Function: Adipocytes Prime Inflammation Independent of Macrophages *Plos One* (2011). Vol 6. Issue 3
- 160 Datseris IE, Sonmezoglu K, Siraj QH, Bomanji JB, Nimmon CC, Nijran KS, Britton KE. Predictive value of captopril transit renography in essential hypertension and diabetic nephropathy. *Nucl Med Commun.* 1995 Jan;16(1):4-9. Source Department of Nuclear Medicine, St Bartholomew's Hospital, London, UK.
- 161 Grande MT, Pascual G, Riobobos AS, Clemente-Lorenzo M, Bardaji B, Barreiro L, Tornavaca O, Meseguer A, López-Novoa JM. Increased oxidative stress, the renin-angiotensin system, and sympathetic overactivation induce hypertension in kidney androgen-regulated protein transgenic mice. *Free Radic Biol Med.* 2011 Nov 15;51(10):1831-41. doi: 10.1016/j.freeradbiomed.2011.08.014. Epub 2011 Aug 25.
- 162 Bichu P., Nistala R., Khan A., Sowers J. And Whaley-Connell A. Angiotensin receptor blockers for the reduction of proteinuria in diabetic patients with overt nephropathy: results from the AMADEO study. *Vascular Health and Risk Management* (2009) 2009:5 129–140.
- 163 <http://www.signaling-gateway.org/molecule/query?afcsid=A000304>
- 164 Masri, B., Knibiehler, B., and Audigier, Y. Apelin signalling: a promising pathway from cloning to pharmacology. *Cell. Signal.* (2005) 17, 415–426.
- 165 Principe A, Melgar-Lesmes P, Fernández-Varo G, del Arbol LR, Ros J, Morales-Ruiz M, Bernardi M, Arroyo V, Jiménez W. The hepatic apelin system: a new therapeutic target for liver disease. *Hepatology* (2008); 48(4):1193-201.
- 166 D.L. Crandall, G.J. Hausman, J.G. Kral, A review of the microcirculation of adipose tissue: anatomic, metabolic, and angiogenic perspectives, *Microcirculation* 4 (1997) 211–232.
- 167 The novel peptide apelin lowers blood pressure via a nitric oxide-dependent mechanism. Tatemoto K, Takayama K, Zou MX, Kumaki I, Zhang W, Kumano K, Fujimiya M. Source Department of Molecular Physiology, Institute for Molecular and Cellular Regulation, Gunma University, 371-8512, Maebashi, Japan. [tatekazu@akagi.sb.gunma-u.ac.jp](mailto:tatekazu@akagi.sb.gunma-u.ac.jp)
- 168 Cheng X, Cheng XS, Pang CC: Venous dilator effect of apelin, an endogenous peptide ligand for the orphan APJ receptor, in conscious rats. *Eur J Pharmacol*, 2003; 470:171–75.

## REFERENCES

- 169** Apelin, a Newly Identified Adipokine Up-Regulated by Insulin and Obesity Jérémie Boucher, Bernard Masri, Danie'le Daviaud, Ste'phane Gesta, Charlotte Guigne', Anne Mazzucotelli, Isabelle Castan-Laurell, Ivan Tack, Bernard Knibiehler, Christian Carpe'ne', Yves Audigier, Jean-Se'bastien Saulnier-Blache, and Philippe Valet *Endocrinology* 146(4):1764–1771
- 170** Muller D. N., et al. Mouse Cyp4a isoforms: enzymatic properties, gender- and strain-specific expression, and role in renal 20-hydroxyeicosatetraenoic acid formation. *Biochemical Society* (2007) 403, 109-118.
- 171** Carlyle M., Jones O., Kuo J. and Hall J. Chronic Cardiovascular and Renal Actions of Leptin: Role of Adrenergic Activity. *Hypertension* 2002;39:496-501. DOI: 10.1161/hy0202.104398.
- 172** Minhas K., Khan S., Raju S., Phan A. et al. Leptin repletion restores depressed  $\beta$ -adrenergic contractility in ob/ob mice independently of cardiac hypertrophy. *J Physiol.* (2005); 565(Pt 2): 463–474. doi: 10.1113/jphysiol.2005.084566.
- 173** Kis A, Murdoch C, Zhang M, Siva A, Rodriguez-Cuenca S, Carobbio S, Lukasik A, Blount M, O'Rahilly S, Gray SL, Shah AM, Vidal-Puig A. Defective peroxisomal proliferators activated receptor gamma activity due to dominant-negative mutation synergizes with hypertension to accelerate cardiac fibrosis in mice. *Eur J Heart Fail.* 2009 Jun;11(6):533-41. doi: 10.1093/eurjhf/hfp048. Epub 2009 Apr 24.
- 174** Liu, et al. PKR regulates proliferation, differentiation, and survival of murine hematopoietic stem/progenitor cells *Blood* 2013 121:3364-3374
- 175** El Hussein D, Boulanger MC, Fournier D, Mahmut A, Bossé Y, Pibarot P, Mathieu P. High expression of the Pi-transporter SLC20A1/Pit1 in calcific aortic valve disease promotes mineralization through regulation of Akt-1. *PLoS One.* 2013;8(1):e53393. doi: 10.1371/journal.pone.0053393. Epub 2013 Jan 4.
- 176** Sarró E, Jacobs-Cachá C, Itarte E, Meseguer A. A pharmacologically-based array to identify targets of cyclosporine A-induced toxicity in cultured renal proximal tubule cells. *Toxicol Appl Pharmacol.* 2012 Jan 15;258(2):275-87. doi: 10.1016/j.taap.2011.11.007. Epub 2011 Dec 3.
- 177** Cebrian, C., Areste, C., Nicolas, A, Olive, P., Carceller, A., Piulats, J., Meseguer, A. (2001) *J. Biol. Chem.*



## **PUBLISHED ARTICLES**

---

*“Once you eliminate the impossible, whatever remains, no matter how improbable, must be the truth.”*

A study in scarlet

Sir Arthur Conan Doyle